



TECHNISCHE
UNIVERSITÄT
DARMSTADT

Generation of Multispecific Antibodies with Immune Cell Modulating Functions

at the Department of Chemistry
of the Technischen Universität Darmstadt

submitted in fulfilment of the requirement for the degree
Doctor rerum naturalium
(Dr. rer. nat.)

Doctoral Thesis
By

Stefania Candela Carrara
from Buenos Aires, Argentina

First reviewer: Prof. Dr. Harald Kolmar
Second reviewer: PD. Dr. Björn Hock
Third reviewer: Prof. Dr. Matthias Peipp

Darmstadt, 2022

Carrara, Stefania Candela: Generation of Multispecific Antibodies with Immune Cell Modulating Functions

Darmstadt, Technische Universität Darmstadt,

Jahr der Veröffentlichung der Dissertation auf TUprints: 2023

URN: urn:nbn:de:tuda-tuprints-230236

URL: <https://tuprints.ulb.tu-darmstadt.de/id/eprint/23023>

Date of submission: 31 October 2022

Date of oral examination: 12 December 2022

Veröffentlicht unter CC BY-SA 4.0 International.

Publications derived from this work

Carrara SC, Ulitzka M, Grzeschik J, Kornmann H, Hock B, Kolmar H (2021). From cell line development to the formulated drug product: The art of manufacturing therapeutic monoclonal antibodies. *International Journal of Pharmaceutics* 10.1016/j.ijpharm.2020.120164.

Carrara SC*, Fiebig D*, Bogen JP*, Grzeschik J, Hock B, Kolmar H (2021). Recombinant Antibody Production Using a Dual-Promoter Single Plasmid System. *Antibodies (Basel)* 10.3390/antib10020018.

Carrara SC*, Bogen JP*, Grzeschik J, Hock B, Kolmar H (2022). Antibody Library Screening Using Yeast Biopanning and Fluorescence-Activated Cell Sorting. *Methods in Molecular Biology* 10.1007/978-1-0716-2285-8_10.

Fiebig D*, Bogen JP*, **Carrara SC***, Deweid L, Zielonka S, Grzeschik J, Hock B, Kolmar H (2022). Streamlining the Transition from Yeast Surface Display of Antibody Fragment Immune Libraries to the Production as IgG format in Mammalian Cells. *Frontiers in Bioengineering & Biotechnology* 10.3389/fbioe.2022.794389.

Carrara SC, Bogen JP, David F, Grzeschik J, Hock B, Kolmar H (2022). Bulk reformatting of antibody fragments displayed on the surface of yeast cells to final IgG format for mammalian production. *Methods in Molecular Biology*, *accepted*.

Carrara SC, Bogen JP, Fiebig D, Grzeschik J, Hock B, Kolmar H (2022). Targeted phagocytosis induction for cancer immunotherapy via bispecific MerTK-engaging antibodies. *International Journal of Molecular Sciences*, 10.3390/ijms232415673.

Carrara SC, Harwardt J, Grzeschik J, Hock B, Kolmar H (2022). TriTECM: A Tetrafunctional T-Cell Engaging Antibody with Built-In Risk Mitigation of Cytokine Release Syndrome. *Frontiers in Immunology* 10.3389/fimmu.2022.1051875.

(* shared first authorship)

Contributions to Publications & Conferences

Publications:

Ulitzka M, **Carrara SC**, Grzeschik J, Kornmann H, Hock B, Kolmar H (2020). Engineering therapeutic antibodies for patient safety: tackling the immunogenicity problem. *Protein Engineering Design & Selection* 10.1093/protein/gzaa025.

Bogen JP, **Carrara SC**, Fiebig D, Grzeschik J, Hock B, Kolmar H (2020). Expeditious Generation of Biparatopic Common Light Chain Antibodies *via* Chicken Immunization and Yeast Display Screening. *Frontiers in Immunology* 10.3389/fimmu.2020.606878.

Bogen JP, **Carrara SC**, Fiebig D, Grzeschik J, Hock B, Kolmar H (2021). Design of a Trispecific Checkpoint Inhibitor and Natural Killer Cell Engager Based on a 2+1 Common Light Chain Antibody Architecture. *Frontiers in Immunology* 10.3389/fimmu.2021.669496.

Pekar L, Klewinghaus D, Arras P, **Carrara SC**, Harwardt J, Krah S, Yanakieva D, Toleikis L, Smider VV, Kolmar H, Zielonka S (2021). Milking the Cow: Cattle-Derived Chimeric Ultralong CDR-H3 Antibodies and Their Engineered CDR-H3-Only Knobbody Counterparts Targeting Epidermal Growth Factor Receptor Elicit Potent NK Cell-Mediated Cytotoxicity. *Frontiers in Immunology* 10.3389/fimmu.2021.742418.

Harwardt J, Bogen JP, **Carrara SC**, Ulitzka M, Grzeschik J, Hock B, Kolmar H (2022). A Generic Strategy to Generate Bifunctional Two-in-One Antibodies by Chicken Immunization. *Frontiers in Immunology* 10.3389/fimmu.2022.888838.

Patent applications:

Kolmar H, Harwardt J, Bogen JP, **Carrara SC**, Ulitzka M (2022). “Two-in-one”-antibodies binding to EGFR/PD-L1-double positive cells. EP22196556.9.

Conferences

Carrara SC, Dávila-Lezama A. Novel *in vitro* functional assays for therapeutic antibody screening (Presentation). *Ciclo de Conferencias*, Foro International UABC, Tijuana (4 December 2020).

Carrara SC, Fiebig D, Bogen JP, Grzeschik J, Hock B, Kolmar H. Production of recombinant antibodies using a dual-promoter single plasmid system (Poster). PepTalk Conference, San Diego (17 – 19 January 2022).

Table of Contents

Publications derived from this work.....	iii
Contributions to Publications & Conferences	iv
Table of Contents	v
Scientific Novelty & Significance	vi
Zusammenfassung und wissenschaftlicher Erkenntnisgewinn	ix
Individual Contributions by S.C. Carrara for Cumulative Section.....	xiii
1 Introduction.....	1
1.1 <i>Immune System</i>	1
1.1.1 Innate Immune System	1
1.1.2 Adaptive Immune System	4
1.1.3 Structure and Function of Antibodies	7
1.2 <i>Therapeutic Antibodies for Immunotherapy</i>	9
1.2.1 Immuno-oncology Applications	12
1.2.2 Severe Adverse Effects – Cytokine Release	14
1.3 <i>Discovery & Generation of Therapeutic Antibodies</i>	16
1.3.1 Discovery of binders	16
1.3.2 Development of therapeutic antibodies	17
1.4 <i>Immune-Cell Engagers</i>	19
1.4.1 T-Cell Engagers	19
1.4.2 Macrophage Engagers	21
1.4.3 Multispecific antibodies	22
2 Objective.....	26
3 References	28
4 Cumulative Section	43
4.1 <i>From cell line development to the formulated drug product: The art of manufacturing therapeutic monoclonal antibodies.</i>	43
4.2 <i>Recombinant Antibody Production Using a Dual-Promoter Single Plasmid System.</i>	58
4.3 <i>Streamlining the Transition from Yeast Surface Display of Antibody Fragment Immune Libraries to the Production as IgG Format in Mammalian Cells</i>	77
4.4 <i>Targeted phagocytosis induction for cancer immunotherapy via bispecific MerTK-engaging antibodies</i>	94
4.5 <i>TriTECM: A Tetrafunctional T-Cell Engaging Antibody with Built-In Risk Mitigation of Cytokine Release Syndrome</i>	122
4.6 <i>Antibody Library Screening Using Yeast Biopanning and Fluorescence-Activated Cell Sorting</i>	145
5 Acknowledgements	163
6 Curriculum Vitae.....	166
7 Erklärung laut Promotionsordnung	167

Scientific Novelty & Significance

Within the field of biologics, monoclonal antibodies have ruled the market with blockbuster and top selling drugs over the last decades. With the advancements in technological discoveries, lightspeed progress has been achieved to discover novel antibodies and mechanisms of action to address unmet needs and indications. Particularly, display technologies, *in vitro* systems, and high/ultra-high-throughput technologies have shown monumental progress to ensure the rapid discovery of novel biological entities.

In the first study presented herein, the focus laid on the generation of a bidirectional plasmid for recombinant antibody production in mammalian cells to facilitate native antibody folding and post-translational modifications. Conventional approaches for transient antibody production utilise co-transfection of heavy and light chain genes encoded on separate plasmids. Here, a single plasmid under the control of two independent promoters, constructed in a bidirectional fashion, is used. This study assessed promoter combinations resulting in the best antibody yields of two U.S. Food and Drug Administration (FDA)-approved antibodies, durvalumab and avelumab. By comparing promoters with varying strengths (CMV, minCMV, EF-1 α and enhanced CMV), gene expression of heavy and light chain genes and subsequent IgG1 yields gave rise to the 2xeCMV combination, consisting of two mirrored eCMV cassettes controlling the expression of the light and heavy chains individually in each direction. This combination effectuated the most promising mRNA synthesis for both chains in two regularly used mammalian cell lines, human embryonic kidney 293 (HEK293) and Chinese hamster ovary (CHO) cells, and the highest yields after IgG quantification, comparable to the conventional co-transfection method. By substituting the co-transfection approach with this bidirectional plasmid, lower plasmid preparation efforts are required and further facilitates the handling of a higher number of mAb candidates simultaneously.

In the second study, the described bidirectional plasmid was put into practise by generating a Fab-presenting yeast surface display (YSD) library from immunised OmniRats. After screening of antibody formats *via* fluorescence-activated cell sorting (FACS), reformation of single candidates into their final IgG format is required, rapidly converting itself into a cumbersome step, and often resulting in the bottleneck to proceed with further characterisation. Within this study, a novel workflow based on Golden Gate Cloning (GGC) was established, allowing the bulk reformatting of antibody candidates after YSD FACS screening. By using an OmniRat-derived Fab library against MerTK, two screening rounds of YSD were performed by FACS. Subsequently, the antibody-encoding genes were transferred into a Mammalian_Destination (MD) vector, which contained a partial hinge-CH2-CH3 sequence, resulting in a full-length heavy chain after GGC with *Esp3I*. In order to produce the full-length variants, the yeast-

specific Gal1,10 promoter was exchanged for the described promoter cassette combinations from the first study, 2xeCMV, by a final GGC step with *BbsI*. After assembly, the resulting MD vector contained the variable domains from the second sorting round with the respective constant domains required for the production of full-length IgG molecules. Next generation sequencing (NGS) of the screening rounds confirmed that the entire VH family diversity was covered in the resulting clones after bulk reformatting. Ten candidates were subsequently transiently expressed in mammalian cells and characterised for target binding and biophysical properties. This workflow presented a two-pot, two-step, PCR-free method to transition from YSD to a mammalian expression vector, eliminating any unwanted polymerase-introduced mutations and allowing for bulk cloning of yeast display-enriched antibody fragments. By this procedure, heavy and light chain pairing is conserved, contrary to other reformatting approaches, and paves the way to accelerate antibody hit discovery campaigns with YSD. Furthermore, this platform is malleable to other antibody formats and immunisation hosts, such as single chain variable fragments (scFvs) and chickens, and has the potential to be developed for bispecific or multispecific antibodies.

Next-generation antibodies, including bi- and multispecific antibodies, have been set under the spotlight for their ability to combine multiple modes of action simultaneously and result in higher efficacy, where monoclonal antibodies are lacking. A special class of such are immune cell engagers which target immune cells and tumour-associated antigens (TAAs) to create an immune synapse. Depending on the effector cell being targeted, specialised killing mechanisms are triggered to efficiently kill the targeted cells. Macrophage engagers are aimed at forcing targeted phagocytosis of the engaged cell type and have typically targeted the CD47/SIRP α axis up to date, known as the “do not eat me” signal. Nevertheless, targeting CD47 lacks specificity due to its ubiquitous expression pattern. On the other hand, T-cell engagers (TCEs) result in very specialised signals by targeting CD3 on T cells and additional TAAs. The hyperactivation of T cells results in a feedback loop through the activation of macrophages and the over-release of cytokines, resulting in cytokine storms or cytokine release syndrome (CRS). If left untreated, these can provoke life-threatening conditions. Thus, macrophage engagers and TCEs require novel cell-specific targets and widening of their therapeutic windows for restored patient alleviation.

In the third study within this cumulative thesis, the first bispecific macrophage engager targeting the receptor tyrosine kinase MerTK and epidermal growth factor receptor (EGFR) is presented. From the 10 antibody candidates derived in the second study, one candidate displayed agonistic properties, detected by the dose-dependent activation of the downstream signalling molecule phospho AKT (pAKT). MerTK's overexpression on macrophages and tumour-associated macrophages within the tumour microenvironment (TME) lays the foundation to generate macrophage-engaging bispecific antibodies for targeted phagocytosis of tumour cells. Therefore, tandem biparatopic EGFR-binding V_{HH} molecules

(termed 7D9G) were combined in different architectures to generate bispecific molecules. By using the Knob-into-Hole technology, a bispecific with a MerTK-binding Fab arm and an EGFR-binding tandem VHH arm were generated, abolishing the agonistic properties of the parental MerTK mAb. On the other hand, a tetravalent bispecific antibody was generated by fusing the tandem V_{HHS} to the C-terminus of the CH3 domain, resulting in intact MerTK-binding Fabs. The bispecific antibodies were able to bind both targets simultaneously in their soluble form and engage macrophages with EGFR⁺ tumour cells. Furthermore, they were able to compete with the binding site of EGF and therefore inhibit EGF-mediated signalling transduction by inhibiting pAKT. EGFR domain mapping of 7D9G by YSD resulted in binding to domain III of the extracellular EGFR domain, confirming its ligand-inhibiting abilities. Moreover, the bispecific antibodies resulted in targeted phagocytosis of EGFR⁺ tumour cells by macrophage-like THP-1 cells. This work represents the first bispecific macrophage-engager targeting MerTK for immunoncology applications by harnessing its expression and role in the tumour microenvironment to selectively phagocytise tumour cells.

In the last study presented here, a trispecific T-cell engager and cytokine release modulating antibody (TriTECM) was generated. In brief, a tetravalent, bispecific two-in-one antibody binding EGFR and PD-L1 simultaneously with a single Fab arm was combined with anti-CD3 and anti-IL-6R scFvs, derived from foralumab or sarilumab, respectively. By testing two TriTECM architectures varying mainly in the anti-CD3 scFv positioning and valency of IL-6R binding, tetraspecific molecules were generated with multiple mechanisms of action. Firstly, increased tumour specificity was ensured by targeting EGFR and PD-L1 with a low nanomolar on-cell affinity. Checkpoint inhibition by blockage of the PD-1/PD-L1 axis was mediated by binding to PD-L1. T-cell engagement and subsequent T-cell-mediated cytotoxicity was attenuated, resulting in reduced pro-inflammatory cytokine release. And lastly, inhibition of the IL-6/IL-6R pathway can modulate cytokine storms after T-cell activation. The attenuation of CD3 binding could allow existing CD3-binders to be used, that were previously shown to result in cytotoxicity. With cytokine release still putting obstacles in the way of novel immune cell engagers, TriTECM designs represent a novel class of therapeutics with the potential to inertly modulate over-activated immune responses and widen the therapeutic index of T-cell-engaging therapeutics.

Zusammenfassung und wissenschaftlicher Erkenntnisgewinn

Auf dem Gebiet der Biologika haben monoklonale Antikörper (mAb) in den letzten Jahrzehnten den Markt mit Blockbustern und umsatzstarken Medikamenten durchdrungen. Fortschritte bei der Entwicklung neuer Technologien gingen einher mit rasanten Fortschritten bei der Entdeckung neuartiger Antikörper und Wirkmechanismen, die es ermöglichen, neue Anwendungsgebiete zu erschließen. Insbesondere Display-Technologien, *In-vitro*-Systeme und Hoch- bzw. Ultra-Hochdurchsatz-Technologien ermöglichen heute die Isolierung von biologischen Wirkstoffkandidaten in relativ kurzen Zeiträumen.

In der ersten hier vorgestellten Studie lag der Schwerpunkt auf der Herstellung eines bidirektionalen Plasmids für die rekombinante Antikörperproduktion in Säugetierzellen, um die native Antikörperfaltung und posttranslationale Modifikationen zu erleichtern. Konventionelle Ansätze für die transiente Antikörperproduktion nutzen die Co-Transfektion von Genen der schweren und der leichten Kette eines Antikörpers, die auf separaten Plasmiden kodiert sind. In der vorgestellten Studie wird nur ein einziges Plasmid unter der Kontrolle von zwei unabhängigen Promotoren eingesetzt. Der Fokus lag dabei auf der Untersuchung, welche Promotorkombination die beste Antikörperausbeute für zwei von der U.S. Food and Drug Administration (FDA) zugelassenen Antikörper, Durvalumab und Avelumab, erbringt. Durch die Kombination von Promotoren unterschiedlicher Stärke (CMV, minCMV, EF-1 α und Enhanced CMV) für die Genexpression der schweren und leichten Kette, waren die IgG-Ausbeuten am höchsten bei der 2xeCMV-Kombination. Bei dieser wurden zwei gespiegelte eCMV-Kassetten eingesetzt, welche die Expression der leichten und schweren Kette individual in jeder Richtung steuerten. Diese Kombination bewirkte eine hohe mRNA-Syntheserate für beide Ketten in zwei standardmäßig eingesetzten Säugetierzelllinien und die höchsten Ausbeuten an Antikörpern, vergleichbar mit der herkömmlichen Co-Transfektionsmethode. Der Ersatz der Co-Transfektionsmethode bei Einsatz zweier Plasmide durch dieses bidirektionale Plasmid verringert den Aufwand für die Plasmidpräparation, was die gleichzeitige Bearbeitung einer größeren Anzahl von Antikörperkandidaten ermöglicht.

In der zweiten Studie wurde das zuvor beschriebene bidirektionale Plasmid verwendet, um eine Fab-Bibliothek aus immunisierten OmniRats zu generieren und die Fab-Varianten im Hefeoberflächendisplay (YSD) zu präsentieren. Nach der Durchmusterung von Antikörperkandidaten mittels fluoreszenz-aktivierter Zellsortierung (FACS) ist die Reformatierung einzelner Kandidaten in ihr endgültiges IgG-Format erforderlich, was mit größerem manuellem Aufwand verbunden ist und oft zu einer zeitlichen Verzögerung bei der weiteren Charakterisierung führt. Im Rahmen dieser Studie wurde ein neuartiger, auf Golden Gate Cloning (GGC)-basierender Arbeitsablauf etabliert, der die Massenreformatierung von Antikörperkandidaten nach dem YSD-FACS-Screening ermöglicht. Unter Verwendung einer von

OmniRat stammenden Fab-Bibliothek gegen MerTK wurden zwei YSD-Durchmusterungsrunden mittels FACS durchgeführt. Anschließend wurden die Antikörper-kodierenden Gene in einen *Mammalian_Destination* (MD)-Vektor übertragen, der eine partielle Hinge-CH2-CH3 Sequenz enthielt, was nach einem GGC-Schritt mit *Esp3I* in einem ORF resultierte, welche die vollständige schwere Kette kodierte. Um die Vollängenvarianten zu erzeugen, wurde der hefespezifische Gal1,10-Promotor in einen abschließenden GGC-Schritt mit *BbsI* gegen die beschriebenen Promotorkassettenkombination aus der ersten Studie, 2xeCMV, ausgetauscht. Nach der Assemblierung enthielt der resultierende MD-Vektor die variablen Domänen aus der zweiten Sortierunde mit den jeweiligen konstanten Domänen, die für die Produktion von IgG-Molekülen erforderlich sind. *Next Generation Sequencing* (NGS) aller Durchmusterungsrunden bestätigte, dass die gesamte Vielfalt der Sequenzen der VH-Familien in den resultierenden Klonen nach der Massenumformatierung wiedergefunden wurde. Zehn Kandidaten wurden anschließend transient in Säugetierzellen exprimiert und hinsichtlich ihrer Antigenbindung und biophysikalischen Eigenschaften charakterisiert. Dieser Arbeitsablauf ermöglicht einen direkten Transfer von Fab Fragmente kodierenden Genen aus einem Hefedisplayvektor in einen Säugetier-Expressionsvektor, vermeidet unerwünschte Polymerase-induzierte Mutationen und erlaubt eine Massenklonierung von angereicherten Antikörperfragmenten. Durch dieses Verfahren bleibt die Paarung von schwerer und leichter Kette im Gegensatz zu anderen Reformatierungsansätzen erhalten und ebnet somit den Weg zur Beschleunigung von Antikörper Durchmusterungskampagnen mit YSD. Darüber hinaus ist diese Plattform für andere Antikörperformate und Immunisierungswirte, wie scFvs und Hühner, anpassbar und hat das Potenzial, für bispezifische oder multispezifische Antikörper entwickelt zu werden.

Antikörper der neuesten Generation, einschließlich bi- und multispezifischer Antikörper, sind in den Fokus der Forschung gerückt, da sie mehrere Wirkmechanismen gleichzeitig kombinieren und eine höhere Wirksamkeit als monoklonale Antikörper erzielen können. Eine besondere Klasse von Antikörpern sind *Immunzell-Engager*, welche gleichzeitig Immunzellen und tumorassoziierte Antigene (TAAs) auf malignen Zellen targetieren, und so eine Immunsynapse schaffen. Je nach adressierter Immunzelle werden spezielle Effektorfunktionen aktiviert, was in der effizienten Tötung der targetierten Zellen resultiert. *Makrophagen-Engager* vermitteln eine gezielte Phagozytose der angegriffenen Zelle und adressierten bisher in dem meisten Fällen die CD47/SIRP α -Achse, welche für sogenannte "Friss mich nicht"-Signale verantwortlich ist. Allerdings wird CD47 ubiquitär exprimiert und ist daher nicht selektiv. *T-Cell Engager* (TCEs) hingegen erkennen zumeist CD3 auf T-Zellen und zusätzlich ein TAA auf einer Tumorzelle. Durch die Bildung einer immunologischen Synapse vermittelt der TCE die Aktivierung der T Zelle, was in einer zytotoxischen Reaktion gegen die Zielzelle resultiert. Die Hyperaktivierung von T-Zellen führt zu einer Rückkopplungsschleife durch die Aktivierung von Makrophagen und damit in der

Folge zur übermäßigen Freisetzung von Zytokinen, was zu Zytokinstürmen oder einem Zytokinfreisetzungssyndrom führen kann, welche unbehandelt lebensbedrohlichen Zustände hervorrufen. Daher benötigen Makrophagen-Engager und TCEs neue, zellspezifische Targets und eine Erweiterung ihres therapeutischen Fensters, um das Auftreten von Nebenwirkungen im Patienten zu verhindern.

In der dritten Studie, die im Rahmen dieser kumulativen Dissertation vorgestellt wird, wurde der erste bispezifische Makrophagen-Engager generiert, welcher den Rezeptor-Tyrosinkinase MerTK und den epidermalen Wachstumsfaktor-Rezeptor (EGFR) targetierte. Von den zehn Antikörperkandidaten, die in der zweiten Studie entwickelt wurden, zeigte ein Kandidat ein agonistisches Wirkprofil, welches durch die dosisabhängige Aktivierung eines nachgeschalteten Signalmoleküls, phospho-AKT, nachgewiesen wurde. Die Überexpression von MerTK auf Makrophagen und tumorassoziierten Makrophagen in der Tumormikroumgebung bildet die Grundlage für die Entwicklung von Makrophagen-aktivierenden bispezifischen Antikörpern zur gezielten Phagozytose von Tumorzellen. Daher wurden biparatopische EGFR-bindende tandem-VHH-Moleküle (bezeichnet als 7D9G) in verschiedenen Architekturen mit dem MerTK mAb kombiniert, um bispezifische Moleküle zu erzeugen. Mit Hilfe der „Knob-into-Hole“-Technologie wurde ein bispezifischer Antikörper designt, welcher mit einem Fab-Arm MerTK adressiert und ein weiterer Arm durch die EGFR-bindenden tandem-VHH dargestellt wurde. Dieses Konstrukt zeigte jedoch keine agonistische MerTK Bindung. Durch die Fusion der tandem VHHs an den C-terminus der CH3-Domäne des anti-MerTK IgGs, wurde die agonistische Bindungseigenschaft wiederhergestellt. Die bispezifischen Antikörper waren in der Lage, beide Zielmoleküle gleichzeitig in ihrer löslichen Form zu binden und Makrophagen mit EGFR-positiven Tumorzellen in Kontakt zu bringen. Darüber hinaus waren sie in der Lage, mit der Bindung von EGF, dem natürlichen Liganden von EGFR, zu kompetieren und somit die EGF-vermittelte Signaltransduktion durch Hemmung von phospho-AKT zu inhibieren. Des Weiteren führten die bispezifischen Antikörper zu einer gezielten Phagozytose von EGFR-positiven Tumorzellen durch makrophagenartige THP-1-Zellen. In dieser Arbeit wurde der erste bispezifische Makrophagen-Aktivator generiert, welcher MerTK adressiert und für immunonkologische Anwendungen geeignet ist, indem er dessen Expression und Rolle in der Mikroumgebung des Tumors für die selektive Phagozytose von Tumorzellen nutzt.

In der letzten hier vorgestellten Studie wurde ein trispezifischer *T-Cell Engager* und Zytokinfreisetzungsmodulierender Antikörper (TriTECM) entwickelt. Hierzu wurde ein tetravalenter bispezifischer Zwei-in-Eins-Antikörper, der EGFR und PD-L1 gleichzeitig mit einem einzigen Fab-Arm bindet, mit Anti-CD3- und Anti-IL-6R-Einzelketten-Variablen-Fragmenten (scFvs) kombiniert, welche von Foralumab bzw. Sarilumab abgeleitet wurden. Es wurden zwei TriTECM-Architekturen erzeugt, die sich hauptsächlich in

der Positionierung der Anti-CD3-scFvs und der Valenz der IL-6R-Bindung unterschieden, welche mehreren Wirkmechanismen vereinten. Zunächst wurde eine erhöhte Tumorspezifität gewährleistet, indem EGFR und PD-L1 mit einer niedrigen nanomolaren Affinität auf doppelt-positive Zielzellen gebunden werden. Durch Bindung an PD-L1 wurde die PD-1/PD-L1-Achse blockiert und dieser Immuncheckpoint inhibiert. Die T-Zell-Bindung und die anschließende T-Zell-vermittelte Zytotoxizität wurden abgeschwächt, was zu einer verringerten Freisetzung von pro-inflammatorischen Zytokinen führte. Abschließend kann die Hemmung des IL-6/IL-6R-Signalwegs die Zytokinausschüttung nach der T-Zell-Aktivierung herunterreguliert. Die Abschwächung der CD3-Bindung könnte es ermöglichen, Literatur-bekanntes CD3-Binder zu verwenden, die zuvor nachweislich Zytotoxizität bewirkten. Angesichts der Tatsache, dass die Freisetzung von Zytokinen immer noch eine Problematik bei der Entwicklung neuartiger Immunzellen-targetierender Antikörper darstellt, sind TriTECM eine neue Klasse von Therapeutika, die das Potenzial haben, überaktivierte Immunantworten gezielt zu modulieren und den therapeutischen Index von T-Zell-aktivierenden Therapeutika zu erweitern.

Individual Contributions by S.C. Carrara for Cumulative Section

1) Carrara SC, Ulitzka M, Grzeschik J, Kornmann H, Hock B, Kolmar H (2021). From cell line development to the formulated drug product: The art of manufacturing therapeutic monoclonal antibodies. *International Journal of Pharmaceutics* 10.1016/j.ijpharm.2020.120164.

Contributions by S.C. Carrara:

- Literature search
- Summarising data from literature and planning manuscript
- Writing of original manuscript draft
- Generation of all figures

The contribution of S.C. Carrara totalled 90%. The remaining 10% were distributed between M. Ulitzka, J. Grzeschik, H. Kornmann, B. Hock, and H. Kolmar for reading and correcting the manuscript.

2) Carrara SC*, Fiebig D*, Bogen JP*, Grzeschik J, Hock B, Kolmar H (2021). Recombinant Antibody Production Using a Dual-Promoter Single Plasmid System. *Antibodies (Basel)* 10.3390/antib10020018.
(* shared first authorship)

Contributions by S.C. Carrara:

- Experimental testing of variants generated by D. Fiebig and J.P. Bogen
- Writing of manuscript together with D. Fiebig and J.P. Bogen
- Generation of figures together with D. Fiebig and J.P. Bogen

The contributions of S.C. Carrara totalled 30%. The remaining first co-authors D. Fiebig and J.P. Bogen also contributed 30% each, with the remaining 10% spread across J. Grzeschik, B. Hock and H. Kolmar for their scientific advice and revising the manuscript.

3) Fiebig D*, Bogen JP*, **Carrara SC***, Deweid L, Zielonka S, Grzeschik J, Hock B, Kolmar H (2022). Streamlining the Transition from Yeast Surface Display of Antibody Fragment Immune Libraries to the Production as IgG Format in Mammalian Cells. *Frontiers in Bioengineering & Biotechnology* 10.3389/fbioe.2022.794389.

(* shared first authorship)

Contributions by S.C. Carrara:

- Production of antibody hits from YSD-derived screening campaigns
- Characterisation of antibody hits
- Writing of manuscript together with D. Fiebig and J.P. Bogen
- Generation of figures

The contributions of S.C. Carrara totalled 30%. As first co-authors, D. Fiebig and J.P. Bogen each contributed 30%. The remaining 10% was spread across J. Grzeschik, B. Hock and H. Kolmar for their scientific advice and revising the manuscript.

4) **Carrara SC**, Bogen JP, Fiebig D, Grzeschik J, Hock B, Kolmar H (2022). Targeted phagocytosis induction for cancer immunotherapy via bispecific MerTK-engaging antibodies. *International Journal of Molecular Sciences*, 10.3390/ijms232415673.

Contributions by S.C. Carrara:

- Initial idea
- Cloning and production of bispecific variants
- Testing of variants on cell lines and isolated PBMCs
- Writing of manuscript
- Generation of all figures

The contribution of S.C. Carrara totalled 90%. The remaining 10% were distributed between J.P. Bogen, D. Fiebig, J. Grzeschik, B. Hock, and H. Kolmar for their scientific advice and writing/reviewing of the manuscript.

5) Carrara SC, Harwardt J, Grzeschik J, Hock B, Kolmar H (2022). TriTECM: A Tetrafunctional T-Cell Engaging Antibody with Built-In Risk Mitigation of Cytokine Release Syndrome. *Frontiers in Immunology* 10.3389/fimmu.2022.1051875.

Contributions by S.C. Carrara:

- Initial idea
- Cloning and production of bi-, tri- and tetraspecific variants
- Testing of variants on cell lines and isolated PBMCs
- Writing of manuscript
- Generation of all figures

The contribution of S.C. Carrara totalled 90%. The remaining 10% were distributed between J. Harwardt, J. Grzeschik, B. Hock, and H. Kolmar for their scientific advice and revising of the manuscript.

6) Carrara SC*, Bogen JP*, Grzeschik J, Hock B, Kolmar H (2022). Antibody Library Screening Using Yeast Biopanning and Fluorescence-Activated Cell Sorting. *Methods in Molecular Biology* 10.1007/978-1-0716-2285-8_10.

(* shared first authorship)

Contributions by S.C. Carrara:

- Writing of manuscript together with J.P. Bogen
- Design and generation of figures with J.P. Bogen

The contributions of S.C. Carrara totalled 45%. J.P. Bogen also contributed 45% as the co-first author. The remaining 10% were contributed by J. Grzeschik, B. Hock, and H. Kolmar for revising and correcting the manuscript.

7) Carrara SC, Bogen JP, Fiebig D, Grzeschik J, Hock B, Kolmar H (2022). Bulk reformatting of antibody fragments displayed on the surface of yeast cells to final IgG format for mammalian production. *Methods in Molecular Biology*, accepted.

Contributions by S.C. Carrara:

- Writing of manuscript
- Generation of all figures

The contribution of S.C. Carrara was 85%. The remaining 15% were distributed between J.P. Bogen, D. Fiebig, J. Grzeschik, B. Hock, and H. Kolmar for revising and correcting the manuscript.

1 Introduction

1.1 Immune System

Vertebrates have the most advanced immune system, composed of a complex network of signalling molecules, immune cells, organs and tissues. The immune system protects the human body from disease-causing substances, such as germs, bacteria, viruses, parasites or fungi (1). It is composed of two main systems: the innate and the adaptive immune system. The innate immune response represents a rapid, general immunological response. On the other hand, the adaptive immune system is considered a specialised, antigen-specific response, representing a slower reaction. While the innate system is evolutionarily older and found in virtually all living organisms, the adaptive response was first discovered approximately 500 million years ago in jawed fish and has since only been found in vertebrates (2,3). Both systems will be reviewed in 1.1.1 and 1.1.2, accordingly.

1.1.1 Innate Immune System

The first line of defence comprises three different types of barriers: structural, chemical and biological barriers. Structural barriers include the outermost layer of the body, the skin, composed of a number of structural cells (4–6) and mucosal membranes found within close proximity of body cavities (7–9). These membranes prevent the infiltration of inhaled or ingested foreign pathogens. Additionally, the mucosa of vertebrates serves as a chemical and biological barrier by secreting bioactive molecules including pro-inflammatory cytokines and lysozyme (9,10). Lysozyme is further present in nasal secretions, tears and saliva and inhibits microbial growth (11–13). Chemical barriers include regions of lowered pH, i.e., as found within the stomach and mucous membranes to avoid microbial growth and invasion.

Once pathogens penetrate anatomical barriers, an immune cascade is started to immediately fight against possible infection. This system is known as the innate immune response and is the first line of defence against a pathogen that was able to intrude the chemical and physical barriers. As a fast response is required to clear pathogens before causing more damage, the innate immune response occurs immediately or within a maximum of hours after encountering a pathogen-derived antigen, thus it is known as an antigen-independent, non-specific defence mechanism (14). Pathogens entering the body must fulfil a number of requirements in order to be efficiently cleared by the immune system. One of these requirements is the presence of conserved molecular patterns and structures across large groups of pathogens, which are the main target of innate immune recognition. These patterns are known as pathogen-associated molecular patterns (PAMPs) (15) or more recently as microbe-associated molecular patterns (MAMPs) (16,17). Examples of PAMPs include lipopolysaccharides (LPS), lipoproteins, peptidoglycans and oligosaccharides, all often found on the surface of pathogens (18). Furthermore,

dangerous endogenous signals that may contribute to tissue stress are designated damage-associated molecular patterns (DAMPs) (19,20).

While PAMPs and MAMPs originate from external pathogens, DAMPs generally play a physiological role within the body but transform into danger signals when exposed to external environments, for example after being released from dying cells (21). PAMPs, MAMPs, and DAMPs can be recognised due to their conserved molecular patterns, hence the receptors that do such were termed pattern-recognition receptors (PRRs) (22). As PAMPs are broadly expressed on pathogens but not in host cells, PRRs are able to discriminate between self and non-self, as first proposed by Janeway in the early 1990s (23,24). PRRs are germline-coded receptors that can either be present on the surface of sensor cells important for detecting pathogen infection, such as monocytes, macrophages, dendritic cells (DCs), epithelial and endothelial cells, and fibroblasts (25,26), or can be found in soluble forms (18). PRRs can be divided into four subclasses, based on their downstream signal transduction activation and their residency location. The Toll-like receptors (TLRs) and C-type lectin receptors (CLRs) are both transmembrane receptors that detect PAMPs either on the cell surface or the lumen of intracellular vesicles. TLRs are the most well-studied class of PRRs and can be classified into two subfamilies. Cell surface TLRs, including TLR1, TLR2, TLR4, TLR5, TLR6 and TLR10, recognise microbial membrane components (lipids, lipoproteins). For example, TLR4 specifically recognises bacterial LPS. The second subfamily comprises intracellular TLRs that recognise nucleic acids from bacteria or viruses and additionally recognise self-nucleic acids in autoimmunity. These include TLR3, TLR7, TLR8, TLR11, TLR12, and TLR13 (27,28). Two further PRR subclasses exist that were recently shown to detect intracellular PAMPs cytosolically, namely retinoic acid-inducible gene I-like receptors (RLRs) and nucleotide-binding oligomerisation domain-like receptors (NLRs) (25,26). Once the innate immune system detects and recognises foreign molecules *via* PRRs on sensor cells, a downstream signalling cascade is activated leading to the secretion of inflammatory mediators, including cytokines, chemokines, interferons, and antimicrobial peptides (AMPs) (29–33).

A further system within innate immune responses is the complement system. It is composed of over 40 proteins found in the plasma and on cellular surfaces and constitutes over 15% of the globular fraction of plasma. Its versatile functions include pathogen opsonisation through complement opsonin (e.g., C3b), release of pro-inflammatory mediators, and targeted lysis of pathogenic surfaces through membrane-penetrating pores known as the membrane attack complex (MAC). These actions are the result of three complement pathways that are activated and mediated in different ways (34,35).

Integral effector cells of the innate immune system are phagocytic cells, consisting of granulocytes (neutrophils, basophils, eosinophils, mast cells), monocytes/macrophages, and DCs (10). Neutrophils

and monocyte-derived macrophages are known as professional phagocytes, as their precise reason for existing is to engulf pathogens through receptor-mediated endocytosis. The phagocytosis theory originates from Elie Metchnikoff in 1882, for which he was later awarded the 1908 Nobel Prize together with Paul Ehrlich (36,37). Neutrophils make up 40-60% of all leukocytes in human blood and are the first to arrive to an infected scene, hours before monocytes and monocyte-derived macrophages. To recognise phagocytic targets, neutrophils and macrophages express a number of cell-surface PRRs. Neutrophils, for example, express Dectin-1 and Dectin-2, both belonging to the CLR family, recognising β -glucan found in the cell wall of a wide array of microbes and mannose-rich structures present on a range of species, respectively (38–42). Additionally, they possess cell-surface receptors for the Fc portion of antibodies and for the C3b component of the complement system.

Upon encountering pathogens, actin polymerisation is induced at the site of pathogen attachment after ligand binding *via* PRRs. The plasma membrane of phagocytes can subsequently surround the pathogen and results in phagosomes with engulfed pathogens (43). The phagosome fuses with intracellular granules filled with proteases and AMPs to form the phagolysosome, where microbes are subsequently killed. Two main mechanisms exist for killing of microbes: i) de-granulation of granules to expose bacteria to AMPs, enzymes and proteases, or ii) generation of reactive oxygen species (ROS) (44). The former is known as the oxygen-independent mechanism and is predominantly responsible for altering the permeability of bacterial membranes, for example through the release of defensins and cathelicidins such as hCAP-18/LL-37 (45–47). Defensins and cathelicidins predominantly disrupt anionic bacterial surfaces by forming pores in their membranes, rendering bacteria more susceptible to lysis (46). The enzyme lysozyme is also released from neutrophil granules that leads to bacterial killing through the targeted hydrolysis of peptidoglycans (PGs) present on their cell walls (13,48,49). Neutrophil serine proteases (NSPs), including neutrophil elastase (NE) and cathepsin G (CG), also contribute to the non-oxidative pathways of neutrophil-driven killing. Under normal conditions, these inactivated proteases are stored in granules, which are only activated upon release into phagocytic vacuoles (50). The most well-known direct antibacterial function of NSPs is the direct killing of bacterial cells. NE has been shown to directly kill gram-negative bacteria, for example through the degradation of outer membrane protein A (OmpA) in *Escherichia coli* resulting in loss of membrane integrity and bacterial degradation (51). Gram-positive *Streptococcus pneumoniae* are rather killed through the collective action of NE, CG and other proteases (52). Furthermore, NSPs can indirectly result in bacterial killing by other mechanisms, such as generating AMPs through cleavage of host proteins or degrading virulence factors (50).

Monocyte-derived macrophages and tissue-resident macrophages also partake in the onset of an acute inflammatory event but play a more crucial role in the subsequent resolution of inflammation, whereas neutrophils are merely responsible for the initial removal of pathogens (44). Consequently, macrophages

ultimately phagocytose apoptotic neutrophils after pathogen removal. Additionally, macrophages are long-lived cells that are involved in antigen presentation (14). Macrophages are largely influenced by external factors (e.g., cytokines) leading to changes in both their phenotype and function. Two main groups of macrophages are known, namely “classically activated” M1 macrophages which are known to secrete pro-inflammatory cytokines, including tumour necrosis factor α (TNF α) and interleukins (IL)-6, IL-1 β , IL-12, and IL-15. The polarisation to M1 macrophages occurs in response to different stimuli such as exposure to LPS, interferon- γ (IFN γ) and other factors. On the other hand, “alternatively activated” M2 macrophages secrete anti-inflammatory cytokines including transforming growth factor β (TGF β), IL-4, IL-10, and IL-13 and are stimulated by macrophage colony-stimulating factor (M-CSF) and other interleukins. While M1 macrophages play a pro-inflammatory role with anti-microbial and anti-tumoral activity, M2 macrophages exhibit an anti-inflammatory role and aid in tissue homeostasis, wound healing and fighting infections (53–55).

Besides phagocytic cells, antigen-presenting cells (APCs) compose an important share in maintaining innate immunity. Professional APCs consist of macrophages, DCs, and B cells. APCs first recognize their target through binding of PAMPS or DAMPs to PRRs and internalising their target by initiating phagocytosis, pinocytosis, or clathrin-mediated endocytosis. Depending on the PRR family, different pathways of endocytosis are initiated to degrade external PAMPS/DAMPs and display them on major histocompatibility complex (MHC) for further T cell recognition, as discussed in 1.1.2 (56,57). A further group of innate immune cells are natural killer (NK) cells that play a large role in antiviral immunity by destructing virus-infected cells through the release of perforins and granzymes which induce programmed cell death. NK cells are also known as large producers of IFN γ aiding subsequent T cell responses (14,58). APCs, especially dendritic cells, and the complement system represent the linkage between the innate and adaptive immune responses (35,56,59,60).

1.1.2 Adaptive Immune System

The adaptive immune response represents an antigen-specific and memory response, contrary to the non-clonal recognition pathways of cells pertaining to the innate immune system. Responses of the adaptive immune system are mediated by lymphocytes derived from hematopoietic stem cells and can be separated into two broad categories. Cell-mediated immune responses are carried out by T lymphocytes (T cells), whereas antibodies are produced by B lymphocytes (B cells) (43).

T Cells

T cells arise from the bone marrow and migrate to the thymus where somatic gene rearrangement takes place, leading to the expression of a unique antigen-binding molecule, the T cell receptor (TCR). The TCR recognises peptide antigens that have undergone proteolytic cleavage and are presented on a host

cells' MHC molecule. Nucleated cells are capable of expressing MHC class I (human leukocyte antigen HLA A, B, and C) molecules that lead to T cell responses. Further, professional antigen-presenting cells, including B cells, DCs and macrophages, constitutively express MHC class II (HLA DP, DQ and DR) molecules, allowing for an enhanced activation of T cells. MHC class I and II molecules can interact with different TCR co-receptors, such as CD8 and CD4, accordingly, and differ in presenting either endogenous or exogenous peptides, respectively (61). The TCR itself does not consist of any intracellular signalling domains, and instead associates non-covalently with signalling apparatus from co-receptors. This complex consists of CD3 $\epsilon\gamma$ and CD3 $\epsilon\delta$ heterodimers and a CD3 $\zeta\zeta$ homodimer, collectively forming the TCR-CD3 complex (62).

T cells can be separated into two primary types, cytotoxic T cells (CTLs) and T-helper (Th) cells. Upon antigen presentation via MHC molecules, stimulated T cells differentiate either into CD8⁺ CTLs or CD4⁺ Th cells. CD8⁺ CTLs are responsible for killing foreign agents and tumour cells expressing the appropriate antigens by two main mechanisms. The first involves the release of pore-forming perforin, that forms transmembrane channels in the target cell. Proteases, such as granzyme B, are contained in secretory vesicles together with perforin which are released by CTLs through exocytosis. Granzyme B cleaves and activates members of the caspase family of proteases, resulting in a cascade that ultimately arbitrates apoptosis. The second mechanism also involves the activation of the caspase cascade, however through Fas ligand on the cell surface of CTLs binding to Fas on the target cell. Binding results in the activation of the caspase cascade, similarly resulting in apoptosis (43).

On the other hand, CD4⁺ Th cells do not possess cytotoxic activity but are rather involved in maximising an immune response by directing other cell types to kill infected cells or pathogens. Upon activation, Th cells influence the activity of other cell types, including APCs, by releasing cytokines. Th cell responses can be classified into different subsets, depending on the effector mechanisms required for elimination of the presented pathogen. The major subsets include Th1, Th2, Th17, and regulatory T cells (Tregs). The first response to be discovered, Th1, is characterised by the release of IFN γ which leads mainly to the activation of macrophages and further enhances anti-viral immunity. Th2 responses are induced by IL-6 and IL-13 and are characterised by the release of cytokines IL-4, IL-5 and IL-13, playing a role in the development and recruitment of mast cells and eosinophils, an essential response for effective protection against parasites. Furthermore, Th2 responses are involved in B cell-mediated humoral responses, such as the development of immunoglobulin E (IgE)-secreting B cells and enhancing the production of IgG production. Th1 responses also contribute to B cell differentiation, as described below. As the name suggests, Th17 cells are characterised by the production of IL-17 and other IL-17 family members and are associated with chronic infection and disease. Lastly, Tregs control aberrant responses to self-antigens and thus limit and suppress immune responses, playing a large role in controlling the

development of autoimmune disorders. Both CTLs and helper T cells die upon resolution of infection and are cleared by phagocytes, with a few cells remaining as memory cells. Upon encounter with the same antigen, these memory cells can differentiate into effector cells and swiftly resolve infections (14,43,63–66).

B Cells

B cells are derived from the bone marrow where B cell development takes place and mediate antibody responses. The B cell receptor (BCR) undergoes somatic recombination, similar to the TCR, resulting in very high specificity, where each B cell represents a unique BCR. To reach this point, immunoglobulin (Ig) heavy and light chain encoding genes undergo DNA recombination. A detailed description of the structure and function of antibodies is provided in 1.1.3. During B cell development, V(D)J recombination occurs in the bone marrow. Starting at the pro-B cell stage, the Ig heavy chain gene is produced by joining of diversity gene segments (D) to joining gene segments (J_H), resulting in a late pro-B cell. Then, variable heavy chain segment (V_H) is rearranged to the joined DJ_H sequence. Successful heavy chain V gene rearrangement associates with an intact μ chain as a constant (C)-region sequence, and the cell can progress into a pre-B cell, stopping V_H to DJ_H rearrangement and starting to proliferate. In the case where both heavy-chain alleles are non-productive, pro-B cells are unable to receive the proliferation signal and are eliminated. The pre-B-cell receptor consists of the μ heavy chain, and two further proteins made in pro-B cells, $\lambda 5$ and V_{preB} , which pair to form a surrogate light chain. Together with the association of $Ig\alpha$ and $Ig\beta$, the pre-B-cell receptor complex is formed, allowing for signalling and structurally resembling a mature BCR complex. Light chain rearrangement occurs as with the heavy-chain locus. Synthesised light chains after successful rearrangement are combined with the heavy chain to form intact IgM molecules on the surface of B cells, together with $Ig\alpha$ and $Ig\beta$, forming the functional B-cell receptor complex. Throughout this process, recombination-activation genes 1 and 2 (RAG-1 and RAG-2) play a large role in gene rearrangement, forming a RAG-1:RAG-2 dimer that acts as a component of the V(D)J recombinase. Further, terminal deoxynucleotidyl transferase (TdT) adds N-nucleotides at the joints between rearranged gene segments, contributing to the diversity of both B-cell and T-cell receptor repertoires (67–70).

From the intact IgM molecule on the surface of mature B cells, a central tolerance process is initiated to eliminate B cells that have produced autoreactive cells reacting with the body's "self" proteins, leading to autoimmune diseases. Non-reactive cells are then released from the bone marrow into the periphery, where naïve B cells can become activated by contact with antigens. In contrast to T cells which only recognise short peptide sequences presented on MHC molecules, B cells can recognize three-dimensional large antigens (71,72). Somatic hypermutation occurs in the antigen-binding site of BCRs to increase their affinity by hypermutating along the V gene region of the Ig gene (73). This process is mediated by

activation-induced cytidine deaminase (AID) which induces cytosine to uracil deamination. To repair this process, error-prone polymerases are recruited, allowing any base to be incorporated. Here too, tolerance mechanisms result in positive selection for BCRs with the highest affinity and remove low affinity or autoreactive BCRs. Fully differentiated, antibody-secreting B cells are known as plasma cells, which together with memory B cells exist in the germinal centre of secondary lymphoid tissues (74,75). Lastly, high affinity antibodies undergo a class switch from low-affinity IgM or IgD antibodies to matured IgA, IgE and IgG isotypes (76).

Besides their role as antibody-secreting cells, B cells also play a large role as professional APCs for CD4⁺ Th cells through the expression of MHC class II molecules. Hereby, B cells recognise antigens through membrane-bound immunoglobulins and take them up via endocytosis. Through a lowered pH, the Ig is proteolytically cleaved, allowing for peptide generation to occur. Newly synthesized MHC class II molecules are then loaded with peptides and endocytosed to present them to T cells (77,78).

1.1.3 Structure and Function of Antibodies

Antibodies are heterodimeric glycoproteins exerting high affinity and specificity to bind foreign invaders and avoid inflammation. Antibodies can be split into five isotype classes, each employing specific functions and varying mainly in their heavy chain structure: IgA, IgD, IgE, IgG and IgM (Figure 1A). IgMs are the first isotype to be produced upon differentiation of naïve B cells into plasma cells, as described above. They exhibit a pentameric structure and result in avidity effects, compensating for their relatively low affinity and are mainly found in the blood (79,80). IgA is predominantly responsible for mucosal immunity by binding to Fc α RI (CD89) and thus contributes to the first line of defence (81,82). The IgA isotype exists as a monomer in serum, or as a dimer, containing two IgA with one J chain and a secretory component (83). IgD exists in two forms and represents a monomeric structure. Membrane-bound IgD is recognised as B-cell receptors (BCR), while its soluble form is implicated in mucosal innate immunity (84). IgE and IgG are isotypes found exclusively in mammals and both exist only as monomers (85). IgE plays a crucial role in mediating allergic reactions by binding to Fc receptors Fc ϵ RI and Fc ϵ RII (CD23) (86). IgGs are the most abundant class of antibodies, constituting up to 75% of Igs in human serum. From the IgG family, four subclasses exist, namely IgG1, IgG2, IgG3 and IgG4, with minor differences in structure and effector functions. Besides isotypes, IgG heavy chain polymorphisms, known as *allotypes*, add an additional layer of variation (87).

The IgG isotype consists of four polypeptide chains, two identical γ heavy chains (HC) and two identical κ or λ light chains (LC), resulting in a molecule of approximately 150 kilodaltons (kDa). The heavy and light chains are linked together by inter-chain disulphide bonds, while the individual domains of each chain are stabilized by intra-chain disulphides. Variable domains (Fv) are found at the N-terminus of

each chain and consist of VH and VL domains for the heavy and light chain, respectively, that make up the antigen-binding site (paratope). Together with the Fv and a constant domain, fragment antigen binding (Fab) regions are formed by pairing of VL and CL of the light chain with VH and CH1 of the heavy chain (Figure 1B).

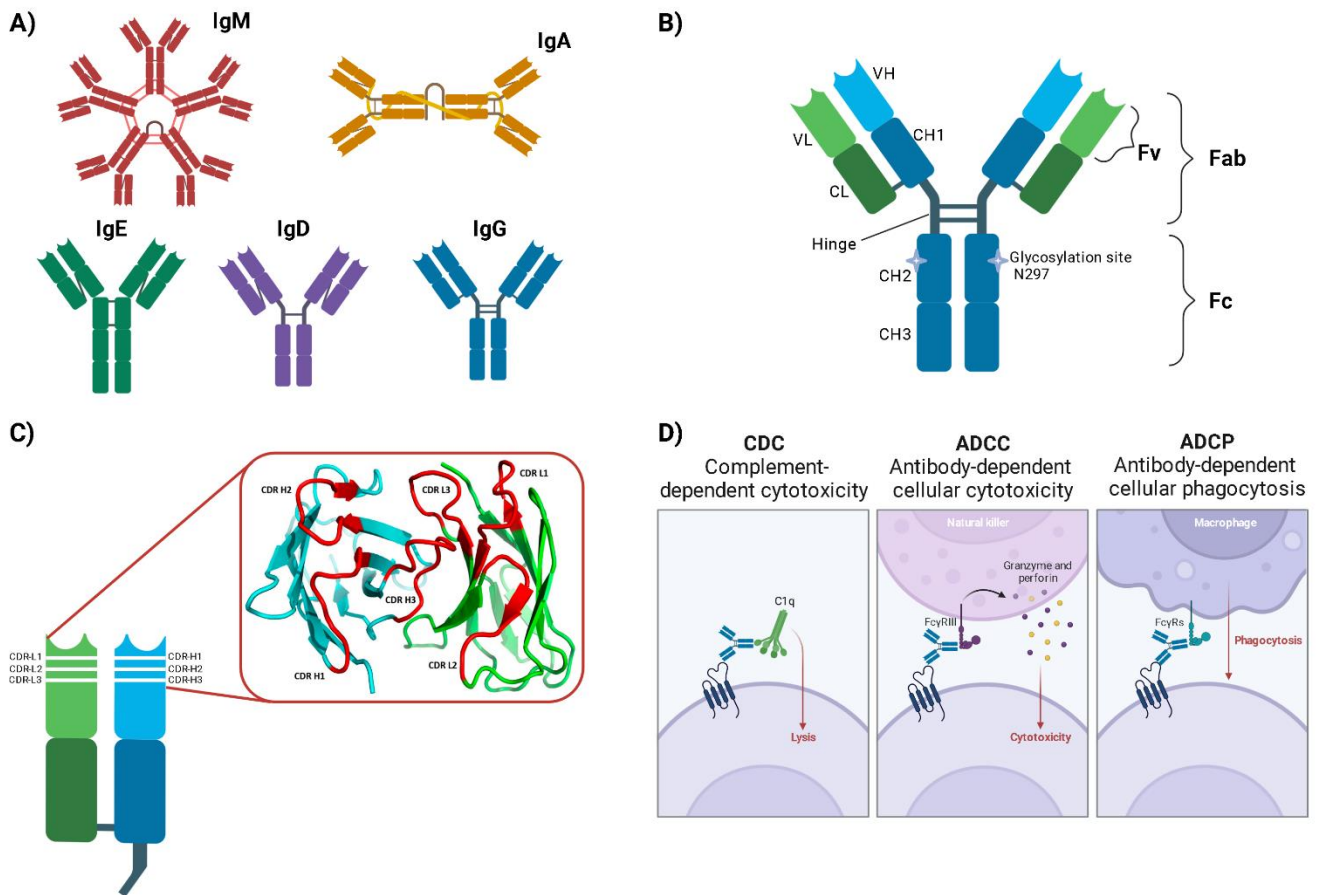


Figure 1: Antibody structure and function. A) Immunoglobulin (Ig) isotypes. B) Structure of IgG antibody. Variable regions are shown in light blue and green for VH and VL, respectively, making up the variable fragment (Fv). Constant domains are in dark blue and green for heavy and light chains, respectively. Stars represent the glycosylation site at N297 in the CH2 domain. C) Zoom-in of a Fab fragment with the complementary-determining regions (CDRs) highlighted in white for VH and VL. The crystal structure of the variable regions and their respective loops is taken from (90). D) Fc-mediated effector functions of IgG molecules. Binding of IgG molecule (blue) to a cell-bound receptor (purple) and simultaneous binding to different effector molecules mitigates CDC, ADCC or ADCP. Figure created in Biorender.com.

Each variable domain contains three hypervariable regions termed complementarity-determining regions (CDRs) that mediate antigen recognition. These six loops, CDR-L1, CDR-L2, CDR-L3 for VL and CDR-H1, CDR-H2, and CDR-H3 for VH, find themselves in close proximity to each other and steer the orientation of VL and VH after formation of the Fv (Figure 1C). The CDR-H3 is the most diverse loop as it is the focal point of V(D)J recombination and is often considered the most important CDR for antigen binding (88,89). Framework regions (Fr) are located between the CDRs of Fv domains and are numbered Fr1 to Fr4.

Heavy chains contain three constant domains: CH1, CH2, and CH3. The crystallisable fragment (Fc) that mediates effector functions consists of domains CH2 and CH3. Joining the CH1 and CH2-CH3 domains is a hinge region, which results in Fab arm flexibility and provides disulphide bonds to join two heavy chains together to form an antibody molecule (87). While light chains only consist of one constant domain (CL), two light chain isotypes are found in humans, κ or λ . The ratio of kappa/lambda antibodies detected strongly depends on the class of antibody heavy chain. Kappa/lambda ratios were reported to be 2.0 for IgG, 1.1 for IgA, and 1.7 for IgM, highlighting the isotype-dependent preferences in light chain isotypes (91,92). Compared to other isotypes, IgG molecules have a single glycosylation site at position N297 of the CH2 domain, except for IgG3 that exhibits an additional glycosylation site (93).

The function of antibodies rests not only in binding to a specific antigen through their Fv regions, but also through Fc-mediated effector functions by binding to Fc gamma receptors (Fc γ R) and the first subcomponent of the C1 complex (C1q) (94). These functions are known as antibody-dependent cellular cytotoxicity (ADCC), complement-dependent cytotoxicity (CDC), and antibody-dependent cellular phagocytosis (ADCP) (Figure 1D). ADCP is reviewed in more detail in 1.4.2. ADCC is mainly mediated by NK cells through binding of Fc γ RIIIa (CD16a) of antibody-opsonised target cells and induces cellular cytotoxicity by the release of perforins and granzymes. The potency of ADCC is influenced not only by the IgG subclass, but also by glycosylation patterns and IgG allotypes. The largest allotype-dependent variations have been reported for IgG3, whereas all IgG1, IgG2 and IgG4 allotypes were shown to behave similarly (95). CDC is triggered in a similar manner, by binding of antibody-coated target cells to C1q through essential residues in the CH2 domain (96). IgM molecules, for example, are exceptionally effective in activating the complement system due to their pentameric structure (97). Additionally, the CH2-CH3 interface of the Fc fragment interacts with the neonatal Fc receptor (FcRn) under acidified conditions and prolongs serum half-life. FcRn recycling avoids intracellular degradation of IgG molecules and extends the serum half-life of IgGs up to 21 days (98).

1.2 Therapeutic Antibodies for Immunotherapy

Harnessing the innate qualities of antibodies, including but not limited to, their high affinity and specificity, their Fc-mediated effector functions, and their ability to modulate biological responses, monoclonal antibody therapy has seen incredible growth as a therapeutic class. The birth of monoclonal antibody production began by the discovery of the hybridoma technology by Köhler and Milstein in 1975. The system consists of fusing mouse antibody-producing B cells isolated from immunised mice together with myeloma cells to generate immortal hybrid cells that produce antibodies in large quantities (99). While the hybridoma technology allowed the fast production of antigen-specific monoclonal antibodies, murine antibodies posed severe immunogenic effects including severe adverse effects such as

anaphylaxis and cytokine release syndrome (100,101). A total of 6 approved antibody therapeutics are murine IgG molecules (either mIgG2a or mIgG1), of which 4 have been withdrawn due to safety or commercial reasons, among them the first antibody to ever receive regulatory approval, anti-CD3 muromonab-CD3 (Orthoclone OKT3) (102). Patients administered with murine monoclonal antibodies showed human anti-murine antibody (HAMA) responses, stagnating the success of mAb therapy (103,104). Thus, the focus shifted towards the generation of less immunogenic molecules by developing chimeric antibodies. Chimeric antibodies combine the murine variable regions with human constant domains and result in better human Fc-mediated effector functions and lower immunogenicity, entailing approximately 60% human components (105,106). Ten chimeric antibodies have successfully been approved for therapy, including the renowned anti-CD20 antibody rituximab (Rituxan), cetuximab (Erbix) binding EGFR, and siltuximab (Sylvant) binding IL-6 (102).

The largest subset of approved and next-generation antibody therapeutics has taken a step further by performing humanisation after discovery of antibody candidates from different origins, representing 56 approved antibodies and a further 11 undergoing regulatory review (102). The most common type of humanisation is known as CDR-grafting, where the heavy and light chain CDRs of the variable domains are grafted onto a human framework, resulting in an antibody that is >90% human when considering the entire antibody molecule. Specificity-determining residue (SDR) grafting further minimises the murine content in the CDRs of CDR-grafted humanised antibodies (107). The first fully human antibody to be approved was the anti-TNF antibody adalimumab (Humira) in 2003 that was discovered through phage display screening (108,109). Adalimumab has achieved blockbuster status, surpassing the \$20 billion mark in sales in 2021 and often emerging in the top drug sales lists (110). The discovery and development of fully human antibodies has been facilitated by powerful technologies, among them phage display and transgenic animals which will be covered in 1.3.1.

Revolutionised by the number of approved drugs on the market, humanised and fully human antibodies make up a large part of approved biologics. Nevertheless, their homology to human proteins does not entirely rule out immunogenic responses. Anti-drug antibodies (ADAs) have been reported after treatment with adalimumab and another fully human anti-TNF mAb golimumab (Simponi), obstructing the drug's bioavailability, altering its pharmacokinetics and pharmacodynamics, and ultimately hampering its efficacy (111,112). Advances in computational power may help predict the immunogenicity of humanised and fully human therapeutics before they reach critical clinical development (113).

In the context of complex diseases, IgG molecules pose several limitations, such as poor tumour penetration due to their large size, and Fc-mediated bystander activation of the immune system, among

others (114). To avoid the latter, antibody engineering approaches have paved the way to abate binding of Fc domains to FcγRs, rendering them “effector silenced”. The first point mutation described was Leu235Glu, resulting in 100x decreased affinity to the FcγRs (115). This initial mutation was investigated further and the double mutant Leu234Ala and Leu235Ala (abbreviated as LALA) was born, reducing binding to FcγRI, FcγRII, and FcγRIIIa for both IgG1 and IgG4 isotypes, diminishing ADCC, ADCP and CDC effector functions (116,117). With the additional substitution of Pro329Gly (PG), the LALA-PG modification abolished binding to FcγRI, FcγRII, FcγRIIIa and C1q, obliterating Fc functions in mouse and human IgGs (118). As interaction of the Fc and FcγRs or C1q is additionally mediated through glycosylation at position Asn297, mutants thereof also resulted in diminished effector functions. These mutations include Asn297Ala (119), and Asn297Gln (120,121). The potential of such mutations to abolish or reduce bystander effects has been spotlighted through clinical development of monoclonal antibodies carrying LALA, LALA-PG or N297 mutations (122).

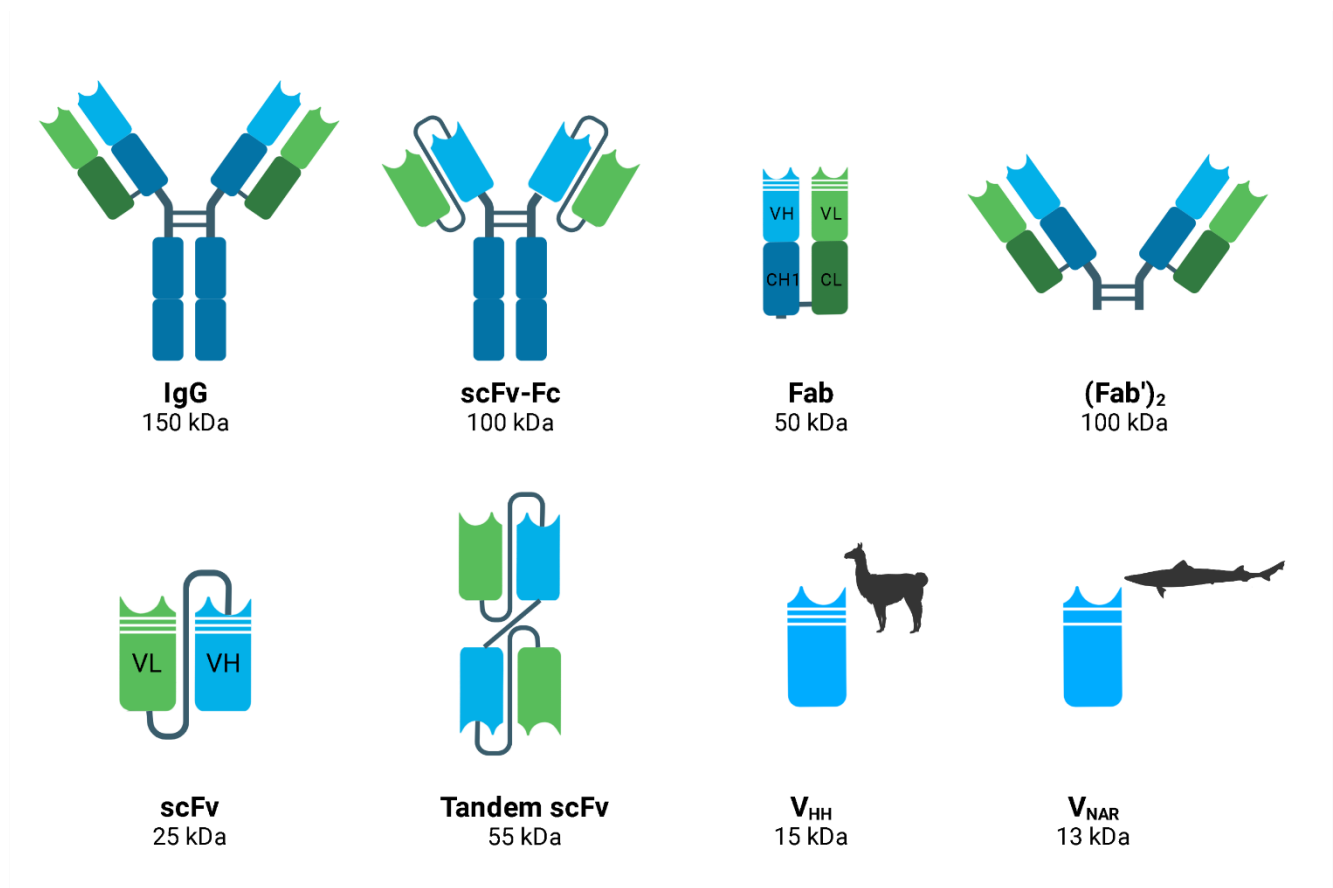


Figure 2: Structure of antibody fragments. The constant domains are depicted in dark blue and green, and the variable chains are coloured in light blue and light green for VH and VL, accordingly. The white lines represent the complementary-determining regions. Abbreviations: Immunoglobulin – Ig, single chain variable fragment – scFv, fragment crystallisable – Fc, antigen binding fragment – Fab. Figure created in Biorender.com.

To overcome the poor penetration of IgG molecules, antibody formats represent an interesting class of therapeutic entities. Antibody fragments include single chain variable fragments (scFvs, 25 kDa), scFv-

Fc (100 kDa), Fabs (50 kDa), nanobody domain antibodies (V_{HH}) (15 kDa), and V_{NAR} (13 kDa) (Figure 2). Fab fragments consist of the VH and VL domains and CL and CH1 constant domains of an IgG molecule, whereas scFvs are composed only of the variable domains connected by a flexible linker. Nanobodies and V_{NARs} originate from camelids and sharks, respectively, and represent single-domain antibodies (sdAbs). Fabs and scFvs contain a total of six CDRs, three from the heavy and three from the light chain, whereas V_{HH} fragments consist of three CDRs. V_{NAR} fragments only consist of two CDRs, equivalent to CDR-H1 and CDR-H3 (123).

Owing to their smaller size and lack of an Fc fragment, antibody fragments demonstrate improved tissue penetration and broader biodistribution, no effector functions and easier manufacturing. Four Fab fragments have made their way into the clinic, with abciximab (Reopro) marking the first antibody fragment to reach the market in 1994. The first scFv fragment to be approved was blinatumomab in 2014, a bispecific T-cell engager (BiTE) that is discussed in 1.4.1. Of the sdAb type, only one humanised nanobody has been approved targeting the von Willebrand factor in 2018. Bivalent or bispecific antibodies can also be generated, for example as F(ab')₂ or by joining two scFvs (termed tandem scFv) (Figure 2). Taken together, both IgG molecules and antibody fragments have shown great success as therapeutic entities and their characteristics can be fine-tuned depending on the disease indication and desired mechanism of action (124,125).

1.2.1 Immuno-oncology Applications

Cancer is one of the leading causes of death, attributing nearly 10 million deaths worldwide in 2020. The cancer types with the highest incidence rates are breast, lung and colorectum cancer, with lung and colorectum cancer accounting for the highest mortality rates (126). Independent of the cancer types, cancer originates from the abnormal and dysregulated proliferation of malignant cells causing the uncontrolled growth to invade healthy tissues and organs, leading to metastatic tumours. New dimensions in the proposed hallmarks of cancer have been described in 2022 to summarize the complexity of different tumour types and find common ground between all types of cancer cells (127). While conventional therapeutic strategies such as chemotherapy or radiation therapy have shown success in shrinking or eradicating tumours in the past, targeted therapy is becoming of utmost importance due to milder adverse effects, high efficacy and reduced off-target toxicities. Close to half of all approved monoclonal antibodies are for the treatment of oncology indications (128), with the authorisation of rituximab for the treatment of non-Hodgkin's lymphoma in 1997 marking the first clinically relevant anti-cancer agent. Since then, a number of mAbs have been approved to treat many cancer types, especially for the treatment of breast cancer (129,130), and lung cancer (131,132). The success in the area of oncology is exemplified with Roche's anti-human epidermal growth factor receptor 2 (HER2) antibody trastuzumab (Herceptin) with sales of more than \$5 billion in 2018 (133).

The tumour microenvironment (TME) is composed of a heterogeneous nexus of cancer cells with infiltrating and resident host cells, extracellular matrix and secreted cytokines and chemokines. Immune cells within the TME can promote either an anti-tumour or an immune suppressive environment, depending on the tumour types and form of inflammation that is persistent (134,135). Solid tumours are particularly infiltrated by leukocytes harbouring an immunosuppressive environment, hampering the efficacy of novel therapies (136). In order to efficiently target tumour cells, the tumour microenvironment must also be modified and targeted (137). Tumour types can be further separated into two categories, namely “hot” or “cold” tumours. “Hot” tumours are characterised by the accumulation of pro-inflammatory cytokines and higher infiltration of T cells, whereas “cold” tumours largely lack T cell infiltration. The breakthrough of immune checkpoint inhibitors (ICIs), such as anti-PD-1/PD-L1 (pembrolizumab, nivolumab, avelumab, durvalumab, atezolizumab) or anti-CTLA-4 antibodies (ipilimumab) have shown great promise in anti-cancer therapy. Nonetheless, there is accumulating evidence that only a fraction of patients benefits from ICIs, with the response rates largely being related to tumour-infiltrating lymphocytes (138). Accordingly, “hot” tumours are associated with better ICI efficacy compared to “cold” tumours, posing a challenge for immunotherapy. The focus for novel therapeutic approaches is spotlighted onto turning “cold” tumours into “hot” tumours by improving T-cell infiltration into the TME (139–141).

While the success of mAb therapy is obviated by the number of approved mAbs and the number of candidates in pre-(clinical) phases, their efficacy is sometimes hindered. Among other reasons, the complexity of tumours and their microenvironment further employ strategies to overcome the immune response, the so-called immune escape mechanisms. These mechanisms may include the loss of MHC class I molecules on APCs resulting in a loss of antigenicity and preventing appropriate presentation to T cells, or through the conversion of malignant cells and their environment to an immunosuppressive TME by upregulation of PD-L1 or immunosuppressive cytokines, including IL-10 and TGF β (142). While ICIs have dramatically increased patient’s response rates and survival, novel strategies are required to tackle the TME that poses several obstacles in efficacy in solid and “cold” tumours. Accordingly, bispecific antibodies (bsAbs) binding multiple targets have been set in the spotlight in recent years. Bispecific antibodies have two main mechanisms of action: cell-bridging or non-cell-bridging. Cell-bridging bispecifics will be reviewed in detail in 1.4, but they are able to link immune cells to malignant cells, improving specificity and effectiveness. Non-cell-bridging bispecific antibodies bind two antigens simultaneously and block signals of cell survival and cell growth, enhancing inhibitory or stimulatory effects in malignant cells or immune cells, respectively (143). By combining multiple modes of action and activating immune cells, their therapeutic effect and benefit is greater than monoclonal antibodies. To date, there are 7 approved bispecific antibodies, with more than 180 in pre-clinical development and 50 undergoing clinical investigation. From the approved bsAbs, four target CD3 on T cells with an

additional tumour-associated antigen (TAA) that will be reviewed in 1.4.1. The remaining three bispecific antibodies are non-cell-bridging bsAbs, targeting two receptors to cross-link antigens or combined antagonism of pathways resulting in cell death (144).

1.2.2 Severe Adverse Effects – Cytokine Release

Besides lack of efficacy, many biologics are hampered by severe toxicity in early clinical stages. While the development of humanised and fully human antibodies has drastically improved their *in vivo* tolerability, adverse effects may still occur (145). A severe adverse effect observed after first doses of mAbs is cytokine storm or cytokine release syndrome (CRS). Back in the 1980s, the term was coined after infusion with Muromonab-CD3, due to infusion-related reactions that were observed. CRS is a life-threatening systemic inflammatory syndrome, where elevated levels of cytokines through hyperactivation of immune cells occurs. CRS can be triggered through therapies, pathogens, cancer, and autoimmune reactions, among others, and is one of the most frequent grave adverse effects after T-cell-engaging immunotherapies *via* CD3 binding (146–148). Nonetheless, the onset of CRS is not only characteristic to CD3-binding mAbs but has also been reported after treatment with anti-CD52 alemtuzumab (149), anti-CD20 rituximab (150) and tositumomab (145), anti-CD40 CP-870893 (151), anti-CD2 BTI-322 (152) and anti-CD28 TGN1412 (153) antibodies (154). TGN1412, in particular, displayed a tremendous public outcry for regulatory agencies to standardise *in vitro* and *in vivo* studies prior to first-in-human studies (155).

While the pathophysiology of CRS is not entirely understood, it can be induced by two main mechanisms: direct target cell lysis or activation of T cells through therapeutics. Focusing on T cell-engaging therapeutic-induced CRS, IFN γ is released upon activation of T cells which induces the activation of other immune cells, principally macrophages and DCs. The subsequent activation of macrophages results in excessive amounts of IL-6, TNF α and IL-10 (Figure 3). Excessive amounts of IFN γ and TNF α elicit flu-like symptoms including fever, chills, dizziness, fatigue and diarrhoea (146). IL-6 seems to play a particularly important role in the CRS pathophysiology, as its trans-signalling pathway leads to characteristic symptoms of CRS such as vascular leakage (156), and elevated serum IL-6 levels have been consistently observed in patients with CRS (157–159).

Grade 1 and 2 CRS results in mild reactions including fever and hypotension, where intravenous fluids or low-dose vasopressors are required. Grade 3 CRS results in hospitalisation with the need for high-dose vasopressors, and signs of organ dysfunction appear to instigate. Life-threatening complications are observed with grade 4 CRS where mechanical ventilation support is required, grade 4 organ toxicities are observed and severe hypotension requiring a combination of high-dose vasopressors is exhibited (160). The onset of grade 4 CRS is triggered by the feedback loop between activated T cells and

macrophages, resulting in extremely high serum IL-6 levels of 600-1000 pg/ml compared to normal levels of 7-30 pg/ml (161,162). Due to IL-6's key role in the pathophysiology of CRS, grade 3 and 4 CRS symptoms are managed by treating patients with tocilizumab (Actemra), an anti-IL-6R antibody that blocks receptor activation via both cis- and trans-activation pathways. While tocilizumab was initially approved for treatment of rheumatoid arthritis by the FDA in 2010, it has recently received emergency use authorisation for the management of CRS (163–165).

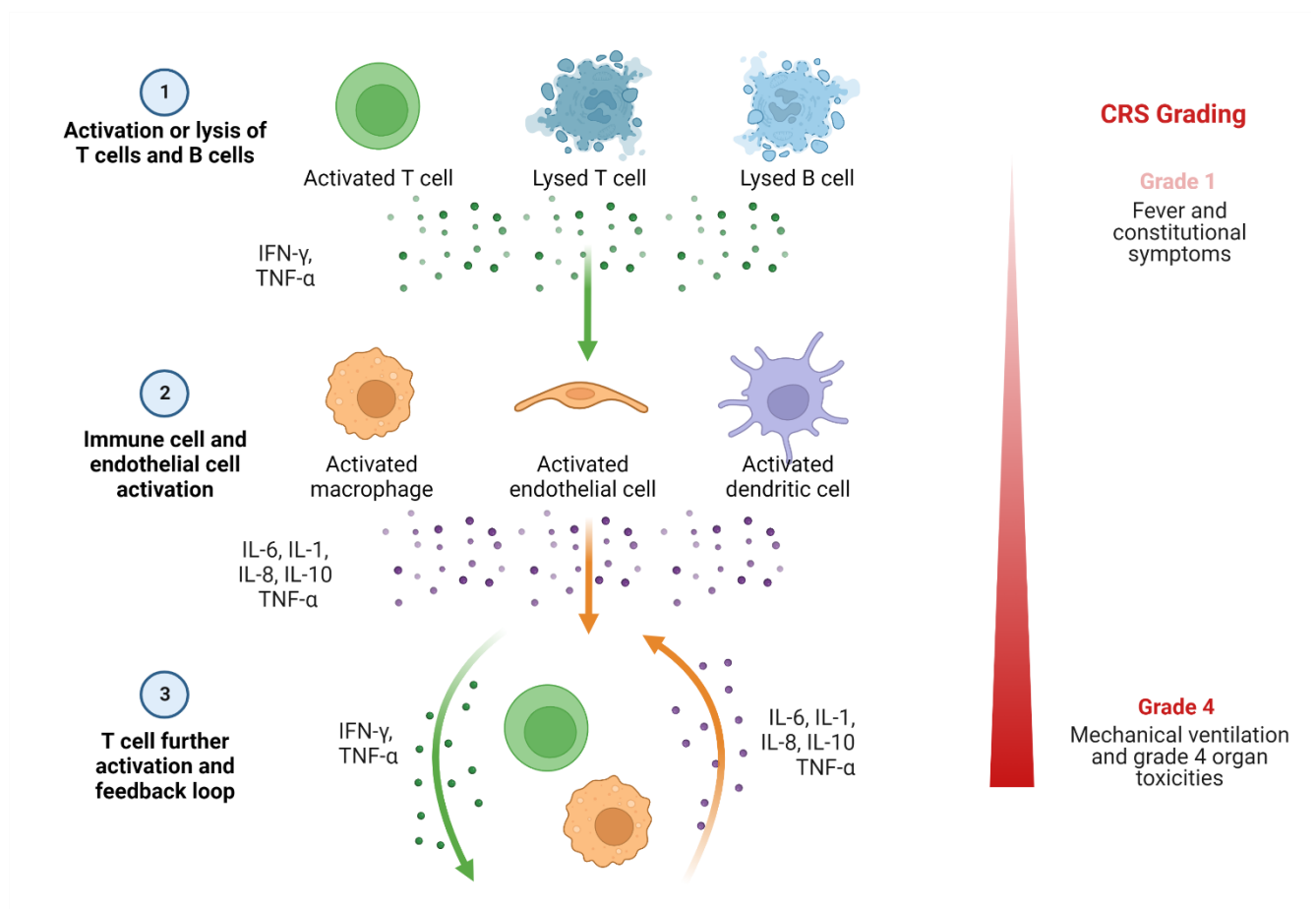


Figure 3: Pathophysiology of cytokine release syndrome. The onset of cytokine release syndrome is depicted, initiating with the activation or lysis of T cells and B cells. Their release of IFN γ and TNF α results in the activation of macrophages, endothelial and dendritic cells. Following the release of inflammatory cytokines from activated immune cells, the further activation of T cells is triggered, and a feedback loop is initiated, resulting in hyperactivation. The third step represents grade 4 CRS where mechanical ventilation and grade 4 organ toxicities are observed. Figure created in Biorender.com and adapted from (146).

Furthermore, in light of the unprecedented COVID-19 pandemic where life-threatening infections resulting in CRS were observed, sarilumab, another therapeutic anti-IL-6R antibody has been investigated in the management of CRS in critically ill patients (166–170). While risk- and grade-management of CRS appears to alleviate patients from life-threatening indications, improvements are required for novel T cell-engaging therapies to widen their therapeutic index and boost their efficacies (171).

1.3 Discovery & Generation of Therapeutic Antibodies

Biotherapeutics are not only relevant in immuno-oncology applications, but also for a plethora of important disease areas such as metabolic diseases (172), neuro-degenerative diseases (173,174), regenerative therapy (175–177), infectious diseases including Ebola (178) or COVID-19 (179,180), and many others (128,181). Advances in protein engineering and platform technologies have facilitated the rapid discovery of novel potential therapeutics. In order to generate novel biotherapeutics, several aspects must be taken into consideration. The discovery and development of antibodies will be discussed in the sections 1.3.1 and 1.3.2, respectively.

1.3.1 Discovery of binders

The discovery of novel therapeutic entities begins with an antibody repertoire from which antigen-specific monoclonal antibodies can be selected. Different sources of antibody libraries exist, with the most common ones being synthetic, naïve or immune libraries. Synthetic antibody repertoires are created by designed synthetic DNA, giving scientists free choice of the framework. Thus, higher stability and low immunogenic variants can be generated by designing optimised human frameworks and diversity can be restricted to four of the six CDRs to generate antigen-binding sites with high specificity (182,183). On the other hand, natural naïve libraries originate from B cells from individuals or donors that were not altered by immunisation. Such libraries are known as “universal libraries” that can be screened against an array of antigens, as the individual/donor did not react to a specific antigen. Limited by the size of the human naïve antibody repertoire, combinatorial libraries of multiple donors can generate large libraries. While naïve libraries can be screened for virtually any antigen of interest and are of human origin, the antibodies exhibit lower affinity compared to other sources due to lacking *in vivo* affinity maturation. Nonetheless, a number of approved antibodies have been selected from natural naïve library sources, such as raxibacumab, necitumumab, and belimumab (184–187). Semisynthetic libraries combine synthetic and naïve libraries by mainly introducing random sequences in the CDR-H3 to increase the affinity of human antibodies (188,189).

Immune libraries originate from cells of immunised animals. A particular antigen of interest is injected in the immunisation host, where genetic rearrangement of antibody germ line genes and somatic hypermutation occurs upon exposure to a foreign antigen. Due to *in vivo* affinity maturation and V gene hypermutation, antibodies from immune libraries generally exhibit higher affinities compared to other sources, however they are antigen-specific libraries against the immunised antigen. The first immunisation hosts described were mice, rats, and rabbits (187,190,191). More recently, chicken immunisation has shown great promise due to the large phylogenetic distance between birds and mammals, resulting in antibody repertoires addressing epitopes that are conserved in rodents. A handful of early-stage chicken-derived antibodies have been described in literature, highlighting their potential

as therapeutic entities (192–199). Independent of the immunisation host, humanisation of antibody candidates is required to avoid immunogenic responses. Advances in antibody engineering have facilitated the humanisation of rodent (200–203), rabbit (191,204), and chicken antibodies (205,206). To circumvent this cumbersome process, transgenic animals have eased the generation of fully human antibodies by integrating human immunoglobulin gene loci in animal strains that can undergo normal processes of rearrangement and hypermutation, resulting in high diversity and specificity (207–209). Transgenic mice were the first of their kind, thereafter followed by rats, chickens and recently cows, as embodied by the OmniAb platform of Ligand Pharmaceuticals (210).

Besides the hybridoma technology, *in vitro* selection technologies have paved the way for the rapid discovery of novel therapeutic biologics. These include phage display (211,212), ribosome display (213), yeast surface display (214), mRNA display (215), and mammalian display (216,217). Phage display represented the first *in vitro* technology to offer fully human antibodies, by containing human VH and VL repertoires (218,219). As not all organisms are capable of efficiently producing full-length glycosylated IgG molecules, display technologies are generally performed with antibody fragments in the form of scFv or Fabs, exhibiting robust display and expression in different systems (220,221). Mammalian display has the particular advantage of screening directly in the final IgG format, not requiring further reformatting of antibodies after screening (216,222,223). Additionally, losses of affinity have been reported after conversion of antibody fragments, particularly scFvs, into the IgG format, requiring subsequent affinity maturation (224). Very recent advances in phage display systems have allowed the construction of full-length IgG antibodies on M13 phages for phage display screening, however the production of IgGs in *Escherichia coli* is limited to aglycosylated mAbs (225).

After screening in antibody formats, antibody hits must be reformatted into the desired IgG subclass, depending on the desired biological activity (226). Reformatting can become a cumbersome approach as the number of antibody hits becomes larger. To this effect, platform technologies have seen advancements in bulk reformatting of entire libraries to their desired final format, e.g., IgG1. In the case of phage-displayed libraries, several approaches have been reported for batch reformatting (227–229). However, no such reports were noted for YSD-derived antibody fragment libraries, still requiring single candidate reformatting in order to avoid losing heavy and light chain pairing.

1.3.2 Development of therapeutic antibodies

Once potential antibody candidates have been selected, reformatted into the desired final format and thoroughly characterised exhibiting the desired affinity, pharmacodynamics and pharmacokinetics (PD/PK) both *in vitro* and *in vivo*, the development of the best antibody candidate may begin. While binding to the target of interest is crucial, therapeutic antibodies must also be free from other attributes,

such as aggregates, heterogeneity or unstable product, known as critical quality attributes (CQA). As the development of a therapeutic mAb carries great time and economic burdens, a developability assessment is required before entering process development to ensure the selected candidate exhibits exceptional biophysical and biochemical behaviour to lower the risk of development. By *in silico* methods, atypical behaviour of mAbs may be evaluated and/or predicted from antibody sequence or molecular dynamics simulations in a more effective and rapid process, based on learnings from previous mAbs that have undergone development. Parameters for *in silico* assessment may include hydrophobicity, net charge, so-called “hot spots” within CDR regions, or post-translational modification sites (230–232). These parameters can lead to suboptimal behaviour, such as high aggregation resulting in immunogenicity and impacting their biological activity (233,234), or high viscosity presenting challenges in formulation development and subcutaneous drug delivery (235). While *in silico* methods provide a good selection criterion for antibody candidates, thorough characterisation by *in vitro* methods including forced degradation studies is still required or may be combined (236).

Antibody variants produced during process development must be kept to a minimum, as they can impair an antibody’s activity, efficacy, safety and PK/PD properties. The introduction of heterogeneous species begins with antibody production in mammalian cells, such as Chinese hamster ovary (CHO) cells. A number of possible modifications exist, increasing the heterogeneity of the drug product. For example, N-terminal modifications (e.g., introduction of pyroglutamate) may occur, altering the mass and charge of antibody molecules, that must then be separated by cation exchange (237). In the case of bispecific antibodies, process development becomes more difficult as the correct heavy chain and light assembly must be ensured to avoid mispairing or heterogeneous molecules. In the case of the Knob-into-Hole technology, extensive chromatography can remove unwanted by-products or impurities (238,239).

When a homogenous product is up to regulatory standards after quality assessments, formulability of antibody molecules must be assessed. Due to their macromolecular structure offering high specificity and efficacy, its complexity poses challenges in formulation and drug delivery. Antibody formulations must fulfil the requirements for the desired route of administration. Intravenous (IV) applications were the most common route of administration for mAbs, now substituted with subcutaneous (SC) delivery for chronic diseases (240,241). Due to platform technologies, advances in process development and *in silico* technologies, the development of mAbs has seen great advances lowering risk and cost for pharmaceutical companies.

1.4 Immune-Cell Engagers

Owing to the heterogeneity of tumours and their microenvironment, ICIs and monotherapy still have exposed limitations. To improve these shortcomings, immune cell engagers (ICEs) have been discovered, generally consisting of bispecific antibodies targeting both immune effector cells and TAAs. By re-directing immune cells and forming immune synapses between effector and tumour cells, MHC-independent tumour cell killing, and successive elimination is ensured, overcoming possible immune escape mechanisms (242). Depending on the type of immune effector cell to be engaged, ICEs can be split into three sub-types: T-cell engagers (TCEs), NK-cell engagers (NKCEs), and phagocytic cell engagers (Figure 4) (243). T-cell engagers will be reviewed in 1.3.1, and macrophage-engagers in 1.3.2.

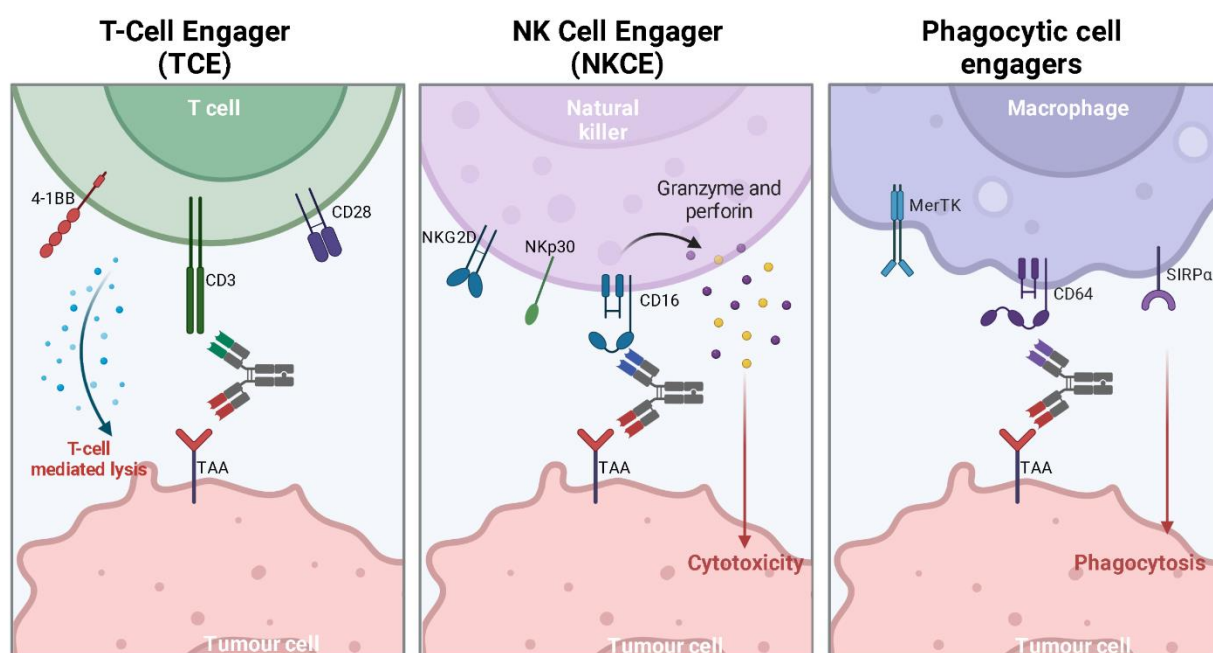


Figure 4: Immune cell engagers. Three types of immune cell engagers are depicted: T-cell engagers (TCE), NK cell engagers (NKCE) and phagocytic cell engagers, from left to right. Generic bispecific antibodies are depicted with the red Fab arm binding to a tumour-associated antigen (TAA) on tumour cells, and the other arm binding immune cell-specific markers. Some immune cell-specific markers are depicted, such as CD3, CD28 and 4-1BB for TCEs, CD16, NKG2D and NKp30 for NKCEs, and CD64, SIRP α and MerTK for macrophage-engagers. Figure created in Biorender.

1.4.1 T-Cell Engagers

The most common category of TCEs is bispecific T-cell engagers (BiTEs) as introduced by Micromet in 2008, where T cells are redirected to tumour cells to employ T-cell mediated cytotoxicity. BiTEs consist of two tandem single-chain variable fragments, one binding a TAA and the other a part of the TCR complex (244–247). Usually, a specific chain of the CD3 complex associated to the TCR complex is targeted and participates in TCR-mediated signalling, resulting in the simultaneous redirection and activation of T cells to the tumour cells. Tumour cell lysis is mediated by the secretion of perforin and granzymes stored in secretory vesicles of cytotoxic T cells (248,249).

The first-in-class BiTE molecule to be approved by the FDA was blinatumomab (Blincyto) in 2014 for treatment of B-cell malignancies, targeting CD19 on B cells and CD3 on T cells (250–252). With a different architecture, catumaxomab (Removab) gained approval by EMA several years before, binding epithelial cell adhesion molecule (EpCAM) and CD3 with a functionalised Fc region to mediate effector functions, resulting in a trifunctional antibody (253,254). Regulatory approval of both molecules validated the breakthrough of bispecific T-cell engagers, however they both come with limitations. Treatment with blinatumomab was reported to be associated with a high risk of CRS due to T cell over-activation, narrowing its therapeutic window and additionally requiring frequent infusion due to its short half-life as it lacks an Fc fragment (146,255–258). Similarly, catumaxomab exhibited very high affinity for CD3 and led to CRS events, and it was later withdrawn due to commercial reasons (259).

As is the case for existing TCEs, the development of novel T-cell-redirecting molecules is often hampered by high toxicities in early stages of preclinical or clinical development. To this end, next generation TCEs have laid the focus on CD3 affinity to improve the therapeutic index of TCEs by lowering the affinity to CD3. These next generation TCEs have resulted in less critical cytokine release profiles as T cells were not over-stimulated (260–264). Moreover, trispecific T-cell engagers (TriTEs) have been recently described and their efficacy has been validated *in vivo*. One strategy described a CD3-specific scFv flanked by two different tumour-targeting V_{HH} antibody fragments targeting EGFR and EpCAM for the treatment of colorectal cancer (265). Another elegant approach using a cross-over dual variable (CODV) bispecific antibody format was described by Sanofi by targeting not only CD3 and a TAA, but also CD3's co-stimulatory receptor CD28 in order to enhance T cell activation and the efficacy of T-cell redirecting antibodies (SAR442257, NCT04401020) (266). Treatment with this trispecific T-cell engager in humanised mouse models resulted in suppressed tumour growth and stimulation of effector T cell proliferation. Moreover, a novel T-cell engager format was developed by Harpoon Therapeutics using their Trispecific T-cell Activating Construct (TriTACs) platform. They comprise two sdAbs and a CD3-specific scFv. Due to their small size, TriTACs aim to achieve superior efficacy through penetrating the TME of solid tumours, and a half-life extender has been built-in by incorporating an albumin-binding V_{HH} (267). The second nanobody can be exchanged to target different tumour types. Three clinical candidates are being evaluated for different indications: HPN328 targeting DLL3 for small cell lung cancer (NCT04471727) (268), HPN217 binding BCMA for multiple myeloma (NCT04184050) (269), and HPN536 targeting MSLN for ovarian cancer (NCT03872206) (270).

As of date, there are a significant number of CD3-targeting bispecific antibodies in early-phase development, including TNB-383B (NCT03933735) and REGN5458 (NCT03761108, NCT05167054) both targeting BCMAxCD3, and talquetamab targeting GPRC5DxCD3 (NCT0464552) all for relapsed or refractory multiple myeloma. Three further candidates are in phase II development: odronextamab

targeting CD20xCD3 (NCT03888105), flotetuzumab targeting CD123xCD3 (NCT04582864, DART format), and tarlatamab binding DLLxCD3 (NCT05060016). Phase III clinical candidates include glofitamab (NCT04408638) and epcoritamab (NCT04628494, DuoBody) targeting CD20xCD3 for diffuse large B cell lymphoma. A further BCMAxCD3 bispecific for treatment of multiple myeloma, elranatamab, is also in late-stage clinical development (NCT05317416). Surprisingly, the previously withdrawn catumaxomab binding EpCAMxCD3 is being evaluated in phase III clinical trials for advanced gastric cancer with peritoneal metastasis (NCT04222114) and in early-stage clinical investigation for non-muscle invasive bladder cancer (NCT04799847) (144).

In 2022, three bispecific T-cell-engaging immunotherapies have been approved by the European Medicines Agency (EMA), two of which have also received approval by the FDA. At the beginning of the year, tebentafusp-tebn (Kimmtrak) targeting gp100xCD3 was approved for treatment of patients with unresectable or metastatic uveal melanoma. By June 2022, mosunetuzumab (Lunsumio) binding CD20xCD3 was approved by EMA for relapsed or refractory follicular lymphoma. Teclistamab (Tecvayli), a first-in-class bispecific antibody for the treatment of patients with multiple myeloma, has been granted conditional marketing authorisation by EMA in August 2022. Teclistamab binds and redirects CD3-positive T cells to B-cell maturation antigen (BCMA)-expressing myeloma cells to induce T-cell-mediated killing of tumour cells (271,272). Together, bi- and trispecific T-cell engagers represent a promising platform for cancer immunotherapy for a plethora of tumour types and highlights the unmet need and interest in pursuing T cell-activating immunotherapies with widened therapeutic windows.

1.4.2 Macrophage Engagers

One of the prominent strategies to target macrophages and exploit their phagocytic capabilities to engulf tumour cells is antibody-dependent cellular phagocytosis (ADCP) (273). ADCP is a well-known mechanism of action of several therapeutic antibodies, such as rituximab (274) and trastuzumab (275). All subclasses of IgGs can elicit such responses due to binding to different Fc gamma receptors expressed on macrophages. Triggering of phagocytosis is mediated after binding of the Fab domain of the antibody to target cells and clustering to generate avidity, where signalling is activated on macrophages (276). As the FcγRs contain immunoreceptor tyrosine-based activation motifs (ITAMs), these motifs become phosphorylated upon binding and a downstream signalling pathway is activated. Among others, the MAPK and PI3K/AKT pathways are activated, leading to actin remodelling, engulfment and phagocytosis of the tumour cell (277,278).

Even though a number of therapeutic antibodies have a functional Fc domain capable of ADCP and other effector functions, this effect relies on clustering of antibody molecules on tumour cells in order to elicit a good response. To improve this, bispecific macrophage-engagers (BiMEs) have been developed,

targeting different TAAs and an additional macrophage-specific receptor. Phagocytosis checkpoint inhibitors, such as CD47, have shown great promise, as blocking the CD47/SIRP α axis by CD47 blockage induces phagocytosis (279–281). By combining CD47 blockers with tumour-specific binding moieties, targeted phagocytosis can be induced and additionally improves binding specificity, as CD47 is ubiquitously expressed throughout the body. Similar to CD3 affinity for TCEs, BiMEs also benefit from lower affinity to CD47 compared to the TAA-arm (282). A variety of antibody formats co-targeting the CD47/SIRP α axis are currently being evaluated in clinical trials, including AK117 (anti-CD47; NCT04980885, NCT04728334, NCT05235542), HX009 (anti-CD47/anti-PD-L1 bispecific; NCT05189093, NCT04886271), IBI188 (anti-CD47; NCT03763149), IBI322 (anti-CD47/anti-PD-L1 bispecific, NCT04338659), STI-6643 (anti-CD47; NCT04900519), Hu5F9-G4 (anti-CD47; NCT02216409, NCT02678338), IMM2902 (anti-Her2/SIRP α antibody-receptor trap; NCT05076591), ALX148 (anti-CD47; NCT05025800). This non-exhaustive list highlights the potential of targeting macrophages to use their innate function to specifically eradicate tumorous cells (283).

Besides indications within the oncology field, macrophage-engagers have been described for autoimmune disorders including rheumatoid arthritis. The receptor tyrosine kinase belonging to Tyro3, Axl, Mer (TAM) receptor family, MerTK, is expressed on macrophages and has been shown to play a crucial role in the clearance of apoptotic cells to prevent inflammation and autoimmunity. Further, it promotes anti-inflammatory functions by suppressing TLR-mediated cytokine production and inhibiting NF- κ B signalling. Thus, MerTK-mediated phagocytosis may be an interesting approach to avoid the pro-inflammatory cytokine release that occurs through the engagement of IgG molecules with activating Fc γ Rs (ADCP). By activating the MerTK-specific signalling pathway, phagocytic clearance may be achieved in an immunologically silent manner. As shown by Kedage *et al.*, combining a MerTK agonist with anti-CD20 or anti-A β to generate MerTKxCD30 or MerTKxA β bispecifics resulted in targeted phagocytosis of live cells or protein aggregates, respectively (284). In summary, macrophages or tumour-associated macrophages (TAMs) play key roles in the regulation of the TME and thus specific targeting of macrophages may also contribute to eradicate tumours. Targeted phagocytosis approaches still require further clinical investigation due to the widespread expression of targets such as CD47.

1.4.3 Multispecific antibodies

Due to the ever-evolving understanding of the immensely complex pathogenesis of cancer, monospecific therapies only targeting single signalling pathways often result in moderate efficacy. Besides bispecific antibodies targeting two distinct antigens, multispecific antibodies are gaining momentum to address unmet therapeutic needs (285,286). Such molecules can take on different architectures, mainly split into two categories: IgG-like antibody formats carrying an Fc domain, and non-IgG-like antibody formats lacking an Fc domain. IgG-like formats possess binding to the neonatal Fc receptor FcRn and result in

better pharmacokinetic properties and may exert additional effector functions (ADCP, ADCC, CDC). On the other hand, non-IgG-like formats are generally smaller in size and permit greater penetration to tumour sites, which can result in enhanced efficacy. They also exhibit a relatively short half-life compared to IgG-like formats as they are cleared faster (287). A handful of next generation multispecific antibodies are highlighted in Figure 5.

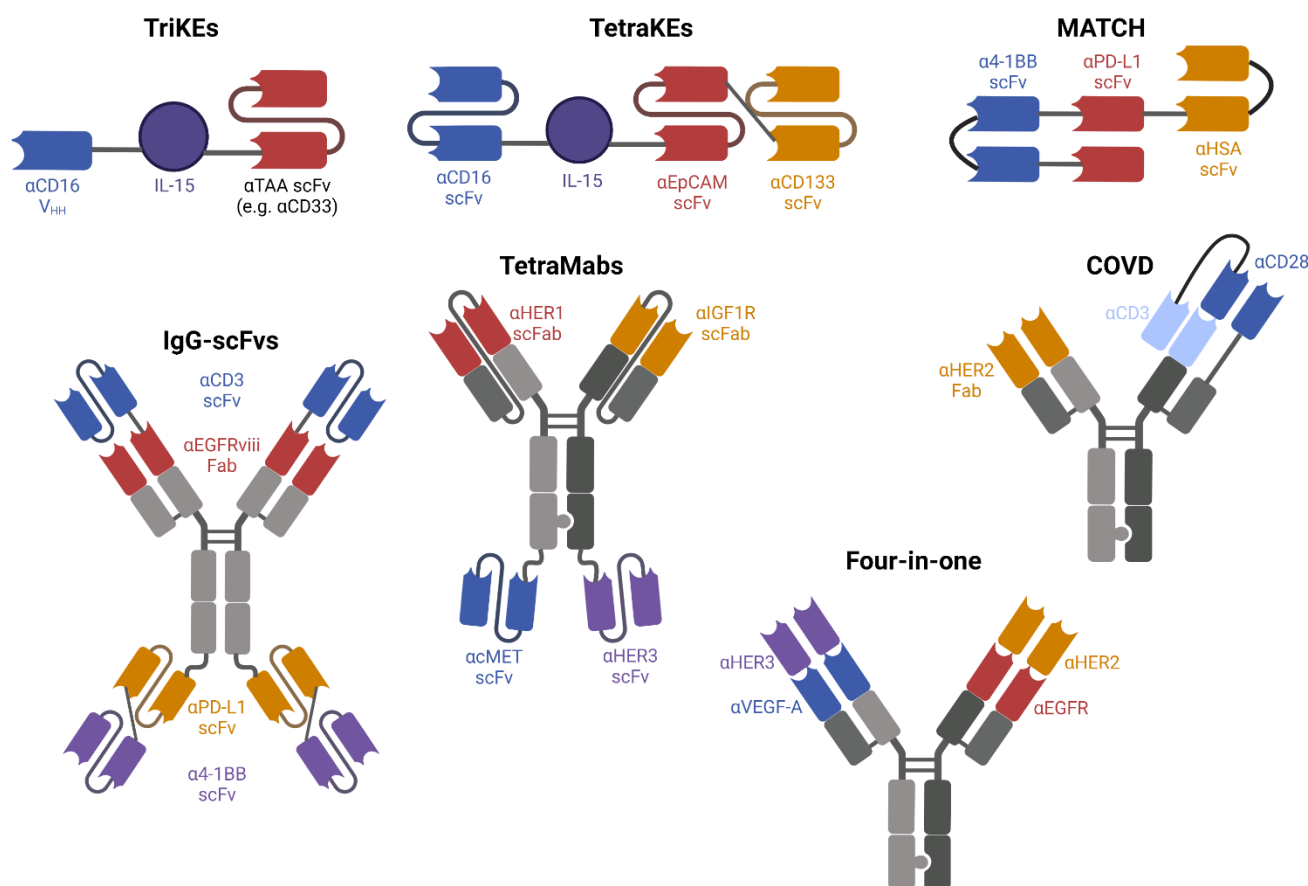


Figure 5: Multispecific antibodies in development. The Fc domain and constant regions of both heavy and light chains are depicted in grey. Heterodimeric chains with Knob-into-Hole technology are displayed with different shading of grey and a representative “knob-into-hole” schematic. Where relevant, the region binding effector cells is depicted in blue. Abbreviations: VHH – single variable domain on a heavy chain/nanobody; scFv – single chain variable fragment; scFab – single chain Fab fragment. Figure created in Biorender.com.

Facilitated by advances in antibody engineering over the years, complex molecules can be generated to combine several mechanisms of action. Besides the trispecific T-cell engagers described in 1.4.2, trispecific NK-cell engagers (TriKEs) have also emerged as potent immune cell engagers, redirecting NK cells to the tumour site and mediating elevated NK cell activity and potent ADCC (288). A few TriKEs are currently in (pre-)clinical development by GT Pharma, with the most advanced program, GT-3550, consisting of two scFvs binding CD16xCD33 together with human IL-15, that was shown to be safe and well-tolerated in a Phase I/II clinical study (NCT03214666) (289). Nevertheless, further clinical

development was terminated due to the development of second generation V_{HH} -based TriKEs (NCT03214666). All next generation TriKEs from GT Pharma consist of a V_{HH} binding the CD16 receptor on NK cells, a tumour-specific scFv, and human IL-15 to further activate NK cells and enhance their ability to kill tumour cell (290). Additional TriKE molecules have been reported in literature (288,291). Furthermore, tetraspecific killer engagers (TetraKE) have been described by Schmohl *et al.* (2016) comprising three scFvs binding to CD16xEpCAMxCD133 and cross-linked to human IL-15 for enhanced NK proliferation, combining mechanisms of action of two bispecific molecules to improve activity, proliferation and stimulation of NK cells (292).

Stepping away from killer cell engagers, tri- and tetraspecific antibodies have been described addressing a combination of targets relevant for efficacious tumour clearance. Pharmaceutical companies have developed antibody engineering platforms to generate fast turnaround plug-and-play multispecific antibodies. For example, Numab Therapeutics has developed a heterodimeric “multispecific antibody-based therapeutics by cognate heterodimerisation” (MATCH) platform which can incorporate up to six lambda-capped variable fragments (293). Promising clinical data was achieved with their first clinical candidate, NM21-1480, targeting 4-1BBxPD-L1xHSA, with HSA as a half-life extender (NCT04442126).

To circumvent half-life extenders, IgG-like architectures are also being investigated within the multispecific antibody space. Tetraspecific IgG-scFv-conjugates of Baili Pharmaceuticals represent the most trivial form of multispecific antibodies resulting in symmetrical, octavalent molecules. GNC-038 binding PD-L1x4-1BBxCD3xCD19 is the first tetraspecific antibody under clinical investigation for recurrent or refractory non-Hodgkin’s lymphoma (NCT04606433) (294). Two further tetraspecifics have been protected under patent by exchanging the specificity of the Fab arm for other tumour markers, including EGFRvIII (GNC-039) and ROR1 (GNC-035) (295).

TetraMabs with binding specificities for four oncogenic RTKs have been described by designing HER1 and IGF1R-specific scFabs instead of generic Fabs and C-terminal scFv fusions. By the Knob-into-Hole technology, tetraspecificity can be introduced, as reported by Castoldi *et al.* (2016), for HER1xcMETxHER3xIGF1R (296). Further complex IgG-like architectures for tetraspecific antibodies include “four-in-one” antibodies, where two “two-in-one” antibodies are combined by using Knob-into-Hole, CrossMab and DVD-Ig technology to ensure heterodimerisation of the heavy chains, correct light-chain/heavy-chain interactions and tetraspecificity. A four-in-one antibody binding EGFRxHER2xHER3xVEGF displayed increased *in vitro* and *in vivo* efficacy compared to bispecific antibodies, presumably due to combined signal pathway inhibition and limiting drug resistance (297). Additional IgG-like tri- and tetraspecific antibodies have been patented by Roche. To ensure heterodimerisation, the Knob-into-Hole technology was applied. Correct heavy- and light-chain pairing

was guaranteed through different strategies, among them the replacement of specific domains with each other from a single arm, including CL/CH1, VL/VH or a combination of both (298). Multispecific antibodies show tremendous potential in revolutionising the fight against different cancers due to their combined mechanism of actions, however hitches concerning developability, stability, and large-scale manufacturability still require great improvements. All in all, such molecules might represent the next wave of next-generation therapies.

2 Objective

Before reaching clinical development, antibodies must first be discovered and thoroughly characterised to ensure their attributes are appropriate and in-line with their desired functionality. Great progress has been made to streamline antibody hit discovery workflows to ensure the faster turnaround of novel biologics. Yeast surface display (YSD), in particular, has shown to be a robust, high-throughput screening technology for isolating high-affinity binders from immune and naïve libraries. YSD libraries are screened by fluorescence-activated cell sorting (FACS), from which single clone analysis can be performed. Subsequently, the most interesting candidates are reformatted into the final IgG format (or desired format) for their *in vitro* characterisation after production in mammalian cells to ensure the correct folding and glycosylation pattern. Reformation of antibody candidates after YSD is a laborious and time-intensive process, habitually ensuing the bottleneck of antibody hit discovery campaigns as a method for bulk reformatting is yet to be described.

State-of-the-art antibody production in mammalian cells is performed by co-transfection of heavy and light chain genes encoded on different plasmids. The first aim of this study was to develop a bidirectional vector encoding both heavy and light chain genes on a single plasmid under the control of individual promoters for transfection of IgG molecules in mammalian cells. By using two FDA-approved antibodies, different promoter and enhancer element combinations were evaluated by analysing heavy and light chain mRNA expression after transient transfection in commercial cell lines apt for antibody production. Subsequent quantification of fully folded IgG molecules was used to confirm the most suitable promoter combination resulting in yields comparable to conventional methods to facilitate small-scale mAb production with a single vector in a cost- and time-efficient manner.

Having found a suitable bidirectional plasmid for mammalian expression of IgG molecules, the second goal of this study was to simplify the transition of Fab-displaying YSD libraries to the production of full-length mAbs in mammalian cells. To this end, a Fab-displaying YSD library was constructed from genetically immunised transgenic OmniRats against MerTK. The library was screened using FACS and then transferred into designed vectors exhibiting type II restriction enzyme cleavage sites for Golden Gate Cloning (GGC). The diversity of the initial library and the reformatted candidates was investigated by Next-Generation Sequencing. Lastly, the verification of successful reformation was performed by transiently transfecting Expi293 cells with the resulting bidirectional vectors encoding single antibody candidates.

While mAbs targeting single antigens have shown great promise, they carry their own limitations, in that their efficacy is often hampered by immune escape mechanisms. Due to the complex disease

environment, multiple mechanisms of action are required to improve tumour penetration and increase the efficacy of drugs. Immune cell engagers represent a class of bispecific antibodies that bridge immune cells, such as macrophages or T cells, with tumour cells to form immune synapses and harness the innate power of immune cells to kill tumour cells, pertaining to so-called next-generation antibodies. These bi- or multispecific antibodies result in increased efficacy but issues with toxicity and severe adverse effects are often faced.

The third goal of this study was to generate the first bispecific macrophage engaging antibodies by harnessing the expression of MerTK on tumour-associated macrophages for oncology indications. From the OmniRat-derived screened library after reformation, single clones were functionally characterised by investigating MerTK's downstream signalling cascade. The most suitable candidate was selected for the generation of bispecific molecules. This mAb was then fused with tandem, biparatopic V_{HH} fragments binding EGFR, to generate a MerTK/EGFR bispecific. The biophysical properties of the bispecific molecules were investigated to ensure specific binding to both targets in a simultaneous manner. Ultimately, targeted phagocytosis of tumour cells through macrophages was investigated.

Besides macrophage engagers, the efficacy of T-cell engaging immunotherapies are often hampered by high toxicities and adverse effects, mainly resulting in cytokine release syndrome (CRS). Within the last aim of this thesis, the first tetraspecific T-cell engaging antibody with built-in risk mitigation of cytokine release events (TriTECM) was generated. By using a two-in-one antibody binding to EGFR and PD-L1 and fusing single-chain variable fragments (scFvs) targeting CD3 and IL-6R, different TriTECM architectures were investigated. The tetraspecificity of the molecules was determined by specific binding to both soluble proteins and target-specific cell lines. Functional cell-based assays were performed to validate the concept of an attenuated T-cell engager with an additional IL-6R binding moiety to inhibit the IL-6/IL-6R pathway. Finally, peripheral blood mononuclear cells (PBMCs) isolated from healthy human subjects were used to study the cytokine release profiles after treatment with TriTECM molecules.

3 References

1. Yatim KM, Lakkis FG. A Brief Journey through the Immune System. *Clinical Journal of the American Society of Nephrology*. 2015 Jul 7;10(7):1274–81.
2. Buchmann K. Evolution of Innate Immunity: Clues from Invertebrates via Fish to Mammals. *Front Immunol*. 2014 Sep 23;5.
3. Flajnik MF, Kasahara M. Origin and evolution of the adaptive immune system: genetic events and selective pressures. *Nat Rev Genet*. 2010 Jan 8;11(1):47–59.
4. Chambers ES, Vukmanovic-Stejic M. Skin barrier immunity and ageing. *Immunology*. 2020 Jun 4;160(2):116–25.
5. Nguyen A v., Soulika AM. The Dynamics of the Skin's Immune System. *Int J Mol Sci*. 2019 Apr 12;20(8):1811.
6. Afshar M, Gallo RL. Innate immune defense system of the skin. *Vet Dermatol*. 2013 Feb;24(1):32-e9.
7. Sperandio B, Fischer N, Sansonetti PJ. Mucosal physical and chemical innate barriers: Lessons from microbial evasion strategies. *Semin Immunol*. 2015 Mar;27(2):111–8.
8. Wang K, Wu L yi, Dou C zi, Guan X, Wu H gan, Liu H rong. Research Advance in Intestinal Mucosal Barrier and Pathogenesis of Crohn's Disease. *Gastroenterol Res Pract*. 2016;2016:1–6.
9. Riera Romo M, Pérez-Martínez D, Castillo Ferrer C. Innate immunity in vertebrates: an overview. *Immunology*. 2016 Jun;148(2):125–39.
10. Anaya JM, Shoenfeld Y, Rojas-Villarraga A, Cervera R. Chapter 2: Innate immune system. In: *Autoimmunity from Bench to Bedside*. Bogota: El Rosario University Press; 2013.
11. Starling S. A new way out for lysozyme. *Nat Rev Immunol*. 2017 Sep 14;17(9):532–532.
12. Ferraboschi P, Ciceri S, Grisenti P. Applications of Lysozyme, an Innate Immune Defense Factor, as an Alternative Antibiotic. *Antibiotics*. 2021 Dec 14;10(12):1534.
13. Ragland SA, Criss AK. From bacterial killing to immune modulation: Recent insights into the functions of lysozyme. *PLoS Pathog*. 2017 Sep 21;13(9):e1006512.
14. Marshall JS, Warrington R, Watson W, Kim HL. An introduction to immunology and immunopathology. *Allergy, Asthma & Clinical Immunology*. 2018 Sep 12;14(S2):49.
15. Medzhitov R, Janeway CA. Innate immunity: impact on the adaptive immune response. *Curr Opin Immunol*. 1997 Feb;9(1):4–9.
16. Gallo J, Raska M, Kontinen YT, Nich C, Goodman SB. Innate Immunity Sensors Participating in Pathophysiology of Joint Diseases: A Brief Overview. *J Long Term Eff Med Implants*. 2014;24(4):297–317.
17. Schlee M. Master sensors of pathogenic RNA – RIG-I like receptors. *Immunobiology*. 2013 Nov;218(11):1322–35.
18. Basset C, Holton J, O'Mahony R, Roitt I. Innate immunity and pathogen–host interaction. *Vaccine*. 2003 Jun;21:S12–23.
19. Roh JS, Sohn DH. Damage-Associated Molecular Patterns in Inflammatory Diseases. *Immune Netw*. 2018;18(4).
20. Solari JIG, Filippi-Chiela E, Pilar ES, Nunes V, Gonzalez EA, Figueiró F, et al. Damage-associated molecular patterns (DAMPs) related to immunogenic cell death are differentially triggered by clinically relevant chemotherapeutics in lung adenocarcinoma cells. *BMC Cancer*. 2020 Dec 26;20(1):474.
21. Vénéreau E, Ceriotti C, Bianchi ME. DAMPs from Cell Death to New Life. *Front Immunol*. 2015 Aug 18;6.
22. Thomas CJ, Schroder K. Pattern recognition receptor function in neutrophils. *Trends Immunol*. 2013 Jul;34(7):317–28.
23. Janeway CA. Approaching the Asymptote? Evolution and Revolution in Immunology. *Cold Spring Harb Symp Quant Biol*. 1989 Jan 1;54(0):1–13.
24. Coers J. Self and Non-self Discrimination of Intracellular Membranes by the Innate Immune System. *PLoS Pathog*. 2013 Sep 19;9(9):e1003538.

25. Jang JH, Shin HW, Lee JM, Lee HW, Kim EC, Park SH. An Overview of Pathogen Recognition Receptors for Innate Immunity in Dental Pulp. *Mediators Inflamm.* 2015;2015:1–12.
26. Kawai T, Akira S. The roles of TLRs, RLRs and NLRs in pathogen recognition. *Int Immunol.* 2009 Apr 1;21(4):317–37.
27. Peter Christmas. Toll-Like Receptors: Sensors that Detect Infection. *Nature.* 2010;3(9).
28. Kawasaki T, Kawai T. Toll-Like Receptor Signaling Pathways. *Front Immunol.* 2014 Sep 25;5.
29. Skarnes RC, Watson DW. ANTIMICROBIAL FACTORS OF NORMAL TISSUES AND FLUIDS. *Bacteriol Rev.* 1957 Dec;21(4):273–94.
30. Liang W, Diana J. The Dual Role of Antimicrobial Peptides in Autoimmunity. *Front Immunol.* 2020 Sep 2;11.
31. Ganz T. The Role of Antimicrobial Peptides in Innate Immunity. *Integr Comp Biol.* 2003 Apr 1;43(2):300–4.
32. Diamond G, Beckloff N, Weinberg A, Kisich K. The Roles of Antimicrobial Peptides in Innate Host Defense. *Curr Pharm Des.* 2009 Jul 1;15(21):2377–92.
33. Gallo RL, Nizet V. Innate barriers against skin infection and associated disorders. *Drug Discov Today Dis Mech.* 2008 Jun;5(2):e145–52.
34. Merle NS, Noe R, Halbwachs-Mecarelli L, Fremeaux-Bacchi V, Roumenina LT. Complement System Part II: Role in Immunity. *Front Immunol.* 2015 May 26;6.
35. Dunkelberger JR, Song WC. Complement and its role in innate and adaptive immune responses. *Cell Res.* 2010 Jan 15;20(1):34–50.
36. Tauber AI. Metchnikoff and the phagocytosis theory. *Nat Rev Mol Cell Biol.* 2003 Nov;4(11):897–901.
37. Schmalstieg FC, Goldman AS. Ilya Ilich Metchnikoff (1845–1915) and Paul Ehrlich (1854–1915): The Centennial of the 1908 Nobel Prize in Physiology or Medicine. *J Med Biogr.* 2008 May 1;16(2):96–104.
38. Rahar S, Swami G, Nagpal N, Nagpal M, Singh G. Preparation, characterization, and biological properties of β -glucans. *J Adv Pharm Technol Res.* 2011;2(2):94.
39. Kennedy AD, Willment JA, Dorward DW, Williams DL, Brown GD, DeLeo FR. Dectin-1 promotes fungicidal activity of human neutrophils. *Eur J Immunol.* 2007 Feb;37(2):467–78.
40. Saijo S, Iwakura Y. Dectin-1 and Dectin-2 in innate immunity against fungi. *Int Immunol.* 2011 Aug 1;23(8):467–72.
41. Taylor PR, Brown GD, Reid DM, Willment JA, Martinez-Pomares L, Gordon S, et al. The β -Glucan Receptor, Dectin-1, Is Predominantly Expressed on the Surface of Cells of the Monocyte/Macrophage and Neutrophil Lineages. *The Journal of Immunology.* 2002 Oct 1;169(7):3876–82.
42. Ifrim DC, Bain JM, Reid DM, Oosting M, Verschueren I, Gow NAR, et al. Role of Dectin-2 for Host Defense against Systemic Infection with *Candida glabrata*. *Infect Immun.* 2014 Mar;82(3):1064–73.
43. Alberts B, Johnson A, Lewis J, Raff M, Roberts K, Walter P. *Molecular Biology of the Cell.* 4th ed. New York: Garland Science; 2002.
44. Lim JJ, Grinstein S, Roth Z. Diversity and Versatility of Phagocytosis: Roles in Innate Immunity, Tissue Remodeling, and Homeostasis. *Front Cell Infect Microbiol.* 2017 May 23;7.
45. van Wetering S, Tjabringa GS, Hiemstra PS. Interactions between neutrophil-derived antimicrobial peptides and airway epithelial cells. *J Leukoc Biol.* 2005 Apr;77(4):444–50.
46. Mariano FS, Campanelli AP, Nociti Jr. FH, Mattos-Graner RO, Gonçalves RB. Antimicrobial peptides and nitric oxide production by neutrophils from periodontitis subjects. *Brazilian Journal of Medical and Biological Research.* 2012 Nov;45(11):1017–24.
47. Puklo M, Guentsch A, Hiemstra PS, Eick S, Potempa J. Analysis of neutrophil-derived antimicrobial peptides in gingival crevicular fluid suggests importance of cathelicidin LL-37 in the innate immune response against periodontogenic bacteria. *Oral Microbiol Immunol.* 2008 Aug;23(4):328–35.
48. Lollike K, Kjeldsen L, Sengeløv H, Borregaard N. Lysozyme in human neutrophils and plasma. A parameter of myelopoietic activity. *Leukemia.* 1995 Jan;9(1):159–64.

-
49. Karle H, Hansen NE, Killmann SA. Intracellular Lysozyme in Mature Neutrophils and Blast Cells in Acute Leukemia. *Blood*. 1974 Aug 1;44(2):247–55.
 50. Stapels DA, Geisbrecht B v, Rooijackers SH. Neutrophil serine proteases in antibacterial defense. *Curr Opin Microbiol*. 2015 Feb;23:42–8.
 51. Belaouaj A azzaq, Kim KS, Shapiro SD. Degradation of Outer Membrane Protein A in *Escherichia coli* Killing by Neutrophil Elastase. *Science* (1979). 2000 Aug 18;289(5482):1185–7.
 52. Standish AJ, Weiser JN. Human Neutrophils Kill *Streptococcus pneumoniae* via Serine Proteases. *The Journal of Immunology*. 2009 Aug 15;183(4):2602–9.
 53. Troidl C, Möllmann H, Nef H, Masseli F, Voss S, Szardien S, et al. Classically and alternatively activated macrophages contribute to tissue remodelling after myocardial infarction. *J Cell Mol Med*. 2009 Sep;13(9b):3485–96.
 54. Myers K v., Amend SR, Pienta KJ. Targeting Tyro3, Axl and MerTK (TAM receptors): implications for macrophages in the tumor microenvironment. *Mol Cancer*. 2019 Dec 14;18(1):94.
 55. Jayasingam SD, Citartan M, Thang TH, Mat Zin AA, Ang KC, Ch'ng ES. Evaluating the Polarization of Tumor-Associated Macrophages into M1 and M2 Phenotypes in Human Cancer Tissue: Technicalities and Challenges in Routine Clinical Practice. *Front Oncol*. 2020 Jan 24;9.
 56. Gaudino SJ, Kumar P. Cross-Talk Between Antigen Presenting Cells and T Cells Impacts Intestinal Homeostasis, Bacterial Infections, and Tumorigenesis. *Front Immunol*. 2019 Mar 6;10.
 57. Eiz-Vesper B, Schmetzer HM. Antigen-Presenting Cells: Potential of Proven und New Players in Immune Therapies. *Transfusion Medicine and Hemotherapy*. 2020;47(6):429–31.
 58. Vivier E, Raulet DH, Moretta A, Caligiuri MA, Zitvogel L, Lanier LL, et al. Innate or Adaptive Immunity? The Example of Natural Killer Cells. *Science* (1979). 2011 Jan 7;331(6013):44–9.
 59. Frei R, Steinle J, Birchler T, Loeliger S, Roduit C, Steinhoff D, et al. MHC Class II Molecules Enhance Toll-Like Receptor Mediated Innate Immune Responses. *PLoS One*. 2010 Jan 20;5(1):e8808.
 60. Karp CL. Links between Innate and Adaptive Immunity. In: *Fundamentals of Inflammation*. Cambridge University Press; 2010. p. 28–38.
 61. Artyomov MN, Lis M, Devadas S, Davis MM, Chakraborty AK. CD4 and CD8 binding to MHC molecules primarily acts to enhance Lck delivery. *Proceedings of the National Academy of Sciences*. 2010 Sep 28;107(39):16916–21.
 62. Birnbaum ME, Berry R, Hsiao YS, Chen Z, Shingu-Vazquez MA, Yu X, et al. Molecular architecture of the $\alpha\beta$ T cell receptor–CD3 complex. *Proceedings of the National Academy of Sciences*. 2014 Dec 9;111(49):17576–81.
 63. Andersen MH, Schrama D, thor Straten P, Becker JC. Cytotoxic T Cells. *Journal of Investigative Dermatology*. 2006 Jan;126(1):32–41.
 64. Whitacre JM, Lin J, Harding A. T Cell Adaptive Immunity Proceeds through Environment-Induced Adaptation from the Exposure of Cryptic Genetic Variation. *Front Genet*. 2012;3.
 65. Pennock ND, White JT, Cross EW, Cheney EE, Tamburini BA, Kedl RM. T cell responses: naïve to memory and everything in between. *Adv Physiol Educ*. 2013 Dec;37(4):273–83.
 66. Ait-Oufella H, Sage AP, Mallat Z, Tedgui A. Adaptive (T and B Cells) Immunity and Control by Dendritic Cells in Atherosclerosis. *Circ Res*. 2014 May 9;114(10):1640–60.
 67. Nguyen TV, Pawlikowska P, Firlej V, Rosselli F, Aoufouchi S. V(D)J recombination process and the Pre-B to immature B-cells transition are altered in *Fanca*^{-/-} mice. *Sci Rep*. 2016 Dec 24;6(1):36906.
 68. González D, van der Burg M, García-Sanz R, Fenton JA, Langerak AW, González M, et al. Immunoglobulin gene rearrangements and the pathogenesis of multiple myeloma. *Blood*. 2007 Nov 1;110(9):3112–21.
 69. Roth DB. V(D)J Recombination: Mechanism, Errors, and Fidelity. *Microbiol Spectr*. 2014 Nov 21;2(6).
 70. Janeway CA, Travers P, Walport M, Schlomchik MJ. *Immunobiology: The Immune System in Health and Disease*. In: 5th ed. New York: Garland Science; 2001.
 71. Nemazee D. Mechanisms of central tolerance for B cells. *Nat Rev Immunol*. 2017 May 3;17(5):281–94.

72. Pelanda R, Torres RM. Central B-Cell Tolerance: Where Selection Begins. *Cold Spring Harb Perspect Biol.* 2012 Apr 1;4(4):a007146–a007146.
73. Gatto D, Brink R. The germinal center reaction. *Journal of Allergy and Clinical Immunology.* 2010 Nov;126(5):898–907.
74. Merlo LMF, Mandik-Nayak L. Adaptive Immunity. In: *Cancer Immunotherapy.* Elsevier; 2013. p. 25–40.
75. Stavnezer J, Guikema JEJ, Schrader CE. Mechanism and Regulation of Class Switch Recombination. *Annu Rev Immunol.* 2008 Apr 1;26(1):261–92.
76. Adler LN, Jiang W, Bhamidipati K, Millican M, Macaubas C, Hung S chen, et al. The Other Function: Class II-Restricted Antigen Presentation by B Cells. *Front Immunol.* 2017 Mar 23;8.
77. Janeway CA, Ron J, Katz ME. The B cell is the initiating antigen-presenting cell in peripheral lymph nodes. *J Immunol.* 1987 Feb 15;138(4):1051–5.
78. Fellah JS, Wiles M v., Charlemagne J, Schwager J. Evolution of vertebrate IgM: complete amino acid sequence of the constant region of *Ambystoma mexicanum* μ chain deduced from cDNA sequence. *Eur J Immunol.* 1992 Oct;22(10):2595–601.
79. Oostindie SC, Lazar GA, Schuurman J, Parren PWHI. Avidity in antibody effector functions and biotherapeutic drug design. *Nat Rev Drug Discov.* 2022 Oct 5;21(10):715–35.
80. Otten MA, van Egmond M. The Fc receptor for IgA (Fc α RI, CD89). *Immunol Lett.* 2004 Mar;92(1–2):23–31.
81. Woof JM, Kerr MA. The function of immunoglobulin A in immunity. *J Pathol.* 2006 Jan;208(2):270–82.
82. Kumar Bharathkar S, Parker BW, Malyutin AG, Haloi N, Huey-Tubman KE, Tajkhorshid E, et al. The structures of secretory and dimeric immunoglobulin A. *Elife.* 2020 Oct 27;9.
83. Nguyen TG. The therapeutic implications of activated immune responses via the enigmatic immunoglobulin D. *Int Rev Immunol.* 2022 Mar 4;41(2):107–22.
84. Bengtén E, Wilson M, Miller N, Clem LW, Pilström L, Warr GW. Immunoglobulin Isotypes: Structure, Function, and Genetics. In 2000. p. 189–219.
85. Sutton B, Davies A, Bax H, Karagiannis S. IgE Antibodies: From Structure to Function and Clinical Translation. *Antibodies.* 2019 Feb 22;8(1):19.
86. Vidarsson G, Dekkers G, Rispens T. IgG Subclasses and Allotypes: From Structure to Effector Functions. *Front Immunol.* 2014 Oct 20;5.
87. Weitzner BD, Dunbrack RL, Gray JJ. The Origin of CDR H3 Structural Diversity. *Structure.* 2015 Feb;23(2):302–11.
88. Morea V, Tramontano A, Rustici M, Chothia C, Lesk AM. Conformations of the third hypervariable region in the VH domain of immunoglobulins 1 1 Edited by I. A. Wilson. *J Mol Biol.* 1998 Jan;275(2):269–94.
89. Chiu ML, Goulet DR, Teplyakov A, Gilliland GL. Antibody Structure and Function: The Basis for Engineering Therapeutics. *Antibodies.* 2019 Dec 3;8(4):55.
90. Haraldsson Á, Kock-Jansen MJH, Jaminon M, v Eck-Arts PBJM, de Boo T, Weemaes CMR, et al. Determination of Kappa and Lambda Light Chains in Serum Immunoglobulins G, A and M. *Annals of Clinical Biochemistry: International Journal of Laboratory Medicine.* 1991 Sep 29;28(5):461–6.
91. Molé CM, Béné MC, Montagne PM, Seilles E, Faure GC. Light chains of immunoglobulins in human secretions. *Clinica Chimica Acta.* 1994 Jan;224(2):191–7.
92. Maverakis E, Kim K, Shimoda M, Gershwin ME, Patel F, Wilken R, et al. Glycans in the immune system and The Altered Glycan Theory of Autoimmunity: A critical review. *J Autoimmun.* 2015 Feb;57:1–13.
93. van Erp EA, Luytjes W, Ferwerda G, van Kasteren PB. Fc-Mediated Antibody Effector Functions During Respiratory Syncytial Virus Infection and Disease. *Front Immunol.* 2019 Mar 22;10.
94. de Taeye SW, Bentlage AEH, Mebius MM, Meesters JI, Lissenberg-Thunnissen S, Falck D, et al. Fc γ R Binding and ADCC Activity of Human IgG Allotypes. *Front Immunol.* 2020 May 6;11.
95. Moore GL, Chen H, Karki S, Lazar GA. Engineered Fc variant antibodies with enhanced ability to recruit complement and mediate effector functions. *MAbs.* 2010 Mar 27;2(2):181–9.

-
96. Sharp TH, Boyle AL, Diebolder CA, Kros A, Koster AJ, Gros P. Insights into IgM-mediated complement activation based on in situ structures of IgM-C1-C4b. *Proceedings of the National Academy of Sciences*. 2019 Jun 11;116(24):11900–5.
 97. Pyzik M, Rath T, Lencer WI, Baker K, Blumberg RS. FcRn: The Architect Behind the Immune and Nonimmune Functions of IgG and Albumin. *The Journal of Immunology*. 2015 May 15;194(10):4595–603.
 98. KÖHLER G, MILSTEIN C. Continuous cultures of fused cells secreting antibody of predefined specificity. *Nature*. 1975 Aug 1;256(5517):495–7.
 99. Hansel TT, Kropshofer H, Singer T, Mitchell JA, George AJT. The safety and side effects of monoclonal antibodies. *Nat Rev Drug Discov*. 2010 Apr 22;9(4):325–38.
 100. Dillman RO, Beauregard JC, Halpern SE, Clutter M. Toxicities and side effects associated with intravenous infusions of murine monoclonal antibodies. *J Biol Response Mod*. 1986 Feb;5(1):73–84.
 101. The Antibody Society. Therapeutic monoclonal antibodies approved or in review in the EU or US [Internet]. [cited 2022 Sep 13]. Available from: <https://www.antibodysociety.org/resources/approved-antibodies/>
 102. Khazaeli M, Conry R, LoBuglio A. Human immune response to monoclonal antibodies. In: *Journal of Immunotherapy with Emphasis on Tumor Immunology*. 1994. p. 42–52.
 103. Tjandra JJ, Ramadi L, McKenzie IFC. Development of human anti-murine antibody (HAMA) response in patients. *Immunol Cell Biol*. 1990 Dec;68(6):367–76.
 104. Shin SU. Chimeric antibody: Potential applications for drug delivery and immunotherapy. *Biotherapy*. 1991 Jan;3(1):43–53.
 105. Almagro JC, Daniels-Wells TR, Perez-Tapia SM, Penichet ML. Progress and Challenges in the Design and Clinical Development of Antibodies for Cancer Therapy. *Front Immunol*. 2018 Jan 4;8.
 106. Safdari Y, Farajnia S, Asgharzadeh M, Khalili M. Antibody humanization methods – a review and update. *Biotechnol Genet Eng Rev*. 2013 Oct;29(2):175–86.
 107. Osbourn J, Groves M, Vaughan T. From rodent reagents to human therapeutics using antibody guided selection. *Methods*. 2005 May;36(1):61–8.
 108. Pelechas E, Voulgari P v, Drosos AA. Preclinical discovery and development of adalimumab for the treatment of rheumatoid arthritis. *Expert Opin Drug Discov*. 2021 Mar 4;16(3):227–34.
 109. Buntz B. 50 of 2021's best-selling pharmaceuticals [Internet]. *Drug Discovery Trends*. 2022 [cited 2022 Oct 13]. Available from: <https://www.drugdiscoverytrends.com/50-of-2021s-best-selling-pharmaceuticals/>
 110. Harding FA, Stickler MM, Razo J, DuBridg R. The immunogenicity of humanized and fully human antibodies. *MAbs*. 2010 May 27;2(3):256–65.
 111. Vaisman-Mentesh A, Gutierrez-Gonzalez M, DeKosky BJ, Wine Y. The Molecular Mechanisms That Underlie the Immune Biology of Anti-drug Antibody Formation Following Treatment with Monoclonal Antibodies. *Front Immunol*. 2020 Aug 18;11.
 112. Liang S, Zhang C. Prediction of immunogenicity for humanized and full human therapeutic antibodies. *PLoS One*. 2020 Aug 31;15(8):e0238150.
 113. Thurber GM, Schmidt MM, Wittrup KD. Antibody tumor penetration: Transport opposed by systemic and antigen-mediated clearance. *Adv Drug Deliv Rev*. 2008 Sep;60(12):1421–34.
 114. Alegre ML, Collins AM, Pulito VL, Brosius RA, Olson WC, Zivin RA, et al. Effect of a single amino acid mutation on the activating and immunosuppressive properties of a 'humanized' OKT3 monoclonal antibody. *J Immunol*. 1992 Jun 1;148(11):3461–8.
 115. Saunders KO. Conceptual Approaches to Modulating Antibody Effector Functions and Circulation Half-Life. *Front Immunol*. 2019 Jun 7;10.
 116. Lund J, Winter G, Jones PT, Pound JD, Tanaka T, Walker MR, et al. Human Fc gamma RI and Fc gamma RII interact with distinct but overlapping sites on human IgG. *J Immunol*. 1991 Oct 15;147(8):2657–62.

117. Lo M, Kim HS, Tong RK, Bainbridge TW, Vernes JM, Zhang Y, et al. Effector-attenuating Substitutions That Maintain Antibody Stability and Reduce Toxicity in Mice. *Journal of Biological Chemistry*. 2017 Mar;292(9):3900–8.
118. Bolt S, Routledge E, Lloyd I, Chatenoud L, Pope H, Gorman SD, et al. The generation of a humanized, non-mitogenic CD3 monoclonal antibody which retains in vitro immunosuppressive properties. *Eur J Immunol*. 1993 Feb;23(2):403–11.
119. Tao MH, Morrison SL. Studies of aglycosylated chimeric mouse-human IgG. Role of carbohydrate in the structure and effector functions mediated by the human IgG constant region. *J Immunol*. 1989 Oct 15;143(8):2595–601.
120. Wang X, Mathieu M, Brezski RJ. IgG Fc engineering to modulate antibody effector functions. *Protein Cell*. 2018 Jan 6;9(1):63–73.
121. Wilkinson I, Anderson S, Fry J, Julien LA, Neville D, Qureshi O, et al. Fc-engineered antibodies with immune effector functions completely abolished. *PLoS One*. 2021 Dec 21;16(12):e0260954.
122. Cheong WS, Leow CY, Abdul Majeed AB, Leow CH. Diagnostic and therapeutic potential of shark variable new antigen receptor (VNAR) single domain antibody. *Int J Biol Macromol*. 2020 Mar;147:369–75.
123. Strohl W, Strohl L. Antibody fragments as therapeutics. In: *Therapeutic Antibody Engineering*. Elsevier; 2012. p. 265–595.
124. Kholodenko R v., Kalinovskiy D v., Doronin II, Ponomarev ED, Kholodenko I v. Antibody Fragments as Potential Biopharmaceuticals for Cancer Therapy: Success and Limitations. *Curr Med Chem*. 2019 Mar 26;26(3):396–426.
125. World Health Organization. Estimated number of deaths in 2020, World, both sexes, all ages (excl. NMSC). *Cancer Today*. 2020.
126. Hanahan D. Hallmarks of Cancer: New Dimensions. *Cancer Discov*. 2022 Jan 1;12(1):31–46.
127. Kaplon H, Chenoweth A, Crescioli S, Reichert JM. Antibodies to watch in 2022. *MAbs*. 2022 Dec 31;14(1).
128. Torres ETR, Emens LA. Emerging combination immunotherapy strategies for breast cancer: dual immune checkpoint modulation, antibody–drug conjugates and bispecific antibodies. *Breast Cancer Res Treat*. 2022 Jan 30;191(2):291–302.
129. Krasniqi E, Barchiesi G, Pizzuti L, Mazzotta M, Venuti A, Maugeri-Saccà M, et al. Immunotherapy in HER2-positive breast cancer: state of the art and future perspectives. *J Hematol Oncol*. 2019 Dec 29;12(1):111.
130. Lemjabbar-Alaoui H, Hassan OU, Yang YW, Buchanan P. Lung cancer: Biology and treatment options. *Biochimica et Biophysica Acta (BBA) - Reviews on Cancer*. 2015 Dec;1856(2):189–210.
131. Silva APS, Coelho P v., Anazetti M, Simioni PU. Targeted therapies for the treatment of non-small-cell lung cancer: Monoclonal antibodies and biological inhibitors. *Hum Vaccin Immunother*. 2017 Apr 3;13(4):843–53.
132. Biopharma Dealmakers. Moving up with the monoclonals [Internet]. *Nature*. 2019 [cited 2022 Sep 13]. Available from: <https://www.nature.com/articles/d43747-020-00765-2>
133. Anderson NM, Simon MC. The tumor microenvironment. *Current Biology*. 2020 Aug;30(16):R921–5.
134. Labani-Motlagh A, Ashja-Mahdavi M, Loskog A. The Tumor Microenvironment: A Milieu Hindering and Obstructing Antitumor Immune Responses. *Front Immunol*. 2020 May 15;11.
135. Shiao SL, Ganesan AP, Rugo HS, Coussens LM. Immune microenvironments in solid tumors: new targets for therapy. *Genes Dev*. 2011 Dec 15;25(24):2559–72.
136. Sounni NE, Noel A. Targeting the Tumor Microenvironment for Cancer Therapy. *Clin Chem*. 2013 Jan 1;59(1):85–93.
137. Naimi A, Mohammed RN, Raji A, Chupradit S, Yumashev AV, Suksatan W, et al. Tumor immunotherapies by immune checkpoint inhibitors (ICIs); the pros and cons. *Cell Communication and Signaling*. 2022 Dec 7;20(1):44.
138. Bonaventura P, Shekarian T, Alcazer V, Valladeau-Guilemond J, Valsesia-Wittmann S, Amigorena S, et al. Cold Tumors: A Therapeutic Challenge for Immunotherapy. *Front Immunol*. 2019 Feb 8;10.

139. Duan Q, Zhang H, Zheng J, Zhang L. Turning Cold into Hot: Firing up the Tumor Microenvironment. *Trends Cancer*. 2020 Jul;6(7):605–18.
140. Liu YT, Sun ZJ. Turning cold tumors into hot tumors by improving T-cell infiltration. *Theranostics*. 2021;11(11):5365–86.
141. Beatty GL, Gladney WL. Immune Escape Mechanisms as a Guide for Cancer Immunotherapy. *Clinical Cancer Research*. 2015 Feb 15;21(4):687–92.
142. Wang S, Chen K, Lei Q, Ma P, Yuan AQ, Zhao Y, et al. The state of the art of bispecific antibodies for treating human malignancies. *EMBO Mol Med*. 2021 Sep 7;13(9).
143. Biopharma PEG. Bispecific Antibodies - Current Status and Prospects [Internet]. 2022 [cited 2022 Sep 27]. Available from: <https://www.biochempeg.com/article/252.html>
144. Sathish JG, Sethu S, Bielsky MC, de Haan L, French NS, Govindappa K, et al. Challenges and approaches for the development of safer immunomodulatory biologics. *Nat Rev Drug Discov*. 2013 Apr 28;12(4):306–24.
145. Shimabukuro-Vornhagen A, Gödel P, Subklewe M, Stemmler HJ, Schlößer HA, Schlaak M, et al. Cytokine release syndrome. *J Immunother Cancer* [Internet]. 2018 Dec 15;6(1):56. Available from: <https://jitc.bmj.com/lookup/doi/10.1186/s40425-018-0343-9>
146. Fajgenbaum DC, June CH. Cytokine Storm. *New England Journal of Medicine*. 2020 Dec 3;383(23):2255–73.
147. Tang XD, Ji TT, Dong JR, Feng H, Chen FQ, Chen X, et al. Pathogenesis and Treatment of Cytokine Storm Induced by Infectious Diseases. *Int J Mol Sci*. 2021 Nov 30;22(23):13009.
148. Thomas K, Eisele J, Rodriguez-Leal FA, Hainke U, Ziemssen T. Acute effects of alemtuzumab infusion in patients with active relapsing-remitting MS. *Neurology - Neuroimmunology Neuroinflammation*. 2016 Jun 29;3(3):e228.
149. Winkler U, Jensen M, Manzke O, Schulz H, Diehl V, Engert A. Cytokine-Release Syndrome in Patients with B-Cell Chronic Lymphocytic Leukemia and High Lymphocyte Counts After Treatment With an Anti-CD20 Monoclonal Antibody (Rituximab, IDEC-C2B8). *Blood*. 1999 Oct 1;94(7):2217–24.
150. Beatty GL, Torigian DA, Chiorean EG, Saboury B, Brothers A, Alavi A, et al. A Phase I Study of an Agonist CD40 Monoclonal Antibody (CP-870,893) in Combination with Gemcitabine in Patients with Advanced Pancreatic Ductal Adenocarcinoma. *Clinical Cancer Research*. 2013 Nov 15;19(22):6286–95.
151. Nizet Y, Chentoufi AA, de la Parra B, Lewalle P, Rouas R, Cornet A, et al. The experimental (in vitro) and clinical (in vivo) immunosuppressive effects of a rat IgG2b anti-human CD2 mAb, LO-CD2a/BTI-322. *Transplantation*. 2000 Apr 15;69(7):1420–9.
152. Suntharalingam G, Perry MR, Ward S, Brett SJ, Castello-Cortes A, Brunner MD, et al. Cytokine Storm in a Phase 1 Trial of the Anti-CD28 Monoclonal Antibody TGN1412. *New England Journal of Medicine*. 2006 Sep 7;355(10):1018–28.
153. Bugelski PJ, Achuthanandam R, Capocasale RJ, Treacy G, Bouman-Thio E. Monoclonal antibody-induced cytokine-release syndrome. *Expert Rev Clin Immunol*. 2009 Sep 10;5(5):499–521.
154. Kenter M, Cohen A. Establishing risk of human experimentation with drugs: lessons from TGN1412. *The Lancet*. 2006 Oct;368(9544):1387–91.
155. Tanaka T, Narazaki M, Kishimoto T. Immunotherapeutic implications of IL-6 blockade for cytokine storm. *Immunotherapy*. 2016 Jul;8(8):959–70.
156. Pabst T, Joncourt R, Shumilov E, Heini A, Wiedemann G, Legros M, et al. Analysis of IL-6 serum levels and CAR T cell-specific digital PCR in the context of cytokine release syndrome. *Exp Hematol*. 2020 Aug;88:7-14.e3.
157. Moore JB, June CH. Cytokine release syndrome in severe COVID-19. *Science (1979)*. 2020 May;368(6490):473–4.
158. Maude SL, Barrett D, Teachey DT, Grupp SA. Managing Cytokine Release Syndrome Associated with Novel T Cell-Engaging Therapies. *The Cancer Journal*. 2014 Mar;20(2):119–22.
159. Lee DW, Santomasso BD, Locke FL, Ghobadi A, Turtle CJ, Brudno JN, et al. ASTCT Consensus Grading for Cytokine Release Syndrome and Neurologic Toxicity Associated with Immune Effector

- Cells. *Biology of Blood and Marrow Transplantation* [Internet]. 2019 Apr;25(4):625–38. Available from: <https://linkinghub.elsevier.com/retrieve/pii/S1083879118316914>
160. Chen LYC, Hoiland RL, Stukas S, Wellington CL, Sekhon MS. Confronting the controversy: interleukin-6 and the COVID-19 cytokine storm syndrome. *European Respiratory Journal*. 2020 Oct;56(4):2003006.
161. Pabst T, Joncourt R, Shumilov E, Heini A, Wiedemann G, Legros M, et al. Analysis of IL-6 serum levels and CAR T cell-specific digital PCR in the context of cytokine release syndrome. *Exp Hematol*. 2020 Aug;88:7-14.e3.
162. Si S, Teachey DT. Spotlight on Tocilizumab in the Treatment of CAR-T-Cell-Induced Cytokine Release Syndrome: Clinical Evidence to Date. *Ther Clin Risk Manag*. 2020;16:705–14.
163. Le RQ, Li L, Yuan W, Shord SS, Nie L, Habtemariam BA, et al. FDA Approval Summary: Tocilizumab for Treatment of Chimeric Antigen Receptor T Cell-Induced Severe or Life-Threatening Cytokine Release Syndrome. *Oncologist* [Internet]. 2018 Aug 1;23(8):943–7. Available from: <https://academic.oup.com/oncolo/article/23/8/943/6439647>
164. Kadauke S, Myers RM, Li Y, Aplenc R, Baniewicz D, Barrett DM, et al. Risk-Adapted Preemptive Tocilizumab to Prevent Severe Cytokine Release Syndrome After CTL019 for Pediatric B-Cell Acute Lymphoblastic Leukemia: A Prospective Clinical Trial. *J Clin Oncol* [Internet]. 2021;39(8):920–30. Available from: <http://www.ncbi.nlm.nih.gov/pubmed/33417474>
165. REMAP-CAP. Interleukin-6 Receptor Antagonists in Critically Ill Patients with Covid-19. *New England Journal of Medicine* [Internet]. 2021 Apr 22;384(16):1491–502. Available from: <http://www.nejm.org/doi/10.1056/NEJMoa2100433>
166. Chamlagain R, Shah S, Sharma Paudel B, Dhital R, Kandel B. Efficacy and Safety of Sarilumab in COVID-19: A Systematic Review. Lanzafame M, editor. *Interdiscip Perspect Infect Dis* [Internet]. 2021 Oct 22;2021:1–8. Available from: <https://www.hindawi.com/journals/ipid/2021/8903435/>
167. Corominas H, Castellví I, Diaz-Torné C, Matas L, de la Rosa D, Mangues MA, et al. Sarilumab (IL-6R antagonist) in critically ill patients with cytokine release syndrome by SARS-CoV2. *Medicine* [Internet]. 2021 May 14;100(19):e25923. Available from: <https://journals.lww.com/10.1097/MD.00000000000025923>
168. Mariette X, Hermine O, Tharaux PL, Resche-Rigon M, Porcher R, Ravaut P, et al. Sarilumab in adults hospitalised with moderate-to-severe COVID-19 pneumonia (CORIMUNO-SARI-1): An open-label randomised controlled trial. *Lancet Rheumatol* [Internet]. 2022 Jan;4(1):e24–32. Available from: <https://linkinghub.elsevier.com/retrieve/pii/S2665991321003155>
169. León López R, Fernández SC, Limia Pérez L, Romero Palacios A, Fernández-Roldán MC, Aguilar Alonso E, et al. Efficacy and safety of early treatment with sarilumab in hospitalised adults with COVID-19 presenting cytokine release syndrome (SARICOR STUDY): protocol of a phase II, open-label, randomised, multicentre, controlled clinical trial. *BMJ Open* [Internet]. 2020 Nov 14;10(11):e039951. Available from: <https://bmjopen.bmj.com/lookup/doi/10.1136/bmjopen-2020-039951>
170. Lee DW, Gardner R, Porter DL, Louis CU, Ahmed N, Jensen M, et al. Current concepts in the diagnosis and management of cytokine release syndrome. *Blood* [Internet]. 2014 Jul 10;124(2):188–95. Available from: <https://ashpublications.org/blood/article/124/2/188/32896/Current-concepts-in-the-diagnosis-and-management>
171. Ahrens B. Antibodies in metabolic diseases. *N Biotechnol*. 2011 Sep;28(5):530–7.
172. Mortada I, Farah R, Nabha S, Ojcius DM, Fares Y, Almawi WY, et al. Immunotherapies for Neurodegenerative Diseases. *Front Neurol*. 2021 Jun 7;12.
173. Yu YJ, Watts RJ. Developing Therapeutic Antibodies for Neurodegenerative Disease. *Neurotherapeutics*. 2013 Jul 3;10(3):459–72.
174. Freire MO, Kim HK, Kook JK, Nguyen A, Zadeh HH. Antibody-Mediated Osseous Regeneration: The Early Events in the Healing Response. *Tissue Eng Part A*. 2013 May;19(9–10):1165–74.
175. Ross KG, Omuro KC, Taylor MR, Munday RK, Hubert A, King RS, et al. Novel monoclonal antibodies to study tissue regeneration in planarians. *BMC Dev Biol*. 2015 Dec 21;15(1):2.

176. McClung MR, Lewiecki EM, Cohen SB, Bolognese MA, Woodson GC, Moffett AH, et al. Denosumab in Postmenopausal Women with Low Bone Mineral Density. *New England Journal of Medicine*. 2006 Feb 23;354(8):821–31.
177. Baseler L, Chertow DS, Johnson KM, Feldmann H, Morens DM. The Pathogenesis of Ebola Virus Disease. *Annual Review of Pathology: Mechanisms of Disease*. 2017 Jan 24;12(1):387–418.
178. Corti D, Purcell LA, Snell G, Vesler D. Tackling COVID-19 with neutralizing monoclonal antibodies. *Cell*. 2021 Jun;184(12):3086–108.
179. Shanmugaraj B, Siri wattananon K, Wangkanont K, Phoolcharoen W. Perspectives on monoclonal antibody therapy as potential therapeutic intervention for Coronavirus disease-19 (COVID-19). *Asian Pac J Allergy Immunol* [Internet]. 2020; Available from: <http://apjai-journal.org/wp-content/uploads/2020/03/2.pdf>
180. Lu ZJ. Frontier of therapeutic antibody discovery: The challenges and how to face them. *World J Biol Chem*. 2012;3(12):187.
181. Sidhu SS, Fellouse FA. Synthetic therapeutic antibodies. *Nat Chem Biol*. 2006 Dec;2(12):682–8.
182. Rajan S, Sidhu SS. Simplified Synthetic Antibody Libraries. In 2012. p. 3–23.
183. Strohl W, Strohl L. Sources of antibody variable chains. In: *Therapeutic Antibody Engineering*. Elsevier; 2012. p. 77–595.
184. Chan SK, Rahumatullah A, Lai JY, Lim TS. Naïve Human Antibody Libraries for Infectious Diseases. In 2017. p. 35–59.
185. Lim BN, Chin CF, Choong YS, Ismail A, Lim TS. Generation of a naïve human single chain variable fragment (scFv) library for the identification of monoclonal scFv against Salmonella Typhi Hemolysin E antigen. *Toxicon*. 2016 Jul;117:94–101.
186. Hentrich C, Ylera F, Frisch C, ten Haaf A, Knappik A. Monoclonal Antibody Generation by Phage Display. In: *Handbook of Immunoassay Technologies*. Elsevier; 2018. p. 47–80.
187. Braunagel M. Construction of a semisynthetic antibody library using trinucleotide oligos. *Nucleic Acids Res*. 1997 Nov 15;25(22):4690–1.
188. Barbas CF, Bain JD, Hoekstra DM, Lerner RA. Semisynthetic combinatorial antibody libraries: a chemical solution to the diversity problem. *Proceedings of the National Academy of Sciences*. 1992 May 15;89(10):4457–61.
189. Soon Lim T, Khim Chan S. Immune Antibody Libraries: Manipulating the Diverse Immune Repertoire for Antibody Discovery. *Curr Pharm Des*. 2017 Jan 11;22(43):6480–9.
190. Rader C, Ritter G, Nathan S, Elia M, Gout I, Jungbluth AA, et al. The Rabbit Antibody Repertoire as a Novel Source for the Generation of Therapeutic Human Antibodies. *Journal of Biological Chemistry*. 2000 May;275(18):13668–76.
191. Tsai KC, Chang CD, Cheng MH, Lin TY, Lo YN, Yang TW, et al. Chicken-Derived Humanized Antibody Targeting a Novel Epitope F2pep of Fibroblast Growth Factor Receptor 2: Potential Cancer Therapeutic Agent. *ACS Omega*. 2019 Jan 31;4(1):2387–97.
192. Grzeschik J, Yanakieva D, Roth L, Krah S, Hinz SC, Elter A, et al. Yeast Surface Display in Combination with Fluorescence-activated Cell Sorting Enables the Rapid Isolation of Antibody Fragments Derived from Immunized Chickens. *Biotechnol J*. 2019 Apr 28;14(4):1800466.
193. Bogen JP, Carrara SC, Fiebig D, Grzeschik J, Hock B, Kolmar H. Design of a Trispecific Checkpoint Inhibitor and Natural Killer Cell Engager Based on a 2 + 1 Common Light Chain Antibody Architecture. *Front Immunol*. 2021 May 10;12.
194. Harwardt J, Bogen JP, Carrara SC, Ullitzka M, Grzeschik J, Hock B, et al. A Generic Strategy to Generate Bifunctional Two-in-One Antibodies by Chicken Immunization. *Front Immunol*. 2022 Apr 11;13.
195. Bogen JP, Storka J, Yanakieva D, Fiebig D, Grzeschik J, Hock B, et al. Isolation of Common Light Chain Antibodies from Immunized Chickens Using Yeast Biopanning and Fluorescence-Activated Cell Sorting. *Biotechnol J*. 2021 Mar 8;16(3):2000240.
196. Elter A, Yanakieva D, Fiebig D, Hallstein K, Becker S, Betz U, et al. Protease-Activation of Fc-Masked Therapeutic Antibodies to Alleviate Off-Tumor Cytotoxicity. *Front Immunol*. 2021 Aug 3;12.

197. Hinz SC, Elter A, Rammo O, Schwämmle A, Ali A, Zielonka S, et al. A Generic Procedure for the Isolation of pH- and Magnesium-Responsive Chicken scFvs for Downstream Purification of Human Antibodies. *Front Bioeng Biotechnol.* 2020 Jun 23;8.
198. Bogen JP, Carrara SC, Fiebig D, Grzeschik J, Hock B, Kolmar H. Expeditious Generation of Biparatopic Common Light Chain Antibodies via Chicken Immunization and Yeast Display Screening. *Front Immunol.* 2020 Dec 23;11.
199. Roguska MA, Pedersen JT, Keddy CA, Henry AH, Searle SJ, Lambert JM, et al. Humanization of murine monoclonal antibodies through variable domain resurfacing. *Proceedings of the National Academy of Sciences.* 1994 Feb;91(3):969–73.
200. Lee EC, Liang Q, Ali H, Bayliss L, Beasley A, Bloomfield-Gerdes T, et al. Complete humanization of the mouse immunoglobulin loci enables efficient therapeutic antibody discovery. *Nat Biotechnol.* 2014 Apr 16;32(4):356–63.
201. Hsieh YC, Liao J min, Chuang KH, Ho KW, Hong ST, Liu HJ, et al. A universal in silico V(D)J recombination strategy for developing humanized monoclonal antibodies. *J Nanobiotechnology.* 2022 Dec 31;20(1):58.
202. Zhang D, Chen CF, Zhao BB, Gong LL, Jin WJ, Liu JJ, et al. A Novel Antibody Humanization Method Based on Epitopes Scanning and Molecular Dynamics Simulation. *PLoS One.* 2013 Nov 21;8(11):e80636.
203. Zhang YF, Ho M. Humanization of rabbit monoclonal antibodies via grafting combined Kabat/IMGT/Paratome complementarity-determining regions: Rationale and examples. *MABs.* 2017 Apr 3;9(3):419–29.
204. Elter A, Bogen JP, Hinz SC, Fiebig D, Macarrón Palacios A, Grzeschik J, et al. Humanization of Chicken-Derived scFv Using Yeast Surface Display and NGS Data Mining. *Biotechnol J.* 2021 Mar 9;16(3):2000231.
205. Nishibori N, Horiuchi H, Furusawa S, Matsuda H. Humanization of chicken monoclonal antibody using phage-display system. *Mol Immunol.* 2006 Feb;43(6):634–42.
206. Brüggemann M, Spicer C, Buluwela L, Rosewell I, Barton S, Surani MA, et al. Human antibody production in transgenic mice: expression from 100 kb of the human IgH locus. *Eur J Immunol.* 1991 May;21(5):1323–6.
207. Brüggemann M, Osborn MJ, Ma B, Hayre J, Avis S, Lundstrom B, et al. Human Antibody Production in Transgenic Animals. *Arch Immunol Ther Exp (Warsz).* 2015 Apr 3;63(2):101–8.
208. Brüggemann M, Caskey HM, Teale C, Waldmann H, Williams GT, Surani MA, et al. A repertoire of monoclonal antibodies with human heavy chains from transgenic mice. *Proceedings of the National Academy of Sciences.* 1989 Sep;86(17):6709–13.
209. Ligand Pharmaceuticals Inc. OmniAb Technologies [Internet]. [cited 2022 Sep 21]. Available from: <https://www.ligand.com/technologies/omniab>
210. McCafferty J, Griffiths AD, Winter G, Chiswell DJ. Phage antibodies: filamentous phage displaying antibody variable domains. *Nature.* 1990 Dec;348(6301):552–4.
211. Dübel S, Breitling F, Fuchs P, Braunagel M, Klewinghaus I, Little M. A family of vectors for surface display and production of antibodies. *Gene.* 1993 Jun;128(1):97–101.
212. Hanes J, Plückthun A. In vitro selection and evolution of functional proteins by using ribosome display. *Proceedings of the National Academy of Sciences.* 1997 May 13;94(10):4937–42.
213. Boder ET, Wittrup KD. Yeast surface display for screening combinatorial polypeptide libraries. *Nat Biotechnol.* 1997 Jun;15(6):553–7.
214. Roberts RW, Szostak JW. RNA-peptide fusions for the in vitro selection of peptides and proteins. *Proceedings of the National Academy of Sciences.* 1997 Nov 11;94(23):12297–302.
215. Ho M, Pastan I. Mammalian Cell Display for Antibody Engineering. In 2009. p. 337–52.
216. Dyson MR, Masters E, Pazeraitis D, Perera RL, Syrjanen JL, Surade S, et al. Beyond affinity: selection of antibody variants with optimal biophysical properties and reduced immunogenicity from mammalian display libraries. *MABs.* 2020 Jan 1;12(1).
217. Frenzel A, Kügler J, Helmsing S, Meier D, Schirrmann T, Hust M, et al. Designing Human Antibodies by Phage Display. *Transfusion Medicine and Hemotherapy.* 2017;44(5):312–8.

218. Pini A, Viti F, Santucci A, Carnemolla B, Zardi L, Neri P, et al. Design and Use of a Phage Display Library. *Journal of Biological Chemistry*. 1998 Aug;273(34):21769–76.
219. Ledsgaard L, Ljungars A, Rimbault C, Sørensen C v., Tulika T, Wade J, et al. Advances in antibody phage display technology. *Drug Discov Today*. 2022 Aug;27(8):2151–69.
220. Sivelles C, Sierocki R, Ferreira-Pinto K, Simon S, Maillere B, Nozach H. Fab is the most efficient format to express functional antibodies by yeast surface display. *MAbs*. 2018 Jul 4;10(5):720–9.
221. Zhou C, Shen WD. Mammalian Cell Surface Display of Full Length IgG. In: *Antibody Engineering* [Internet]. 2012. p. 293–302. Available from: http://link.springer.com/10.1007/978-1-61779-974-7_17
222. Robertson N, Lopez-Anton N, Gurjar SA, Khalique H, Khalaf Z, Clerkin S, et al. Development of a novel mammalian display system for selection of antibodies against membrane proteins. *Journal of Biological Chemistry*. 2020 Dec;295(52):18436–48.
223. Steinwand M, Droste P, Frenzel A, Hust M, Dübel S, Schirrmann T. The influence of antibody fragment format on phage display based affinity maturation of IgG. *MAbs*. 2014 Jan 26;6(1):204–18.
224. Zhang L, Cong Y, Li H, Chen L, Li B, Huang JX, et al. Construction of a full-length antibody phage display vector. *J Immunol Methods*. 2021 Jul;494:113052.
225. Yu J, Song Y, Tian W. How to select IgG subclasses in developing anti-tumor therapeutic antibodies. *J Hematol Oncol*. 2020 Dec 5;13(1):45.
226. Chen CG, Fabri LJ, Wilson MJ, Panousis C. One-step zero-background IgG reformatting of phage-displayed antibody fragments enabling rapid and high-throughput lead identification. *Nucleic Acids Res*. 2014 Feb 1;42(4):e26–e26.
227. Liu Y, Gu M, Wu Y, Wang W, Wang R, Du M, et al. High-throughput reformatting of phage-displayed antibody fragments to IgGs by one-step emulsion PCR. *Protein Engineering, Design and Selection*. 2018 Nov 1;31(11):427–36.
228. Reader RH, Workman RG, Maddison BC, Gough KC. Advances in the Production and Batch Reformatting of Phage Antibody Libraries. *Mol Biotechnol*. 2019 Nov 29;61(11):801–15.
229. Sharma VK, Patapoff TW, Kabakoff B, Pai S, Hilario E, Zhang B, et al. In silico selection of therapeutic antibodies for development: Viscosity, clearance, and chemical stability. *Proceedings of the National Academy of Sciences*. 2014 Dec 30;111(52):18601–6.
230. Raybould MIJ, Marks C, Krawczyk K, Taddese B, Nowak J, Lewis AP, et al. Five computational developability guidelines for therapeutic antibody profiling. *Proceedings of the National Academy of Sciences*. 2019 Mar 5;116(10):4025–30.
231. Xu Y, Wang D, Mason B, Rossomando T, Li N, Liu D, et al. Structure, heterogeneity and developability assessment of therapeutic antibodies. *MAbs*. 2019 Feb 17;11(2):239–64.
232. Joshi V, Yadav N, Rathore AS. Aggregation of Monoclonal Antibody Products: Formation and Removal [Internet]. *BioPharm International*. 2013 [cited 2022 Sep 27]. Available from: <https://www.biopharminternational.com/view/aggregation-monoclonal-antibody-products-formation-and-removal>
233. Bansal R, Dash R, Rathore AS. Impact of mAb Aggregation on Its Biological Activity: Rituximab as a Case Study. *J Pharm Sci*. 2020 Sep;109(9):2684–98.
234. Buck PM, Chaudhri A, Kumar S, Singh SK. Highly Viscous Antibody Solutions Are a Consequence of Network Formation Caused by Domain–Domain Electrostatic Complementarities: Insights from Coarse-Grained Simulations. *Mol Pharm*. 2015 Jan 5;12(1):127–39.
235. Wolf Pérez AM, Sormanni P, Andersen JS, Sakhnini LI, Rodriguez-Leon I, Bjelke JR, et al. In vitro and in silico assessment of the developability of a designed monoclonal antibody library. *MAbs*. 2019 Feb 17;11(2):388–400.
236. Beck A, Liu H. Macro- and Micro-Heterogeneity of Natural and Recombinant IgG Antibodies. *Antibodies* [Internet]. 2019 Feb 19;8(1):18. Available from: <http://www.mdpi.com/2073-4468/8/1/18>
237. Giese G, Williams A, Rodriguez M, Persson J. Bispecific antibody process development: Assembly and purification of knob and hole bispecific antibodies. *Biotechnol Prog*. 2018 Mar;34(2):397–404.

238. Reichert J, Hutchinson N. Development and Manufacture of Therapeutic Bispecific Antibodies [Internet]. BioProcess International. 2022 [cited 2022 Sep 27]. Available from: <https://bioprocessintl.com/2022/january-february-2022-featured-report/development-and-manufacture-of-therapeutic-bispecific-antibodies/>
239. Matucci A, Vultaggio A, Danesi R. The use of intravenous versus subcutaneous monoclonal antibodies in the treatment of severe asthma: a review. *Respir Res*. 2018 Dec 16;19(1):154.
240. Pitiot A, Heuzé-Vourc'h N, Sécher T. Alternative Routes of Administration for Therapeutic Antibodies—State of the Art. *Antibodies*. 2022 Aug 26;11(3):56.
241. Fucà G, Spagnoletti A, Ambrosini M, de Braud F, di Nicola M. Immune cell engagers in solid tumors: promises and challenges of the next generation immunotherapy. *ESMO Open*. 2021 Feb;6(1):100046.
242. Shin HG, Yang HR, Yoon A, Lee S. Bispecific Antibody-Based Immune-Cell Engagers and Their Emerging Therapeutic Targets in Cancer Immunotherapy. *Int J Mol Sci*. 2022 May 19;23(10):5686.
243. Zhou S, Liu M, Ren F, Meng X, Yu J. The landscape of bispecific T cell engager in cancer treatment. *Biomark Res* [Internet]. 2021 Dec 26;9(1):38. Available from: <https://biomarkerres.biomedcentral.com/articles/10.1186/s40364-021-00294-9>
244. Elshiaty M, Schindler H, Christopoulos P. Principles and Current Clinical Landscape of Multispecific Antibodies against Cancer. *Int J Mol Sci* [Internet]. 2021 May 26;22(11):5632. Available from: <https://www.mdpi.com/1422-0067/22/11/5632>
245. Cheadle EJ. MT-103 Micromet/MedImmune. *Curr Opin Mol Ther*. 2006 Feb;8(1):62–8.
246. Gupta A, Kumar Y. Bispecific antibodies: a novel approach for targeting prominent biomarkers. *Hum Vaccin Immunother*. 2020 Nov 1;16(11):2831–9.
247. Hombach A, Köhler H, Rappl G, Abken H. Human CD4+ T Cells Lyse Target Cells via Granzyme/Perforin upon Circumvention of MHC Class II Restriction by an Antibody-Like Immunoreceptor. *The Journal of Immunology*. 2006 Oct 15;177(8):5668–75.
248. Krähenbühl O, Tschopp J. Involvement of granule proteins in T-cell-mediated cytotoxicity. *Nat Immun Cell Growth Regul*. 1990;9(4):274–82.
249. Goebeler ME, Bargou R. Blinatumomab: a CD19/CD3 bispecific T cell engager (BiTE) with unique anti-tumor efficacy. *Leuk Lymphoma* [Internet]. 2016 May 3;57(5):1021–32. Available from: <http://www.tandfonline.com/doi/full/10.3109/10428194.2016.1161185>
250. Wu J, Fu J, Zhang M, Liu D. Blinatumomab: a bispecific T cell engager (BiTE) antibody against CD19/CD3 for refractory acute lymphoid leukemia. *J Hematol Oncol* [Internet]. 2015 Dec 4;8(1):104. Available from: <http://www.jhoonline.org/content/8/1/104>
251. Burt R, Warcel D, Fielding AK. Blinatumomab, a bispecific B-cell and T-cell engaging antibody, in the treatment of B-cell malignancies. *Hum Vaccin Immunother* [Internet]. 2019 Mar 4;15(3):594–602. Available from: <https://www.tandfonline.com/doi/full/10.1080/21645515.2018.1540828>
252. Linke R, Klein A, Seimetz D. Catumaxomab. *MAbs* [Internet]. 2010 Mar 27;2(2):129–36. Available from: <http://www.tandfonline.com/doi/abs/10.4161/mabs.2.2.11221>
253. Wu Y, Yi M, Zhu S, Wang H, Wu K. Recent advances and challenges of bispecific antibodies in solid tumors. *Exp Hematol Oncol* [Internet]. 2021 Dec 18;10(1):56. Available from: <https://ehoonline.biomedcentral.com/articles/10.1186/s40164-021-00250-1>
254. Jain T, Litzow MR. Management of toxicities associated with novel immunotherapy agents in acute lymphoblastic leukemia. *Ther Adv Hematol* [Internet]. 2020 Jan 20;11:204062071989989. Available from: <http://journals.sagepub.com/doi/10.1177/2040620719899897>
255. Frey N v., Porter DL. Cytokine release syndrome with novel therapeutics for acute lymphoblastic leukemia. *Hematology* [Internet]. 2016 Dec 2;2016(1):567–72. Available from: <https://ashpublications.org/hematology/article/2016/1/567/20992/Cytokine-release-syndrome-with-novel-therapeutics>
256. Li X, Shao M, Zeng X, Qian P, Huang H. Signaling pathways in the regulation of cytokine release syndrome in human diseases and intervention therapy. *Signal Transduct Target Ther* [Internet]. 2021 Dec 20;6(1):367. Available from: <https://www.nature.com/articles/s41392-021-00764-4>

-
257. Teachey DT, Rheingold SR, Maude SL, Zugmaier G, Barrett DM, Seif AE, et al. Cytokine release syndrome after blinatumomab treatment related to abnormal macrophage activation and ameliorated with cytokine-directed therapy. *Blood*. 2013 Jun 27;121(26):5154–7.
258. Ma J, Mo Y, Tang M, Shen J, Qi Y, Zhao W, et al. Bispecific Antibodies: From Research to Clinical Application. *Front Immunol* [Internet]. 2021 May 5;12. Available from: <https://www.frontiersin.org/articles/10.3389/fimmu.2021.626616/full>
259. Chen W, Yang F, Wang C, Narula J, Pascua E, Ni I, et al. One size does not fit all: navigating the multi-dimensional space to optimize T-cell engaging protein therapeutics. *MAbs* [Internet]. 2021 Jan 1;13(1). Available from: <https://www.tandfonline.com/doi/full/10.1080/19420862.2020.1871171>
260. Wang S, Chen K, Lei Q, Ma P, Yuan AQ, Zhao Y, et al. The state of the art of bispecific antibodies for treating human malignancies. *EMBO Mol Med* [Internet]. 2021 Sep 7;13(9). Available from: <https://onlinelibrary.wiley.com/doi/10.15252/emmm.202114291>
261. Haber L, Olson K, Kelly MP, Crawford A, DiLillo DJ, Tavaré R, et al. Generation of T-cell-redirecting bispecific antibodies with differentiated profiles of cytokine release and biodistribution by CD3 affinity tuning. *Sci Rep* [Internet]. 2021 Dec 13;11(1):14397. Available from: <http://www.nature.com/articles/s41598-021-93842-0>
262. Dang K, Castello G, Clarke SC, Li Y, Balasubramani A, Boudreau A, et al. Attenuating CD3 affinity in a PSMAxCD3 bispecific antibody enables killing of prostate tumor cells with reduced cytokine release. *J Immunother Cancer* [Internet]. 2021 Jun 4;9(6):e002488. Available from: <https://jitc.bmj.com/lookup/doi/10.1136/jitc-2021-002488>
263. Staffin K, Zuch de Zafra CL, Schutt LK, Clark V, Zhong F, Hristopoulos M, et al. Target arm affinities determine preclinical efficacy and safety of anti-HER2/CD3 bispecific antibody. *JCI Insight* [Internet]. 2020 Apr 9;5(7). Available from: <https://insight.jci.org/articles/view/133757>
264. Tapia-Galisteo A, Sánchez Rodríguez Í, Aguilar-Sopeña O, Harwood SL, Narbona J, Ferreras Gutierrez M, et al. Trispecific T-cell engagers for dual tumor-targeting of colorectal cancer. *Oncoimmunology* [Internet]. 2022 Dec 31;11(1). Available from: <https://www.tandfonline.com/doi/full/10.1080/2162402X.2022.2034355>
265. Wu L, Seung E, Xu L, Rao E, Lord DM, Wei RR, et al. Trispecific antibodies enhance the therapeutic efficacy of tumor-directed T cells through T cell receptor co-stimulation. *Nat Cancer* [Internet]. 2020 Jan 18;1(1):86–98. Available from: <https://www.nature.com/articles/s43018-019-0004-z>
266. Austin RJ, Lemon BD, Aaron WH, Barath M, Culp PA, DuBridg RB, et al. TriTACs, a Novel Class of T-Cell-Engaging Protein Constructs Designed for the Treatment of Solid Tumors. *Mol Cancer Ther*. 2021 Jan 1;20(1):109–20.
267. Johnson ML, Dy GK, Mamdani H, Dowlati A, Schoenfeld AJ, Pacheco JM, et al. Interim results of an on-going Phase 1/2 study of HPN328, a tri-specific half-life extended DLL3-targeting T-cell engager, in patients with small cell lung cancer and other neuroendocrine cancers. In: American Society of Clinical Oncology Annual Meeting. 2022.
268. Madan S, Abdallah AO, Cowan A, Bensinger W, Hillengass J, Leleu X, et al. An interim report on a Phase 1/2 study of HPN217, a half-life extended tri-specific T cell activating construct (TriTAC) targeting B cell maturation antigen for the treatment of relapsed/refractory multiple myeloma. In: American Society of Hematology Annual Meeting. 2021.
269. Molloy ME, Austin RJ, Lemon BD, Aaron WH, Ganti V, Jones A, et al. Preclinical Characterization of HPN536, a Trispecific, T-Cell-Activating Protein Construct for the Treatment of Mesothelin-Expressing Solid Tumors. *Clinical Cancer Research*. 2021 Mar 1;27(5):1452–62.
270. Moreau P, Garfall AL, van de Donk NWCJ, Nahi H, San-Miguel JF, Oriol A, et al. Teclistamab in Relapsed or Refractory Multiple Myeloma. *New England Journal of Medicine*. 2022 Aug 11;387(6):495–505.
271. Pillarisetti K, Powers G, Luistro L, Babich A, Baldwin E, Li Y, et al. Teclistamab is an active T cell-redirecting bispecific antibody against B-cell maturation antigen for multiple myeloma. *Blood Adv*. 2020 Sep 22;4(18):4538–49.
272. Chen S, Lai SWT, Brown CE, Feng M. Harnessing and Enhancing Macrophage Phagocytosis for Cancer Therapy. *Front Immunol*. 2021 Mar 10;12.
-

-
273. Yasunaga M. Antibody therapeutics and immunoregulation in cancer and autoimmune disease. *Semin Cancer Biol.* 2020 Aug;64:1–12.
274. Shi Y, Fan X, Deng H, Brezski RJ, Ryczyn M, Jordan RE, et al. Trastuzumab Triggers Phagocytic Killing of High HER2 Cancer Cells In Vitro and In Vivo by Interaction with Fcγ Receptors on Macrophages. *The Journal of Immunology.* 2015 May 1;194(9):4379–86.
275. Stewart R, Hammond SA, Oberst M, Wilkinson RW. The role of Fc gamma receptors in the activity of immunomodulatory antibodies for cancer. *J Immunother Cancer.* 2014 Dec 19;2(1):29.
276. Abdin SM, Paasch D, Morgan M, Lachmann N. CARs and beyond: tailoring macrophage-based cell therapeutics to combat solid malignancies. *J Immunother Cancer.* 2021 Aug 30;9(8):e002741.
277. Nimmerjahn F, Ravetch J v. Fcγ receptors as regulators of immune responses. *Nat Rev Immunol.* 2008 Jan;8(1):34–47.
278. van Duijn A, van der Burg SH, Scheeren FA. CD47/SIRPα axis: bridging innate and adaptive immunity. *J Immunother Cancer.* 2022 Jul 13;10(7):e004589.
279. Andrejeva G, Capoccia BJ, Hiebsch RR, Donio MJ, Darwech IM, Puro RJ, et al. Novel SIRPα Antibodies That Induce Single-Agent Phagocytosis of Tumor Cells while Preserving T Cells. *The Journal of Immunology.* 2021 Feb 15;206(4):712–21.
280. Chauchet X, Cons L, Chatel L, Daubeuf B, Didelot G, Moine V, et al. CD47xCD19 bispecific antibody triggers recruitment and activation of innate immune effector cells in a B-cell lymphoma xenograft model. *Exp Hematol Oncol.* 2022 Dec 10;11(1):26.
281. Yang Y, Yang Z, Yang Y. Potential Role of CD47-Directed Bispecific Antibodies in Cancer Immunotherapy. *Front Immunol.* 2021 Jul 8;12.
282. Reis-Sobreiro M, Teixeira da Mota A, Jardim C, Serre K. Bringing Macrophages to the Frontline against Cancer: Current Immunotherapies Targeting Macrophages. *Cells.* 2021 Sep 9;10(9):2364.
283. Kedage V, Ellerman D, Chen Y, Liang WC, Borneo J, Wu Y, et al. Harnessing MerTK agonism for targeted therapeutics. *MAbs.* 2020 Jan 1;12(1).
284. Elshiaty M, Schindler H, Christopoulos P. Principles and Current Clinical Landscape of Multispecific Antibodies against Cancer. *Int J Mol Sci.* 2021 May 26;22(11):5632.
285. Jin S, Sun Y, Liang X, Gu X, Ning J, Xu Y, et al. Emerging new therapeutic antibody derivatives for cancer treatment. *Signal Transduct Target Ther.* 2022 Dec 7;7(1):39.
286. Brinkmann U, Kontermann RE. The making of bispecific antibodies. *MAbs.* 2017 Feb 17;9(2):182–212.
287. Felices M, Lenvik TR, Davis ZB, Miller JS, Vallera DA. Generation of BiKEs and TriKEs to Improve NK Cell-Mediated Targeting of Tumor Cells. In 2016. p. 333–46.
288. Felices M, Warlick E, Juckett M, Weisdorf D, Vallera D, Miller S, et al. 444 GTB-3550 tri-specific killer engager TriKE™ drives NK cells expansion and cytotoxicity in acute myeloid leukemia (AML) and myelodysplastic syndromes (MDS) patients. *J Immunother Cancer.* 2021 Nov;9(Suppl 2):A473–A473.
289. GT Biopharma Inc. Pipeline [Internet]. [cited 2022 Sep 13]. Available from: <https://www.gtbiopharma.com/product-pipeline/overview>
290. Felices M, Kodal B, Hinderlie P, Kaminski MF, Cooley S, Weisdorf DJ, et al. Novel CD19-targeted TriKE restores NK cell function and proliferative capacity in CLL. *Blood Adv.* 2019 Mar 26;3(6):897–907.
291. Schmohl JU, Felices M, Todhunter D, Taras E, Miller JS, Vallera DA. Tetraspecific scFv construct provides NK cell mediated ADCC and self-sustaining stimuli via insertion of IL-15 as a cross-linker. *Oncotarget.* 2016 Nov 8;7(45):73830–44.
292. Egan TJ, Diem D, Weldon R, Neumann T, Meyer S, Urech DM. Novel multispecific heterodimeric antibody format allowing modular assembly of variable domain fragments. *MAbs.* 2017 Jan 2;9(1):68–84.
293. NCI Dictionaries. anti-CD19/CD3/PD-L1/4-1BB tetra-specific antibody GNC-038 [Internet]. [cited 2022 Sep 13]. Available from: <https://www.cancer.gov/publications/dictionaries/cancer-drug/def/emfizatamab>

-
294. Innostar. The first tetraspecific antibody declared clinically: PD-L1/4-1BB/CD3/CD19 of Baily Pharmaceutical Co., Ltd. [Internet]. 2020 [cited 2022 Sep 13]. Available from: <https://www.innostar.cn/en/index/Lists/show/catid/21/id/205.html>
 295. Castoldi R, Schanzer J, Panke C, Jucknischke U, Neubert NJ, Croasdale R, et al. TetraMabs: simultaneous targeting of four oncogenic receptor tyrosine kinases for tumor growth inhibition in heterogeneous tumor cell populations. *Protein Engineering Design and Selection*. 2016 Oct;29(10):467–75.
 296. Hu S, Fu W, Xu W, Yang Y, Cruz M, Berezov SD, et al. Four-in-One Antibodies Have Superior Cancer Inhibitory Activity against EGFR, HER2, HER3, and VEGF through Disruption of HER/MET Crosstalk. *Cancer Res*. 2015 Jan 1;75(1):159–70.
 297. Croasdale R, Klein C, Schaefer W, Schanzer JM. Tri- or tetraspecific antibodies. Switzerland: F. Hoffmann-La Roche; WO 2010/136172, 2010.

4 Cumulative Section

4.1 From cell line development to the formulated drug product: The art of manufacturing therapeutic monoclonal antibodies.

Title:

From cell line development to the formulated drug product: The art of manufacturing therapeutic monoclonal antibodies

Authors:

Stefania Candela Carrara, Michael Ulitzka, Julius Grzeschik, Henri Kornmann, Björn Hock, Harald Kolmar

Bibliographic Data:

Journal – *International Journal of Pharmaceutics*

Volume 594

Article published: 10th December 2020

DOI: 10.1016/j.ijpharm.2020.120164

PMID: 33309833

Copyright © 2020. Published by Elsevier B.V.

Contribution by S.C. Carrara:

- Literature search and summarizing ideas
- Manuscript writing
- Generation of all figures



Review

From cell line development to the formulated drug product: The art of manufacturing therapeutic monoclonal antibodies

Stefania C. Carrara^{a,b}, Michael Ulitzka^{a,b}, Julius Grzeschik^b, Henri Kornmann^c, Björn Hock^{c,*}, Harald Kolmar^{a,**}

^a Institute for Organic Chemistry and Biochemistry, Technische Universität Darmstadt, Alarich-Weiss-Strasse 4, D-64287 Darmstadt, Germany

^b Ferring Darmstadt Laboratory, Alarich-Weiss-Strasse 4, D-64287 Darmstadt, Germany

^c Ferring International Center SA, CH-1162 Saint-Prex, Switzerland



ARTICLE INFO

Keywords:

Therapeutic antibodies
Manufacturing
Formulation
QbD
Route of administration

ABSTRACT

Therapeutic monoclonal antibodies and related products have steadily grown to become the dominant product class within the biopharmaceutical market. Production of antibodies requires special precautions to ensure safety and efficacy of the product. In particular, minimizing antibody product heterogeneity is crucial as drug substance variants may impair the activity, efficacy, safety, and pharmacokinetic properties of an antibody, consequently resulting in the failure of a product in pre-clinical and clinical development. This review will cover the manufacturing and formulation challenges and advances of therapeutic monoclonal antibodies, focusing on improved processes to minimize variants and ensure batch-to-batch consistency. Processes put in place by regulatory agencies, such as Quality-by-Design (QbD) and current Good Manufacturing Practices (cGMP), and how their implementation has aided drug development in pharmaceutical companies will be reviewed. Advances in formulation and considerations on the intended use of a therapeutic antibody, including the route of administration and patient compliance, will be discussed.

1. Introduction to therapeutic antibodies

Over the past 20 years, therapeutic monoclonal antibodies (mAbs) have become increasingly important in the fight against various diseases. Across several therapeutic areas, such as oncology, hematology, and immunology, mAbs have become the treatment modality of choice (Lu et al., 2020). As of August 18th, 2020, 97 therapeutic mAbs have been approved in the United States or Europe by the U.S. Federal Drug and Food Administration (FDA) or European Medicines Agency (EMA), respectively, of which more than one third are for the treatment of different cancers ('The Antibody Society', 2020). The first mAb approved for therapeutic use was in 1986, namely orthoclone OKT3 (Muromonab®), a murine monoclonal antibody targeting CD3, which was approved for the treatment of kidney transplantation rejection (Kung et al., 1979; Ribatti, 2014). The latest FDA-approved mAb is satralizumab (Enspryng®), approved in August 2020, for the treatment of neuromyelitis optica spectrum disorders by targeting interleukin 6 receptor (IL-6R) ('The Antibody Society', 2020). As of 2018, the global

mAb market was valued at US\$115.2 billion and is expected to continue growing at an increasing pace, reaching US\$300 billion by 2025. Seven companies rule 87% of the market, i.e., Genentech, AbbVie, Johnson & Johnson, Bristol-Myers Squibb, Merck Sharpe & Dohme, Novartis, and Amgen, with all other companies making up the remaining 13%. Adalimumab (Humira®), targeting TNF α , has reported the highest sales figures for a biopharmaceutical in history, with nearly US\$20 billion in sales in 2018 (Lu et al., 2020). A detailed list of U.S. FDA-approved mAbs was recently reviewed by Lu and co-workers and can be found elsewhere (Lu et al., 2020). Additionally, there are currently 88 antibodies under late-stage clinical trials for several indications, with a handful for the treatment of COVID-19. Several mAbs have been summarized in Table 1; however, a full list is available from 'The Antibody Society' (2020). Due to platform-based approaches, mAb products are easily adjusted for production and demonstrate a lower safety risk in clinical trials compared to other modalities. Thus, mAbs have become the go-to modality for first drug candidates against new targets, as they provide a rapid route for new therapeutics or proof-of-concept studies, thus

* Corresponding author at: Global Pharmaceutical Research and Development, Ferring Pharmaceuticals, CH-1162 Saint-Prex, Switzerland.

** Corresponding author.

E-mail addresses: bjorn.hock@ferring.com (B. Hock), kolmar@biochemie-tud.de (H. Kolmar).

<https://doi.org/10.1016/j.ijpharm.2020.120164>

Received 3 September 2020; Received in revised form 23 November 2020; Accepted 6 December 2020

Available online 10 December 2020

0378-5173/© 2020 Elsevier B.V. All rights reserved.

driving the continued growth of the mAb market (Ecker et al., 2015).

The use and success of monoclonal antibodies for therapeutic applications is mainly due to their high specificity, resulting from their complex glycoprotein structure. mAbs are immunoglobulins (Ig), of which there are five sub-classes: IgA, IgD, IgE, IgG, and IgM, with IgG being the most relevant isotype for therapeutic use (Awwad and Angkawinitwong, 2018). IgGs have a molecular weight of approximately 150 kilodalton (kDa) and are Y-shaped molecules consisting of three equal-sized parts connected with a flexible hinge. IgG molecules are made up of four polypeptide chains, comprising two heavy (H) chains, of roughly 50 kDa, and two light (L) chains of 25 kDa. The two arms of the Y-shaped structures, termed fragment antigen-binding (Fab) fragments, include the so-called variable regions that vary between different mAbs, and are responsible for antigen-binding. On the other hand, the stem of the Y, termed the constant region, is less variable and interacts with effector cells and molecules, known as the Fc fragment (Fig. 1).

With the development of hybridoma technology in 1975, Köhler and Milstein have paved the way for modern mAb technologies (Köhler and Milstein, 1975). In addition, display technologies such as phage display (Smith, 1985) or yeast display (Boder and Wittrup, 1998) are nowadays used for the generation of antibodies (Liu, 2014). Technological advances in the generation of mAbs are not within this review's scope but have been recently reviewed by Lu et al. (2020). Drug discovery begins with millions of potential drug candidates. Nonetheless, resource-intensive steps, such as developing a manufacturing process, are typically only carried out for a single variant after extensive screening and characterization. These qualification studies include *in vitro* and *in vivo* pharmacokinetic (PK) and pharmacodynamic (PD) experiments, as well as animal safety studies (Jarasch et al., 2015).

In theory, mAbs are defined by a unique primary structure of amino acids. However, in reality, a single dose of a mAb product represents a plethora of variants inherent to the biotechnological procedure used to manufacture these drug products. Heterogeneity of monoclonal antibodies arises from different sources throughout process development, but variations may start through errors during gene transcription and translation. The use of protein engineering and improved manufacturability techniques can be applied to minimize mAb variants and increase

batch-to-batch consistency. The reduction of such variants is a crucial requirement as they may impair an antibody's activity, efficacy, safety, and/or pharmacokinetic properties, ultimately resulting in the failure of a product in pre-clinical and clinical trials. Manufacturing and formulation of lead candidates are critical aspects that are often overlooked in drug discovery and early drug development. This review summarizes the challenges and recent technological advances used to minimize mAb heterogeneity during the manufacturing process and improve the formulability of a drug product.

2. Manufacturing of therapeutic antibodies

2.1. Industrial process of manufacturing and current GMP milestones

Throughout the years, optimization efforts in process development have been devoted to decrease process time, and development costs per antibody (Gronemeyer et al., 2014). Moreover, reducing mAb variants, process impurities, and delivering batch-to-batch consistency are key deliverables of process development. The manufacturing process can be summarized into five steps: (1) development of a stable and productive cell line expressing the gene of interest, (2) production of the desired antibody in host cells in high titres, (3) drug substance purification, (4) formulation steps and appropriate dosage forms (Fill & Finish), and (5) analytical testing methods to monitor the processes and evaluate the final product. The first two stages correspond to upstream processing (USP) operations, while the next three are considered downstream processing (DSP) activities and analytical testing operations carried out in quality control laboratories (Steinmeyer and McCormick, 2008). Owing to the structural similarity of mAbs, platform process technologies can be developed. The platform process includes the host system for cell culture, pre-engineered vectors for transformation, pre-defined cell amplification scheme, bioreactor conditions, high performance purification systems and well-validated analytical methods (Steinmeyer and McCormick, 2008).

During mAb production, one of the most critical steps is the choice of a cell line. The cells must propagate well, be highly stable in culture and produce high mAb titres in its active form, meaning the protein is folded

Table 1

Summary of mAb candidates in late-stage clinical trials. Data was extracted from 'The Antibody Society' (2020).

INN or code name – Sponsoring company	Molecular format	Target	Phase	Indication (pivotal phase 2, phase 2/3, or phase 3)
Envaflimab (KN035) – Alphamab Oncology	Single domain mAb	PD-L1	Phase 3	Bile tract carcinoma (NCT03478488)
Balstilimab (AGEN2034) – Agenus Inc.	Human IgG4	PD-1	Phase 2 (pivotal)	Cervical cancer (NCT03894215, NCT03104699, NCT03495882)
Utomilumab – Pfizer	Human IgG2	4-1BB (CD137)	Phase 3	Diffuse large B cell lymphoma (NCT02951156)
Zolbetuximab – Astellas Pharma Inc.	Chimeric IgG1	Claudin-18.2	Phase 3	Gastro-esophageal junction adenocarcinoma (NCT03653507, NCT03504397)
GX3359609 – GlaxoSmithKline	Humanized IgG4	ICOS	Phase 2/3	Head and neck squamous cell carcinoma (NCT04128696)
TJ202, MOR202 – I-Mab Biopharma, Morphosys	Human IgG1	CD38	Phase 3	Multiple myeloma (NCT03952091)
Sabatolimab (MBG453) – Novartis Pharmaceuticals Corp.	Humanized IgG4	TIM-3	Phase 3	Myelodysplastic syndromes (NCT03946670, NCT04266301)
Lenzilumab – Humanigen, Inc.	Human IgG1	GM-CSF	Phase 3	COVID-19 (NCT04351152)
Vilobelimab (IFX-1, CaCP29) – InflaRx GmbH	Chimeric IgG4	C5a	Phase 2/3	COVID-19 (NCT04333420)
Mavrilimumab – Kiniksa Pharmaceuticals, Ltd.	Human IgG4	GM-CSFR	Phase 2/3	COVID-19 (NCT04447469)
REGN10933 + REGN10987 – Regeneron Pharmaceuticals, Inc.	Human mAbs	SARS CoV-2	Phase 3	COVID-19 (NCT04452318)
Brazikumab – Allergan	Human IgG2	IL-23	Phase 3	Crohn's disease (NCT03961815, NCT03759288)
Lecanemab (BAN2401) – Eisai Inc.	Humanized IgG1	Amyloid β protofibrils	Phase 3	Early Alzheimer's disease (NCT03887455)
Marstacimab – Pfizer	Human IgG1	Tissue factor pathway inhibitor	Phase 3	Hemophilia A or B (NCT03938792)
Ublituximab – TG Therapeutics	Chimeric IgG1	CD20	Phase 3; Phase 2/3	Multiple sclerosis (NCT03277261, NCT03277248, NCT04130997); chronic lymphocytic leukemia (NCT02301156, NCT02612311); Non-Hodgkin's Lymphoma (Phase 2/3, NCT02793583)

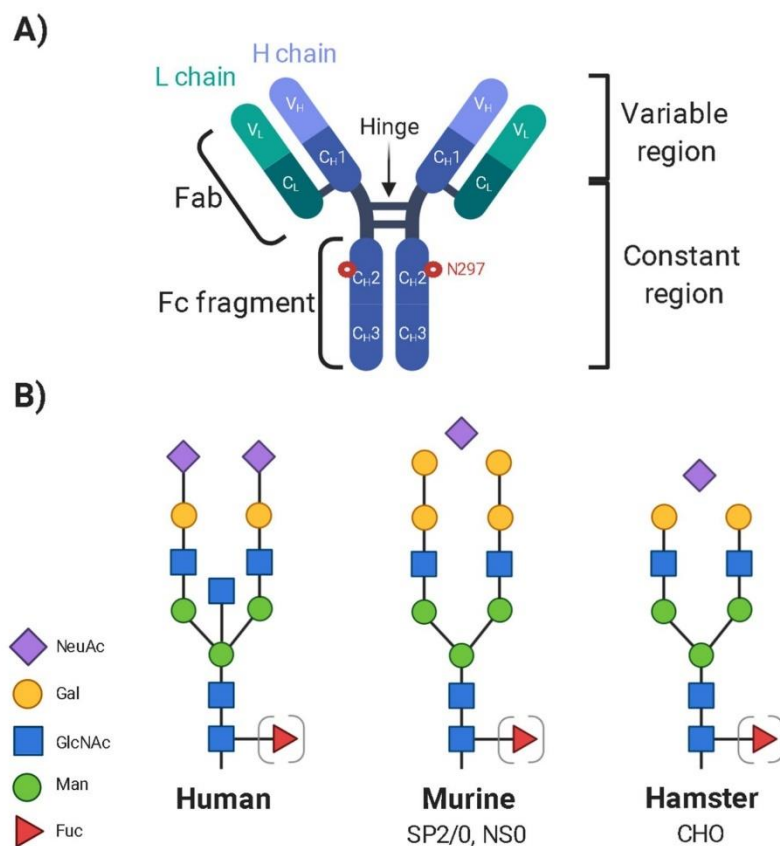


Fig. 1. Overview of IgG antibodies. A) Structure of IgG showing light (L) chains and heavy (H) chains in green and blue, respectively. The glycan-modification position N297 is depicted with red stars. B) N-glycan structure of monoclonal antibodies in different species. Abbreviations: NeuAc: N-acetylneuraminic acid, Man: mannose, Fuc: fucose, GlcNAc: N-acetylglucosamine, Gal: galactose. Adapted from Gomord et al., 2010. Created with BioRender.com. (For interpretation of the references to colour in this figure legend, the reader is referred to the web version of this article.)

correctly, glycosylated, and not aggregated. Thus, based on these requirements, mammalian cells are most commonly used as they are adapted for the production, processing, and secretion of highly complex molecules (Carvalho et al., 2017). Historically, the host cell line commonly used was NS0, a murine myeloma cell line. The widespread adoption of NS0 cells as a host cell system was hindered by the production of live murine leukaemia virus that required inactivation (Taylor et al., 2000). Used as the expression system for tissue plasminogen activator, one of the first approved biopharmaceuticals in 1986, Chinese hamster ovary (CHO) cells were used, and have remained the preferred choice for production since (Dahodwala et al., 2019; Dangi et al., 2018; Hogwood et al., 2013; Kunert and Reinhart, 2016; Park et al., 2017; Zhu, 2012). The preference for CHO cells is attributable to their rapid propagation and high expression titres, along with the absence of two glycan epitopes for humans, which are present in murine cell lines, e.g., NS0 and Sp2/0 (Fig. 1) (Gomord et al., 2010; Gronemeyer et al., 2014; Jefferis, 2009; Kelley, 2009; Kunert and Reinhart, 2016). Other human cell lines, such as human embryonic kidney (HEK) or PER. C6 cells, are also considered an adequate expression host. However, reports have shown increased *in vivo* heterogeneity compared to CHO cells (Kunert and Reinhart, 2016).

Cell line engineering and development aims at achieving higher cell titres to improve productivity and product quality. Optimisation efforts in cell culture medium, feed development, bioprocess development, and scale-up experiments are extensively reviewed by Gronemeyer et al. (2014). Engineering of CHO cells, for example, has resulted in cell lines capable of secreting up to 100 pg/cell/day of humanized mAbs (Page

and Sydenham, 1991) or 80–110 pg/cell/day of chimerized mAb (Fouser et al., 1992) in perfusion cultures. Nevertheless, the feed method implemented has a direct influence on mAb titres. The different feed methods are batch, fed-batch, or perfusion. In the batch method, all nutrients are added into the initial medium, whereas in fed-batch, nutrients are added as they become depleted. Perfusion means the medium is being circulated through the growing culture while keeping the cells in the bioreactor via filtration, removing waste, and supplying fresh nutrients to the cells (Dorceus et al., 2017). Fed-batch processing leads to mAb titres of 1–5 g/L, with some companies reporting up to 13 g/L using extended culturing conditions (Kelley, 2009). The different processes have been compared in the literature (Carvalho et al., 2017; Fan et al., 2018; Kunert and Reinhart, 2016; Ritacco et al., 2018).

At the heart of the biopharmaceutical process, cell culture medium provides the host cells with essential nutrients and the environment to achieve high viable cell density and efficient mAb expression ('CHO Media Development for Therapeutic Protein Production', 2019). Cell culture medium development for a fed-batch process consists of batch medium and feed concentrate development and feed strategy optimization. Due to the different nutrient consumption and metabolism of cell lines, this optimization stage is considered to be cell line-dependent. For decades, fully chemically-defined media have been employed in large-scale mAb production. The use of animal-derived raw materials, such as bovine serum, is avoided due to safety concerns for transmissible spongiform encephalopathy and other transmissible contaminants (Li et al., 2010; Ling, 2015; Pérez-Rodríguez et al., 2020).

Nevertheless, fully chemically-defined media do not always yield

high titres, and thus animal component-free hydrolysates are added to the media to increase cell density, viability, and productivity (Li et al., 2010). A detailed list of cell culture medium components and their effect on critical quality attributes is shown in Table 2. With perfusion cultures gaining tract, Kuiper and co-workers have developed a method for deriving perfusion culture media based on fed-batch media and feeds. While further optimization can be performed, the CHO cultures resulted in high productivity and product quality from a rapidly derived perfusion medium (Kuiper et al., 2019). Along with the cell culture nutrients, it has been shown that controlling the proliferation and maintaining a high viable cell density can lead to higher product yields (Oguchi et al., 2002). Changes in temperature, pH, or CO₂ levels can drastically influence their productivity (Becker et al., 2019; Kim and Lee, 2007; Oguchi et al., 2002; Seo et al., 2013). As shown by Kim and Lee (2007), even for two CHO-derived clones from the same parental clone, the cell lines exhibited different responses to culture conditions and maximum antibody concentration (Kim and Lee, 2007). While cell culture medium development is labor-intensive and time-consuming, high throughput scale-down screening in deep-96-well format can be performed to cut development time (Ritacco et al., 2018; Rouiller et al., 2013; Wang et al., 2018; Media Development, 2019).

Over the years, USP operations have seen titre and stability increases, and the focus has shifted to the optimization of DSP operations, particularly on improving yield, purity, and reducing mAb heterogeneity. After mAb production, DSP is responsible for the delivery of the active pharmaceutical ingredient (API), also referred to as bulk drug substance or drug substance (DS), to formulation and filling (Fill &

Finish). The formulated DS is then referred to as the drug product (DP) and is ready to be administered to patients. Novel technologies and the establishment of platform technologies based on Quality-by-Design (QbD) approaches have allowed for advancements in DSP operations. Focusing on chromatographic separations, mainly using Protein A chromatography, progress in column characteristics, including higher flow rate, longer life cycles, reduced run times, and increased binding capacity, has brought advances into DSP operations. However, non-chromatographic separations are of growing interest due to the high costs associated with chromatography. Non-chromatographic separation methods include the use of filtration, aqueous two-phase separations, precipitation, or crystallization methods (Gronemeyer et al., 2014; Kruse et al., 2019; O'Kennedy et al., 2016). These allow for high-volume feeds and rapid liquid removal, aiming at cost and process time reduction, as well as improved impurities and yield losses (Gronemeyer et al., 2014; Großhans et al., 2018; Thömmes et al., 2017).

Continuous manufacturing has combined the advantages of improved process performances and flexible manufacturing (Chahar et al., 2020; Großhans et al., 2018; Pollard et al., 2016). Compared to batch or hybrid manufacturing systems, continuous bioprocessing offers many advantages across several issues. Not only does it offer reduced capital investment costs, but it also allows for a flexible and standardized manufacturing process, facilitating the ability to meet demands in a timely manner. The reduction of molecule residence time in a bioreactor by using continuous technology also brings quality benefits. mAb modifications associated with bioreactor conditions (pH and temperature), e.g., deamidation, could be minimized through continuous

Table 2

Components of cell culture medium and their influence on critical quality attributes (CQAs). Data gathered and modified from Rathore et al. (2017).

Quality modification	Amino Acids	Sugars	Proteins	Lipids	Vitamins	Salt and trace elements	Others
Cell growth / titre	L-glutamine L-lysine	Maltose	Insulin Albumin Transferrin	Linoleic acid Lipoic acid	Inositol Riboflavin Folic acid Thiamine	Fe ²⁺ , Fe ³⁺ Zinc	Sodium butyrate / propionate Growth factors and hormones
Glycosylation	L-asparagine L-glutamine L-serine L-threonine	Mannose Galactose D-glucose				MgCl ₂ Zinc Copper sulfate	EDTA
Glycation	L-cysteine L-histidine	Galactose D-glucose				Cobalt MgCl ₂ MgSO ₄ Zinc Copper sulfate	
Fucosylation	L-cysteine L-glutamine	Mannose D-glucose					Kifunensine
Galatosylation	L-asparagine L-glutamine	Fructose Galactose D-glucose				MgCl ₂ MgSO ₄ Zinc Copper sulfate	
Sialylation	L-asparagine Aspartic acid L-cysteine L-glutamine L-isoleucine L-leucine L-tryptophan Valine	Galactose D-glucose		Glycerol		MnCl ₂	
Charge variants	L-cysteine L-lysine L-tryptophan	Mannose Sucrose D-glucose		Glycerol	Inositol Tocopherol Pyridoxine Vitamin B ₁₂	MnCl ₂ Fe ²⁺ , Fe ³⁺ NaCl Zinc Copper sulfate	Glutathione DMSO
Aggregates	L-cysteine	Trehalose		Glycerol		Fe ²⁺ , Fe ³⁺ NaCl Copper sulfate	Glutathione DMSO
LMW/HMW	L-cysteine					MnCl ₂ Fe ²⁺ , Fe ³⁺ Zinc Copper sulfate Cobalt	EDTA
Misincorporation	L-asparagine L-serine						

cultivation (Konstantinov and Cooney, 2015).

Trends have led to the use of disposables, with the benefits of having lower capital investment and operational costs, increased flexibility, improved production scheduling, and higher process replication (Eibl & Eibl, 2019; Gronemeyer et al., 2014). Single-use bioreactors and technologies are applicable to Good Manufacturing Practice (GMP) regulations and are available in sizes up to 2000 L (Gronemeyer et al., 2014; Jossen et al., 2019; Langer and Rader, 2019).

As the resulting drug product from downstream processing is ready to be administered to patients, precautions and regulations must be taken and followed to achieve product quality, safety, traceability, and reproducibility. Regulatory health authorities such as the World Health Organization (WHO), FDA, and EMA have described and constantly audit the so-called *current Good Manufacturing Practices* (cGMP). cGMP outlines measures to ensure that processes necessary for production and testing are clearly defined, validated, reviewed, and documented. By these definitions, products are ensured to be produced and controlled according to quality standards appropriate for their intended use and as required by product specification. Manufacturers and their facilities located in the European Economic Area (EEA) must hold authorization issued by a competent national authority and must comply with the European Union (EU) GMP requirements to obtain approval. The national authorities are then responsible for inspecting manufacturing sites and ensuring they are effectively following the EU GMP guidelines (European Medicines Agency, 2016). The GMP guidelines are based on the principles summarized in Fig. 2 (WHO, 1998). With the strict implementation and control of GMP, the drug product is traceable. Deviations and variations can be easily tracked, and action can be taken

accordingly to avoid putting the patient at risk or losing drug efficacy throughout the process.

2.2. Improved manufacturability of mAb variants

In the pharmaceutical and biotechnology industry, development programs of therapeutic mAbs may be delayed due to poor manufacturability. To circumvent any problems associated with protein stability, solubility, or sensitivity to stress, developability studies are performed early during the process. These experiments include short-term stability studies at different temperatures, freeze–thaw cycles, forced degradation studies, and viscosity determination at high sample concentrations (Yang et al., 2013). Considering that drug substance and drug product quality attributes are affected by minimal changes in the manufacturing process, all steps may be critical to material quality and patient safety. Thus, it is mandatory to minimize and control the level of antibody variants in the drug product.

As early as translation, variants can be formed in production cell lines through the misincorporation of amino acids, such as the incorporation of serine instead of asparagine in CHO cells. While both are neutral, polar amino acids with similar physical properties, this results in the generation of a different amino acid sequence, a phenomenon found to be caused by the starvation of a particular amino acid in cell medium (Khetan et al., 2010; Parker et al., 1978; Wen et al., 2009; Yu et al., 2009). Despite this, most variants originate from post-translational modifications (PTMs) or are generated during the manufacturing process. Alterations of a drug are considered critical quality attributes (CQA) if linked to stability, activity, or efficacy (Jacobi

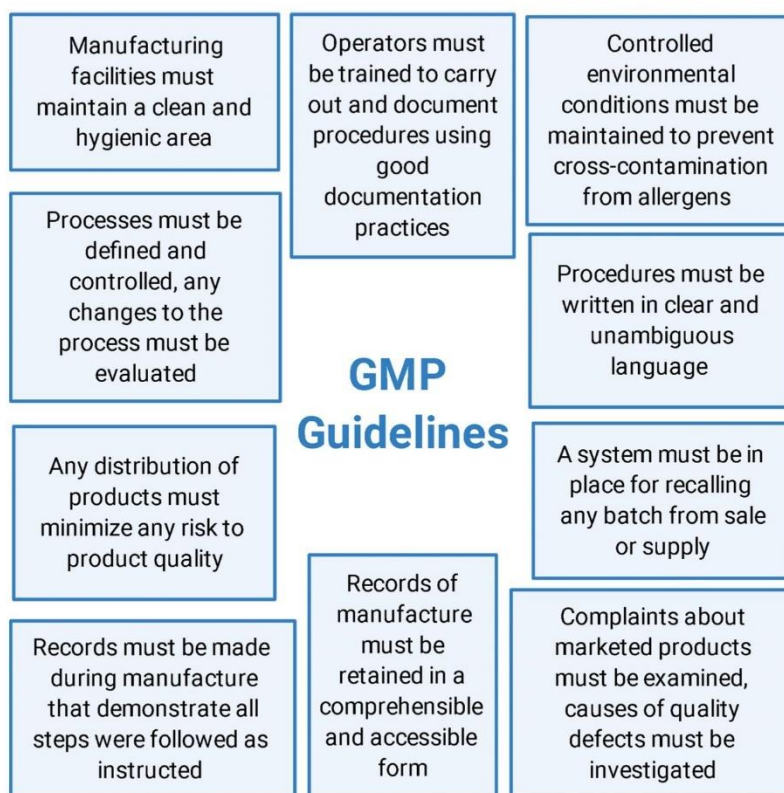


Fig. 2. Good Manufacturing Practices guidelines from World Health Organisation (WHO, 1998). Abbreviations: GMP: Good Manufacturing Practices. Created with BioRender.com.

et al., 2014). Thus, it is critical to thoroughly characterise and control PTMs throughout the process that may potentially impact the drug product's efficacy or safety (Zhou et al., 2020).

Major quality modifications are extensively described in the literature (Jacobi et al., 2014; Sissolak et al., 2019), and glycosylation variants are commonly known to influence pharmacokinetics, antigen-binding, and immunogenicity (Eon-Duval et al., 2012; Mimura et al., 2018). *A priori* knowledge and glycoengineering advances of therapeutic IgG antibodies provide opportunities to optimize safety, functionality, and efficacy of the drug (Sissolak et al., 2019). Examples of applying protein engineering techniques include amino acid exchanges to prevent aggregation, or avoiding methionine residues in complementary-determining regions (CDRs) to prevent impactful oxidation. mAb oxidation occurs primarily on methionine residues, leading to more polar side chains by the formation of methionine sulfoxide. Additionally, replacement of N-terminal residues by glutamine can be designed to reduce the number of charge variants arising upon pyroglutamate formation (Beck et al., 2010; Liu et al., 2011). Improvements in protein sequence modifications by *in silico* engineering and structure-based rational design simulations have provided advancements in predicting aggregation-prone regions, stability calculations, and solubility of a

monoclonal antibody (Arslan et al., 2019; Kuroda and Tsumoto, 2020; Sormanni et al., 2017). Furthermore, improvement of the thermodynamic stability of a monoclonal antibody can be monitored by experimental stress studies, including temperature, pH, and protease incubations, to select molecules more resistant to aggregation (Arslan et al., 2019; Enever et al., 2015; Tesar et al., 2017). Monoclonal antibody structures may be altered when exposed to different temperatures, pH and stress conditions, causing unwanted products that may exhibit increased immunogenicity and reduced efficacy and activity (Cui et al., 2017). Other protein engineering approaches have been described elsewhere (Chiu and Gilliland, 2016; Popplewell, 2015; Ulitzka et al., 2020; Yang et al., 2018). Table 3 summarizes the common mAb modifications leading to heterogeneous drug products and how these modifications are being addressed to reduce mAb variants during process development.

To detect and characterize heterogeneity caused by PTMs, researchers are constantly establishing sensitive and quantitative state-of-the-art technologies. Recent reports have shown the use of low-flow sheath-less capillary electrophoresis-mass spectrometry (Haselberg et al., 2018). Micro-heterogeneity can be detected utilizing a mass spectrometry (MS)-based approach composed of high-resolution native

Table 3

Modifications commonly found during mAb development. The type of heterogeneity caused by the modification, its potentially detrimental effect on the mAb, its causes, and possible solutions either in DSP operations or through protein engineering techniques are described.

Modification	Heterogeneity	Potential detrimental effects	Causes	Possible solutions or separation techniques	Reference
N-terminal modifications (PyroGlu, truncation, signal peptides)	Different mass and charge for Gln to PyroGlu	No expected detrimental effect on efficacy or safety	Environmental causes such as buffer composition, pH, and temperature during cell culture and purification	mAbs with pyroglutamate elute earlier than glutamine in cation exchange	(Beck and Liu, 2019; Beyer et al., 2018; Liu et al., 2014)
Asparagine (Asn) deamidation	Mass and charge	Potential impact on potency and immunogenicity, deamidation in CDR leads to diminished antigen binding	Abundant modification; pH- and temperature-dependent during manufacturing and storage	Structure-based predictions of deamidation propensity to design more stable mAbs, and recently applying machine learning to large LC-MS/MS datasets	(Beck and Liu, 2019; Delnar et al., 2019; Lu et al., 2019; Yan et al., 2018)
Aspartate (Asp) isomerization	Charge and hydrophobicity	Isomerization in CDRs lead to decreased antigen-binding affinity and may trigger an immune response	pH- and temperature-dependent chemical modification	Peptide mapping by LC-MS/MS to detect and minimize method-induced isomerization	(Lu et al., 2019; Rouse et al., 2017; Wakankar et al., 2007; Zhou et al., 2020)
Methionine (Met) Oxidation	Mass and hydrophobicity	Oxidation of Met in Fc showed impaired Fc-mediated activity, while oxidation in CDRs exhibits reduced antigen binding, and affects serum half-life	Caused by oxidation through radicals or singlet oxygen produced under thermal or light stress during storage, respectively	Avoiding methionine residues in CDRs. Oxidation species can be separated from the main antibody by chromatographic methods	(Beck et al., 2010; Beck and Liu, 2019; Dashivets et al., 2016; Masato et al., 2016; Mo et al., 2016; Sankar et al., 2018)
Cysteine-related modifications (trisulfide bond, interchain disulfide bond reduction)	Mass and charge	Interchain disulfide bond reduction: loss of product, reduced drug product stability Trisulfide bond: no impact on antigen binding or thermal stability, but appear to be more acidic	Interchain disulfide bond reduction: mechanical shear forces used for harvesting of cell culture supernatant Trisulfide bond: culture duration and feeding method	Interchain disulfide bond reduction: Cell culture redox potential control via an online redox probe Trisulfide bond: changing feeding strategy in cell culture, removing cysteine wash step during Protein A chromatography	(Beck and Liu, 2019; Du et al., 2018; Gu et al., 2010; Handlogten et al., 2020; Seibel et al., 2017)
Glycosylation	Mass and charge	May affect mAb stability, <i>in vivo</i> efficacy, and Fc-mediated effector functions	Glucose limitation in cell culture medium, as well as other cell culture conditions (pH, shear stress)	Feeding methods of cultures alter the glycosylation heterogeneity. Methods for the detection of glycosylation patterns include NMR, MS, HPLC, and CE. Engineering of CHO cells leading to defucosylation or sialylation improves properties of mAbs	(Esser-Skala et al., 2020; Irvine and Alter, 2020; Torkashvand and Vaziri, 2017; Q. Wang et al., 2018; Wang et al., 2020; Zheng et al., 2011)
Glycation	Mass and charge	Increased propensity of aggregation	Sugars used in cell culture medium composition, decomposition during storage to a lower degree	Reduction of glucose in fed batch cultures. Glycation species can be measured using boronate affinity HPLC. The recent development of kinetic models elucidates the contribution of factors to glycation	(Agarwal et al., 2019; Beck and Liu, 2019; Jacobitz et al., 2020; Miller et al., 2011; Quan et al., 2008; Yuk et al., 2011)

MS and targeted glycan profiling (Yang et al., 2017), or by combining multiple technologies as recently described by Camperi et al. (2020). A multidimensional setup involving a 4D-LC/MS method (Protein A reduction – RPLC – Digestion – RPLC/MS) allows the determination of PTM levels, including oxidation, deamidation, and succinimide formation by online peptide mapping analysis. For the accurate detection of mAb glycosylation patterns, a 3D-LC/MS workflow was developed using the same chromatographic system. The implementation of such multidimensional workflows demonstrates the potential to perform fast and reliable PTM monitoring during the manufacturing process (Camperi et al., 2020). Chemical modifications, such as oxidation, deamidation, and fragmentation, result in charge variants, which may influence both the *in vitro* and *in vivo* behavior of mAbs. By changing the binding behavior to their targets, tissue penetration, distribution, and pharmacokinetics may be impaired, and analysis of charge variants is therefore crucial. With a focus on acidic variants produced by modifications, Liu et al. (2020) described the use of free flow electrophoresis combined with MS. This allowed for the continuous sample separation and fluid phase fractionation of antibody charge isoforms, striving towards the separation of different charge isoforms and minimizing drug product heterogeneity.

Along with protein engineering efforts, the central goal of process development of biologics is the establishment of manufacturing technologies and processes that will generate consistency in different batches (Carson, 2005). Quality-by-design (QbD) was established and first developed by Joseph M. Juran in the early 1990s, who believed that quality should be designed into a product and that most quality crises and complications arose from the way a product was designed (Juran, 1992). Along with GMP, regulatory agencies encourage risk-based

approaches and have adopted the QbD principles since the early 2000s (Yu et al., 2014). By providing guidance on pharmaceutical development, QbD aims at facilitating the design of products and processes, ultimately maximizing the product's efficacy and safety profile while enhancing product manufacturability (Alt et al., 2016). The principles are described by the International Council for Harmonisation of Technical Requirements for Pharmaceuticals for Human Use (ICH) guideline documents, ICH Q8-11 (ICH; Yu et al., 2014). The objectives of pharmaceutical QbD include: (1) achieving meaningful product quality specifications based on clinical performance; (2) increasing process capability and reducing product variability and defects by enhancing product and process design; (3) facilitating the ability to identify root causes of failures; and (4) improving product development and manufacturing efficiencies (Yu et al., 2014). Of the QbD milestones, *critical quality attributes* (CQA) identifies the crucial characteristics of a product required to ensure quality from a patient's perspective. By identifying specifications or numerical ranges for CQAs, candidates may be ranked and discarded accordingly (Somma, 2007). Several QbD milestones are summarized in Fig. 3.

For improved manufacturability, the QbD paradigm has been incorporated into mAb-specific scenarios. Karlberg et al. (2018) reported the adoption of quantitative structure-activity relationship (QSAR)-type modelling by exploiting the structural characteristics of mAbs for directed QbD implementation, increasing both product and process understanding. For upstream processes, Nagashima et al. (2013) applied the QbD approach to mAb production in CHO cells, focusing on quality risk management using failure mode and effects analysis. By doing so, the authors identified potential critical process parameters (CPPs) and key performance indicators (KPI) that may impact quality

Target Product Profile (TPP)	Quality TPP (QTTP)	Process Risk Assessment (PRA)	Process Characterisation Study
Describe the intent of a product, and its desired features (indication, efficacy, safety, drug format, etc.)	Define quality characteristics of product to ensure quality is achieved. Attributes include: RoA, dosage form, bioavailability, stability, strength	Identify parameters for each manufacturing step and define critical quality attributes (CQA)	Examine variation of parameters identified by PRA to determine limits of variation. Leads to definition of CPP and non-CPP
Design Space	Control Strategy	Qualification Studies	Continued Process Verification
Represents combination and interaction of input variables and CPPs that demonstrate guarantee of quality	Description of: Input Materials Controls, In-process Controls, Parameter Controls, Product Characterisation, Process Monitoring	Studies of facilities, utilities and equipment. PPQ performed at full-scale to mimic the manufacturing operation	Demonstrate that process validation remains up-to-date across lifecycle of product Post-marketing activities

Fig. 3. Summary of Quality-by-Design milestones. Adapted from ICHQ11 guidelines document. *Abbreviations:* TPP: Target product profile, QTTP: quality target product profile, PRA: process risk assessment, CPP: critical process parameters, non-CPP: non-critical process parameters, PPQ: process performance qualification study. Created with BioRender.com.

attributes and gained further knowledge to mitigate any future cell culture-related issues (Nagashima et al., 2013). On a scale beyond single processes, Genentech participated in a pilot program launched in 2008 by the FDA in an effort to expand the implementation of QbD, leading to imperative improvement of QbD tools and concepts for following products (Alt et al., 2016; Finkler and Krummen, 2016). A recent report has also demonstrated the efficient implementation and feasibility of using QbD-based similarity assessment of a biosimilar mAb, using an adalimumab biosimilar to Humira® (E. Zhang et al., 2020). Today, QbD activities are fully integrated into product development phases and have led to more robust, and high-yielding manufacturing processes, ultimately resulting in increased clinical efficiency (Gronemeyer et al., 2014).

3. Formulation development

Compared to small molecules, biopharmaceutical drugs such as mAbs offer high specificity and potency, arising from their macromolecular structure. However, their structural complexity is the cause for challenges in formulation and delivery (Mitragotri et al., 2014). Formulability is defined as the suitability of a drug product to be formulated in a way appropriate for the desired route of administration (RoA) or delivery method. Its quality attributes include, but are not limited to, solubility, stability, viscosity, and aggregation. Early formulability assessment is an essential aspect in the development program of any new biopharmaceutical and is often not emphasized enough (Zurdo, 2013). In line with the QbD paradigm, the intended use of an antibody is considered and defined in the target product profile (TPP), usually during early stages of drug development. By completing a TPP, considerations into RoA, dosage form, bioavailability, and stability can be addressed in early stages (Fig. 3). Ultimately, every single aspect of development that affects the efficacy, cost, or simplicity of an antibody can become the difference between success and failure of a drug (Zurdo, 2013).

3.1. Route of administration

For pharmaceutical products, the preferred RoA is through oral administration (non-parental) due to increased safety, good patient compliance, ease of ingestion, and cost-effectiveness. However, the pitfall of macromolecular biopharmaceuticals is their limited bioavailability of only 1–2% by oral administration due to limited penetration across the intestinal epithelium, and increased susceptibility to enzymatic degradation in the intestinal lumen, owing to the polar surface charge and large MW of mAbs (Ovacik and Lin, 2018; Sifniotis et al., 2019; Zhao et al., 2013). In recent years, therapeutic antibodies with diverse RoA have been approved for the treatment of diseases. The most common RoA for mAbs are intravenous (IV), intramuscular (IM), or subcutaneous (SC) administrations, with injections being the principal source of delivery (Table 4) (Zurdo, 2013). Other administration methods, e.g., ocular delivery, also exist for site-specific drug administration and lowering of side effects by localized therapy (Homayun et al., 2019; Mandal et al., 2018). When compared to SC or IV, IM administration is not the ideal route of administration for mAbs due to low bioavailability (Homayun et al., 2019). IV administration is generally used for mAbs, whereas IM injections are most commonly used for vaccines (Mitragotri et al., 2014). Compared to other parental RoAs, SC injections are the most convenient as they facilitate patient self-administration and are the least invasive (Mitragotri et al., 2014; Zurdo, 2013). Despite that, however, SC formulations place considerable constraints in terms of stability, aggregation, and viscosity due to the need for high concentrated doses in low injection volumes (Viola et al., 2018; Zurdo, 2013).

In terms of pharmacokinetics, IV appears to be superior to SC injections due to faster absorption, higher bioavailability, shorter time to reach maximum serum concentration (T_{max}), and similar elimination

Table 4

Properties of different routes of administration (RoA) for monoclonal antibodies. Data gathered from Ortega et al. (2014), Ryman & Meibohm (2017), and Zhao et al. (2013).

RoA:	Intravenous (IV)	Subcutaneous (SC)	Intramuscular (IM)
Delivery frequency	Low frequency	High frequency	High frequency
Delivery time	Hours	Seconds	Seconds
Absorption	Fast absorption (T_{max} 0.5–4 h)	Slow absorption (T_{max} 1.7–13.5 days)	Slow absorption (T_{max} 2–14 days)
Bioavailability	100%	~65%	~80%
Half-Life	Similar for all routes		
Dose	Low	High	High
Concentration	Diluted solutions	High concentrations	High concentrations
Volume	High injection volume	Low injection volume	Low injection volume
Injection device	Saline drips, syringe	Vial and syringe, pre-filled syringe, pre-filled pen, autoinjectors	Syringe
Formulation for storage	Lyophilized powder for reconstitution, liquid formulations in vials or syringes	Liquid formulations containing excipients in single use syringes/pens	Lyophilized powder for reconstitution, liquid formulations in vials or syringes
Injection angle	25°	45°	90°
Immunogenicity	Low	Higher ADA events	Low
Patient compliance	Low (invasive, need for professional assistance)	Higher (self-administration, less invasive)	Low (invasive)

half-life (Table 4) (Matucci et al., 2018). Subcutaneous route results in slow absorption, with a slow increase in plasma concentration and delayed time of T_{max} , ranging from 1.7 to 13.5 days (Ortega et al., 2014; Ryman and Meibohm, 2017; Zhao et al., 2013). The longer T_{max} associated with slow lymphatic uptake is due to the limited flow rate of 1–2 mg kg⁻¹ h⁻¹ in the thoracic duct (Zhao et al., 2012). While the SC route offers more convenience to patients compared to IV administration, it was reported that SC administration resulted in a higher risk of immunogenicity (Hamuro et al., 2017). This observation was investigated by comparing the immunogenicity profiles of marketed mAbs by monitoring the formation and persistence of anti-drug antibody (ADA) events with either SC- or IV-formulations (Hamuro et al., 2017). ADA events can potentially impact the pharmacokinetics of the product by increasing or decreasing drug clearance or affecting its pharmacodynamics and efficacy. Tocilizumab (Actemra®), a humanized mAb against interleukin 6 receptor (IL-6R) for the treatment of rheumatoid arthritis (RA), was studied by IV and SC formulations in a phase 3 study in a Japanese cohort. After 24 weeks of treatment, ADAs were detected in 3.5% and 0% of patients for SC or IV administration, respectively. Trastuzumab (Herceptin®), a humanized IgG1 mAb against HER2, was first approved for IV injections and became the standard treatment for patients with HER2-positive breast cancer. An SC formulation was offered as a fixed-dose alternative to the weight-adjusted IV-formulated product, and a 2-fold increase in ADA incidence was observed for SC (14.6%) compared to IV (7.6%) route. Rituximab (MabThera®), an anti-CD20 chimeric IgG1 approved for non-Hodgkin's lymphoma, has a similar SC formulation to trastuzumab, but no difference in ADA incidence was reported between SC and IV routes (Hamuro et al., 2017). Further examples comparing IV and SC routes for therapeutic mAbs are described in the literature (Blair and Duggan, 2018; Matucci et al., 2018), and additional examples of dosing and administration methods of FDA- and EMA-approved mAbs are listed in Table 5. Despite the majority of therapeutic mAbs being administered through IV or SC routes, early drug development programs are still exploring novel delivery

Table 5

Characteristics (route of administration, mode of delivery, and dose strength) of several therapeutic mAbs approved by the FDA. **Abbreviations:** RoA: route of administration, IV: intravenous, SC: subcutaneous, IVP: intravenous pyelogram, PFS: pre-filled syringe, AI: autoinjector. Information gathered from [MedScape \(2020\)](#) and [Drugs@FDA \(2020\)](#).

INN (Trade Name)	Target	Indication	RoA	Dose strength	Mode of delivery
Erenumab (Alimovig®)	CGRP receptor	Migraines	SC	70 or 140 mg/ml	PFS, SureClick AI
Sarilumab (Kevzara®)	IL-6 receptor	Rheumatoid arthritis	SC	150 mg/1.14 ml, 200 mg/1.14 ml	PFS, pre-filled pen
Emicizumab (Hemlibra®)	Factor IXa / X	Haemophilia A	SC	30 mg/ml, 150 mg/ml	Injection, IV solution vial
Denosumab (Prolia®)	RANK L	Postmenopausal osteoporosis	SC	Prolia: 60 mg/ml Xgeva: 70 mg/ml	PFS or vial
Adalimumab (Humira®)	TNF-α	Rheumatoid arthritis	SC	40 mg/0.8 ml	PFS, pre-filled pen or vial
Trastuzumab (Herceptin®)	HER2	Breast cancer	IV/SC	IV: 21 mg/ml SC: (120 mg/2000units)/ml	IV: lyophilized powder, vial SC: single-dose vial
Rituximab (Mabthera)	CD20	Non-Hodgkin's lymphoma	IV/SC	IV: 10 mg/ml (10 and 50 ml vials) SC: (120 mg/2000units)/ml	IV: prepare and dilute in IV bag SC: Single-dose vial
Teprotumumab (Tepezza®)	IGF-R1	Thyroid eye disease	IV	500 mg/single-dose vial	Lyophilized powder
Belimumab (Benlysta®)	BLyS	Systemic lupus erythematosus	IV/SC	IV: 120 or 400 mg/vial SC: 200 mg/ml	IV: lyophilized powder SC: PFS or AI
Palivizumab (Synagis®)	RSV	Respiratory syncytial virus	IM	100 mg/ml	Powder for reconstitution
Muromonab (OKT3) (<i>discontinued</i>)	CD3	Transplantation rejection	IVP	1 mg/ml	Injectable solution
Genotuzumab (Mylotarg®) (<i>discontinued</i>)	CD33	Acute myeloid leukaemia (AML)	IV	4.5 mg/ml	Single-dose vial

systems for biopharmaceuticals. Examples of these delivery systems are ones that can pass the intestinal tract without being digested or administration through pulmonary or nasal routes (Anselmo et al., 2019; Bequignon et al., 2019; Kumar et al., 2018; Mitragotri et al., 2014). With superior attributes compared to the currently established formulations, drug carrier technologies, e.g., nanoparticle or microencapsulation formulations, have become of increasing interest as they allow enhanced stability and controlled release of the drug while being less invasive inhaled formulations (Abdelaziz et al., 2018; Anselmo et al., 2019; Jani and Krupa, 2019; Sifniotis et al., 2019).

One of the main limitations of the SC route is the limited dosing volume, which requires high mAb concentrations. However, advances in SC administration technologies have alleviated injection volume limitations. Higher volumes are now facilitated through the use of on-body SC delivery systems such as intradermal and patchable pumps for 5–10 ml injection volumes, and reports of novel technologies allowing volumes of 30 ml in self-administration SC routes are predicted to be feasible within the next decade (Datta-Mannan, 2019; Viola et al., 2018). The use of large volume wearable injector devices (LVD) also aims at overcoming volume limitations of SC or IM injections, allowing up to 10 ml with slower bolus injection rates (Li and Easton, 2018).

3.2. Formulation into the drug product

Formulation development is a critical aspect as the degradation of a mAb product can affect its stability and efficacy. In early clinical development, IV administration is often the preferred RoA, especially when dose-ranging clinical studies are carried out. During early stages, the target dose is unknown, thus putting emphasis on allowing dose-flexibility by IV administration, ensuring 100% bioavailability, and allowing comprehensive PK studies in humans during these critical early phase clinical trials (Li and Easton, 2018).

Depending on the administration, different formulations will be favoured to increase product stability and ensure product quality. For IV administration, a lyophilized powder for reconstitution and further dilution is typically prepared for increased product stability. However, during the drying process, this technology leads to physical stress, potentially inducing instability and degradation, and resulting in decreased efficacy. Today, lyophilized formulations are not preferred as they are expensive to manufacture and require further dilution prior to administration. SC and injectable administrations are prepared and stored as liquid formulations in self-administration devices. However, the pitfall of liquid formulations is an increased susceptibility to physicochemical degradation and lower stability, which can impact shelf-life

and product quality (Sifniotis et al., 2019). With injections being the primary delivery method for antibody products, different products exist: Traditional vial and syringe (VS), pre-filled syringes (PFS), pre-filled pens, or auto-injectors (AI). While the use of PFS brings advantages such as user-friendly design and both patient and economic benefits, formulation issues arise due to solubility, aggregation, and viscosity complications. The requirement for high protein concentrations of up to 200 mg/ml to achieve a therapeutic dose are thus limited by development difficulties (Li and Easton, 2018).

Aggregation is thought to result from the hydrophobic areas on the surface amino acid sequence, representing the most common form of instability of protein drugs. As it decreases the available efficacious product during treatment and often leads to increased side effects and immunogenicity, it is very much undesirable in a drug product (Cui et al., 2017; Giannos et al., 2018). To reduce protein degradation and aggregation, excipients are added to injectable formulations, adhering to the International Pharmaceutical Excipient Council Europe (IPEC) guidelines that describe what an excipient should look like in terms of quality (Madani et al., 2020). Commonly used excipients include salts, amino acids, or sugars to balance repulsion and attraction forces by intermediate ionic strength or by adjusting the pH of the solution (Kemter et al., 2018). Sugars are efficacious in stabilizing mAbs by protecting against aggregation and denaturation in both dried and solution states, along with increasing their melting temperatures in solution (Ohtake et al., 2011; Y. Zhang et al., 2020). Surfactants, such as polysorbates, are also used in biologics as stabilizing agents, but the addition of such agents in high concentrations may denature proteins and cause adverse side effects such as injection site reactions (Sifniotis et al., 2019).

Amino acid-based formulations containing single amino acids at high concentrations serve to stabilize and reduce viscosity (Awwad and Angkawitwong, 2018; Kemter et al., 2018). Hung et al. (2018) reported the improved use of concentrated proline in mAb formulations to increase stability and reduce viscosity at pH 6, compared to using glycine or trehalose (Hung et al., 2018). Cryoprotectants, such as sucrose or trehalose, are commonly added to improve long-term stability as a frozen liquid and to avoid aggregation and denaturation (Cui et al., 2017). The use of excipient listings, such as the "Inactive Ingredient Search for Approved Drug Products" offered by the FDA (www.accessdata.fda.gov/scripts/cder/iig/index.cfm), provides formulation scientists with excipients from approved products. Such listings avoid extensive formulation screening experiments. Nevertheless, challenges remain in achieving target pH and excipient concentrations in high-concentration doses, which can be overcome by using viscosity-

lowering excipients or altered cassettes for ultrafiltration, as recently reviewed by Holstein et al. (2020).

High-throughput technologies for the screening of pre-formulations has allowed for the selection of candidates which are better suited for specific formulation and delivery requirements, as well as providing valuable information to improve process design and leading to increased yields and quality (Johnson et al., 2009; Maddux et al., 2011; Razinkov et al., 2015; Whitaker et al., 2017). Further, the use of novel and emerging technologies such as small-angle X-ray scattering (SAXS) together with differential scanning calorimetry (DSC), dynamic light scattering (DLS), and viscosity measurements can be used to characterize and optimize the appropriate excipient formulation for a mAb product (Xu et al., 2019). A recent review by Le Basle et al. (2020) describes further advances used to analyse the stability and physico-chemical properties of mAbs. Improvements in formulation to increase the duration of action of therapeutic antibodies may also be achieved through the use of nanomaterials, such as hydrogels, liposomes, micelles, or nanoparticles (Awwad and Angkawitwong, 2018; Carrillo-Conde et al., 2015; Farahavar et al., 2019; Yang et al., 2019). The use of nanomaterials allows for sustained oral delivery of therapeutic antibodies while avoiding degradation in the GI tract and preserving antibody stability and function. This allows for the administration of therapeutics to treat infections or local conditions located in the GI tract or systemic conditions such as rheumatoid arthritis (Carrillo-Conde et al., 2015).

3.3. Patient compliance

At the core of drug development and the intended use of an antibody is *patient centricity*. While some formulations were developed for improved PK/PD properties or safety concerns, others were developed for increased patient compliance. The subcutaneous route has shown to be the most convenient administration route due to self-administration possibilities, with increased flexibility and potential to reduce costs for patients, payers, and providers. The use of autoinjectors, PFS, or mini-needles for SC administrations has led to increased patient acceptability and compliance, with the exception of potentially eliciting a higher immunological response (Datta-Mannan, 2019; Homayun et al., 2019). Using the aforementioned trastuzumab as an example, the successfully repurposed SC formulation allows for administration using a hand-held syringe or single-use injection device (Jackisch et al., 2015). A study by Pivot et al. reported that 88.9% of patients treated with trastuzumab, both IV and SC, preferred administration by SC route, with "time-saving" being the main reason for their preference (Pivot et al., 2014). Nevertheless, potential higher immunological ADA response, needle-associated phobia and pain, unsafe needle use, and improper disposal must also be considered (Homayun et al., 2019).

Considerations for the intended use of an antibody must also be suitable for treating the desired disease. While parenteral administration is preferred for acute and emergency responses, non-parenteral and less invasive methods are more suitable for sustained therapy and chronic delivery (Homayun et al., 2019). Patient adherence is a critical aspect of achieving successful treatment outcomes. Reports have revealed that patient adherence rates for chronic therapies in developed countries are only 50%, being even lower in developing countries (Li and Easton, 2018). Considering this, novel technologies have been developed, such as large-volume wearable injector device (LVD), allowing self-administration of a drug at a flexible time and location, with the hope of joining patient factors and promoting consistent use of a drug in chronic diseases (Li and Easton, 2018). To increase patient compliance and reduce invasive treatments, promising advances have been reported by assessing different RoA for mAb treatment of diabetic retinopathy and potentially other chronic retinal pathologies in mice (Barcelona et al., 2018).

Special populations must also be examined, particularly if there is a specific correlation between a disease and a given population. The

disease status of patients with renal or hepatic impairment or pediatric or elderly patients will not only influence a drug's PK properties, but may also impact safety and efficacy profiles (Mould and Meibohm, 2016). Defining patient's physical and cognitive limitations and capabilities could also affect the ability to safely and effectively use a certain drug delivery device. Such impairments could include visual, cognitive, or manual dexterity. For example, patients with rheumatoid arthritis or those eliciting involuntary hand movements due to Parkinson's disease may not be capable of using fine motor skills to control and stabilize a syringe with a narrow needle (Strochlic and Davis, 2017). The high costs of monoclonal antibody therapy by achieving patient-convenient self-administration formulations may also hamper the success of a drug on the market (Li and Easton, 2018). Thus, when evaluating the intended use of a therapeutic monoclonal antibody, all these attributes must be taken into consideration to find the balance between the needs, interests, and limitations of both the patient and the manufacturer.

4. Conclusion & outlook

The success of therapeutic monoclonal antibodies throughout the years is, in part, accredited to improvements in manufacturing and formulation, allowing for the development of more efficient and cost-effective mAbs. Efforts to minimize mAb heterogeneity using protein engineering and the implementation of regulatory agency guidelines to ensure reproducibility, safety, and traceability, such as GMP and QbD milestones discussed herein, have shown remarkable advances in pharmaceutical and biotechnology companies. Further improvements to process development involve implementing single-use strategies to reduce cost and increase the flexibility of platform processes. At the current growth rate, novel computational-based approaches will become an integral part of process development and facilitate predictions of post-translational modifications, kinetic properties, and pre-formulation screening, among others.

When talking about the intended use of a therapeutic antibody, it is important to note that several factors must be considered deeply in order to make adequate decisions, ranging from choosing the RoA to the drug delivery system and appropriate formulation, and even the patient population. Tuning of PK/PD properties of a monoclonal antibody not only leads to increased safety and efficacy but may facilitate increased patient acceptability and compliance, lower doses or dose frequency, and lead to improved therapeutic outcomes. Consideration of the TPP in early development is an important advancement in process development, as RoA, protein modifications, and mAb heterogeneity may all influence the behaviour and safety of a therapeutic mAb in humans. Early pre-formulation experiments and assessments to determine which excipients are compatible and to investigate the ideal conditions for the stability of the API, e.g., temperature, pH, etc. should be performed to improve the formulation development of a drug product.

Ultimately, the aim is to minimize potential errors and variability throughout the entire process, potentially hindering product quality and causing safety or efficacy concerns. While progress in the manufacturing and formulation of mAb drugs continues to be made through the advancement of high-throughput technologies and low-cost alternatives, drawbacks are nevertheless present. Compared to other drug modalities, protein pharmaceuticals tend to have higher cost of goods. Consequently, a drug product with high immunogenicity and poor bioavailability would be too costly to manufacture. Therefore, strict understanding and control of every step of the process are fundamental to the success of a therapeutic monoclonal antibody, while always keeping in mind that "*the process is the product*" (Kuehn, 2014).

CRediT authorship contribution statement

Stefania C. Carrara: Conceptualization, Writing - original draft, Writing - review & editing. **Michael Ulitzka:** Writing - review & editing. **Julius Grzeschik:** Writing - review & editing. **Henri Kornmann:**

Conceptualization, Writing - review & editing. **Björn Hock:** Conceptualization, Writing - review & editing, Supervision. **Harald Kolmar:** Conceptualization, Writing - review & editing, Supervision.

Declaration of Competing Interest

The authors declare that they have no known competing financial interests or personal relationships that could have appeared to influence the work reported in this paper.

References

- Abdelaziz, H.M., Gaber, M., Abd Elwakil, M.M., Mabrouk, M.T., Elgohary, M.M., Kamel, N.M., Kabary, D.M., Freag, M.S., Samaha, M.W., Mortada, S.M., Elkhodairy, K.A., Fang, J.-Y., Elzoghby, A.O., 2018. Inhalable particulate drug delivery systems for lung cancer therapy: Nanoparticles, microparticles, nanocomposites and nanoaggregates. *J. Control. Release* 269, 374–392. <https://doi.org/10.1016/j.jconrel.2017.11.036>.
- Agarwal, N., Mason, A., Pradhan, R., Kemper, J., Bosley, A., Serfiotis-Mitsa, D., Wang, J., Lindo, V., Aluja, S., Hatton, D., Savery, J., Miro-Quesada, G., 2019. Kinetic modeling as a tool to understand the influence of cell culture process parameters on the glycation of monoclonal antibody biotherapeutics. *Biotechnol. Prog.* 35 <https://doi.org/10.1002/btpr.2865>.
- Alt, N., Zhang, T.Y., Motchnik, P., Taticek, R., Quarnby, V., Schlothauer, T., Beck, H., Emrich, T., Harris, R.J., 2016. Determination of critical quality attributes for monoclonal antibodies using quality by design principles. *Biologicals* 44, 291–305. <https://doi.org/10.1016/j.biologics.2016.06.005>.
- Anselmo, A.C., Gokarn, Y., Mitragotri, S., 2019. Non-invasive delivery strategies for biologics. *Nat. Rev. Drug Discov.* 18, 19–40. <https://doi.org/10.1038/nrd.2018.183>.
- Arslan, M., Karadag, D., Kalyoncu, S., 2019. Protein engineering approaches for antibody fragments: directed evolution and rational design approaches. *Turkish J. Biol.* 43, 1–12. <https://doi.org/10.3906/biy-1809-28>.
- Awad, S., Angkawitwong, U., 2018. Overview of antibody drug delivery. *Pharmaceutics* 10, 1–24. <https://doi.org/10.3390/pharmaceutics10030083>.
- Barcelona, P.F., Galan, A., Nedeve, H., Jian, Y., Sarunic, M.V., Uri Saragovi, H., 2018. The route of administration influences the therapeutic index of an anti-proNGF neutralizing mAb for experimental treatment of Diabetic Retinopathy. *PLoS One* 13, 1–19. <https://doi.org/10.1371/journal.pone.0199079>.
- Beck, A., Liu, H., 2019. Macro- and micro heterogeneity of natural and recombinant IgG antibodies. *Antibodies* 8, 18. <https://doi.org/10.3390/antib8010018>.
- Beck, A., Wurch, T., Bailly, C., Corvaia, N., 2010. Strategies and challenges for the next generation of therapeutic antibodies. *Nat. Rev. Immunol.* 10, 345–352. <https://doi.org/10.1038/nri2747>.
- Becker, M., Junghans, L., Teleki, A., Bechmann, J., Takors, R., 2019. The less the better: how suppressed base addition boosts production of monoclonal antibodies with chinese hamster ovary cells. *Front. Biotechnol.* 7 <https://doi.org/10.3389/fbioe.2019.00076>.
- Bequignon, E., Dhommée, C., Angely, C., Thomas, L., Bottier, M., Escudier, E., Isabey, D., Coste, A., Louis, B., Papon, J.-F., Guilleux-Griart, V., 2019. FcRn-Dependent transcytosis of monoclonal antibody in human nasal epithelial cells in vitro: a prerequisite for a new delivery route for therapy? *Int. J. Mol. Sci.* 20, 1379. <https://doi.org/10.3390/ijms20061379>.
- Beyer, B., Schuster, M., Jungbauer, A., Lingg, N., 2018. Microheterogeneity of recombinant antibodies: analytics and functional impact. *Biotechnol. J.* 13, 1700476. <https://doi.org/10.1002/biot.201700476>.
- Blair, H.A., Duggan, S.T., 2018. Belimumab: a review in systemic lupus erythematosus. *Drugs* 78, 355–366. <https://doi.org/10.1007/s40265-018-0872-z>.
- Boder, E.T., Wittrup, K.D., 1998. Optimal screening of surface-displayed polypeptide libraries. *Biotechnol. Prog.* 14, 55–62. <https://doi.org/10.1021/bp970144q>.
- Camperi, J., Dai, L., Guillaume, D., Stella, C., 2020. Fast and automated characterization of monoclonal antibody minor variants from cell cultures by combined Protein-A and multidimensional LC/MS methodologies. *Anal. Chem.* 92, 8506–8513. <https://doi.org/10.1021/acs.analchem.0c01250>.
- Carrillo-Conde, B.R., Brewer, E., Lowman, A., Peppas, N.A., 2015. Complexation hydrogels as oral delivery vehicles of therapeutic antibodies: an in vitro and ex vivo evaluation of antibody stability and bioactivity. *Ind. Eng. Chem. Res.* 54, 10197–10205. <https://doi.org/10.1021/acs.iecr.5b01193>.
- Carson, K.L., 2005. Flexibility - the guiding principle for antibody manufacturing. *Nat. Biotechnol.* 23, 1054–1058. <https://doi.org/10.1038/nbt09051054>.
- Carvalho, L.S., Bravim da Silva, O., Carneiro de Almeida, G., Davies de Oliveira, J., Parachin, N.S., Carmo, T.S., 2017. Production processes for monoclonal antibodies. *Intech i*, 13.
- Chahar, D.S., Ravindran, S., Pisal, S.S., 2020. Monoclonal antibody purification and its progression to commercial scale. *Biologicals* 63, 1–13. <https://doi.org/10.1016/j.biologics.2019.09.007>.
- Chiu, M.L., Gilliland, G.L., 2016. Engineering antibody therapeutics. *Curr. Opin. Struct. Biol.* 38, 163–173. <https://doi.org/10.1016/j.sbi.2016.07.012>.
- CHO Media Development for Therapeutic Protein Production [WWW Document], 2019. *Am. Pharm. Rev.* <https://www.americanpharmaceuticalreview.com/Featured-Articles/559489-CHO-Media-Development-for-Therapeutic-Protein-Production/>.
- Cui, Y., Cui, P., Chen, B., Li, S., Guan, H., 2017. Monoclonal antibodies: formulations of marketed products and recent advances in novel delivery system. *Drug Dev. Ind. Pharm.* 43, 519–530. <https://doi.org/10.1080/03639045.2017.1278768>.
- Dahodwala, H., Kanshik, P., Tejawani, V., Kuo, C. C., Menard, P., Henry, M., Voldborg, B. G., Lewis, N.E., Meleady, P., Sharfstein, S.T., 2019. Increased mAb production in amplified CHO cell lines is associated with increased interaction of CREB1 with transgene promoter. *Curr. Res. Biotechnol.* 1, 49–57. <https://doi.org/10.1016/j.crbiot.2019.09.001>.
- Dangi, A.K., Sinha, R., Dwivedi, S., Gupta, S.K., Shukla, P., 2018. Cell line techniques and gene editing tools for antibody production: a review. *Front. Pharmacol.* 9 <https://doi.org/10.3389/fphar.2018.00630>.
- Dashivets, T., Stracke, J., Dengl, S., Knaupp, A., Pollmann, J., Buchner, J., Schlothauer, T., 2016. Oxidation in the complementarity-determining regions differentially influences the properties of therapeutic antibodies. *MAbs* 8, 1525–1535. <https://doi.org/10.1080/19420862.2016.1231277>.
- Datta-Mannan, A., 2019. Mechanisms influencing the pharmacokinetics and disposition of monoclonal antibodies and peptides. *Drug Metab. Dispos.* 47, 1100–1110. <https://doi.org/10.1124/dmd.119.086488>.
- Delmar, J.A., Wang, J., Choi, S.W., Martins, J.A., Mikhail, J.P., 2019. Machine learning enables accurate prediction of asparagine deamidation probability and rate. *Mol. Ther. - Methods Clin. Dev.* 15, 264–274. <https://doi.org/10.1016/j.omtm.2019.09.008>.
- Dorceus, M., Willard, S.S., Suttle, A., Han, K., Chen, P.-J., Sha, M., 2017. Comparing culture methods in monoclonal antibody production: Batch, fed-batch, and perfusion [WWW Document]. *Bioprocess Int.* URL <https://bioprocessintl.com/analytical/upstream-development/comparing-culture-methods-monoclonal-antibody-production-batch-fed-batch-perfusion/> (accessed 4.12.20).
- Du, C., Huang, Y., Borwankar, A., Tan, Z., Cura, A., Yee, J.C., Singh, N., Ludwig, R., Borys, M., Ghose, S., Mussa, N., Li, Z.J., 2018. Using hydrogen peroxide to prevent antibody disulfide bond reduction during manufacturing process. *MAbs* 10, 500–510. <https://doi.org/10.1080/19420862.2018.1424609>.
- Ecker, D.M., Jones, S.D., Levine, H.L., 2015. The therapeutic monoclonal antibody market. *MAbs* 7, 9–14. <https://doi.org/10.4161/19420862.2015.989042>.
- Eibl, D., Eibl, R., 2019. Single-use equipment in biopharmaceutical manufacture: a brief introduction. In: Eibl, R., Eibl, D. (Eds.), *Single Use Technology in Biopharmaceutical Manufacture*. Wiley, pp. 1–11. <https://doi.org/10.1002/9781119477891>.
- Enever, C., Pupecka Swider, M., Sepp, A., 2015. Stress selections on domain antibodies: 'What doesn't kill you makes you stronger'. *Protein Eng. Des. Sel.* 28, 59–66. <https://doi.org/10.1093/protein/gzu057>.
- Eon-Duval, A., Broly, H., Gleixner, R., 2012. Quality attributes of recombinant therapeutic proteins: an assessment of impact on safety and efficacy as part of a quality by design development approach. *Biotechnol. Prog.* 28, 608–622. <https://doi.org/10.1002/btpr.1548>.
- Esser-Skala, W., Wohlschlager, T., Regl, C., Huber, C.G., 2020. A simple strategy to eliminate hexosylation bias in the relative quantification of N-glycosylation in biopharmaceuticals. *Angew. Chemie Int. Ed. anie.* 202002147 <https://doi.org/10.1002/anie.202002147>.
- European Medicines Agency, 2016. Guideline on development, production, characterisation and specification for monoclonal antibodies and related products. *Guideline 44*. <https://doi.org/EMA/CHMP/BWP/157653/2007>.
- Fan, Y., Ley, D., Andersen, M.R., 2018. Fed-batch CHO cell culture for lab-scale antibody production. pp. 147–161. https://doi.org/10.1007/978-1-4939-7312-5_12.
- Farahavar, G., Abolmaali, S.S., Gholijani, N., Nejatollahi, F., 2019. Antibody-guided nanomedicines as novel breakthrough therapeutic, diagnostic and theranostic tools. *Biomater. Sci.* 7, 4000–4016. <https://doi.org/10.1039/C9BM00931K>.
- Finkler, C., Krummen, L., 2016. Introduction to the application of QbD principles for the development of monoclonal antibodies. *Biologicals* 44, 282–290. <https://doi.org/10.1016/j.biologics.2016.07.004>.
- Fousser, I.A., Swanberg, S.L., Lin, B. Y., Benedict, M., Kelleher, K., Cumming, D.A., Riedel, G.E., 1992. High level expression of a chimeric anti-ganglioside GD2 antibody: genomic kappa sequences improve expression in COS and CHO cells. *Nat. Biotechnol.* 10, 1121–1127. <https://doi.org/10.1038/nbt10921121>.
- Giannos, S.A., Kraft, E.R., Zhao, Z.Y., Merkley, K.H., Cai, J., 2018. Formulation stabilization and disaggregation of Bevacizumab, Ranibizumab and Aflibercept in dilute solutions. *Pharm. Res.* 35, 1–15. <https://doi.org/10.1007/s11095-018-2368-7>.
- Gomord, V., Fitchette, A.-C., Menu-Bouaouiche, L., Saint-Jore-Dupas, C., Plasson, C., Michaud, D., Faye, L., 2010. Plant-specific glycosylation patterns in the context of therapeutic protein production. *Plant Biotechnol. J.* 8, 564–587. <https://doi.org/10.1111/j.1467-7652.2009.00497.x>.
- Gronemeyer, P., Ditz, R., Strube, J., 2014. Trends in upstream and downstream process development for antibody manufacturing. *Bioengineering* 1, 188–212. <https://doi.org/10.3390/bioengineering1040188>.
- Großhans, S., Wang, G., Fischer, C., Hubbuch, J., 2018. An integrated precipitation and ion-exchange chromatography process for antibody manufacturing: process development strategy and continuous chromatography exploration. *J. Chromatogr. A* 1533, 66–76. <https://doi.org/10.1016/j.chroma.2017.12.013>.
- Gu, S., Wen, D., Weinreb, P.H., Sun, Y., Zhang, L., Foley, S.F., Kshirsagar, R., Evans, D., Mi, S., Meier, W., Pepinsky, R.B., 2010. Characterization of trisulfide modification in antibodies. *Anal. Biochem.* 400, 89–98. <https://doi.org/10.1016/j.ab.2010.01.019>.
- Hanuro, L., Kijanka, G., Kinderman, F., Kropshofer, H., Bu, D. xiu, Zepeda, M., Jawa, V., 2017. Perspectives on subcutaneous route of administration as an immunogenicity risk factor for therapeutic proteins. *J. Pharm. Sci.* 106, 2946–2954. <https://doi.org/10.1016/j.xphs.2017.05.030>.

- Handlogten, M.W., Wang, J., Ahuja, S., 2020. Online control of cell culture redox potential prevents antibody interchain disulfide bond reduction. *Biotechnol. Bioeng.* 117, 1329–1336. <https://doi.org/10.1002/bit.27281>.
- Haselberg, R., De Vijlder, T., Heukers, R., Smit, M.J., Romijn, E.P., Somsen, G.W., Domínguez-Vega, E., 2018. Heterogeneity assessment of antibody derived therapeutics at the intact and middle-up level by low-flow sheathless capillary electrophoresis-mass spectrometry. *Anal. Chim. Acta* 1044, 181–190. <https://doi.org/10.1016/j.aca.2018.08.024>.
- Hogwood, C.E., Bracewell, D.G., Smales, C.M., 2013. Host cell protein dynamics in recombinant CHO cells. *Biotechnol. Bioeng.* 117, 288–291. <https://doi.org/10.1016/j.biotech.2013.08.024>.
- Holstein, M., Hung, J., Feroz, H., Ranjan, S., Du, C., Ghose, S., Li, Z.J., 2020. Strategies for high-concentration drug substance manufacturing to facilitate subcutaneous administration: a review. *Biotechnol. Bioeng.* 122, 27510. <https://doi.org/10.1002/bit.27510>.
- Homayun, B., Lin, X., Choi, H.J., 2019. Challenges and recent progress in oral drug delivery systems for biopharmaceuticals. *Pharmaceutics* 11, 103029. <https://doi.org/10.3390/pharmaceutics1103029>.
- Hung, J.J., Dear, B.J., Dini, A.K., Borwankar, A.U., Mehta, S.K., Truskett, T.T., Johnston, K.P., 2018. Improving viscosity and stability of a highly concentrated monoclonal antibody solution with concentrated proline. *Pharm. Res.* 35, 133. <https://doi.org/10.1007/s11095-018-2398-1>.
- ICH, 2009. ICH guidelines [WWW Document]. accessed 4.12.20. <https://www.ich.org/page/ich-guidelines>.
- Irvine, E.B., Alter, G., 2020. Understanding the role of antibody glycosylation through the lens of severe viral and bacterial diseases. *Glycobiology* 30, 241–253. <https://doi.org/10.1093/glycob/cwaa018>.
- Jackisch, C., Kim, S.B., Semiglazov, V., Melicher, B., Pivov, X., Hillenbach, C., Stroyakovskiy, D., Lum, B.L., Elliott, R., Weber, H.A., Ismael, G., 2015. Subcutaneous versus intravenous formulation of trastuzumab for HER2-positive early breast cancer: updated results from the phase III HannahH study. *Ann. Oncol.* 26, 320–325. <https://doi.org/10.1093/annonc/mdl524>.
- Jacobi, A., Enekel, B., Garidel, P., Eckermann, C., Knappenberg, I.P., Kaufmann, H., 2014. Process development and manufacturing of therapeutic antibodies, in: Reichert, S.D., and J.M. (Eds.), *Handbook of Therapeutic Antibodies*. Wiley VCH Verlag GmbH & Co, pp. 601–663.
- Jacobitz, A.W., Dykstra, A.B., Spahr, C., Agrawal, N.J., 2020. Effects of buffer composition on site specific glycation of lysine residues in monoclonal antibodies. *J. Pharm. Sci.* 109, 293–300. <https://doi.org/10.1016/j.xphs.2019.05.025>.
- Jani, R.K., Krupa, G., 2019. Active targeting of nanoparticles: an innovative technology for drug delivery in cancer therapeutics. *J. Drug Deliv. Ther.* 9, 408–415. <https://doi.org/10.22270/jddt.v9i1.s2356>.
- Jarascch, A., Koll, H., Regula, J.T., Bader, M., Papadimitriou, A., Kettenberger, H., 2015. Developability assessment during the selection of novel therapeutic antibodies. *J. Pharm. Sci.* 104, 1885–1898. <https://doi.org/10.1002/jps.24430>.
- Jefferis, R., 2009. Glycosylation as a strategy to improve antibody-based therapeutics. *Nat. Rev. Drug Discov.* 8, 226–234. <https://doi.org/10.1038/nrd2804>.
- Johnson, D.H., Parupudi, A., Wilson, W.W., DeLucas, L.J., 2009. High throughput self-interaction chromatography: applications in protein formulation prediction. *Pharm. Res.* 26, 296–305. <https://doi.org/10.1007/s11095-008-9737-6>.
- Jossen, V., Eibl, R., Eibl, D., 2019. Single-use bioreactors – an overview. In: Eibl, R., Eibl, D. (Eds.), *Single-Use Technology in Biopharmaceutical Manufacture*. Wiley, pp. 37–52. <https://doi.org/10.1002/9781119477891>.
- Juran, J.M., 1992. Departmental quality planning. *Natl. Product. Rev.* 11, 287–300. <https://doi.org/10.1002/npr.4040110302>.
- Karlberg, M., von Stosch, M., Glassey, J., 2018. Exploiting mAb structure characteristics for a directed QBD implementation in early process development. *Crit. Rev. Biotechnol.* 38, 957–970. <https://doi.org/10.1080/07388551.2017.1421899>.
- Kelley, B., 2009. Industrialization of mAb production technology: the bioprocessing industry at a crossroads. *MABS* 1, 443–452. <https://doi.org/10.4161/mabs.1.5.9448>.
- Kenner, K., Altrichter, J., Derwand, R., Kriehuber, T., Reinauer, E., Scholz, M., 2018. Amino acid-based advanced liquid formulation development for highly concentrated therapeutic antibodies balances physical and chemical stability and low viscosity. *Biotechnol. J.* 13, 1700523. <https://doi.org/10.1002/biot.201700523>.
- Khetan, A., Huang, Y., Dolnikova, J., Pederson, N.E., Wen, D., Yusuf-Makgiansar, H., Chen, P., Ryll, T., 2010. Control of misincorporation of serine for asparagine during antibody production using CHO cells. *Biotechnol. Bioeng.* 107, 116–123. <https://doi.org/10.1002/bit.22771>.
- Kim, H.S., Lee, G.M., 2007. Differences in optimal pH and temperature for cell growth and antibody production between two Chinese hamster ovary clones derived from the same parental clone. *J. Microbiol. Biotechnol.* 17, 712–720.
- Köhler, G., Milstein, C., 1975. Continuous cultures of fused cells secreting antibody of predefined specificity. *Nature* 256, 495–497. <https://doi.org/10.1038/256495a0>.
- Konstantinov, K.B., Cooney, C.L., 2015. White paper on continuous bioprocessing May 20–21 2014 continuous manufacturing symposium. *J. Pharm. Sci.* 104, 813–820. <https://doi.org/10.1002/jps.24268>.
- Kruse, T., Schmidt, A., Kampmann, M., Strube, J., 2019. Integrated clarification and purification of monoclonal antibodies by membrane based separation of aqueous two-phase systems. *Antibodies* 8, 40. <https://doi.org/10.3390/antib8030040>.
- Kuehn, S.E., 2014. The process is the product [WWW Document]. *Pharm. Manuf.* <https://www.pharmamanufacturing.com/articles/2014/the-process-is-the-product/> (accessed 4.13.20).
- Kuiper, M., Spencer, C., Fäldt, E., Vuilleme, A., Holmes, W., Samuelsson, T., Gruber, D., Castan, A., 2019. Repurposing fed batch media and feeds for highly productive CHO perfusion processes. *Biotechnol. Prog.* 35. <https://doi.org/10.1002/btpr.2821>.
- Kumar, N.N., Lochhead, J.J., Pizzo, M.E., Nehra, G., Boroumand, S., Greene, G., Thorne, R.G., 2018. Delivery of immunoglobulin G antibodies to the rat nervous system following intranasal administration: distribution, dose response, and mechanisms of delivery. *J. Control. Release* 286, 467–484. <https://doi.org/10.1016/j.jconrel.2018.08.006>.
- Kunert, R., Reinhardt, D., 2016. Advances in recombinant antibody manufacturing. *Appl. Microbiol. Biotechnol.* 100, 3451–3461. <https://doi.org/10.1007/s00253-016-7388-9>.
- Kung, P., Goldstein, G., Reinherz, E., Schlossman, S., 1979. Monoclonal antibodies defining distinctive human T cell surface antigens. *Science* (80-) 206, 347–349. <https://doi.org/10.1126/science.314668>.
- Kuroda, D., Tsunoto, K., 2020. Engineering stability, viscosity, and immunogenicity of antibodies by computational design. *J. Pharm. Sci.* 109, 1631–1651. <https://doi.org/10.1016/j.xphs.2020.01.011>.
- Langer, E.S., Rader, R.A., 2019. Biopharmaceutical manufacturing is shifting to single-use systems. Are the dinosaurs, the large stainless steel facilities, becoming extinct? *Am. Pharm. Rev.*
- Le Basle, Y., Chemell, P., Tokhadze, N., Astier, A., Sautou, V., 2020. Physicochemical stability of monoclonal antibodies: a review. *J. Pharm. Sci.* 109, 169–190. <https://doi.org/10.1016/j.xphs.2019.08.009>.
- Li, F., Vijayasankaran, N., Shen, A., Kiss, R., Amanullah, A., 2010. Cell culture processes for monoclonal antibody production. *MABS* 2, 466–479. <https://doi.org/10.4161/mabs.2.5.12720>.
- Li, Z., Easton, R., 2018. Practical considerations in clinical strategy to support the development of injectable drug device combination products for biologics. *MABS* 10, 18–33. <https://doi.org/10.1080/19420862.2017.1392424>.
- Ling, W.L., 2015. Development of protein free medium for therapeutic protein production in mammalian cells: recent advances and perspectives. *Pharm. Bioprocess.* 3, 215–226. <https://doi.org/10.4155/pbp.15.8>.
- Liu, H., Ponniah, G., Zhang, H.-M., Nowak, C., Neill, A., Gonzalez-Lopez, N., Patel, R., Cheng, G., Kita, A.Z., Andrien, B., 2014. In vitro and in vivo modifications of recombinant and human IgG antibodies. *MABS* 6, 1145–1154. <https://doi.org/10.4161/mabs.29883>.
- Liu, J.K.H., 2014. The history of monoclonal antibody development – progress, remaining challenges and future innovations. *Ann. Med. Surg.* 3, 113–116. <https://doi.org/10.1016/j.amsu.2014.09.001>.
- Liu, S., Madren, S., Feng, P., Sosic, Z., 2020. Characterization of the acidic species of a monoclonal antibody using free flow electrophoresis fractionation and mass spectrometry. *J. Pharm. Biomed. Anal.* 185, 113217. <https://doi.org/10.1016/j.jpba.2020.113217>.
- Liu, Y.D., Goetze, A.M., Bass, R.B., Flynn, G.C., 2011. N-terminal glutamate to pyroglutamate conversion in vivo for human IgG2 antibodies. *J. Biol. Chem.* 286, 11211–11217. <https://doi.org/10.1074/jbc.M110.185041>.
- Liu, R.M., Hwang, Y.C., Liu, L.J., Lee, C.C., Tsai, H.Z., Li, H.J., Wu, H.C., 2020. Development of therapeutic antibodies for the treatment of diseases. *J. Biomed. Sci.* 27, 1–30. <https://doi.org/10.1186/s12929-019-0592-z>.
- Liu, X., Nobrega, R.P., Lynaugh, H., Jain, T., Barlow, K., Boland, T., Sivasubramanian, A., Vasquez, M., Xu, Y., 2019. Deamidation and isomerization liability analysis of 131 clinical-stage antibodies. *MABS* 11, 45–57. <https://doi.org/10.1080/19420862.2018.1548233>.
- Madani, F., Hsein, H., Busignies, V., Tchoreloff, P., 2020. An overview on dosage forms and formulation strategies for vaccines and antibodies oral delivery. *Pharm. Dev. Technol.* 25, 133–148. <https://doi.org/10.1080/10837450.2019.1689402>.
- Maddux, N.R., Joshi, S.B., Volkin, D.B., Ralston, J.P., Middaugh, C.R., 2011. Multidimensional methods for the formulation of biopharmaceuticals and vaccines. *J. Pharm. Sci.* 100, 4171–4197. <https://doi.org/10.1002/jps.22618>.
- Mandal, A., Pal, D., Agrahari, V., Trinh, H.M., Joseph, M., Mitra, A.K., 2018. Ocular delivery of proteins and peptides: challenges and novel formulation approaches. *Adv. Drug Deliv. Rev.* 126, 67–95. <https://doi.org/10.1016/j.addr.2018.01.008>.
- Massato, A., Kiichi, F., Uchiyama, S., 2016. Suppression of methionine oxidation of a pharmaceutical antibody stored in a polymer-based syringe. *J. Pharm. Sci.* 105, 623–629. <https://doi.org/10.1002/jps.24675>.
- Matucci, A., Vultaggio, A., Danesi, R., 2018. The use of intravenous versus subcutaneous monoclonal antibodies in the treatment of severe asthma: a review. *Respir. Res.* 19, 1–10. <https://doi.org/10.1186/s12931-018-0859-z>.
- MedScape [WWW Document], 2020. <https://reference.medscape.com/> (accessed 4.11.20).
- Miller, A.K., Hambly, D.M., Kerwin, B.A., Treuheit, M.J., Gadgil, H.S., 2011. Characterization of site-specific glycation during process development of a human therapeutic monoclonal antibody. *J. Pharm. Sci.* 100, 2543–2550. <https://doi.org/10.1002/jps.22504>.
- Minura, Y., Katoh, T., Saldova, R., O'Flaherty, R., Izumi, T., Minura-Kimura, Y., Utsunomiya, T., Mizukami, Y., Yamamoto, K., Matsumoto, T., Rudd, P.M., 2018. Glycosylation engineering of therapeutic IgG antibodies: challenges for the safety, functionality and efficacy. *Protein Cell* 9, 47–62. <https://doi.org/10.1007/s13238-017-0433-3>.
- Mitragotri, S., Burke, P.A., Langer, R., 2014. Overcoming the challenges in administering biopharmaceuticals: formulation and delivery strategies. *Nat. Rev. Drug Discov.* 13, 655–672. <https://doi.org/10.1038/nrd4363>.
- Mo, J., Yan, Q., So, C.K., Soden, T., Lewis, M.J., Hu, P., 2016. Understanding the impact of methionine oxidation on the biological functions of IgG1 antibodies using hydrogen/deuterium exchange mass spectrometry. *Anal. Chem.* 88, 9495–9502. <https://doi.org/10.1021/acs.analchem.6b01958>.
- Mould, D.R., Meibohm, B., 2016. Drug development of therapeutic monoclonal antibodies. *BioDrugs* 30, 275–293. <https://doi.org/10.1007/s40259-016-0181-6>.

- Nagashima, H., Watari, A., Shinoda, Y., Okamoto, H., Takuma, S., 2013. Application of a quality by design approach to the cell culture process of monoclonal antibody production, resulting in the establishment of a design space. *J. Pharm. Sci.* 102, 4274–4283. <https://doi.org/10.1002/jps.23744>.
- O'Kennedy, R., Murphy, C., Devine, T., 2016. Technology advancements in antibody purification. *Antib. Technol. J.* 6, 17–32. <https://doi.org/10.2147/ANTI.S64762>.
- Oguchi, S., Saito, H., Tsukahara, M., Tsumura, H., 2002. Control of temperature and pH enhances human monoclonal antibody production in CHO cell culture. In: Yagasaki, K., Miura, Y., Hatori, M., Nomura, Y. (Eds.), *Animal Cell Technology: Basic & Applied Aspects*. Springer-Science+Business Media, B.V., Fuchu, pp. 169–172.
- Ohtake, S., Kita, Y., Arakawa, T., 2011. Interactions of formulation excipients with proteins in solution and in the dried state. *Adv. Drug Deliv. Rev.* 63, 1053–1073. <https://doi.org/10.1016/j.addr.2011.06.011>.
- Ortega, H., Yancey, S., Cozens, S., 2014. Pharmacokinetics and absolute bioavailability of nopolizumab following administration at subcutaneous and intramuscular sites. *Clin. Pharmacol. Drug Dev.* 3, 57–62. <https://doi.org/10.1002/cpdd.60>.
- Ovacik, M., Lin, K., 2018. Tutorial on monoclonal antibody pharmacokinetics and its considerations in early development. *Clin. Transl. Sci.* 11, 540–552. <https://doi.org/10.1111/cts.12567>.
- Page, M.J., Sydenham, M.A., 1991. High level expression of the humanized monoclonal antibody CAMPATH-1H in Chinese Hamster Ovary cells. *Nat. Biotechnol.* 9, 64–68. <https://doi.org/10.1038/nbt0191-64>.
- Park, J.H., Jin, J.H., Lim, M.S., An, H.J., Kim, J.W., Lee, G.M., 2017. Proteomic analysis of host cell protein dynamics in the culture supernatants of antibody-producing CHO cells. *Sci. Rep.* 7, 44246. <https://doi.org/10.1038/srep44246>.
- Parker, J., Pollard, J.W., Friesen, J.D., Stanners, C.P., 1978. Stuttering: high level mistranslation in animal and bacterial cells. *Proc. Natl. Acad. Sci. United States* 75, 1091–1095.
- Pérez-Rodríguez, S., Ramírez-Lira, M. de J., Trujillo-Roldán, M.A., Valdez-Cruz, N.A., 2020. Nutrient supplementation strategy improves cell concentration and longevity, monoclonal antibody production and lactate metabolism of Chinese hamster ovary cells. *Bioengineered* 11, 463–471. <https://doi.org/10.1080/21655979.2020.1744266>.
- Pivot, X., Gligorov, J., Müller, V., Curigliano, G., Knoop, A., Verma, S., Jenkins, V., Scotto, N., Osborne, S., Fallowfield, L., Fallowfield, Lesley, Jenkins, Valerie, Kilkerr, J., Langridge, C., Monson, K., Jakobsen, E.H., Nielsen, M.H., Linnet, S., Knoop, Ann, Pivot, Xavier, Bonnefoi, H., Mousseau, M., Zelek, L., Bourgeois, H., Lefeuvre, C.P., Bachelot, T., Petit, T., Brain, E., Levy, C., Gligorov, Joseph, Augustin, D., Graf, H., Heinrich, G., Kroening, H., Kuenmel, S., Müller, Volkmar, Overkamp, F., Park Simon, T. W., Schmidt, M., Perlova Griff, L., Wolf, C., Colleani, M., Ballestrero, A., Bernardo, A., Ribocco, A.S., Gianni, L., Curigliano, Giuseppe, Brewczynska, E., Jassen, J., Shirinkin, V., Manikhas, A., Dvornichenko, V., Lichinitser, M., Semiglazov, V., Mukhametshina, G., Bulavina, I., Arranz, E.E., Ocon, F.C., Vivanco, G.L., Bofill, J.S., Quintela, I.P., Muñoz, A.S., Pérez, Y.F., Espinosa, J.C., Alvarez, J.V., del Prado, R.L., De Merino, L.C., Garcia, J. M.P., Frances, S.E., Edlund, P., Norberg, B., Wennstig, A.-K., Lind, P., Hauser, N., Tausch, C., Camci, C., Arcpaci, F., Abali, H., Uslu, R., Tahir, S., Wheatley, D., Chan, S., Barrett Lee, P., McAdam, K., Simcock, R., Burcombe, R., El Maraghi, R., Califaretti, N., Spadafora, S., Scheld, S., Sami, A., Verma, Sumil, 2014. Patients' preferences for subcutaneous trastuzumab versus conventional intravenous infusion for the adjuvant treatment of HER2-positive early breast cancer: final analysis of 488 patients in the international, randomized, two-cohort PreHer study. *Ann. Oncol.* 25, 1979–1987. <https://doi.org/10.1093/annonc/ndu364>.
- Pollard, D., Brower, M., Abe, Y., Lopes, A.G., Sinclair, A., 2016. Standardized economic cost modeling for next-generation mAb production [WWW Document]. *Bioprocess Int.* <https://bioprocessintl.com/business/economics/standardized-economic-cost-modeling-next-generation-mab-production/> (accessed 4.12.20).
- Popplewell, A.G., 2015. Protein engineering: applications to therapeutic proteins and antibodies. *Pharm. Sci. Encycl.* 1–11. <https://doi.org/10.1002/9780470571224.pse537>.
- Quan, C., Alcalá, E., Petkovska, I., Matthews, D., Canova Davis, E., Taticek, R., Ma, S., 2008. A study in glycation of a therapeutic recombinant humanized monoclonal antibody: Where it is, how it got there, and how it affects charge-based behavior. *Anal. Biochem.* 373, 179–191. <https://doi.org/10.1016/j.ab.2007.09.027>.
- Rathore, A., Kaur, R., Borgayari, D., 2017. Impact of Media Components on CQAs of Monoclonal Antibodies [WWW Document]. *BioPharm Int.* <http://www.processdevelopmentforum.com/articles/impact-of-media-components-on-cqas-of-monoclonal-antibodies/>.
- Razinkov, V.I., Treuheit, M.J., Becker, G.W., 2015. Accelerated formulation development of monoclonal antibodies (MABS) and mab-based modalities: review of methods and tools. *J. Biomol. Screen.* 20, 468–483. <https://doi.org/10.1177/1087057114565593>.
- Ribatti, D., 2014. From the discovery of monoclonal antibodies to their therapeutic application: an historical reappraisal. *Immunol. Lett.* 161, 96–99. <https://doi.org/10.1016/j.imlet.2014.05.010>.
- Ritacco, F.V., Wu, Y., Khetani, A., 2018. Cell culture media for recombinant protein expression in Chinese hamster ovary (CHO) cells: history, key components, and optimization strategies. *Biotechnol. Prog.* 34, 1407–1426. <https://doi.org/10.1002/btpr.2706>.
- Rouiller, Y., Périlleux, A., Collet, N., Jordan, M., Stettler, M., Broly, H., 2013. A high-throughput media design approach for high performance mammalian fed-batch cultures. *MABS* 5, 501–511. <https://doi.org/10.4161/mabs.23942>.
- Rouise, J.C., Stephens, E., Philip, S., English, A.M., Marzilli, L.A., 2017. Minimizing method induced deamidation and isomerization during antibody characterization to ensure optimal understanding of product quality attributes. *Chromatogr. Online* 15, 6–14.
- Ryman, J.T., Meibohm, B., 2017. Pharmacokinetics of monoclonal antibodies. *CPT Pharmacometrics Syst. Pharmacol.* 6, 576–588. <https://doi.org/10.1002/psp4.12224>.
- Sankar, K., Hoi, K.H., Yin, Y., Ramachandran, P., Andersen, N., Hilderbrand, A., McDonald, P., Spiess, C., Zhang, Q., 2018. Prediction of methionine oxidation risk in monoclonal antibodies using a machine learning method. *MABS* 10, 1281–1290. <https://doi.org/10.1080/19420862.2018.1518887>.
- Seibel, R., Maier, S., Schnellbaecher, A., Bohl, S., Welsling, M., Zeck, A., Zimmer, A., 2017. Impact of S-sulfolcysteine on fragments and trisulfide bond linkages in monoclonal antibodies. *MABS* 9, 889–897. <https://doi.org/10.1080/19420862.2017.1333212>.
- Seo, J.S., Kim, Y.J., Cho, J.M., Baek, E., Lee, G.M., 2013. Effect of culture pH on recombinant antibody production by a new human cell line, F2N78, grown in suspension at 33.0 °C and 37.0 °C. *Appl. Microbiol. Biotechnol.* 97, 5283–5291. <https://doi.org/10.1007/s00253-013-4849-2>.
- Sifiotis, V., Cruz, E., Eroglu, B., Kayser, V., 2019. Current advancements in addressing key challenges of therapeutic antibody design, manufacture, and formulation. *Antibodies* 8, 36. <https://doi.org/10.3390/antib8020036>.
- Sissolak, B., Ling, N., Sommeregger, W., Striedner, G., Vorauer-Uhl, K., 2019. Impact of mammalian cell culture conditions on monoclonal antibody charge heterogeneity: an accessory monitoring tool for process development. *J. Ind. Microbiol. Biotechnol.* 46, 1167–1178. <https://doi.org/10.1007/s10295-019-02202-5>.
- Smith, G., 1985. Filamentous fusion phage: novel expression vectors that display cloned antigens on the virion surface. *Science* (80-) 228, 1315–1317. <https://doi.org/10.1126/science.4001944>.
- Somra, R., 2007. Development knowledge can increase manufacturing capability and facilitate quality by design. *J. Pharm. Innov.* 2, 87–92. <https://doi.org/10.1007/s12247-007-9017-8>.
- Sormanni, P., Amery, L., Ekizoglou, S., Vendruscolo, M., Popovic, B., 2017. Rapid and accurate in silico solubility screening of a monoclonal antibody library. *Sci. Rep.* 7, 8200. <https://doi.org/10.1038/s41598-017-07800-w>.
- Steinmeyer, D.E., McCormick, E.L., 2008. The art of antibody process development. *Drug Discov. Today* 13, 613–618. <https://doi.org/10.1016/j.drudis.2008.04.005>.
- Strochlic, A., Davis, E., 2017. Optimize combination products: Select a drug delivery device that meets user needs [WWW Document]. *MedTech Intell.* https://www.medtechintelligence.com/feature_article/optimize-combination-products-select-drug-delivery-device-meets-user-needs/.
- Taylor, F.R., Ferrant, J.L., Foley, S.F., Zeng, C., Sernatinger, J., Juffras, R., Pepinsky, R.B., 2000. Biochemical analysis of retroviral structural proteins to identify and quantify retroviruses expressed by an NS0 murine myeloma cell line. *J. Biotechnol.* 84, 33–43. [https://doi.org/10.1016/S0168-1656\(00\)00335-7](https://doi.org/10.1016/S0168-1656(00)00335-7).
- Tesar, D., Luoma, J., Wyatt, E.A., Shi, C., Shatz, W., Hass, P.E., Mathieu, M., Yi, L., Corn, J.E., Maass, K.F., Wang, K., Dion, M.Z., Andersen, N., Loyet, K.M., van Lookeren Campagne, M., Rajagopal, K., Dickmann, L., Scheer, J.M., Kelley, R.F., 2017. Protein engineering to increase the potential of a therapeutic antibody Fab for long-acting delivery to the eye. *MABS* 9, 1297–1305. <https://doi.org/10.1080/19420862.2017.1372078>.
- The Antibody Society [WWW Document], 2020. <https://www.antibodysociety.org/home/> (accessed 8.18.20).
- Thömmes, J., Twyman, R.M., Gottschalk, U., 2017. Alternatives to packed bed chromatography for antibody extraction and purification. In: *Gottschalk, U. (Ed.), Process Scale Purification of Antibodies*. John Wiley & Sons Inc, pp. 215–231.
- Torkashvand, F., Vaziri, B., 2017. Main quality attributes of monoclonal antibodies and effect of cell culture components. *Iran. Biomed. J.* 21, 131–141. <https://doi.org/10.18869/acadpub.ijb.21.3.131>.
- Ulitzka, M., Carrara, S., Grzeschik, J., Kornmann, H., Hock, B., Kolmar, H., 2020. Engineering therapeutic antibodies for patient safety: tackling the immunogenicity problem. *Protein Eng. Des. Sel.* 33. <https://doi.org/10.1093/protein/gzaa025>.
- United States Food and Drug Administration, 2020. *Drugs@FDA: FDA-Approved Drugs* [WWW Document]. accessed 8.18.20. <https://www.accessdata.fda.gov/scripts/cdr/cdr/fda/>.
- Viola, M., Sequeira, J., Seça, R., Veiga, F., Serra, J., Santos, A.C., Ribeiro, A.J., 2018. Subcutaneous delivery of monoclonal antibodies: how do we get there? *J. Control. Release* 286, 301–314. <https://doi.org/10.1016/j.jconrel.2018.08.001>.
- Wakanikar, A.A., Borchardt, R.T., Eigenbrot, C., Shia, S., Wang, Y.J., Shire, S.J., Liu, J.L., 2007. Aspartate isomerization in the complementarity-determining regions of two closely related monoclonal antibodies †. *Biochemistry* 46, 1534–1544. <https://doi.org/10.1021/bi061500t>.
- Wang, B., Albanetti, T., Miro-Quesada, G., Flack, L., Li, L., Klover, J., Burson, K., Evans, K., Ivory, W., Bowen, M., Schoner, R., Hawley-Nelson, P., 2018. High-throughput screening of antibody expressing CHO clones using an automated shaken deep-well system. *Biotechnol. Prog.* 34, 1460–1471. <https://doi.org/10.1002/btpr.2721>.
- Wang, Q., Chung, C.-Y., Chough, S., Betenbaugh, M.J., 2018. Antibody glycoengineering strategies in mammalian cells. *Biotechnol. Bioeng.* 115, 1378–1393. <https://doi.org/10.1002/bit.26567>.
- Wang, Z., Zhu, J., Lu, H., 2020. Antibody glycosylation: impact on antibody drug characteristics and quality control. *Appl. Microbiol. Biotechnol.* 104, 1905–1914. <https://doi.org/10.1007/s00253-020-10368-7>.
- Wen, D., Vecchi, M.M., Gu, S., Su, L., Dolnikova, J., Huang, Y.-M., Foley, S.F., Garber, E., Pederson, N., Meier, W., 2009. Discovery and investigation of misincorporation of serine at asparagine positions in recombinant proteins expressed in Chinese Hamster Ovary cells. *J. Biol. Chem.* 284, 32686–32694. <https://doi.org/10.1074/jbc.M109.059360>.
- Whitaker, N., Xiong, J., Pace, S.E., Kumar, V., Middaugh, C.R., Joshi, S.B., Volkin, D.B., 2017. A formulation development approach to identify and select stable ultra-high-

- concentration monoclonal antibody formulations with reduced viscosities. *J. Pharm. Sci.* 106, 3230–3241. <https://doi.org/10.1016/j.xphs.2017.06.017>.
- WHO, 1998. WHO good manufacturing practices for pharmaceutical products: Main principles. *WHO GMP Annex 2*, 170–170 p.
- Xu, Y., Wang, D., Mason, B., Rossomando, T., Li, N., Liu, D., Cheung, J.K., Xu, W., Raghava, S., Katiyar, A., Nowak, C., Xiang, T., Dong, D.D., Sun, J., Beck, A., Liu, H., 2019. Structure, heterogeneity and developability assessment of therapeutic antibodies. *MAbs* 11, 239–264. <https://doi.org/10.1080/19420862.2018.1553476>.
- Yan, Q., Huang, M., Lewis, M.J., Hu, P., 2018. Structure based prediction of asparagine deamidation propensity in monoclonal antibodies. *MAbs* 10, 901–912. <https://doi.org/10.1080/19420862.2018.1478646>.
- Yang, C., Gao, X., Gong, R., 2018. Engineering of Fc fragments with optimized physicochemical properties implying improvement of clinical potentials for Fc-based therapeutics. *Front. Immunol.* 8 <https://doi.org/10.3389/fimmu.2017.01860>.
- Yang, C., Lee, A., Gao, S., Liu, S., Hedrick, J.L., Yang, Y.Y., 2019. Hydrogels with prolonged release of therapeutic antibody: block junction chemistry modification of 'ABA' copolymers provides superior anticancer efficacy. *J. Control. Release* 293, 193–200. <https://doi.org/10.1016/j.jconrel.2018.11.026>.
- Yang, X., Xu, W., Dukleska, S., Benchaar, S., Mengisen, S., Antochshuk, V., Cheung, J., Mann, L., Babadjanova, Z., Rowand, J., Gunawan, R., McCampbell, A., Beaumont, M., Meininger, D., Richardson, D., Ambrogely, A., 2013. Developability studies before initiation of process development: improving manufacturability of monoclonal antibodies. *MAbs* 5, 787–794. <https://doi.org/10.4161/mabs.25269>.
- Yang, Y., Wang, G., Song, T., Lebrilla, C.B., Heck, A.J.R., 2017. Resolving the micro-heterogeneity and structural integrity of monoclonal antibodies by hybrid mass spectrometric approaches. *MAbs* 9, 638–645. <https://doi.org/10.1080/19420862.2017.1290033>.
- Yt, L.X., Amidon, G., Khan, M.A., Hoag, S.W., Polli, J., Raju, G.K., Woodcock, J., 2014. Understanding pharmaceutical quality by design. *AAPS J.* 16, 771–783. <https://doi.org/10.1208/s12248-014-9598-3>.
- Yu, X.C., Borisov, O.V., Alvarez, M., Michels, D.A., Wang, Y.J., Ling, V., 2009. Identification of codon-specific serine to asparagine mistranslation in recombinant monoclonal antibodies by high-resolution mass spectrometry. *Anal. Chem.* 81, 9282–9290. <https://doi.org/10.1021/ac901541h>.
- Yuk, I.H., Zhang, B., Yang, Y., Dutina, G., Leach, K.D., Vijayasankaran, N., Shen, A.Y., Andersen, D.C., Sneedcor, B.R., Joly, J.C., 2011. Controlling glycation of recombinant antibody in fed-batch cell cultures. *Biotechnol. Bioeng.* 108, 2600–2610. <https://doi.org/10.1002/bit.23218>.
- Zhang, E., Xie, L., Qin, P., Lu, L., Xu, Y., Gao, W., Wang, L., Xie, M.H., Jiang, W., Liu, S., 2020. Quality by Design-based assessment for analytical similarity of adalimumab biosimilar HLX03 to Humira®. *AAPS J.* 22, 69. <https://doi.org/10.1208/s12248-020-00454-z>.
- Zhang, Y., III, R.O.W., Tucker, H.O., 2020. Formulation strategies in immunotherapeutic pharmaceutical products. *World J. Clin. Oncol.* 11, 275–282. <https://doi.org/10.5306/wjco.v11.i5.275>.
- Zhao, L., Ji, P., Li, Z., Roy, P., Sahajwalla, C.G., 2013. The antibody drug absorption following subcutaneous or intramuscular administration and its mathematical description by coupling physiologically based absorption process with the conventional compartment pharmacokinetic model. *J. Clin. Pharmacol.* 53, 314–325. <https://doi.org/10.1002/jcph.4>.
- Zhao, L., Ren, T.H., Wang, D.D., 2012. Clinical pharmacology considerations in biologics development. *Acta Pharmacol. Sin.* 33, 1339–1347. <https://doi.org/10.1038/aps.2012.51>.
- Zheng, K., Bantog, C., Bayer, R., 2011. The impact of glycosylation on monoclonal antibody conformation and stability. *MAbs* 3, 568–576. <https://doi.org/10.4161/mabs.3.6.17922>.
- Zhou, K., Cao, X., Bautista, J., Chen, Z., Hershey, N., Ludwig, R., Tao, L., Zeng, M., Das, T. K., 2020. Structure-function assessment and high-throughput quantification of site-specific aspartate isomerization in monoclonal antibody using a novel analytical kit. *J. Pharm. Sci.* 109, 422–428. <https://doi.org/10.1016/j.xphs.2019.08.018>.
- Zhu, J., 2012. Mammalian cell protein expression for biopharmaceutical production. *Biotechnol. Adv.* 30, 1158–1170. <https://doi.org/10.1016/j.biotechadv.2011.08.022>.
- Zurdo, J., 2013. Developability assessment as an early de-risking tool for biopharmaceutical development. *Pharm. Bioprocess.* 1, 29–50. <https://doi.org/10.4155/pbp.13.3>.

4.2 Recombinant Antibody Production Using a Dual-Promoter Single Plasmid System.

Title:

Recombinant Antibody Production Using a Dual-Promoter Single Plasmid System.

Authors:

Stefania Candela Carrara*, David Fiebig*, Jan Patrick Bogen*, Julius Grzeschik, Björn Hock, Harald Kolmar.

(* shared first authorship)

Bibliographic data:

Journal – *Antibodies (Basel)*

Volume 10, Issue 2

Article published: 13th May 2021

DOI: 10.3390/antib10020018.

PMID: 34068440

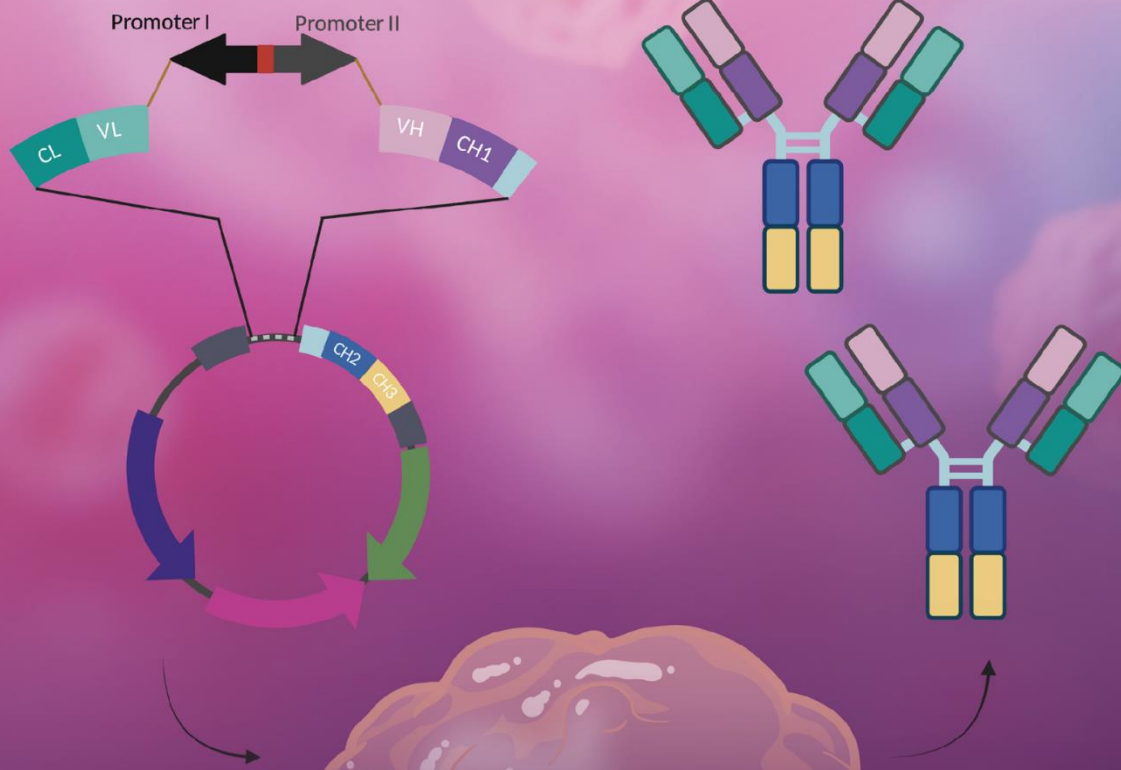
Contributions by S.C. Carrara:

- Experimental testing of variants generated with D. Fiebig and J.P. Bogen.
- Writing of manuscript together with D. Fiebig and J.P. Bogen.
- Generation of figures together with D. Fiebig and J.P. Bogen.

Issue cover for *Antibodies* based on this work:



antibodies



Recombinant Antibody Production Using a Dual-Promoter Single Plasmid System

Volume 10 • Issue 2 | June 2021



mdpi.com/journal/antibodies
ISSN 2073-4468

©Created with Biorender

Article

Recombinant Antibody Production Using a Dual-Promoter Single Plasmid System

Stefania C. Carrara^{1,2,†}, David Fiebig^{1,2,†}, Jan P. Bogen^{1,2,†}, Julius Grzeschik², Björn Hock³ and Harald Kolmar^{1,*} 

¹ Institute for Organic Chemistry and Biochemistry, Technische Universität Darmstadt, Alarich-Weiss-Str. 4, D-64287 Darmstadt, Germany; stefania.carrara@ferring.com (S.C.C.); fiebig@biochemie-tud.de (D.F.); bogen@biochemie-tud.de (J.P.B.)

² Ferring Darmstadt Laboratories, Alarich-Weiss-Str. 4, D-64287 Darmstadt, Germany; julius.grzeschik@ferring.com

³ Ferring International Center S.A, Chemin de la Vergognausaz 50, CH-1162 Saint Prex, Switzerland; bjorn.hock@ferring.com

* Correspondence: Kolmar@biochemie-TUD.de

† These authors contributed equally to this work.

Abstract: Monoclonal antibodies (mAbs) have demonstrated tremendous effects on the treatment of various disease indications and remain the fastest growing class of therapeutics. Production of recombinant antibodies is performed using mammalian expression systems to facilitate native antibody folding and post-translational modifications. Generally, mAb expression systems utilize co-transfection of heavy chain (*hc*) and light chain (*lc*) genes encoded on separate plasmids. In this study, we examine the production of two FDA-approved antibodies using a bidirectional (BiDi) vector encoding both *hc* and *lc* with mirrored promoter and enhancer elements on a single plasmid, by analysing the individual *hc* and *lc* mRNA expression levels and subsequent quantification of fully-folded IgGs on the protein level. From the assessment of different promoter combinations, we have developed a generic expression vector comprised of mirrored enhanced CMV (eCMV) promoters showing comparable mAb yields to a two-plasmid reference. This study paves the way to facilitate small-scale mAb production by transient cell transfection with a single vector in a cost- and time-efficient manner.

Keywords: monoclonal antibodies; promoters; bidirectional; antibody production; upstream processing



Citation: Carrara, S.C.; Fiebig, D.; Bogen, J.P.; Grzeschik, J.; Hock, B.; Kolmar, H. Recombinant Antibody Production Using a Dual-Promoter Single Plasmid System. *Antibodies* **2021**, *10*, 18. <https://doi.org/10.3390/antib10020018>

Academic Editor: Itai Benhar

Received: 24 March 2021

Accepted: 10 May 2021

Published: 13 May 2021

Publisher's Note: MDPI stays neutral with regard to jurisdictional claims in published maps and institutional affiliations.



Copyright: © 2021 by the authors. Licensee MDPI, Basel, Switzerland. This article is an open access article distributed under the terms and conditions of the Creative Commons Attribution (CC BY) license (<https://creativecommons.org/licenses/by/4.0/>).

1. Introduction

With the growing interest in monoclonal antibodies (mAbs) for therapeutic applications, advances in antibody production have improved drastically over the last decades. Due to the more complex structure of antibodies, their production requires host cells capable of natively folding and modifying the mAb. Modifications include post-translational glycosylation, which is, among other functional properties, critical to reduce their immunogenicity [1]. For this purpose, mammalian cells fulfil the requirements as appropriate hosts for antibody production [2,3]. Advances in transfection protocols and cell engineering have boosted the use of suspension cell lines with the ability to grow at high densities, and increased production yields [4,5]. Further within the drug discovery and development process, stable cell lines are generated for the most promising candidate(s), while transient transfection is performed at earlier stages to yield research quantities of mAbs, sufficient for characterization of lead candidates. The accessibility of commercially available transfection reagents with high efficiencies and the use of disposable materials makes transient expression an efficient and cost-effective strategy during early drug discovery [6]. Human Embryonic Kidney 293 (HEK293) and Chinese Hamster Ovary (CHO) cells are commonly used for transient antibody expression, due to their high expression yields and human-like glycosylation patterns [1,7,8].

The basis of successful antibody production is the correct folding of individual chains, followed by their accurate assembly, resulting in functional heterotetrameric glycoproteins. Misfolded or partially folded antibodies are degraded by the host cell's intrinsic quality control system, resulting in low production yields. Furthermore, antibodies with undesired folding are not able to effectively engage their target antigen or to mediate effector functions, have unfavourable pharmacokinetics, and tend to aggregate. Besides these biological limitations, purification of antibody products contaminated with aggregated or misfolded mAbs is a major hindrance in the downstream processing of therapeutic molecules and is currently the topic of numerous studies [9–12].

Antibody folding starts upon co-translational translocation into the endoplasmic reticulum (ER) [13]. Following the homodimerization of the two heavy chains (HC), the light chains (LC) are associated and covalently linked via disulphide bonds [14]. The glycosylation at Asn297 is linked to the CH2 backbone in a co-translational manner [15]. During translation, chaperones are involved to ensure the correct folding of the individual domains, as well as the final assembly of the tetrameric mAb [16].

At present, the largest part of transient production of mAbs is carried out using a two-plasmid system, also known as co-transfection, for the expression of *lc* and *hc*, with each gene driven by its own promoter and transcribed separately [17,18]. These are carried out, for the most part, with an equimolar ratio of heavy chain and light chain genes. Nonetheless, contradictory results have been reported using Expi293-F cells. While some publications report that an equimolar gene ratio results in the highest yield of fully assembled IgGs [8], others have described optimal expression with a 1:2 ratio of heavy and light chain genes, respectively [19].

A large drawback of the two-plasmid system is the moderate control over the relative expression of *lc* and *hc*, with fluctuating cell-to-cell transfection efficiencies [17]. On the other hand, a bidirectional (BiDi) vector with a dual-promoter can ensure the introduction of both *hc* and *lc* genes into each cell in equal amounts. However, for some applications it could be beneficial to have a stronger expression of one chain over the other. By choosing two suitable promoters controlling the transcription of *hc* and *lc*, different ratios can be achieved [20]. While diverse approaches have been developed throughout the years to advance and facilitate recombinant antibody production, the design of expression vectors plays a large role for optimization of expression yields. Recently, Bayat and colleagues (2018) compared the use of three different vector design strategies for the expression of IgG1 antibodies in CHO cells, namely using the conventional two-vector approach with *hc* and *lc* encoded separately, a bicistronic vector based on internal ribosome entry sites (IRES), and a dual-promoter single vector approach. All vectors were under the control of a human cytomegalovirus (CMV) promoter. Expression analysis revealed that the dual-promoter vector system resulted in the highest mAb yield [21].

Andersen and co-workers have previously shown the ability of the CMV enhancer to control two core CMV promoters simultaneously, resulting in efficient antibody expression [22]. With this basis, we sought to investigate different promoters in a bidirectional format to facilitate transient transfection, avoiding co-transfections. We also sought to simplify *hc* and *lc* gene cloning by establishing a one-step Golden Gate cloning procedure that relies on the simultaneous plasmid incorporation of *hc* and *lc* genes together with the bidirectional promoter sequence. By analysing *hc* and *lc* gene expression, as well as through subsequent quantification of fully-folded IgGs, promoter and enhancer element combinations were compared. Here, we show the use of a dual-promoter, single plasmid approach using divergent promoters for the transient expression of two FDA-approved antibodies, Durvalumab and Avelumab, using both Expi293-F and ExpiCHO-S cell systems. This work lays the foundation to facilitate small-scale mAb production in drug discovery programs in a more efficient manner.

2. Materials and Methods

2.1. Plasmids & Cloning of Constructs

To allow the individual exchange of different variable domains, the utilization of κ and λ isotypes, as well as the usage of different BiDi promoter combinations, the backbone of the mammalian destination (MD) vector was built in a cassette-like manner. For vector amplification in *E. coli*, a chloramphenicol resistance was utilized, adjacent to the *colE1* and the *f1* origins. A stuffer sequence, flanked by *Esp31* restriction sites, was downstream of an inverse-orientated SV40 polyA sequence that was intended to be a terminator signal for the light chain cassette. Upstream of the stuffer sequence, a partial hinge followed by the CH2 and CH3 domains of a human IgG1 were encoded. Again, a SV40 polyA signal sequence served as a terminator signal (Figure 1A). The plasmid was de novo designed in silico and ordered at GeneArt (Regensburg, Germany).

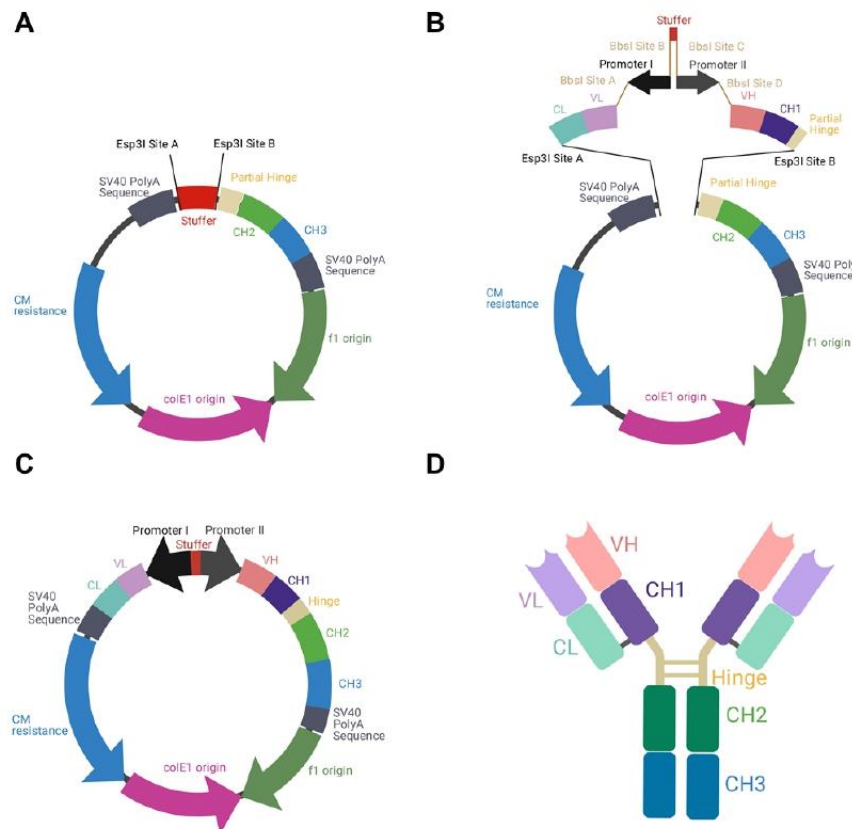


Figure 1. Schematic illustration of BiDi promoter system for antibody production. (A) The MD vector was designed to exhibit a 200-bp stuffer, flanked by *Esp31* restriction sites (*Esp31* sites A and B), adjacent to a SV40 polyA signal sequence and the regions encoding for hinge-CH2-CH3, terminated by a SV40 polyA signal sequence. (B) VL-CL and VH-CH1 amplicons can be inserted into MD by Golden Gate cloning utilizing *Esp31* restriction sites (*Esp31* sites A and B). The BiDi promoter can be chosen individually and is flanked by *BbsI* sites (*BbsI* sites A–D), compatible with the VL and VH sequences. (C) Golden Gate assembly results in a fully functional and re-circularized vector, with the light chain under the control of promoter I and the heavy chain under the control of promoter II. (D) Schematic representation of the resulting heterotetrameric IgG1 antibody using the same colour code as for the genetic elements.

The selected promoter sequences were either ordered as gene strings at Twist Bioscience (EF-1 α , minCMV-enh-CMV (GenBank: MK764037) or PCR-amplified from the pTT5

CMV promoter cassette between bases 42–1185 (hereinafter referred to as eCMV) [23]. To allow for the correct orientation of the promoter sequences, individual primers were used to introduce the respective *Bbs*I Golden Gate cloning (GGC) signature overhangs. Genes for VH-CH1 and VL-CL of Durvalumab (Imfinzi, κ light chain) and Avelumab (Bavencio, λ light chain) were also ordered as gene strings, already bearing suitable signature sequences for *Esp*3I and *Bbs*I as well as their respective leader sequences. The 200-bp stuffer used between individual promoters consists of the non-functional 3' coding region of the amp resistance gene for beta-lactamase, followed by ~40 bp of non-coding DNA. Assembly of the MD expression constructs was conducted with 75 ng destination vector and equimolar amounts of the respective fragments, 20 U *Bbs*I-HF, 10 U *Esp*3I, and 200 U T4-DNA ligase (NEB, Frankfurt, Germany) for 30 cycles (1 min; 16 °C; 37 °C). For the reference constructs, VH and VL genes were amplified incorporating *Sap*I restriction sites and then inserted into a pTT5-derived vector utilizing CH1-CH2-CH3 or κ/λ entry vectors using GGC as described before [24,25]. PCR reactions were performed utilizing Q5 polymerase (NEB) according to the manufacturer's protocol and purified using the Wizard SV Gel and PCR Clean-up System (Promega, Walldorf, Germany). All primers can be found in Table S1. The DNA sequence for the 2xeCMV BiDi construct can be found in Sequence S1 in the Supplementary Information.

E. coli XL1-blue were transformed utilizing the Golden Gate reaction mixtures and cultivated on chloramphenicol or ampicillin DYT agar plates for MD or pTT5 constructs, respectively. Resulting colonies were sequenced at MicroSynth SeqLab (Göttingen, Germany), and positive clones were utilized to inoculate 50 mL overnight cultures. Plasmid DNA for transient transfection was isolated using the PureYield Plasmid Midiprep System (Promega, Walldorf, Germany).

2.2. Cell Lines

Expi293-F and ExpiCHO-S cells were obtained from Thermo Fisher Scientific. Cells were incubated at 37 °C, 8% CO₂, 110 rpm, and sub-passaged every 3–4 days in their respective expression media, as described in the manufacturer's protocol (Thermo Fisher Scientific, Schwerte, Germany). Cell count and viability were measured using an automated cell counter (Bio-Rad TC-20) based on trypan blue staining. Cell densities were maintained between $0.3\text{--}4 \times 10^6$ cells/mL and $0.2\text{--}6 \times 10^6$ cells/mL for Expi293-F and ExpiCHO-S, respectively.

2.3. 24-Well Transfection

For gene expression and protein quantification, small-scale transfections using Axygen 24-well deep-well plates (Corning, New York, NY, USA) were performed. One day prior to transfection, cells were seeded into wells at a final cell density of 1.8×10^6 or 3×10^6 viable cells/mL in 2.5 mL expression medium for Expi293-F or ExpiCHO-S, respectively, and incubated under shaking conditions in a humidified atmosphere at 37 °C, 8% CO₂, 225 rpm. The following day, the cell density was adjusted to 3×10^6 or 6×10^6 viable cells/mL in 2.5 mL expression medium for Expi293-F or ExpiCHO-S, respectively. DNA:Expifectamine complexes were incubated at room temperature with either 3 μ g BiDi plasmid or 2 μ g heavy and 2 μ g light chain plasmid for co-transfections (two-plasmid reference) for 20 or 1 min for Expi293-F or ExpiCHO-S, respectively, before adding dropwise to the cells. Feeding procedures were carried out according to manufacturer's instructions. For gene expression analysis, cells were harvested 3 days post-transfection, while protein quantification was carried out 6 days post-transfection.

2.4. RNA Isolation

Three days post-transfection, Expi293-F or ExpiCHO-S cells were harvested by centrifugation and cell pellets were processed through a QIAshredder column (QIAGEN, Hilden, Germany). Total RNA extraction was carried out using RNeasy Mini Kit (QIAGEN) following the manufacturer's instructions. RNA concentration was determined spectro-

scopically using a NanoDrop One (Thermo Fisher), ensuring pure RNA was isolated with a A260/280 ratio of 2.0.

2.5. Gene Expression Analysis by Reverse Transcription Quantitative Polymerase Chain Reaction (RT-qPCR)

Expression levels of heavy and light chain (both κ and λ) were analysed using 100 ng RNA per well in Hard-Shell[®] 96-well PCR plates (Bio-Rad, Hercules, CA, USA) and iTaq Universal SYBR Green One-step Kit (Bio-Rad) with designed SYBR Green primers (Sigma Aldrich, Munich, Germany) using a CFX96 qPCR instrument (Bio-Rad). Relative expression levels were analysed using the integrated software from Bio-Rad (CFX Manager, Hercules, CA, USA) and normalized to housekeeping genes GAPDH and RPLP0 (IDT, Coralville, IA, USA). The primers used can be found in Table S2.

2.6. Protein Purification

To purify the antibodies from small-scale transfections, cells were harvested by centrifugation and cell culture supernatants were purified using Protein A HP SpinTrap columns (Cytiva, Freiburg im Breisgau, Germany) following the manufacturer's protocol. Antibodies were eluted in 0.1 M glycine-HCl, pH 2.7. Protein concentration was determined using a NanoDrop One (Thermo Fisher) using the corresponding molecular weights and extinction coefficients.

2.7. Protein Quantification and Affinity Determination Using Biolayer Interferometry (BLI)

Six days post-transfection, cells were harvested by centrifugation and the cell culture supernatants were sterile-filtered (0.45 μ m). BLI experiments were performed on an Octet Red96 (FortéBio, Fremont, CA, USA). Using Protein A biosensors (Sartorius, Göttingen, Germany) for quantification, mAb concentration was measured from the cell culture supernatants. An in-house produced mAb was used as a standard within the range of 3.13–400 μ g/mL.

For affinity determination, anti-human Fab-CH1 2nd generation (FAB2G) biosensors (Sartorius) were used. Purified antibodies were loaded onto the tips at 10 μ g/mL until a layer thickness of 1 nm was reached. Association was measured using a serial dilution of His-PD-L1-TwinStrep (produced in-house). Kinetics were determined using Savitzky-Golay filtering and a 1:1 Langmuir binding model.

3. Results

To produce full-length antibodies in a bidirectional manner, we first designed the respective vector in silico. This vector encoded the fragment crystallizable (Fc) region of an IgG1, which is the most common isotype found in therapeutic antibodies [26]. In order to allow the flexible use for a variety of binders, the fragment antigen binding (Fab), which can be of the κ or λ isotype, was not encoded on the plasmid. Instead, a stuffer sequence, flanked by *Esp3I* sites was incorporated (Figure 1A).

As a reference antibody to establish different promoter combinations, the Fab of Durvalumab, an FDA-approved anti-PD-L1 antibody of the κ type, was chosen [27]. PCR amplicons of VH-CH1 and VL-CL were generated introducing *Esp3I* and *BbsI* restriction sites. By utilization of a BiDi promoter system, flanked by *BbsI* sites, a Golden Gate reaction resulted in a re-circularized vector (Figure 1B,C). In this process, the stuffer that was included in the parental MD vector was replaced by a CL-VL-PromoterI-Stuffer-PromoterII-VH-CH1 sequence. Owing to this cloning strategy, a straightforward exchange of different Fabs and different BiDi promoters is feasible. The resulting vector exhibited the functional ORFs for the heavy and the light chains, resulting in the production of full-length antibodies (Figure 1D).

3.1. Cloning Promoter Combinations

Based on the findings from Andersen et al. [22] that a single enhancer adjacent to a bidirectional CMV promoter allows for efficient antibody production using a single expression plasmid, six different bidirectional promoter complexes were generated comprising not only the minCMV-CMV cassette, but also combinations of other strong promoters including their individual enhancer elements, such as the CMV with its major immediate early enhancer (MIE), the optimized CMV cassette from pTT5 (denoted as eCMV in this study), and the human translation elongation factor 1 alpha (EF-1 α) promoter, that were selected based on their capability to produce fully-folded IgG molecules.

The MIE-CMV promoter, being one of the most commonly used in mammalian expression vectors, is designated as a strong driver for recombinant protein expression [28,29]. As shown before by Andersen and colleagues [22], the MIE enhancer is also capable of facilitating elevated expression levels in the divergently oriented minCMV promoter, although to a lesser extent. This was based on the presumption that the formation of the large transcription complex might be sterically hindered. As a reference, we selected a similar bidirectional promoter setup lacking the unique sequence upstream of the enhancer. Additionally, we went for a mirror-symmetric approach comprised of two individual CMV promoters, each having adjacent MIE enhancers that were separated by a 200-bp-stuffer. The eCMV cassette comprises—besides the MIE enhancer and core promoter—several additional regulatory elements that have been described to increase expression levels. These elements include the non-coding adenoviral tripartite leader sequence (TPL), the adenovirus major late promoter enhancer (MLP enh.), as well as distinct splicing sites allowing for prolonged mRNA stability [30,31]. Furthermore, we also utilized the strong human translation elongation factor 1 alpha promoter (EF-1 α) that has proven to be advantageous over the CMV promoter in some cell types and in the expression of distinct proteins of interests [32,33].

Based on the modular setup of our MD vector and utilization of GGC, we generated different combinations of the aforementioned promoters to analyse for highest full-length antibody expression levels and product yield of Durvalumab. A schematic overview of the BiDi combinations is depicted in Figure 2.

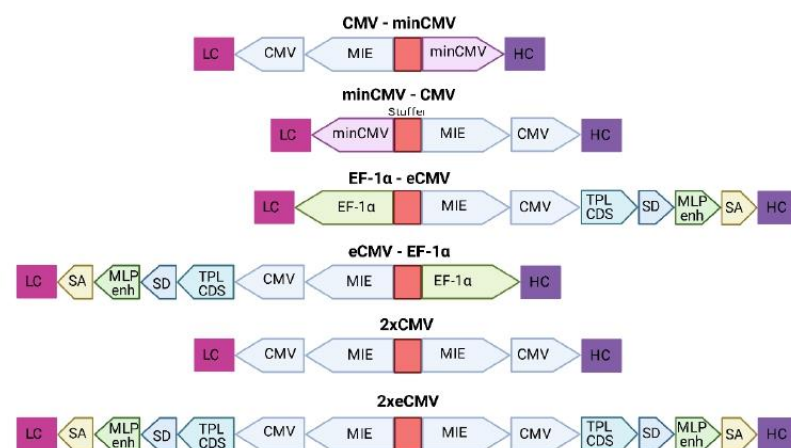


Figure 2. Overview of the different bidirectional combinations tested. The 200-bp stuffer sequence is marked in red for each construct. Abbreviations: minimal CMV (minCMV), cytomegalovirus promoter (CMV), enhanced CMV (eCMV), major immediate early enhancer (MIE), human translation elongation factor 1 alpha (EF-1 α), adenoviral tripartite leader sequence (TPL CDS), adenovirus major late promoter enhancer (MLP enh.), splicing donor site (SD), splicing acceptor site (SA), light chain (LC), heavy chain (HC).

3.2. Gene Expression Analysis in Mammalian Cells

Transient transfections of all six promoter combinations were performed in 24-well plates using Expi293-F cells, an established cell line for transient antibody production. Three days post-transfection, cells were harvested, and RNA was isolated. Relative gene expression of *hc* and *lc* mRNA levels was measured by RT-qPCR (Figure 3).

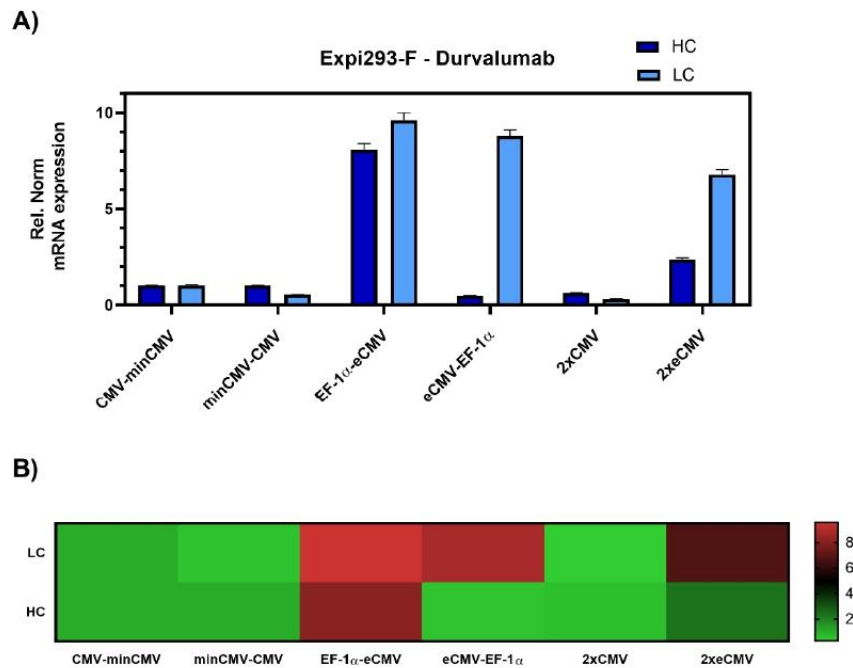


Figure 3. Gene expression analysis of heavy and light chain genes after transient transfection of Durvalumab in Expi293-F cells. (A) Bar chart representing heavy (dark blue) and light (light blue) chain mRNA expression in the different constructs. Values are relative to the CMV-minCMV construct and normalised to housekeeping genes GAPDH and RPLP0. Error bars represent the standard error of the mean of technical triplicates. (B) Heat map representation of gene expression analysis. The relative normalised gene expression for light and heavy chain mRNA is shown on the right.

The data was set relative to the CMV-minCMV construct and normalised to housekeeping genes. Looking at relative mRNA levels, both variants with minCMV and CMV, independent of the promoter orientation, did not yield high mRNA expression for either *lc* or *hc*. Remarkably, the combinations with the EF-1 α promoter and the enhanced CMV cassette (eCMV) showed significant differences in expression levels depending on their orientation. Steering *lc* expression with the EF-1 α promoter (EF-1 α -eCMV) resulted in a 9.5-fold upregulation in *lc* and 8-fold upregulation in *hc* mRNA levels. Conversely, having the more potent eCMV in the light chain direction and EF-1 α in the heavy chain direction (eCMV-EF-1 α) led to a 9-fold *lc* upregulation, and low relative *hc* expression levels. Based on these results, mirrored constructs containing both promoter and enhancer cassettes in both directions were tested, one with the traditional CMV promoter (2xCMV), and the other with the eCMV cassette (2xeCMV). Interestingly, the 2xCMV construct did not result in increased *lc* or *hc* mRNA levels compared to the bidirectional construct containing two identical eCMV promoters or constructs containing two different promoters. The BiDi combination of two mirrored eCMV promoter cassettes (2xeCMV) yielded in a 7-fold upregulation of *lc* mRNA and a modest upregulation in *hc* levels.

As promoter strength may vary depending on the cell line, particularly for the CMV promoter [33], ExpiCHO-S cells were also investigated. Gene expression analysis resulted in similar results as in Expi293-F cells, with the 2xeCMV complex showing the

strongest upregulation in both *hc* and *lc* mRNA levels compared to the other promoter combination, namely a modest 10-fold upregulation of *hc*, and a 20-fold upregulation of *lc* mRNA (Figure 4).

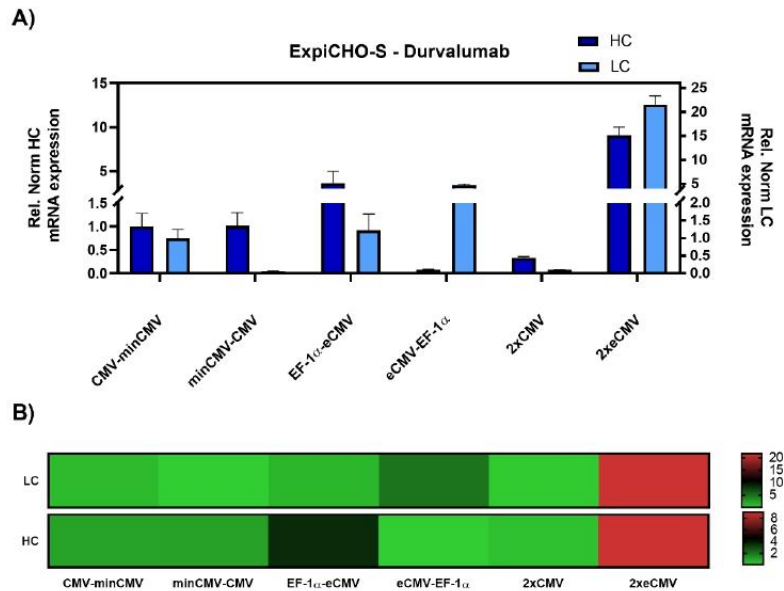


Figure 4. Gene expression analysis of heavy and light chain genes after transient transfection of Durvalumab in ExpiCHO-S cells. (A) Bar chart representing heavy (dark blue) and light (light blue) chain mRNA expression in the different constructs. Values are relative to the CMV-minCMV construct and normalised to housekeeping genes GAPDH and RPLP0. Error bars represent the standard error of the mean of technical triplicates. (B) Heat map representation of gene expression analysis. The relative normalised gene expression for light and heavy chain mRNA is shown on the right with their respective scales.

3.3. Protein Yield Determination via BLI

As mRNA transcript levels do not indicate successful secretion of fully functional recombinant antibodies, protein quantification studies were performed. Expi293-F cells were transiently transfected and the amount of secreted therapeutic antibody Durvalumab [27] was quantified by biolayer interferometry (BLI) using sterile-filtered cell culture supernatants six days post-transfection. The mAb concentrations for the different constructs were interpolated from a standard curve generated using an in-house produced mAb. In line with the gene expression analysis, protein quantification resulted in a clear ranking of the different promoter combinations (Figure 5).

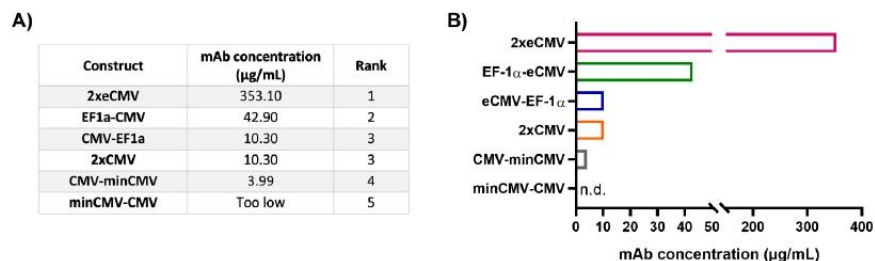


Figure 5. Protein quantification of Durvalumab in cell culture supernatants from transfected Expi293-F cells. (A) Table showing the mAb concentrations from 24-well transient transfections, listed according to their rank. The ranks 1–5 were set based on the mAb concentration of the different BiDi combinations. (B) Bar chart representation of BiDi mAb concentrations.

From the bidirectional combinations tested with transient transfections, the 2xeCMV BiDi construct showed the highest mAb concentration with 353 $\mu\text{g/mL}$ (Figure 5). Interestingly, mRNA expression was higher for EF-1 α -eCMV compared to 2xeCMV for both *hc* and *lc*, but antibody yield was significantly reduced in Expi293-F cells (Figure 3). This may likely be due to the fact that EF-1 α -eCMV displayed similar *hc* and *lc* mRNA expression patterns, while 2xeCMV revealed a higher accumulation of the *lc* compared to the *hc* mRNA. It is well known that the expression of excess light chain over heavy chain is often beneficial for antibody production [34–37]. These findings corroborate that 2xeCMV resulted in the most promising bidirectional promoter combination, particularly in view of the fact that the usage of this promoter combination resulted, both in Expi293-F and ExpiCHO-S cell lines, in significantly enhanced mRNA synthesis with an excess of *lc* over *hc*.

3.4. Correlation of mRNA and Protein Levels

After performing both mRNA and protein studies, the correlation of the cycle threshold (Ct) values from RT-qPCR and the mAb concentrations from protein quantification in Expi293-F was determined (Figure 6A). Overall, a Pearson's coefficient of -0.6407 was calculated, indicating, as expected, a negative correlation between Ct values and mAb concentration. Looking at the respective Ct values of either the *hc* or *lc* for 2xeCMV, one can observe they have a low Ct value and resulted in the largest mAb yield. While some claim that abundance of *hc* may hinder productivity, it appears that the excess of *lc* allowing for correct mAb folding and assembly is sufficient for higher mAb yields. On the contrary, the Ct values of eCMV-EF-1 α *lc* is similar to that of 2xeCMV, with the only difference being in the *hc* expression, ultimately resulting in much lower yields. Thus, this further shows the importance of a fine-tuned *hc* and *lc* expression, substantiating the potential of 2xeCMV for a BiDi antibody production system.

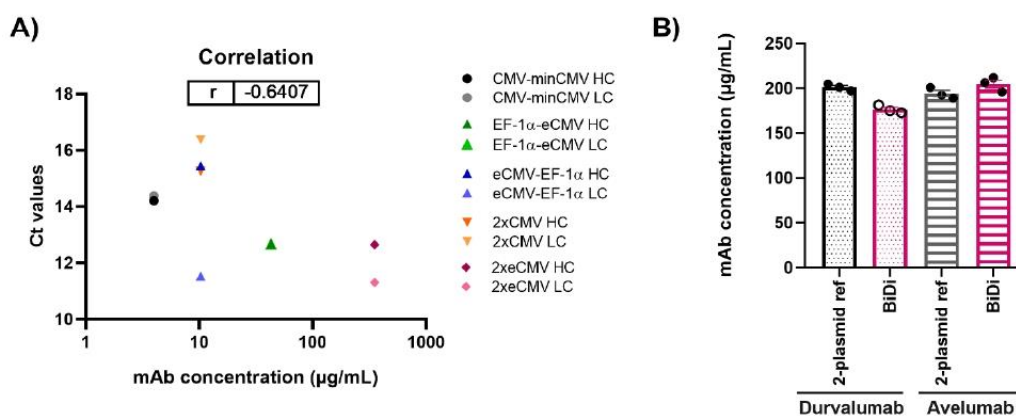


Figure 6. (A) Correlation of mAb concentration and Ct values for both heavy and light chain expression in Expi293-F for production of Durvalumab. (B) Quantification of antibody concentration for the production of Durvalumab and Avelumab using either a 2-plasmid reference or the BiDi 2xeCMV construct. Error bars represent the standard error of the mean of biological triplicates, while the symbols represent the individual measurements.

3.5. Antibody—And Light Chain-Independence

To ensure the promoter combination used for our BiDi technology was not antibody- or light chain isotype-dependent, the FDA-approved anti-PD-L1 antibody Avelumab of the λ isotype was also tested [38]. As 70% of approved antibodies belong to the κ type [39,40], only the most promising 2xeCMV construct was used to validate the established system for a λ -based mAb, compared to the conventional co-transfection approach. For co-transfection, Expi293-F cells were transfected using a 1:1 ratio of HC and LC DNA, with each plasmid carrying the same promoter and enhancer cassette as the bidirectional vector, namely eCMV. As can be appreciated from Figure 6B, there was no significant variation in antibody yield

between transfections with BiDi and the two-plasmid reference for either Durvalumab or Avelumab. Similarly, no variation was observed in ExpiCHO-S production (data not shown). Kinetics determination of both antibodies produced with either the two-plasmid reference or our established 2xeCMV BiDi plasmid bound to its target PD-L1 with comparable affinities (Table 1, Figures S1 and S2). Additionally, SDS-PAGE analysis under reducing conditions resulted in the expected heavy and light chains bands (Figure S3).

Table 1. Affinity determination of Avelumab and Durvalumab using either co-transfection or 2xeCMV BiDi plasmid.

	Antibody	K _D [pM]	
		2-Plasmid Ref.	BiDi
Expi293-F	Durvalumab	594	364
	Avelumab	205	195
ExpiCHO-S	Durvalumab	562	522
	Avelumab	148	267

Thus, this indicated the established system is compatible with different binders and can be employed for both κ - and λ -light chain isotypes.

4. Discussion

This work describes the generation of a bidirectional vector construct for recombinant antibody expression using two eCMV promoter cassettes, controlling the expression of *lc* and *hc* individually in each direction. By performing a thorough analysis of different bidirectional promoter combinations with varying lengths and strengths, the 2xeCMV combination showed the most promising *hc* and *lc* mRNA synthesis in two regularly used mammalian cell lines, and, more importantly, the highest yields after protein quantification comparable to those using the conventional two-plasmid system. Other BiDi constructs showed potentially promising gene expression profiles, such as EF-1 α -eCMV combination, with high relative mRNA levels of both *hc* and *lc* mRNA. Nonetheless, having higher levels of *hc* mRNA in the cells appear to curb productivity of fully folded IgG formation, resulting in drastically decreased antibody yields compared to both the two-plasmid reference and the 2xeCMV BiDi vector.

While using a bidirectional approach takes away some flexibility in terms of being able to alter the *hc:lc* ratios during co-transfection, the overexpression of both genes and, especially the excess *lc* expression, results in sufficient material for antibody hit screening. For convenience, we established a one-step cloning procedure for simultaneous plasmid incorporation of the heavy and light chain encoding segments obviating the need for generating two separate plasmids. Not only does this approach lower plasmid preparation efforts, but it also increases handling for transfection of numerous mAbs during screening and characterization as only a single plasmid is required. The use of two FDA-approved antibodies with either a κ - or λ -light chain shows there is no antibody- or light chain-dependence using this system, indicating that it can be implemented ubiquitously. Further options remain to increase the yields of IgG molecules, such as optimization of the stuffer region between the two eCMV promoter cassettes, potentially reducing any steric hinderance and increasing transcription efficiency [22,41].

In conclusion, this work displays the benefits of using a one-plasmid bidirectional system with 2xeCMV promoters for fully folded IgGs within drug discovery. In terms of practicality, handling of a single plasmid for antibody production may be superior to the conventional way. Moreover, yields of fully folded IgGs are comparable between the two systems. Future directions for this technology go beyond recombinant production of classical antibody formats, as reduction of the number of plasmid constructs could also be considered feasible for the expression of bispecific antibodies and other antibody formats in the frame of antibody drug discovery.

Supplementary Materials: The following are available online at <https://www.mdpi.com/article/10.3390/antib10020018/s1>, Table S1: Primers used for cloning of bidirectional constructs, Table S2: RT-qPCR primers for HC and LC constant regions, Figure S1: Affinity determination by BLI of antibodies produced in Expi293-F, Figure S2: Affinity determination by BLI of antibodies produced in ExpiCHO-S, Figure S3: SDS-PAGE analysis of purified antibodies, Sequence S1: DNA sequence of the designed Durvalumab-2xeCMV insert.

Author Contributions: Conceptualization, S.C.C., D.F., J.P.B., J.G. and H.K.; methodology, S.C.C., D.F., J.P.B.; investigation S.C.C., D.F. and J.P.B. data curation, S.C.C., D.F., J.P.B. and J.G. supervision B.H. and H.K. writing original draft, S.C.C., D.F. and J.P.B. writing review & editing S.C.C., D.F., J.P.B., J.G., B.H. and H.K. All authors have read and agreed to the published version of the manuscript.

Funding: This work was funded by the Ferring Darmstadt Labs at the Technical University of Darmstadt and by GPRD at Ferring Holding S.A., Saint Prex.

Institutional Review Board Statement: Not applicable.

Informed Consent Statement: Not applicable.

Data Availability Statement: The data presented in this study are available within this article and its Supplementary Materials.

Acknowledgments: S.C.C., D.F. and J.P.B. contributed equally to this work. The authors would like to thank GPRD for funding. The funders had no role in study design, data collection, data analysis, decision to publish, or preparation of the manuscript. We acknowledge support by the Deutsche Forschungsgemeinschaft (DFG—German Research Foundation) and the Open Access Publishing Fund of the Technical University of Darmstadt. Figures were created with Biorender and data was processed using GraphPad Prism 8.

Conflicts of Interest: J.G. and B.H. are employees of Ferring Pharmaceuticals, while S.C.C., D.F. and J.P.B. are employed by the Technische Universität Darmstadt in frame of a collaboration with Ferring Pharmaceuticals. All authors declare no conflicts of interest.

References

1. Vink, T.; Oudshoorn-Dickmann, M.; Roza, M.; Reitsma, J.-J.; De Jong, R.N. A simple, robust and highly efficient transient ex-pression system for producing antibodies. *Methods* **2014**, *65*, 5–10. [[CrossRef](#)]
2. Carvalho, L.S.; Bravim da Silva, O.; Carneiro de Almeida, G.; Davies de Oliveira, J.; Parachin, N.S.; Carmo, T.S. Production processes for monoclonal antibodies. *Intech* **2017**. [[CrossRef](#)]
3. Li, F.; Vijayasankaran, N.; Shen, A.; Kiss, R.; Amanullah, A. Cell culture processes for monoclonal antibody production. *MAbs* **2010**, *2*, 466–479. [[CrossRef](#)] [[PubMed](#)]
4. Carrara, S.C.; Ullitzka, M.; Grzeschik, J.; Kornmann, H.; Hock, B.; Kolmar, H. From cell line development to the formulated drug product: The art of manufacturing therapeutic monoclonal antibodies. *Int. J. Pharm.* **2021**, *594*, 120164. [[CrossRef](#)]
5. Kunert, R.; Reinhart, D. Advances in recombinant antibody manufacturing. *Appl. Microbiol. Biotechnol.* **2016**, *100*, 3451–3461. [[CrossRef](#)] [[PubMed](#)]
6. Zhang, R.Y.; Shen, W.D. Monoclonal Antibody Expression in Mammalian. *Cells* **2012**, *907*, 341–358.
7. Graham, F.L.; Russell, W.C.; Smiley, J.; Nairn, R. Characteristics of a Human Cell Line Transformed by DNA from Human Adenovirus Type. *J. Gen. Virol.* **1977**, *36*, 59–72. [[CrossRef](#)]
8. Vazquez-Lombardi, R.; Nevoltris, D.; Luthra, A.; Schofield, P.; Zimmermann, C.; Christ, D. Transient expression of human an-tibodies in mammalian cells. *Nat. Protoc.* **2018**, *13*, 99–117. [[CrossRef](#)]
9. Gronemeyer, P.; Ditz, R.; Strube, J. Trends in Upstream and Downstream Process Development for Antibody Manufacturing. *Bioengineering* **2014**, *1*, 188–212. [[CrossRef](#)]
10. Shukla, A.A.; Hubbard, B.; Tressel, T.; Guhan, S.; Low, D. Downstream processing of monoclonal antibodies—Application of platform approaches. *J. Chromatogr. B* **2007**, *848*, 28–39. [[CrossRef](#)]
11. Van der Kant, R.; Karow-Zwick, A.R.; Van Durme, J.; Blech, M.; Gallardo, R.; Seeliger, D.; Rousseau, F. Prediction and reduction of the aggregation of monoclonal antibodies. *J. Mol. Biol.* **2017**, *429*, 1244–1261. [[CrossRef](#)]
12. Li, W.; Prabakaran, P.; Chen, W.; Zhu, Z.; Feng, Y.; Dimitrov, D.S. Antibody Aggregation: Insights from Sequence and Structure. *Antibodies* **2016**, *5*, 19. [[CrossRef](#)]
13. Bergman, L.W.; Kuehl, W.M. Formation of an intrachain disulfide bond on nascent immunoglobulin light chains. *J. Biol. Chem.* **1979**, *254*, 8869–8876. [[CrossRef](#)]
14. Bauml, R.; Potter, M.; Scharff, M.D. Synthesis, assembly, and secretion of gamma globulin by mouse myeloma cells. *J. Exp. Med.* **1971**, *134*, 1316–1334. [[CrossRef](#)] [[PubMed](#)]

15. Bergman, L.W.; Kuehl, W.M. Temporal relationship of translation and glycosylation of immunoglobulin heavy and light chains. *Biochemistry* **1978**, *17*, 5174–5180. [CrossRef]
16. Feige, M.J.; Hendershot, L.M.; Buchner, J. How antibodies fold. *Trends Biochem. Sci.* **2010**, *35*, 189–198. [CrossRef] [PubMed]
17. Ho, S.C.; Bardor, M.; Feng, H.; Mariati, Tong, Y.W.; Song, Z.; Yap, M.G.; Yang, Y. IRES-mediated Tricistronic vectors for enhancing generation of high monoclonal antibody expressing CHO cell lines. *J. Biotechnol.* **2012**, *157*, 130–139. [CrossRef]
18. Rita Costa, A.; Elisa Rodrigues, M.; Henriques, M.; Azeredo, J.; Oliveira, R. Guidelines to cell engineering for monoclonal antibody production. *Eur. J. Pharm. Biopharm.* **2010**, *74*, 127–138. [CrossRef] [PubMed]
19. Liu, C.Y.; Liu, J.; Yan, W.; Williston, K.; Irvin, K.; Chou, H.; Zmuda, J. Strategies for High-Titer Protein Expression Using the ExpiCHO and Expi293 Transient Expression Systems. Available online: <https://assets.thermofisher.com/TFS-Assets/BID/posters/high-titer-protein-expression-expicho-exp293-poster.pdf> (accessed on 5 March 2021).
20. Wodarczyk, C.; Reichenbacher, B.; Schulze, A.; Köhler, J.; Gerster, A.; Rehberger, B.; Müller, D. Increased antibody yield due to modification of LC and HC expression by gene regulatory elements. Available online: https://www.rentschler-biopharma.com/fileadmin/user_upload/Scientific-Posters/Rentschler_Poster_ESACT_2015.pdf (accessed on 17 February 2021).
21. Bayat, H.; Hossienzadeh, S.; Pourmaleki, E.; Ahani, R.; Rahimpour, A. Evaluation of different vector design strategies for the expression of recombinant monoclonal antibody in CHO cells. *Prep. Biochem. Biotechnol.* **2018**, *48*, 160–164. [CrossRef] [PubMed]
22. Andersen, C.R.; Nielsen, L.S.; Baer, A.; Tolstrup, A.B.; Weiglun, D. Efficient Expression from One CMV Enhancer Controlling Two Core Promoters. *Mol. Biotechnol.* **2010**, *48*, 128–137. [CrossRef]
23. Durocher, Y.; Perret, S.; Kamen, A. High-level and high-throughput recombinant protein production by transient transfection of suspension-growing human 293-EBNA1 cells. *Nucleic Acids Res* **2002**, *30*, e9. [CrossRef] [PubMed]
24. Bogen, J.P.; Carrara, S.C.; Fiebig, D.; Grzeschik, J.; Hock, B.; Kolmar, H. Expedient Generation of Biparatopic Common Light Chain Antibodies via Chicken Immunization and Yeast Display Screening. *Front. Immunol.* **2020**, *11*. [CrossRef] [PubMed]
25. Bogen, J.P.; Storka, J.; Yanakieva, D.; Fiebig, D.; Grzeschik, J.; Hock, B.; Kolmar, H. Isolation of Common Light Chain Antibodies from Immunized Chickens Using Yeast Biopanning and Fluorescence-Activated Cell Sorting. *Biotechnol. J.* **2021**, *16*. [CrossRef] [PubMed]
26. Kretschmer, A.; Schwanbeck, R.; Valerius, T.; Rösner, T. Antibody Isotypes for Tumor Immunotherapy. *Transfus. Med. Hemotherapy* **2017**, *44*, 320–326. [CrossRef]
27. Alvarez-Argote, J.; Dasanu, C.A. Durvalumab in cancer medicine: A comprehensive review. *Expert Opin. Biol. Ther.* **2019**, *19*, 927–935. [CrossRef]
28. Boshart, M.; Weber, F.; Jahn, G.; Dorsch, -H.K.; Fleckenstein, B.; Schaffner, W. A very strong enhancer is located upstream of an immediate early gene of human cytomegalovirus. *Cell* **1985**, *41*, 521–530. [CrossRef]
29. Foecking, M.K.; Hofstetter, H. Powerful and versatile enhancer-promoter unit for mammalian expression vectors. *Gene* **1986**, *45*, 101–105. [CrossRef]
30. Ho, S.C.; Yap, M.G.; Yang, Y. Evaluating post-transcriptional regulatory elements for enhancing transient gene expression levels in CHO K1 and HEK293 cells. *Protein Expr. Purif.* **2010**, *69*, 9–15.
31. Sheay, W.; Nelson, S.; Martinez, I.; Chu, T.H.; Bhatia, S.; Dornburg, R. Downstream insertion of the adenovirus tripartite leader sequence enhances expression in universal eukaryotic vectors. *Biotechniques* **1993**, *15*, 856–862. [PubMed]
32. Suter, D.M.; Cartier, L.; Bettiol, E.; Tirefort, D.; Jaconi, M.E.; Dubois-Dauphin, M.; Krause, K.-H. Rapid Generation of Stable Transgenic Embryonic Stem Cell Lines Using Modular Lentivectors. *Stem Cells* **2006**, *24*, 615–623. [CrossRef]
33. Qin, J.Y.; Zhang, L.; Clift, K.L.; Hular, I.; Xiang, A.P.; Ren, B.-Z.; Lahn, B.T. Systematic Comparison of Constitutive Promoters and the Doxycycline-Inducible Promoter. *PLoS ONE* **2010**, *5*, e10611. [CrossRef]
34. Schlatter, S.; Stansfield, S.H.; Dinnis, D.M.; Racher, A.J.; Birch, J.R.; James, D.C. On the Optimal Ratio of Heavy to Light Chain Genes for Efficient Recombinant Antibody Production by CHO Cells. *Biotechnol. Prog.* **2008**, *21*, 122–133. [CrossRef]
35. Gerster, A.; Wodarczyk, C.; Reichenbacher, B.; Köhler, J.; Schulze, A.; Krause, F.; Müller, D. A simple method to determine IgG light chain to heavy chain polypeptide ratios expressed by CHO cells. *Biotechnol. Lett.* **2016**, *38*, 2043–2049. [CrossRef]
36. Vanhove, M.; Usherwood, Y.-K.; Hendershot, L.M. Unassembled Ig Heavy Chains Do Not Cycle from BiP In Vivo but Require Light Chains to Trigger Their Release. *Immunity* **2001**, *15*, 105–114. [CrossRef]
37. Ho, S.C.; Koh, E.Y.; Van Beers, M.; Mueller, M.; Wan, C.; Teo, G.; Song, Z.; Tong, Y.W.; Bardor, M.; Yang, Y. Control of IgG LC:HC ratio in stably transfected CHO cells and study of the impact on expression, aggregation, glycosylation and conformational stability. *J. Biotechnol.* **2013**, *165*, 157–166. [CrossRef]
38. Powles, T.; Park, S.H.; Voog, E.; Caserta, C.; Valderrama, B.P.; Gurney, H.; Kalofonos, H.; Radulović, S.; Demey, W.; Ullén, A.; et al. Avelumab Maintenance Therapy for Advanced or Metastatic Urothelial Carcinoma. *N. Engl. J. Med.* **2020**, *383*, 1218–1230. [CrossRef]
39. Raybould, M.I.J.; Marks, C.; Krawczyk, K.; Taddese, B.; Nowak, J.; Lewis, A.P.; Bujotzek, A.; Shi, J.; Deane, C.M. Five computational developability guidelines for therapeutic antibody profiling. *Proc. Natl. Acad. Sci. USA* **2019**, *116*, 4025–4030. [CrossRef]
40. Grilo, A.L.; Mantalaris, A. The Increasingly Human and Profitable Monoclonal Antibody Market. *Trends Biotechnol.* **2019**, *37*, 9–16. [CrossRef]
41. Curtin, A.J.; Dane, A.P.; Swanson, A.E.; Alexander, I.; Ginn, S.L. Bidirectional promoter interference between two widely used internal heterologous promoters in a late-generation lentiviral construct. *Gene Ther.* **2008**, *15*, 384–390. [CrossRef]

Supplementary Information

Recombinant antibody production using a dual-promoter single plasmid system

Stefania C. Carrara⁺, David Fiebig⁺, Jan P. Bogen⁺, Julius Grzeschik, Björn Hock, and Harald Kolmar

Table S1: Primers used for cloning of bidirectional constructs

AvelumabVH_Sapl_for	AAAAAGCTCTTCAAGTGAAGTTCAGCTGTTGG
AvelumabVH_Sapl_rev	TTTTTTGCTCTTCTGGCAGAGGAGACAGTAACAAGAG
AvelumabVL_Sapl_for	AAAAAGCTCTTCAAGTCAATCCGCCTTGACTC
AvelumabVL_Sapl_rev	TTTTTTTGTCTTTCACCCGAGAAGTGTGACCTTTG
DurvalumabVH_Sapl_for	AAAAAGCTCTTCAAGTGAAGTTCAGCTGTTGG
DurvalumabVH_Sapl_rev	TTTTTTGCTCTTCTGGCAGAGGAGACAGTAACAAGAG
DurvalumabVL_Sapl_for	AAAAAGCTCTTCAAGTGAAGTTCAGCTGTTGG
DurvalumabVL_Sapl_rev	TTTTTTGCTCTTTCACCCGAGAAGTGTGACCTTTG
MD-Leader-VH_Bbsl_for	ATATAGAAGACATCGCTTCCACCATGAC
CH1_MD_Esp3l_rev	ATATATCGTCTCGGTATGGGTCTTGTGCGAGCTCTTGG
MD-Leader-VL_Bbsl_for	ATATAGAAGACATCGCTTCCACCATGAC
Lam-CL_Esp3l_rev	ATATACGTCTCGAGATCTATTAGCTGCACTCGGTGGGGGCCACGGTTTT CTCCACGGTGTGCCCTC
Kap-CL_Esp3l_rev	ATATACGTCTCGAGATCTATTAACACTCTCCCCTGTTGAAGCTC
eCMV-HC_Bbsl_rev	GCGCGGAAGACATAGCGCGTAGAGATCCGTTTAAACTTGG
eCMV-LC_Bbsl_rev	GCGCGGAAGACATGCGACGCTAGAGATCCGTTTAAACTTGG
eCMV_LC-Stuffer-Con_Bbsl_for	GCGCGGAAGACATGATGGTACATTTATATTGGCTCATGTCCAATATGAC CGC
eCMV_HC-Stuffer-Con_Bbsl_for	GCGCGGAAGACATGGCTGTACATTTATATTGGCTCATGTCCAATATGAC CGC
CMV-HC_Bbsl_rev	GCGCGGAAGACATAGCGGATCTGACGGTCTACTAAACCAG
CMV-HC-Stuffer-Con_Bbsl_for	GCGCGGAAGACATGGCTCCGCTTACATAACTTACGGTAAATG
CMV-LC-Bbsl_rev	GCGCGGAAGACATGCGAGATCTGACGGTCTACTAAACCAGC
CMV-LC-Stuffer-Con_Bbsl_for	GCGCGGAAGACATGATGCCGCTTACATAACTTACGGTAAATG
EF1a-LC-Stuffer-Con_Bbsl_for	GCGCGGAAGACATGATGGGC
EF1a-LC_Bbsl_rev	ATATAGAAGACATGCGAAGCCTGCTTTTTGTACAACTTGTAC
HC-minCMV-CMV-LC_Bbsl_rev	GCGCGGAAGACTAAGCGTCTGACGGTCTACTAAACGAGCTCTGC
HC-minCMV-CMV-LC_Bbsl_for	GCGCGGAAGACATGCGAGATCTGACGGTCTACTAAACCAGC

Table S2: RT-qPCR primers for HC and LC constant regions

HC constant_fwd	TTCCAGAACCAGTCACCGTT
HC constant_rev	CCAAAGAAGAAGAGGGGAACA
LC kappa constant_fwd	TGTAGGTGCTGCCTTGCTG
LC kappa constant_rev	CTGTTGTGTGCCTGCTGAAT
LC lambda constant_fwd	GTAGCTCCTGTGGCTTTTC
LC lambda constant_rev	TGATCAGCGACTTCTACCC

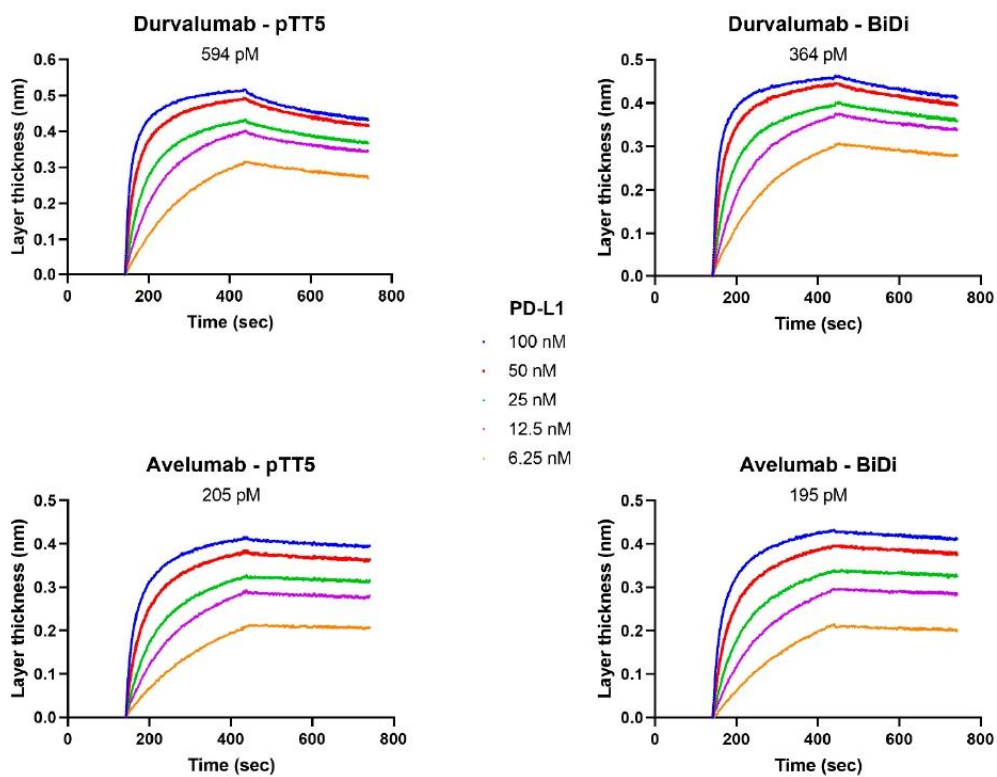


Figure S1: Affinity determination by BLI of antibodies produced in Expi293-F. Binding of Durvalumab and Avelumab produced in Expi293-F cells to PD-L1. Antibodies were either produced by co-transfection (denoted as pTT5) or transfection using 2xcMV BiDi construct (denoted as BiDi). The curves represent binding of 10 µg/mL antibody to different concentrations of PD-L1.

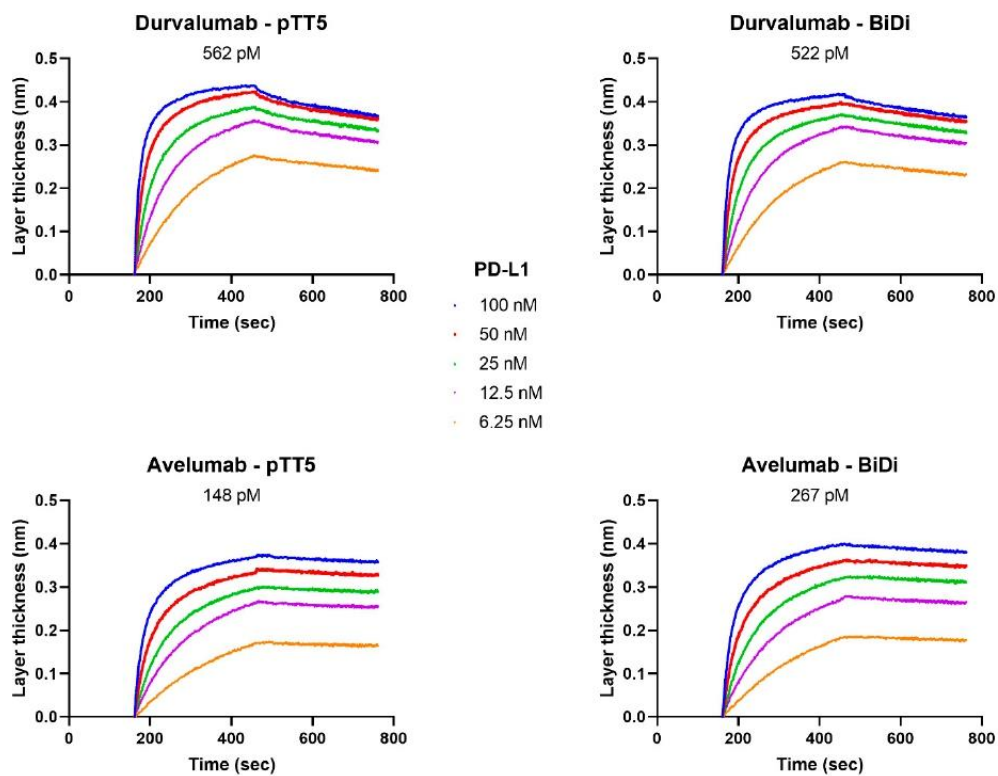


Figure S2: Affinity determination by BLI of antibodies produced in ExpiCHO-S. Binding of Durvalumab and Avelumab produced in ExpiCHO-s cells to PD-L1. Antibodies were either produced by co-transfection (denoted as pTT5) or transfection using 2xeCMV BiDi construct (denoted as BiDi). The curves represent binding of 10 $\mu\text{g}/\text{mL}$ antibody to different concentrations of PD-L1.

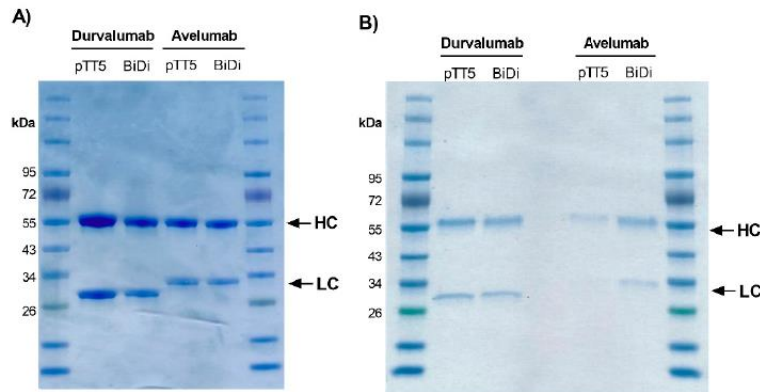


Figure S3: SDS-PAGE analysis of purified antibodies. Heavy and light chain bands at their expected molecular weights. A) represents purified antibodies from an Expi293-F production, while B) represents those produced in ExpiCHO-S cells. After purification, 3 μg or 0.5 μg antibodies were loaded onto an SDS-PAGE gel after Expi293-F and ExpiCHO-S production and purification, respectively.

Sequence S1: DNA sequence of the designed Durvalumab-2xeCMV insert. The colour codes represent the following regions: SV40 polyA signal (grey), **CL Kappa** (cyan), **VL Durvalumab** (magenta), **Signal peptide** (brown), **Enh. MLP** (dark green), **TLF** (red), **CMV promoter** (yellow), **CMV Enhancer** (green), **Stuffer** (blue), **VH Durvalumab** (dark blue), **CH1-CH2-CH3** (black), **Stop codon** (dark yellow).

CGGCAGTGAAAAAATGCTTTATTTGTGAAATTTGTGATGCTATTGCTTTATTTGTAACCATATAAGCTGCAATAAAC
AAGTTAAACAACAACAAATTGCATTCAATTTATGTTTCAGGTTCCAGGGGAGGTGTGGGAGGTTTTTAAAGCAAGTAAA
ACCTCTACAAATGGTATGGCTGATTATGAGCTAGAGATCTATTAACTCTCCCCTGTTGAAGCTCTTTGTGACGGG
CGAGCTCAGGCCCTGATGGGTGACTTCGCAGGCGTAGACTTTGTGTTTCTCGTAGTCTGCTTGTCTCAGCGTCAGGGT
GCTGCTGAGGCTGTAGGTGCTGTCTTGTCTGCTCTGTGACACTCTCTGGGAGTTACCCGATTGGAGGGCGTT
ATCCACCTTCCACTGTACTTTGGCCTCTCTGGGATAGAAGTTATTCAGCAGGCACACAACAGAGGCAGTTCCAGATTTCC
AACTGCTCATCAGATGGCGGGAAGATGAACACAGATGGTGACCCACAGTTCGTTTAATTTTCGACCTTAGTACCTTGG
CCGAATGTCCAAGGGAGACTACCATATTGTTGACAGTAGTAGACTGCAAAATCTTCCGGTCCAGCCGGGAAATTGTA
AGTGTAATAATCTGTGCCGGAACCGCTTCTGAAAACCTATCAGGTATGCCAGTAGCTCTAGAGGATGCGTCATAGATC
AACAGACGCGGTGCTTGCCAGGCTTTTGTGATACCATGCAAGATAGAACTGGATACCCTTTGTGAAGCTCTGCAA
GACAGAGTTGCTCTTACCCCGGGGAGAGACTCAGGGTGCCGGGACTTTGGGTAAAGCACTATTTAGCCAAGGCAAT
ATTAGTTAATCCCAACAATATTGTGAACAGGTAGGTAATAAGAGCGAAAGATAATGTCATGGTGGCTGCGACGCTAG
AGATCCGTTTAACTTGGACCTGGGAGTGGACACCTGTGGAGAGAAAGGCAAAAGTGGATGTCATTGCTCACTCAAGTG
TATGGCCAGATCGGGCCAGGTGAATATCAAACTCTCTCGTTTTTGGAACTGACAATCTTAGCGCAGAAGTAATGCC
CGCTTTTGTGAGAGGGAGTACTCACCCCAACAGCTGGATCTCAAGCCTGCCACCTCACCTCGACCATCCGCCGTCTAAA
GACCGCTACTTTAATTACATCATCAGCAGCACCTCCGCCAGAAACAACCCCGACCGCCACCCGCTGCCGCCGCCACG
GTGCTCAGCCTACTTGGACTGTGACTGGTTAGACGCCTTCTCGAGAGGTTTTCCGATCCGGTTCGATGCGGACTCG
CTCAGGTCCTCGGTGGCGGAGTACCGTTCCGGAGGCCGACGGGTTCCGATCCAAGAGTACTGGAAAGACCCGCGAA
GAGTTTGTCTCAACCGGAGCCCAACAGCTGGCCCTCGCAGACAGCGATGCGGAAGAGAGTGAAGGATCTGACGGTT
CACTAAACGAGCTCTGCTTATATAGACCTCCACCGTACACGCCTACCGCCATTTGCGTCAACGGGGCGGGGTTATTA

CGACATTTTGAAAAGTCCCCTTGATTTTGGTGCCAAAACAACTCCCATTGACGTCAATGGGGTGGAGACTTGAAAAT
CCCCGTGAGTCAAACCGCTATCCACGCCATTGGTGTACTGCCAAAACCGCATCACCATGGTAATAGCGATGACTAAT
ACGTAGATGACTGCCAAGTAGGAAAGTCCCCTAAGGTGATGACTGGGCATATGCCAGGCGGGCCATTACCGTC
ATTGACGTCAATAGGGGGCGGACTTGGCATATGATACACTGATGACTGCCAAGTGGGCAGTTTACCGTAAACTC
CACCCATTGACGTCAATGAAAAGTCCCCTATTGGCGTACTATGGGAACATACGTCATTATTGACGTCAATGGGCGGGG
GTCGTTGGGCGGTCAGCCAGGCGGGCCATTTACCGTAAGTTATGTAACGCGGAACCTCCATATATGGGCTATGAECTA
ATGACCCCGTAATTGATTACTATTAATAACTAGTCAATAATCAATGTCAACATGGCGGTGATATTGGACATGAGCCAAT
ATAAATGTACCATCTAAAGTATATATGAGTAACTTGGTCTGACAGTTACCAATGCTTAATCAGTGAGGCACCTATCTC
AGCGATCTGTCTATTTCTGTTTCATCCATAGTTGCCTGACTCCCGTCTGTAGATAACTACGATACGGGAGGGCTTACCA
TCTGGCCCCAGTCTGCAATGATACCGCGAGATCCACGCTCACCGGCTGTACATTTATATTGGCTCATGTCCAATATGA
CCGCCATGTTGACATTGATTATTGACTAGTTATTAATAGTAATCAATTACGGGGTCAATTAGTTTATAGCCCATATATGG
AGTTCCGCGTTACATAACTTACGGTAAATGGCCCGCTGGCTGACCGCCAACGACCCCGCCATTGACGTCAATAA
TGACGTATGTTCCCATAGTAACGCCAATAGGGACTTTCATTGACGTCAATGGGTGGAGTATTACGGTAAACTGCC
ACTTGGCAGTACATCAAGTGTATCATATGCCAAGTCCGCCCTATTGACGTCAATGACGTAAATGGCCCGCTGGC
ATTATGCCAGTACATGACCTTACGGGACTTCTACTTGGCAGTACATCTACGTATTAGTCATCGCTATTACCATGGTG
ATGCGGTTTTGGCAGTACACCAATGGGCGTGATAGCGGTTTACTCACGGGGATTTCCAAGTCTCCACCCCAATTGAC
GTCAATGGGAGTTTGTGGCACAAAATCAACGGGACTTTCCAAAATGTGTAATAACCCCGCCCGTTGACGCAA
ATGGGCGGTAGGCGTGTACGGTGGGAGGTCTATATAAGCAGAGCTCGTTTAGTGAACCGTCAGATCCCACTCTCTC
CGCATCGTGTCTGCGAGGGCCAGCTGTGGGCTCGCGGTTGAGGACAAACTTTCGCGGCTTCCAGTACTCTGG
ATCGGAAACCCGTGCGCTCCGAACGGTACTCCGCCACCGAGGGACTGAGCGAGTCCGCATCGACCGGATCGGAAA
ACCTCTCGAGAAAGCGTCAACCAGTACAGTCCGAAGTAGGCTGAGCACCGTGGCGGGCGGACGGGTGGCG
GTCGGGGTTGTTTCTGGCGGAGGTGCTGCTGATGATGTAATAAAGTAGGCGGTCTTAGACGGCGGATGGTCGAGG
TGAGGTGTGGCAGGCTTGAGATCCAGCTGTGGGGTGAGTACTCCCTCTCAAAGCGGGCATTACTTCTGCGCTAAG
ATTGTCAAGTTTCCAAAACGAGGAGGATTTGATATTCACCTGGCCCGATCTGGCCATACACTTGAGTGACAATGACAT
CCACTTTGCCCTTCTCTCCACAGGTGTCCACTCCAGGTCCAAGTTAAACGGATCTTAGCGCGCTTCCACCATGACA
TTATCTTTCGCTCATTACCTACCTGTTACAATATTGTTGGGATTAACATAATATTGCCTTGGCAGAGGTTCAACTGTT
GAAAGCGCGGTGGTCTGGTCCAACCTGGTGGTTCTTGGCCTGAGTTGCGCCGCTAGTGCTTCACTTTTAGTCGA
TATTGGATGTCTGGGTACGCCAAGCACCTGGCAAGGGCTTGAATGGGTGGCTAATTAAGCAAGATGGATCAGA
GAAATACTATGTCGACAGCGTAAAAGGGCGGTTACTATTTCTAGGGACAACGAAAGAACTCCCTGTACCTTCAAAT
GAACTCTTTCGCGCTGAGGACACTGCTGTACTACTGCGCCAGGGAGGGAGTTGGTTCGGAGAATGGCATTCC
ATTATTGGGGCCAGGGCACCTCGTTACAGTCTCAAGCGCCTCTACTAAAGGTCCATCTGTTTTTCCATTGGCTCCATCT
TCTAAATCTACATCTGGTGGTACTGCTGCTTTGGGTTGTTGGTTAAGGATTATTTCCAGAACCAGTACCGTTTTCTG
GAATTCTGGTGTCTTACTTCTGGTGTTCATACTTTCCAGCCGATTGCAATCTTCTGGCTTGTATTCTTGTCTCTGT
TGTTACTGTTCCCTCTTCTTCTTGGTACTCAAATTACATCTGCAACGTTAACCATAAGCCATCTAACACCAAGGTTG
ATAAGAGAGTCGAACCTAAGTCTTGTGATAAGACTCATACCTGTCCCTTGTCTGCCCTGAAGCCGCCGGCGGAC
CTTCCGTGTTCTGTTCCCCCAAGCCCAAGGATACCTGATGATCAGCCGACCCCGAAGTGACCTGCGTGGTGG
TGGATGTGTTCCACGAGGACCCTGAAGTGAAGTTCAATTGGTACGTGGACGGCGTGGAAAGTGACAACGCCAAGACC
AAGCCCAGAGAGGAACAGTACAACAGCACCTACCGGGTGGTGTCCGTGCTGACAGTGTGCATCAGGACTGGCTGAA
CGGCAAGAGTACAAGTGAAGGTGTCAACAAGGCCCTGCTGCCCCATCGAGAAAACCATCAGCAAGGCCAAGG
GCCAGCCCGCGAACCCAGGTGTACACTGCCTCCAGCAGGGACGAGCTGACCAAGAACCAGGTGTCCCTGACC
TGTCTGTGAAAGGCTTCTACCCCTCCGATATCGCCGTGGAATGGGAGAGCAATGGCCAGCCCGAGAACAACACTACA
GACCACCCCTGTGCTGGACAGCGACGGCTATTCTTCTGTACAGCAAGCTGACCGTGGACAAGTCCCGTGGCA
GCAGGGCAACGTGTTCACTGTCAGCGTGTGCACGAGGCCCTGCACAACACTACCCAGAAAGTCCCTGAGCCTGA
GCCCCGGCAAATAATGATCCAGAGGATCATAATCAGCCATACCACATTTGTAGAGGTTTACTTGTCTTAAAAAACCTC
CCACACTCCCTGAACTGAAACATAAAATGAATGCAATGTTGTTGTTAACTGTTTATTGACGCTTATAATGGTTA
CAAATAAAGCAATAGCATCACAAATTTCAAATAAAGCATTTTTTCACTGCCCGTGGCGTGGG

4.3 Streamlining the Transition from Yeast Surface Display of Antibody Fragment Immune Libraries to the Production as IgG Format in Mammalian Cells

Title:

Streamlining the Transition from Yeast Surface Display of Antibody Fragment Immune Libraries to the Production as IgG Format in Mammalian Cells

Authors:

David Fiebig*, Jan Patrick Bogen*, Stefania Candela Carrara*, Lukas Deweid, Stefan Zielonka, Julius Grzeschik, Björn Hock, Harald Kolmar

(* shared first authorship)

Bibliographic Data:

Journal – *Frontiers in Bioengineering & Biotechnology*

Volume 10

First online: 10th May 2022

DOI: 10.3389/fbioe.2022.794389

PMID: 35620472

© 2022 Fiebig, Bogen, Carrara, Deweid, Zielonka, Grzeschik, Hock and Kolmar.

Contributions by S.C. Carrara:

- Production of antibody hits from YSD-derived screening campaigns
- Characterisation of antibody hits
- Writing of manuscript together with D. Fiebig and J.P. Bogen
- Generation of all figures



Streamlining the Transition From Yeast Surface Display of Antibody Fragment Immune Libraries to the Production as IgG Format in Mammalian Cells

David Fiebig^{1,2†}, Jan P. Bogen^{1,2†}, Stefania C. Carrara^{1,2†}, Lukas Deweid^{1,2}, Stefan Zielonka¹, Julius Grzeschik³, Björn Hock³ and Harald Kolmar^{1,4*}

¹Institute for Organic Chemistry and Biochemistry, Technical University of Darmstadt, Darmstadt, Germany, ²Ferring Darmstadt Laboratories, Darmstadt, Germany, ³Ferring Biologics Innovation Centre, Epalinges, Switzerland, ⁴Centre for Synthetic Biology, Technical University of Darmstadt, Darmstadt, Germany

OPEN ACCESS

Edited by:

Kequan Chen,
Nanjing Tech University, China

Reviewed by:

Tae Hyeon Yoo,
Ajou University, South Korea
Gordana Wozniak-Knopp,
University of Natural Resources and
Life Sciences, Austria
Xiaoling Wu,
South China University of Technology,
China

*Correspondence:

Harald Kolmar
kolmar@biochemie-tud.de

[†]These authors have contributed
equally to this work and share first
authorship

Specialty section:

This article was submitted to
Bioprocess Engineering,
a section of the journal
Frontiers in Bioengineering and
Biotechnology

Received: 13 October 2021

Accepted: 20 April 2022

Published: 10 May 2022

Citation:

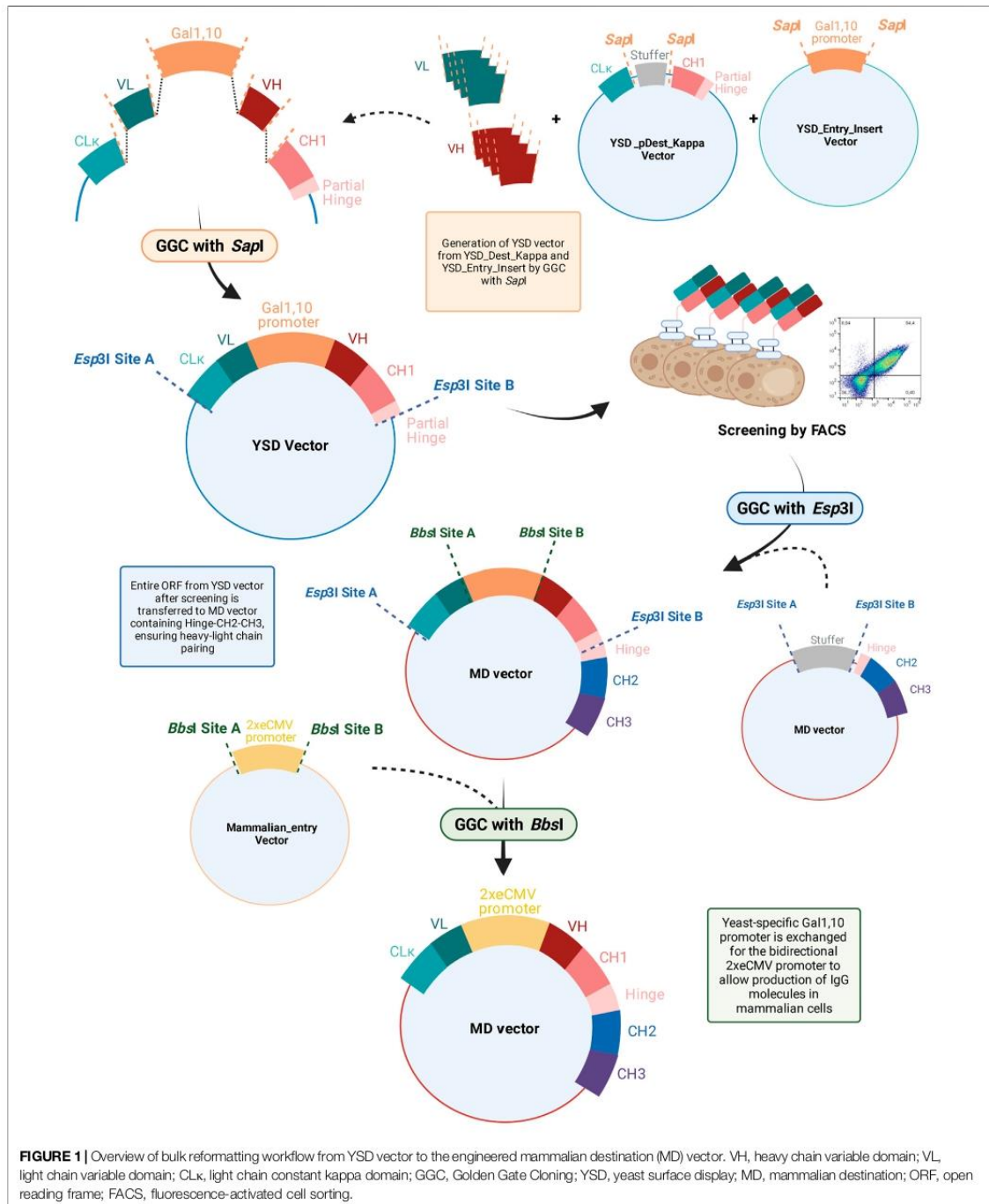
Fiebig D, Bogen JP, Carrara SC,
Deweid L, Zielonka S, Grzeschik J,
Hock B and Kolmar H (2022)
Streamlining the Transition From Yeast
Surface Display of Antibody Fragment
Immune Libraries to the Production as
IgG Format in Mammalian Cells.
Front. Bioeng. Biotechnol. 10:794389.
doi: 10.3389/fbioe.2022.794389

Yeast-surface display (YSD) is commonly applied to screen Fab immune or naïve libraries for binders of predefined target molecules. However, reformatting of isolated variants represents a time-intensive bottleneck. Herein, we present a novel approach to facilitate a lean transition from antibody screening using YSD Fab libraries to the production of full-length IgG antibodies in Expi293-F cells. In this study, utilizing Golden Gate Cloning (GGC) and a bidirectional promoter system, an exemplary Fab-displaying YSD library was generated based on immunised transgene rats. After subsequent screening for antigen-specific antibody candidates by fluorescence-activated cell sorting (FACS), the Fab-encoding genes were subcloned into a bidirectional mammalian expression vector, exhibiting CH2-CH3 encoding genes, in a GGC-mediated, PCR-free manner. This novel, straightforward and time-saving workflow allows the VH/VL pairing to be preserved. This study resulted in antibody variants exhibiting suitable biophysical properties and covered a broad VH diversity after two rounds of FACS screening, as revealed by NGS analysis. Ultimately, we demonstrate that the implication of such a gene transfer system streamlines antibody hit discovery efforts, allowing the faster characterisation of antibodies against a plethora of targets that may lead to new therapeutic agents.

Keywords: antibody hit discovery, bidirectional promoter, reformatting, golden gate cloning, monoclonal antibodies, yeast surface display

INTRODUCTION

Monoclonal antibodies (mAbs) have shown great potential both as therapeutic and diagnostic tools, with the global monoclonal antibody market expected to reach \$300 billion in revenues by 2025 (Lu et al., 2020). Today, a wide variety of display technologies are established for the identification of mAb candidates from immune, synthetic or naïve libraries, among them phage display (McCafferty et al., 1990), ribosome display (Schaffitzel et al., 1999; Lipovsek and Plückthun, 2004), mRNA display (Lipovsek and Plückthun, 2004; Josephson et al., 2014), mammalian display (Parthiban et al., 2019) and yeast display (Boder and Wittrup, 1997). However, all these technologies require laborious subcloning of isolated mAb-encoding genes into protein expression vectors. Even though this



process was improved within the last years, PCR-based subcloning always bears the risk of incorporating unintended mutations. Due to the increasing interest in developing mAbs against a plethora of targets, we sought out to streamline the antibody hit discovery workflow.

Besides phage display, particularly yeast-surface display (YSD) has become widely applicable for screening of large libraries (Boder and Wittrup, 1997). The first approved therapeutic antibody generated *via* YSD was Sintilimab, a PD-1 blocking antibody, approved in 2018 for the treatment of relapsed or refractory classical Hodgkin's lymphoma in China (Hoy, 2019; Valldorf et al., 2021). While advances in YSD technology have facilitated the generation of large Fab antibody libraries using streamlined approaches (Rosowski et al., 2018; Roth et al., 2018), the pitfall that follows antibody screening, namely reformation of Fabs into full-length IgG molecules, remains a tedious procedure. Reformatting into IgG molecules is required in order to fully discover the activity and function of mAbs and to assay their properties, such as Fc-mediated functions (Kapur et al., 2014; Bournazos and Ravetch, 2017). Furthermore, the handling of each antibody individually is required in order to preserve the unique VH and VL pairing.

In recent years, Cruz-Teran and others (2017) have shown that a modification of the yeast cell surface allows one to switch between cell-surface display and secretion of full-length antibodies in order to circumvent subcloning of hit candidates into a suitable expression vector for mammalian expression (Cruz-Teran et al., 2017; Krah et al., 2020). Nevertheless, the glycosylation patterns in baker's yeast cells differ significantly from those in humans (Tanner and Lehle, 1987; Wildt and Gerngross, 2005) and the yields by application of such methods are very limited. On the contrary, two mammalian cell lines are commonly used for small- to mid-scale antibody production due to their human-like glycosylation and high titres, namely Human Embryonic Kidney 293 (HEK293) and Chinese Hamster Ovary (CHO) cells (Li et al., 2010; Vazquez-Lombardi et al., 2018; Carrara et al., 2021a). To continue the production of IgG molecules in mammalian cells and avoid the cumbersome reformatting steps, we have developed a novel two-pot, two-step cloning procedure in order to facilitate the transition of hit candidates from a YSD-display vector to a mammalian bidirectional (BiDi) expression vector. Initial studies were carried out to analyse the most suitable BiDi promoter for both κ - and λ -isotype antibodies (Carrara et al., 2021b). On top of simplifying and facilitating the transition between display on yeast cells to production in mammalian cells, VH and VL pairing is also preserved. To date, a few high-throughput platforms have been described in order to batch reformat from the scFv format to IgG molecules from phage display libraries (Renaut et al., 2012; Batonick et al., 2016; Xiao et al., 2017; Liu et al., 2018; Reader et al., 2019), but to the best of our knowledge, there have been no such reports for YSD Fab libraries.

In this study, we performed an initial proof-of-concept (PoC) experiment with the therapeutic anti-PD-L1 antibody Durvalumab to establish the reformatting workflow (Figure 1) (Alvarez-Argote and Dasanu, 2019). Subsequently, a Fab library resulting from immunised OmniRats against a TAMR was

generated, screened, reformatted, and produced as well as purified using this streamlined approach. The TAM receptors (TAMR), comprising Tyro3, Axl, and MerTK, belong to the family of receptor tyrosine kinases, which have been the focus of several studies over the last decade due to their implications in a number of diseases (Alvarez-Argote and Dasanu, 2019; Reader et al., 2019). The resulting variants unveiled appropriate biophysical properties and covered the entire VH diversity, as revealed by NGS analysis. This method paves the way for facilitating hit discovery processes by expediting the transition between YSD-vectors and mammalian expression of hit candidates.

MATERIALS AND METHODS

Plasmids and Yeast Strains

Plasmids and yeast strains used, as well as their cultivation and media, were previously described in detail elsewhere (Bogen et al., 2020a; Bogen et al., 2020b). For library generation, the yeast destination vector, YSD_pDest_Kappa, comprising a coding sequence for a κ CL and a CH1-hinge-Aga2p fusion, as well as the yeast entry vector, YSD_Entry_Insert, encoding the Gal1,10 promoter were used. By *SapI*-mediated GGC, VH and VL sequences, previously amplified from cDNA (see below) were subcloned into the destination vector, similar to the approach described previously (Rosowski et al., 2018). The mammalian destination (MD) vector was recently described in detail (Carrara et al., 2021b). In brief, the MD vector encodes a stuffer sequence flanked by *Esp3I* sites, adjacent to coding sequences comprising partial hinge-CH2-CH3 domains. By means of Golden Gate cloning, VL-CL and VH-CH1 encoding sequences can be inserted into MD. Additionally, the bidirectional promoter is flanked by *BbsI* sites and can be chosen freely. The 2xcCMV promoter combination was shown to be the most suitable for recombinant antibody production and was thus used herein. The sequence of this promoter construct is available from (Carrara et al., 2021b).

Immunisation

OmniRats (Osborn et al., 2013) were immunised by genetic immunisation encoding TAMR at Aldevron (Freiburg, Germany). After adequate titres were observed, lymph nodes and spleens were extracted. All procedures were carried out in accordance with local animal welfare guidelines and protection laws.

Library Generation

From immunised OmniRats, total RNA was isolated from lymph nodes and spleens using RNeasy Plus Mini Kit (QIAGEN). Subsequently, cDNA was synthesised using SuperScript III First-Strand Kit (Thermo Fisher Scientific) from 25 μ l RNA with random hexamer primers, dNTPs and water to an end volume of 35 μ l. The mixture was first incubated at 65°C for 5 min followed by a 1 min incubation on ice. 35 μ l containing 1x RT-Buffer, MgCl₂, DTT, RNase OUT and 200 U SuperScript III RT were added. The mixture was incubated for 5 min at 25°C and

60 min at 50°C. The reaction was terminated by incubating for 5 min at 80°C. 1 μ l RNase H was added to each tube and incubated for 20 min at 37°C.

With the cDNA, human antibody variable regions from OmniRats were amplified using two successive, nested PCR reactions. For the first PCR, unique forward primers annealing to the leader sequence of VH or VL kappa were combined with reverse primers annealing to rat CH1 or CL domains, respectively, using Q5-High Fidelity DNA Polymerase. After PCR Clean-Up using Wizard SV Gel and PCR Clean-Up System (Promega) and verifying successful amplification by agarose gel electrophoresis, a second PCR was performed to amplify human VH and VL domains and incorporating *SapI* recognition sequences for subsequent Golden Gate Cloning (GGC) into the YSD vector (primer sequences can be found in **Supplementary Table S1**). Therefore, the purified VH and VL PCR products were assembled with the plasmids YSD_Entry_Insert and YSD_pDest_Kappa. For comparison, an additional anti-TAMR Fab library was generated by homologous recombination as described by Benatuil et al. in EBY100 yeast cells (Benatuil et al., 2010).

Library Sorting

For library sorting, 5×10^8 induced yeast cells were washed with PBS containing 0.1% BSA (PBS-B) and incubated with 250 nM TAMR-His₆ for 30 min on ice. After washing with PBS-B, cells were stained with Goat F(ab')₂-anti-human-Kappa PE-conjugate (1:75 dilution, Southern Biotech) to detect surface presentation, with anti-His6 AlexaFluor647-conjugate (1:50 dilution, Thermo Fisher Scientific) for target binding and incubated for 15 min on ice. After a final washing step, cells were analysed by FACS using a Sony Cell Sorter SH800S. Sorting rounds were performed with decreasing target antigen concentrations. For subsequent rounds, TAMR-Fc was used as soluble antigen, staining with an anti-human IgG PE-conjugate (1:50 dilution, Thermo Fisher Scientific).

Next-Generation Sequencing

Plasmids were isolated from yeast cell populations of the initial library, as well as the 1st and 2nd sorting rounds using the Zymoprep Yeast Plasmid Miniprep Kit (Zymo Research). By means of PCR utilizing Q5 High-Fidelity DNA Polymerase (New England Biolabs), the VH and VL genes were amplified and purified by the PCR Clean-Up System (Promega). Next-generation sequencing by Illumina sequencing was performed at Genewiz (Leipzig, Germany) and resulting NGS data were analysed using Geneious Prime 2020.1.2.

Reformatting

Plasmids of yeast cells, enriched during FACS, were isolated using the Zymoprep Yeast Plasmid Miniprep Kit (Zymo Research). Subsequently, plasmids were transformed into chemically competent XL1 blue *E. coli* cells and cultivated overnight in 50 ml dYT media with 100 μ g/ml ampicillin. The next day, plasmids were isolated using the PureYield™ Plasmid Midiprep System (Promega). For reformatting into the

mammalian expression vector, 75 ng of the YSD vector population, encoding the bidirectional CL-VL-Gal1,10-VH-CH1-partial hinge ORFs, was subjected to GGC with 75 ng of the Mammalian Destination (MD) vector, exhibiting the sequences encoding the partial Hinge-CH2-CH3. By *Esp3I*-mediated GGC, the complete bidirectional yeast-derived ORF cassette was inserted into the MD vector. While the 3' end of the CL domain exhibited a stop codon, the CH1-partial hinge region of the yeast vector aligns with the partial-hinge-CH2-CH3 region of the MD vector, resulting in an ORF encoding the complete heavy chain. Subsequently, the Golden Gate products were transformed into chemically competent XL1 blue *E. coli* cells and cultivated overnight in 50 ml dYT media with 25 μ g/ml chloramphenicol. Plasmids were isolated using the PureYield™ Plasmid Midiprep System (Promega) and 75 ng were subsequently subjected to GGC cloning utilizing the Mammalian_entry vector. By *BbsI*-mediated GGC, the Gal1,10 promoter was removed from the vector and exchanged by the bidirectional 2xeCMV promoter cassette. The Golden Gate products were transformed into chemically competent XL1 blue *E. coli* cells and cultivated overnight in 50 ml dYT media with 25 μ g/ml chloramphenicol and subsequently isolated by using the PureYield™ Plasmid Midiprep System (Promega). Golden Gate reactions were performed according to the manufacturer's instruction. In brief, a 20 μ l Golden Gate reaction containing 75 ng of the destination vector, 75 ng of the parental vector harbouring the desired insert, 2 μ l T4 ligase buffer, 1 μ l of the respective type IIS restriction enzyme (*Esp3I* or *BbsI*), and 0.5 μ l T4 ligase was used. All reagents for GGC reactions were supplied by New England Biolabs. Golden Gate cloning was performed in 30 cycles consisting each of 1 min at 37°C and 1 min at 16°C for restriction and ligation steps, respectively.

Transient Transfection and Purification

Expi293-F cells (Thermo Fisher Scientific) were used for transient production of antibodies. The cells were cultured in Expi293 Expression Medium (Thermo Fisher Scientific) at 37°C, 8% CO₂, and 110 rpm, and sub-passaged every 3–4 days. Transfection was carried out using Expifectamine293 according to the manufacturer's manual, using 1 μ g plasmid DNA per ml culture volume. Six days post-transfection, cells were harvested by centrifugation and the cell culture supernatants were sterile filtered before being applied to a HiTrap MabSelect Prisma column (Cytiva) using an ÄKTA Pure 25 system following the manufacturer's instructions. Subsequently, a desalting step against PBS was performed using HiTrap Desalting columns (Cytiva).

Biolayer Interferometry

For kinetics and affinity determination, an Octet Red96 (FortéBio) was utilised. Antibodies were loaded onto anti-human Fc Capture (AHC) biosensor tips (Sartorius) and associated to different concentrations of His-tagged TAMR in the range of 6.25–200 nM. Kinetics were determined using Savitzky-Golay filtering and fitted using a 1:1 Langmuir binding model.

Thermal Stability and Size-Exclusion Chromatography

To evaluate the thermal stability of the isolated and reformatted antibodies, melting points (T_M) were determined utilizing the Prometheus NT.48 NanoDSF Protein Stability Instrument (NanoTemper Technologies) at 0.5 mg/ml between 25–90°C with a heating rate of 1°C/min as previously described (Bogen et al., 2020a). Size exclusion chromatography was carried out using an Agilent Technologies 1260 Infinity system as previously described (Bogen et al., 2020a). In short, 22 μ l of a 0.5 mg/ml protein solution were applied onto a TSKgel SuperSW3000 column (Tosoh) at a constant flow rate of 0.35 ml/min using sterile filtered PBS (pH 7.4) as mobile phase.

RESULTS

Overview of Cloning Strategy From Yeast-Surface Display to Mammalian Destination Vector

To ease the workflow from YSD-mediated antibody discovery to their expression in a mammalian system, we developed a high-throughput, bulk cloning procedure that avoids possible PCR-mediated mutations and conserves heavy chain—light chain pairing while yielding a full-length IgG molecule and significantly reducing hands-on time. In principle, VH and VL genes amplified from virtually any origin, for example, an immunised animal, can be subcloned by *SapI*-mediated GGC into a YSD-vector utilizing the Gal1,10-based bidirectional promoter, similar to the previously described system (Rosowski et al., 2018). Upon transformation in *Saccharomyces cerevisiae* and FACS-assisted enrichment, yeast cells expressing target-specific Fabs are isolated. For subsequent characterization, expression of full-length IgG molecules in mammalian cells is crucial, as this represents the final expression system in the final format for therapeutic mAbs. However, bulk reformatting of multiple antibody candidates from an enriched pool of binders is not feasible with conventional methods as the original heavy chain—light chain pairing is lost during this process. This could be avoided by using scFvs or other single chain antibody formats. However, for most therapeutic applications, IgG antibodies are favoured as demonstrated by the number of approved IgGs in comparison to approved scFv-based drugs (Reichert, 2021). Furthermore, using Fab libraries for YSD allows for screening in an architecture most closely resembling the final IgG format and has shown to result in more promising antibody variants compared to scFv libraries (Sivelle et al., 2018).

Conventionally, the VH and VL sequences are reformatted for each single candidate separately in order to retain the heavy chain—light chain pairing. As more mAb candidates are available, this process becomes more laborious and tedious. Furthermore, PCR-based subcloning bears the risk of introducing unintended mutations, further increasing workload and slowing down the discovery process. To

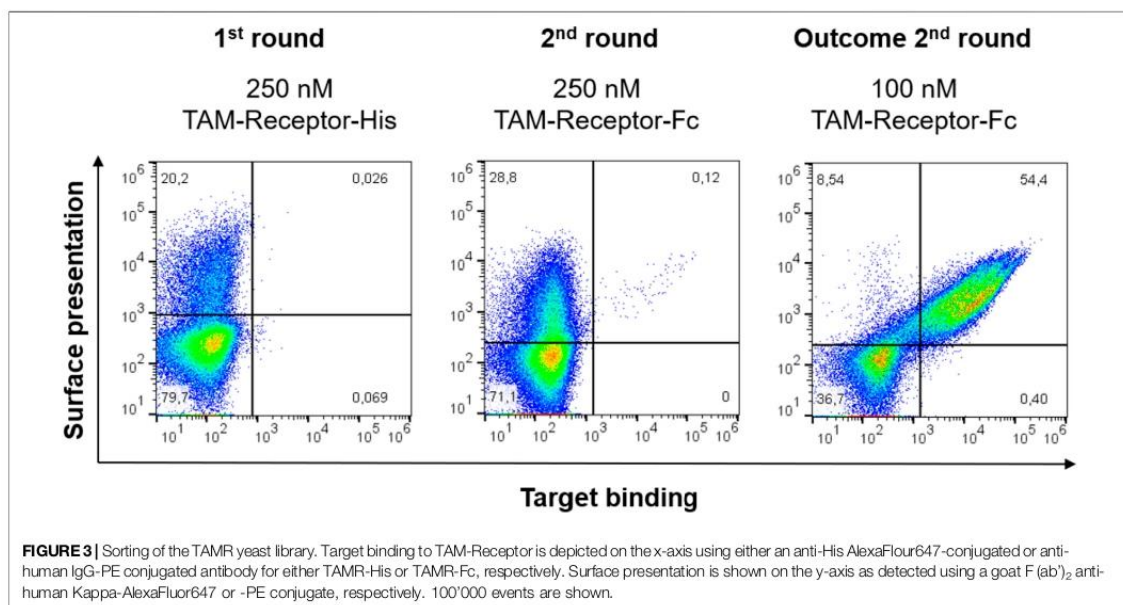
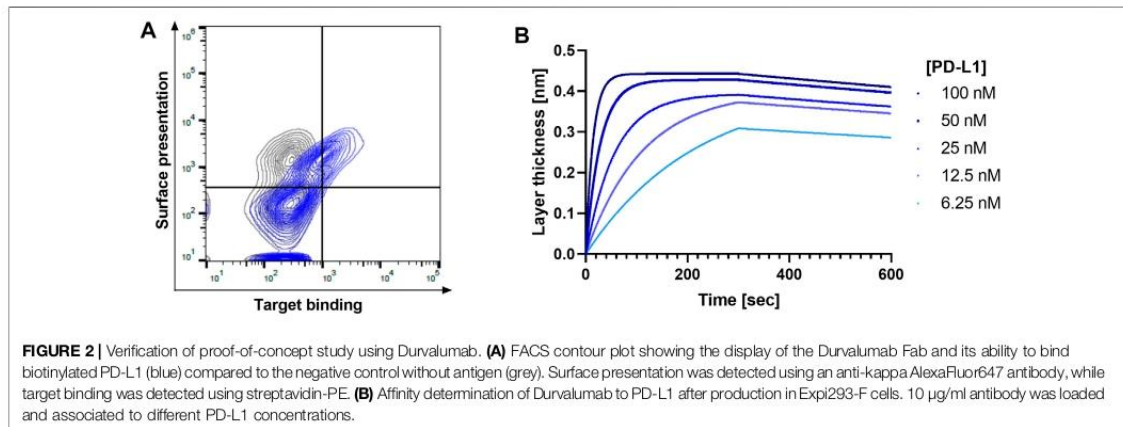
circumvent all these disadvantages, we engineered a mammalian destination vector (MD), encoding a partial hinge region followed by CH2- and CH3-encoding genes. By Golden Gate Cloning using *Esp3I*, the whole CL-VL-Gal1,10-VH-CH1-partial hinge ORF is extracted from the YSD vector and inserted into the MD vector, resulting in a full-length heavy chain ORF, enabling the transfer of a whole population of binding molecules in a one-pot reaction. Due to the physical linkage with the yeast Gal1,10 promoter, heavy chain—light chain coupling is maintained. In the next step, this yeast-specific promoter is exchanged by *BbsI*-mediated Golden Gate Assembly for the 2xeCMV promoter, which was recently demonstrated to be the optimal bidirectional promoter for mAb expression (Carrara et al., 2021b). An overview of the entire procedure is depicted in **Figure 1**. This final vector enables transient transfection of mammalian cells for mAb production and additionally circumvents the need of co-transfecting separate heavy and light chain-encoding plasmids, which is needed in conventional procedures. All vectors were designed *in silico* and subsequently ordered at GeneArt (Thermo Fisher Scientific).

PoC Study With Durvalumab

To verify whether this Golden Gate-assisted discovery process is feasible for subcloning of yeast-displayed Fabs into the mammalian expression vector, we performed a PoC study with the FDA-approved antibody Durvalumab, which recognizes the PD-L1 antigen and blocks the PD-1/PD-L1 axis. The respective VH and VL genes were subcloned into the yeast display vector and upon transformation of yeast cells and subsequent FACS analysis, the display of the respective Fab as well as PD-L1 recognition was verified (**Figure 2A**). Upon *Esp3I*-mediated subcloning of the antibody-encoding genes and the Gal1,10 promoter into the MD vector, followed by promoter exchange in a *BbsI*-assisted manner, a mammalian expression vector was generated. Transient transfection of Expi293-F cells yielded full-length Durvalumab molecules able to recognize PD-L1 in BLI experiments (**Figure 2B**) with an affinity of 364 pM., similar to what has been described in literature (Tan et al., 2018). Encouraged by these initial results, we planned on translating this process to an antibody hit discovery campaign.

Generation of TAMR Library and Screening

We initiated genetic immunisation of transgenic OmniRats, rodents exhibiting a part of the human antibody germline loci (Osborn et al., 2013), with TAMR. Upon cDNA synthesis after total RNA extraction of spleen and lymph node cells, VH- and VL-encoding genes were amplified and subcloned into the yeast display vector using *SapI*-mediated GGC and the YSD_Entry_insert providing the bidirectional Gal1,10 promoter. For library generation, *SapI* was chosen, as this type IIS restriction enzyme does not recognize any antibody germline sequences within OmniRat-derived mAbs. A summary of the cleavage sites within the OmniRat repertoire with the herein used type IIS restriction enzymes,

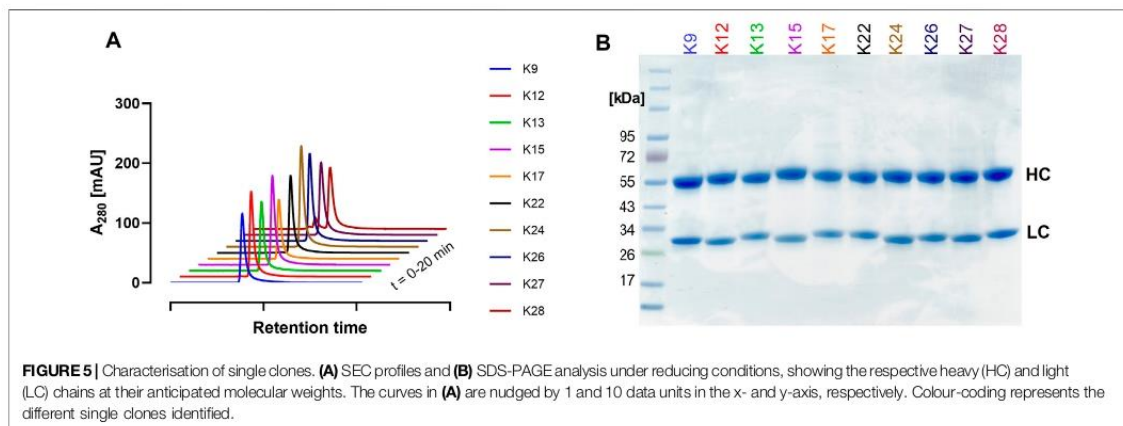
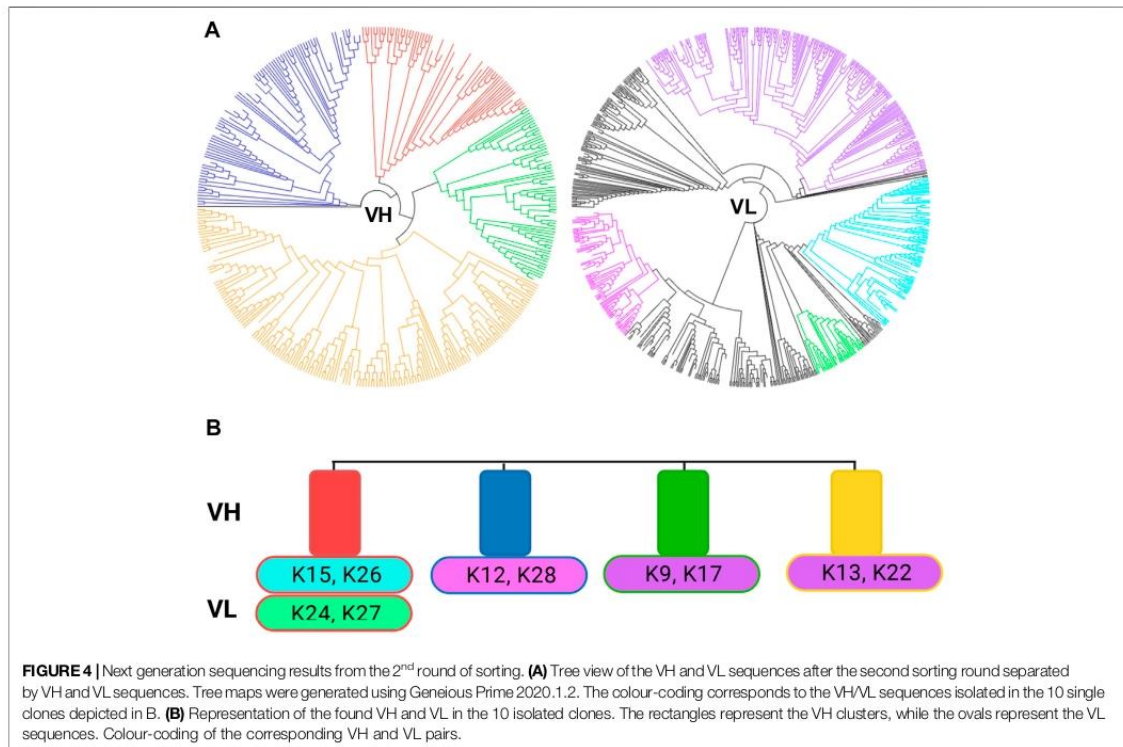


as well as *BsaI* as a reference, is represented in **Supplementary Table S2**.

Upon yeast transformation, the resulting library consisted of 3×10^8 clones and was screened *via* FACS. The first sorting round was performed using 250 nM His-tagged antigen. The subsequent screening round was performed with 250 nM Fc-tagged TAMR, and the outcome of round 2 was stained with 100 nM Fc-tagged TAMR to get higher affinity binders (**Figure 3**). A sufficient enrichment was observed after two sorting rounds, with 54.5% of the Fab-displaying yeast cells binding to the target antigen.

Reformatting of YSD-Enriched Antibodies Into the Mammalian Destination Vector

The antibody-encoding plasmids from the yeast cells after the second sorting round were isolated and antibody-encoding genes were subcloned into the MD vector. Upon promoter exchange from Gal1,10 to 2xeCMV, the obtained final mammalian expression vectors were then subjected to Sanger sequencing. Analysis of 20 single clones revealed 14 unique antibodies, which, in part, originate from multiple clonotypes (**Supplementary Figure S1**). By clustering the sequences based on amino acid differences, especially in the CDR3, ten candidates were chosen



for further analysis. These ten clones were referred to as K9, K12, K13, K15, K17, K22, K24, K26, K27, and K28.

Next-Generation Sequencing

To confirm that no diversity is lost during the subcloning of the Fabs from the library to the expression vector, next-generation sequencing

(NGS) was performed on the initial library as well as the 1st screening round outcome (**Supplementary Figure S2**). The library diversity from the last sorting round was compared to the individual sequences from isolated variants, and colour-coded with the respective sequences from isolated clones (**Figure 4A**). The entire diversity of VH sequence families obtained from library sorting was retained in

TABLE 1 | Affinities of isolated TAMR antibodies determined by BLI measurements using His₆-TAMR.

Clone	Affinity ± S.D. (nM)
K9	43.10 ± 0.65
K13	9.81 ± 0.20
K15	8.23 ± 0.24
K17	10.10 ± 0.21
K22	12.50 ± 0.31
K24	11.90 ± 0.31
K26	7.94 ± 0.26
K27	5.85 ± 0.22
K28	11.10 ± 0.093

the population of reformatted clones, whereas a few VL sequence families were missing. As only 20 clones were inspected, it is probable that more variability could be covered by sequencing a larger sample. Nonetheless, the VH diversity is generally sufficient to obtain highly specific antibodies (Xu and Davis, 2000) and thus is more critical. **Figure 4B** depicts the single clones and their respective VH and VL combinations. From this NGS analysis, one can appreciate that no large diversity was lost within the process as the entire VH repertoire was covered within the single clones.

Transient Expression in Expi293-F Cells, Purification and Characterisation

Ten single clones were produced in Expi293-F cells and purified *via* Protein A to characterise their biophysical properties. Size exclusion chromatography (SEC) revealed favourable aggregation behaviour for most clones, showing minimal aggregation (**Figure 5A**). K28 exhibited the most aggregation behaviour with 15.3% HMW. NanoDSF measurements showed melting temperatures (T_M) between 65 and 70°C, with K13 and K28 exhibiting the lowest and highest T_M values with 65.7 and 70.8°C, respectively (**Supplementary Figure S3**). The observed T_M s represent a high thermal stability and are within a reasonable range for non-glycosylated human IgG1 antibodies (Garber and Demarest, 2007; Dashivets et al., 2015). SDS-PAGE analysis revealed the expected heavy and light chain bands (**Figure 5B**).

Furthermore, kinetics determination *via* BLI indicated a range of single-digit nanomolar affinities to soluble His-tagged TAMR for the vast majority of clones, namely K9, K13, K15, K17, K22, K26, K27, and K28 (**Supplementary Figure S4**). K27 exhibited the highest affinity with 5.85 nM, whereas K9 showed the lowest affinity with 43.1 nM (**Table 1**). Nevertheless, the affinities are within a notable range.

Taken together, the biophysical characterisation revealed 10 promising antibodies targeting TAMR in this proof-of-concept study using the novel approach in order to facilitate the transition from YSD to antibody production in mammalian cells.

DISCUSSION

In this study, we developed a straightforward reformatting approach to yield mammalian expression vectors based on

YSD-screened antibody libraries in a PCR-free manner, based on Golden Gate Cloning. This process allows for bulk cloning of yeast display-enriched antibodies, which was previously not possible due to the loss of the heavy chain–light chain pairing, resulting in reduced hands-on time compared to conventional approaches. Although the issue of cognate heavy and light chain pairing can be omitted by the use of scFvs or scFabs, these molecules come with certain limitations, such as their aggregation behaviour (Röthlisberger et al., 2005; Bates and Power, 2019). Furthermore, the utilization of a Fab-displaying yeast library allows for screening in the final format of the antigen binding site for most therapeutic applications.

However, during library generation, VH and VL genes, amplified from cDNA isolated from immunised animals, are shuffled and therefore their natural pairing is lost. Still, this is also true for conventional yeast libraries, as well as for phage or mammalian display systems. Our novel system could be combined with B cell cloning in the future (Tiller, 2011; Carbonetti et al., 2017; Ouisse et al., 2017), which might allow for a workflow starting from B cells, followed by yeast display screening and mammalian antibody production while maintaining the naturally occurring heavy chain–light chain pairing during the whole antibody discovery process.

Previously, Roth and others have demonstrated the successful generation of a bidirectional YSD vector system to isolate CEACAM6-specific antibodies from immunised OmniRat libraries (Roth et al., 2018). For their library generation, *BsaI* was utilized, which occurs frequently in antibody frameworks (Nelson and Valadon, 2017). To circumvent the risk of losing variants due to internal *BsaI* sites, we chose *SapI* for library generation, which does not occur in OmniRat-derived antibody germlines. As depicted in **Supplementary Table S2**, the other type IIS enzymes employed in this workflow do not have high occurrences within the OmniRat repertoire. Besides human antibodies, chicken-derived antibodies have gained traction within the scientific literature in recent years (Kim et al., 2018; Grzeschik et al., 2019; Bogen et al., 2020a; Bogen et al., 2020b; Bogen et al., 2020c; Hinz et al., 2020; Mwale et al., 2020; Elter et al., 2021). As the chicken germline does not exhibit *SapI* sites either, this workflow can easily be applied to immunised chickens as well, and most likely, to other immunised animals, like mice or rabbits.

Future applications could also include antibody discovery workflows containing a combination of display technologies, for example, by cross-linking phage and yeast display and the presented MD vector for subsequent mammalian production (Patel et al., 2011). Additionally, Akamatsu and others have previously developed a mammalian cell surface display vector to isolate IgG molecules directly using mammalian display (Akamatsu et al., 2007) that can be used to combine yeast surface display with subsequent mammalian display and production. Such workflows can benefit from the advantages of each display technology but are not limited by their own disadvantages. For instance, combining the larger diversity of phage display libraries with the ability to sort for high-affinity antibodies (Marks, 2020) or to perform epitope binning by yeast surface display may ultimately reduce further screening steps within the discovery workflow (e.g., functional assays, binding

affinities, etc.). The herein presented convenient and time-efficient two-pot, two-step method transition from YSD to mammalian expression vector can be further optimized to yield a one-pot, two-step reaction, performing the transfer of antibody VH and VL sequences as well as the promoter exchange within the same “pot”. Furthermore, improvement of the yeast preparation can obviate the need for transformation of *E. coli* and lead to the direct transition from the yeast preparation into the final MD vector for mammalian antibody production. Moreover, a toolbox of different MD vectors containing different Fc variants [e.g., LALA (Lund et al., 1991), N297Q (Wang et al., 2018), RF mutation (Jendeberg et al., 1997)] could be constructed to allow the practical and time-saving exchange for a whole population. This would also pave the way for establishing the methodology for bispecific or multi-specific antibody formats.

Taken together, we designed a straightforward method to preserve heavy chain—light chain pairing while allowing bulk reformatting of YSD-enriched antibody hit candidates into mammalian expression vectors with reduced hands-on time. This procedure has the potential to speed up the drug discovery process and might aid the discovery of therapeutically interesting antibody candidates in the future.

DATA AVAILABILITY STATEMENT

The original contributions presented in the study are included in the article/**Supplementary Material**, further inquiries can be directed to the corresponding author.

REFERENCES

- Akamatsu, Y., Pakabunto, K., Xu, Z., Zhang, Y., and Tsurushita, N. (2007). Whole IgG Surface Display on Mammalian Cells: Application to Isolation of Neutralizing Chicken Monoclonal anti-IL-12 Antibodies. *J. Immunol. Methods* 327, 40–52. doi:10.1016/j.jim.2007.07.007
- Alvarez-Argote, J., and Dasanu, C. A. (2019). Durvalumab in Cancer Medicine: a Comprehensive Review. *Expert Opin. Biol. Ther.* 19, 927–935. doi:10.1080/14712598.2019.1635115
- Bates, A., and Power, C. A. (2019). David vs. Goliath: The Structure, Function, and Clinical Prospects of Antibody Fragments. *Antibodies* 8, 28. doi:10.3390/antib8020028
- Batonick, M., Kiss, M. M., Fuller, E. P., Magadan, C. M., Holland, E. G., Zhao, Q., et al. (2016). pMINERVA: A Donor-Acceptor System for the *In Vivo* Recombineering of scFv into IgG Molecules. *J. Immunol. Methods* 431, 22–30. doi:10.1016/j.jim.2016.02.003
- Benatuil, L., Perez, J. M., Belk, J., and Hsieh, C.-M. (2010). An Improved Yeast Transformation Method for the Generation of Very Large Human Antibody Libraries. *Protein Eng. Des. Sel.* 23, 155–159. doi:10.1093/protein/gzq002
- Boder, E. T., and Wittrup, K. D. (1997). Yeast Surface Display for Screening Combinatorial Polypeptide Libraries. *Nat. Biotechnol.* 15, 553–557. doi:10.1038/nbt0697-553
- Bogen, J. P., Carrara, S. C., Fiebig, D., Grzeschik, J., Hock, B., and Kolmar, H. (2020). Expeditious Generation of Biparatopic Common Light Chain Antibodies via Chicken Immunization and Yeast Display Screening. *Front. Immunol.* 11. doi:10.3389/fimmu.2020.606878
- Bogen, J. P., Grzeschik, J., Krah, S., Zielonka, S., and Kolmar, H. (2020). Rapid Generation of Chicken Immune Libraries for Yeast Surface Display. *Methods Mol. Biology/Genotype Phenotype Coupling* 16 (3), 289–302. doi:10.1007/978-1-4939-9853-1_16
- Bogen, J. P., Storka, J., Yanakieva, D., Fiebig, D., Grzeschik, J., Hock, B., et al. (2020). Isolation of Common Light Chain Antibodies from Immunized Chickens Using Yeast Biopanning and Fluorescence-Activated Cell Sorting. *Biotechnol. J.* 16, 2000240. doi:10.1002/biot.202000240
- Bournazos, S., and Ravetch, J. V. (2017). Diversification of IgG Effector Functions. *Int. Immunol.* 29, 303–310. doi:10.1093/intimm/dxx025
- Carbonetti, S., Oliver, B. G., Vigdorovich, V., Dambruskas, N., Sack, B., Bergl, E., et al. (2017). A Method for the Isolation and Characterization of Functional Murine Monoclonal Antibodies by Single B Cell Cloning. *J. Immunol. Methods* 448, 66–73. doi:10.1016/j.jim.2017.05.010
- Carrara, S. C., Fiebig, D., Bogen, J. P., Grzeschik, J., Hock, B., and Kolmar, H. (2021). Recombinant Antibody Production Using a Dual-Promoter Single Plasmid System. *Antibodies* 10, 18. doi:10.3390/antib10020018
- Carrara, S. C., Ulitzka, M., Grzeschik, J., Kornmann, H., Hock, B., and Kolmar, H. (2021). From Cell Line Development to the Formulated Drug Product: The Art of Manufacturing Therapeutic Monoclonal Antibodies. *Int. J. Pharm.* 594, 120164. doi:10.1016/j.ijpharm.2020.120164
- Cruz-Teran, C. A., Tiruthani, K., Mischler, A., and Rao, B. M. (2017). Inefficient Ribosomal Skipping Enables Simultaneous Secretion and Display of Proteins in *Saccharomyces cerevisiae*. *ACS Synth. Biol.* 6, 2096–2107. doi:10.1021/acssynbio.7b00144
- Dashivets, T., Thomann, M., Rueger, P., Knaupp, A., Buchner, J., and Schlothauer, T. (2015). Multi-Angle Effector Function Analysis of Human Monoclonal IgG Glycovariants. *PLoS One* 10, e0143520. doi:10.1371/journal.pone.0143520
- Elter, A., Bogen, J. P., Hinz, S. C., Fiebig, D., Macarrón Palacios, A., Grzeschik, J., et al. (2021). Humanization of Chicken-Derived scFv Using Yeast Surface Display and NGS Data Mining. *Biotechnol. J.* 16, 2000231. doi:10.1002/biot.202000231
- Garber, E., and Demarest, S. J. (2007). A Broad Range of Fab Stabilities within a Host of Therapeutic IgGs. *Biochem. Biophysical Res. Commun.* 355, 751–757. doi:10.1016/j.bbrc.2007.02.042

AUTHOR CONTRIBUTIONS

DF, JB, SC, and LD performed experiments. DF, JB, SC, LD, JG, and HK analysed the data. SZ, JG, and BH gave scientific advice. DF, JB, and SC wrote the article. All authors contributed to the article and approved the submitted version.

ACKNOWLEDGMENTS

The authors would like to thank Ferring Pharmaceuticals, especially the department of GPRD, for funding. The funders played no role in study design, data collection and analysis, or preparation of the manuscript. The authors would also like to thank Prof. Fessner for the possibility to perform NanoDSF measurements in his laboratory. Figures were created with BioRender.com. We acknowledge support by the Deutsche Forschungsgemeinschaft (DFG—German Research Foundation) and the Open Access Publishing Fund of Technical University of Darmstadt.

SUPPLEMENTARY MATERIAL

The Supplementary Material for this article can be found online at: <https://www.frontiersin.org/articles/10.3389/fbioe.2022.794389/full#supplementary-material>

- Grzeschik, J., Yanakieva, D., Roth, L., Krahl, S., Hinz, S. C., Elter, A., et al. (2019). Yeast Surface Display in Combination with Fluorescence-activated Cell Sorting Enables the Rapid Isolation of Antibody Fragments Derived from Immunized Chickens. *Biotechnol. J.* 14, 1800466. doi:10.1002/biot.201800466
- Hinz, S. C., Elter, A., Rammo, O., Schwämmle, A., Ali, A., Zielonka, S., et al. (2020). A Generic Procedure for the Isolation of pH- and Magnesium-Responsive Chicken scFvs for Downstream Purification of Human Antibodies. *Front. Bioeng. Biotechnol.* 8. doi:10.3389/fbioe.2020.00688
- Hoy, S. M. (2019). Sintilimab: First Global Approval. *Drugs* 79, 341–346. doi:10.1007/s40265-019-1066-z
- Jendeberg, L., Nilsson, P., Larsson, A., Denker, P., Uhlén, M., Nilsson, B., et al. (1997). Engineering of Fc1 and Fc3 from Human Immunoglobulin G to Analyse Subclass Specificity for Staphylococcal Protein A. *J. Immunol. Methods* 201, 25–34. doi:10.1016/S0022-1759(96)00215-3
- Josephson, K., Ricardo, A., and Szostak, J. W. (2014). mRNA Display: from Basic Principles to Macrocyclic Drug Discovery. *Drug Discov. Today* 19, 388–399. doi:10.1016/j.drudis.2013.10.011
- Kapur, R., Einarsdottir, H. K., and Vidarsson, G. (2014). IgG-effector Functions: "The Good, the Bad and the Ugly". *Immunol. Lett.* 160, 139–144. doi:10.1016/j.imlet.2014.01.015
- Kim, Y. M., Park, J. S., Kim, S. K., Jung, K. M., Hwang, Y. S., Han, M., et al. (2018). The Transgenic Chicken Derived Anti-CD20 Monoclonal Antibodies Exhibits Greater Anti-cancer Therapeutic Potential with Enhanced Fc Effector Functions. *Biomaterials* 167, 58–68. doi:10.1016/j.biomaterials.2018.03.021
- Krahl, S., Günther, R., Becker, S., Zielonka, S., and Rhiel, L. (2020). Chemical Modification of the Yeast Cell Surface Allows the Switch between Display and Soluble Secretion of Full-Length Antibodies. *Methods Mol. Biology/Genotype Phenotype Coupling* 2070, 335–349. doi:10.1007/978-1-4939-9853-1_19
- Li, F., Vijayasankaran, N., Shen, A., Kiss, R., and Amanullah, A. (2010). Cell Culture Processes for Monoclonal Antibody Production. *MAbs* 2, 466–479. doi:10.4161/mabs.2.5.12720
- Lipovsek, D., and Plückthun, A. (2004). In-vitro Protein Evolution by Ribosome Display and mRNA Display. *J. Immunol. Methods* 290, 51–67. doi:10.1016/j.jim.2004.04.008
- Liu, Y., Gu, M., Wu, Y., Wang, W., Wang, R., Du, M., et al. (2018). High-throughput Reformatting of Phage-Displayed Antibody Fragments to IgGs by One-step Emulsion PCR. *Protein Eng. Des. Sel.* 31, 427–436. doi:10.1093/protein/gzz004
- Lu, R.-M., Hwang, Y.-C., Liu, I.-J., Lee, C.-C., Tsai, H.-Z., Li, H.-J., et al. (2020). Development of Therapeutic Antibodies for the Treatment of Diseases. *J. Biomed. Sci.* 27, 1. doi:10.1186/s12929-019-0592-z
- Lund, J., Winter, G., Jones, P. T., Pound, J. D., Tanaka, T., Walker, M. R., et al. (1991). Human Fc Gamma RI and Fc Gamma RII Interact with Distinct but Overlapping Sites on Human IgG. *J. Immunol.* 147, 2657–2662.
- Marks, J. D. (2020). "Monoclonal Antibodies From Display Libraries." in *Molecular Biology of B Cells* (Elsevier), 511–531. doi:10.1016/B978-0-12053641-2/50033-2
- McCafferty, J., Griffiths, A. D., Winter, G., and Chiswell, D. J. (1990). Phage Antibodies: Filamentous Phage Displaying Antibody Variable Domains. *Nature* 348, 552–554. doi:10.1038/348552a0
- Mwale, P. F., Lee, C.-H., Lin, L.-T., Leu, S.-J., Huang, Y.-J., Chiang, L.-C., et al. (2020). Expression, Purification, and Characterization of Anti-zika Virus Envelope Protein: Polyclonal and Chicken-Derived Single Chain Variable Fragment Antibodies. *Ijms* 21, 492. doi:10.3390/ijms21020492
- Nelson, R. S., and Valadon, P. (2017). A Universal Phage Display System for the Seamless Construction of Fab Libraries. *J. Immunol. Methods* 450, 41–49. doi:10.1016/j.jim.2017.07.011
- Osborn, M. J., Ma, B., Avis, S., Binnie, A., Dille, J., Yang, X., et al. (2013). High-Affinity IgG Antibodies Develop Naturally in Ig-Knockout Rats Carrying Germline Human IgH/Igk/Igλ Loci Bearing the Rat CHRegion. *J. I.* 190, 1481–1490. doi:10.4049/jimmunol.1203041
- Ouisse, L.-H., Gautreau-Rolland, L., Devilder, M.-C., Osborn, M., Moyon, M., Visentin, J., et al. (2017). Antigen-specific Single B Cell Sorting and Expression-Cloning from Immunoglobulin Humanized Rats: a Rapid and Versatile Method for the Generation of High Affinity and Discriminative Human Monoclonal Antibodies. *BMC Biotechnol.* 17, 3. doi:10.1186/s12896-016-0322-5
- Parthiban, K., Perera, R. L., Sattar, M., Huang, Y., Mayle, S., Masters, E., et al. (2019). A Comprehensive Search of Functional Sequence Space Using Large Mammalian Display Libraries Created by Gene Editing. *MAbs* 11, 884–898. doi:10.1080/19420862.2019.1618673
- Patel, C. A., Wang, J., Wang, X., Dong, F., Zhong, P., Luo, P. P., et al. (2011). Parallel Selection of Antibody Libraries on Phage and Yeast Surfaces via a Cross-Species Display. *Protein Eng. Des. Sel.* 24, 711–719. doi:10.1093/protein/gzr034
- Reader, R. H., Workman, R. G., Maddison, B. C., and Gough, K. C. (2019). Advances in the Production and Batch Reformatting of Phage Antibody Libraries. *Mol. Biotechnol.* 61, 801–815. doi:10.1007/s12033-019-00207-0
- Reichert, J. (2021). *Therapeutic Monoclonal Antibodies Approved or in Review in the European Union or the United States*. The Antibody Society. <https://www.antibodysociety.org/resources/approved-antibodies/>.
- Renaut, L., Monnet, C., Dubreuil, O., Zaki, O., Crozet, F., Bouayadi, K., et al. (2012). Affinity Maturation of Antibodies: Optimized Methods to Generate High-Quality ScFv Libraries and Isolate IgG Candidates by High-Throughput Screening. *Antib. Engineering/Methods Mol. Biol.* 907, 451–461. doi:10.1007/978-1-61779-974-7_26
- Rosowski, S., Becker, S., Toilekis, L., Valldorf, B., Grzeschik, J., Demir, D., et al. (2018). A Novel One-step Approach for the Construction of Yeast Surface Display Fab Antibody Libraries. *Microb. Cell Fact.* 17, 3. doi:10.1186/s12934-017-0853-z
- Roth, L., Grzeschik, J., Hinz, S. C., Becker, S., Toilekis, L., Busch, M., et al. (2018). Facile Generation of Antibody Heavy and Light Chain Diversities for Yeast Surface Display by Golden Gate Cloning. *Biol. Chem.* 400, 383–393. doi:10.1515/hsz-2018-0347
- Röthlisberger, D., Honegger, A., and Plückthun, A. (2005). Domain Interactions in the Fab Fragment: A Comparative Evaluation of the Single-Chain Fv and Fab Format Engineered with Variable Domains of Different Stability. *J. Mol. Biol.* 347, 773–789. doi:10.1016/j.jmb.2005.01.053
- Schaffitzel, C., Hanes, J., Jeremius, L., and Plückthun, A. (1999). Ribosome Display: an *In Vitro* Method for Selection and Evolution of Antibodies from Libraries. *J. Immunol. Methods* 231, 119–135. doi:10.1016/S0022-1759(99)00149-0
- Sivelle, C., Sierocki, R., Ferreira-Pinto, K., Simon, S., Maillere, B., and Nozach, H. (2018). Fab Is the Most Efficient Format to Express Functional Antibodies by Yeast Surface Display. *MAbs* 10, 720–729. doi:10.1080/19420862.2018.1468952
- Tan, S., Liu, K., Chai, Y., Zhang, C. W.-H., Gao, S., Gao, G. F., et al. (2018). Distinct PD-L1 Binding Characteristics of Therapeutic Monoclonal Antibody Durvalumab. *Protein Cell* 9, 135–139. doi:10.1007/s13238-017-0412-8
- Tanner, W., and Lehle, L. (1987). Protein Glycosylation in Yeast. *Biochimica Biophysica Acta (BBA) - Rev. Biomembr.* 906, 81–99. doi:10.1016/0304-4157(87)90006-2
- Tiller, T. (2011). Single B Cell Antibody Technologies. *New Biotechnol.* 28, 453–457. doi:10.1016/j.nbt.2011.03.014
- Valldorf, B., Hinz, S. C., Russo, G., Pekar, L., Mohr, L., Klemm, J., et al. (2021). Antibody Display Technologies: Selecting the Cream of the Crop. *Biol. Chem.* 403, 455–477. doi:10.1515/hsz-2020-0377
- Vazquez-Lombardi, R., Nevoltris, D., Luthra, A., Schofield, P., Zimmermann, C., and Christ, D. (2018). Transient Expression of Human Antibodies in Mammalian Cells. *Nat. Protoc.* 13, 99–117. doi:10.1038/nprot.2017.126
- Wang, X., Mathieu, M., and Brezski, R. J. (2018). IgG Fc Engineering to Modulate Antibody Effector Functions. *Protein Cell* 9, 63–73. doi:10.1007/s13238-017-0473-8
- Wildt, S., and Gerngross, T. U. (2005). The Humanization of N-Glycosylation Pathways in Yeast. *Nat. Rev. Microbiol.* 3, 119–128. doi:10.1038/nrmicro1087
- Xiao, X., Douthwaite, J. A., Chen, Y., Kemp, B., Kidd, S., Percival-Alwyn, J., et al. (2017). A High-Throughput Platform for Population Reformatting and Mammalian Expression of Phage Display Libraries to Enable Functional Screening as Full-Length IgG. *MAbs* 9, 996–1006. doi:10.1080/19420862.2017.1337617
- Xu, J. L., and Davis, M. M. (2000). Diversity in the CDR3 Region of VH Is Sufficient for Most Antibody Specificities. *Immunity* 13, 37–45. doi:10.1016/S1074-7613(00)00006-6

Conflict of Interest: The authors declare that the research was conducted in the absence of any commercial or financial relationships that could be construed as a potential conflict of interest.

Publisher's Note: All claims expressed in this article are solely those of the authors and do not necessarily represent those of their affiliated organizations, or those of the publisher, the editors and the reviewers. Any product that may be evaluated in this article, or claim that may be made by its manufacturer, is not guaranteed or endorsed by the publisher.

Copyright © 2022 Fiebig, Bogen, Carrara, Deweid, Zielonka, Grzeschik, Hock and Kolmar. This is an open-access article distributed under the terms of the Creative Commons Attribution License (CC BY). The use, distribution or reproduction in other forums is permitted, provided the original author(s) and the copyright owner(s) are credited and that the original publication in this journal is cited, in accordance

Supplementary Material

1 Supplementary Figures and Tables

Supplementary Table 1: Primers for 2nd PCR with GGA SapI overhangs for VH and VL kappa

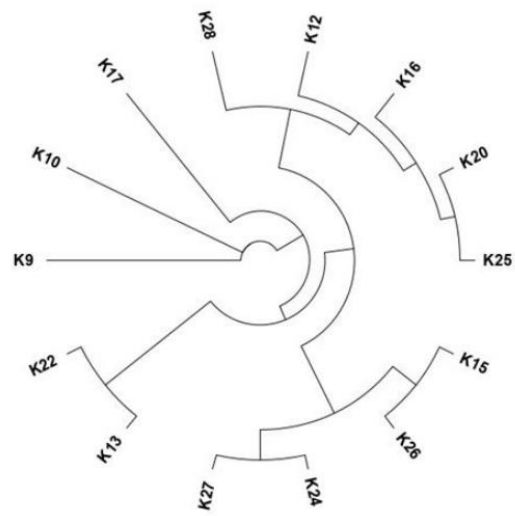
Primer Name	VH/VL	Sequence (5' - 3')
Omni_VH-GGA_1	VH	ATATATGCTCTTCAGCACAGGTBCAGCTGGTGCARTCTGG
Omni_VH-GGA_2	VH	ATATATGCTCTTCAGCACARRTSCAGCTGGTRCAGTCTGG
Omni_VH-GGA_3	VH	ATATATGCTCTTCAGCACAGRTCACCTTGAAGGAGTCTGG
Omni_VH-GGA_4	VH	ATATATGCTCTTCAGCASAGGTGCAGCTGGTGGAGTCYGG
Omni_VH-GGA_5	VH	ATATATGCTCTTCAGCAGARGTGCAGCTGKTGGAGTCTGG
Omni_VH-GGA_6	VH	ATATATGCTCTTCAGCACAGGTGCAGCTACAGCAGTGGGG
Omni_VH-GGA_7	VH	ATATATGCTCTTCAGCACAGSTGCAGCTGCAGGAGTCGGG
Omni_VH-GGA_8	VH	ATATATGCTCTTCAGCAGAGGTGCAGCTGGTGCAGTCTGG
Omni_VH-GGA_9	VH	ATATATGCTCTTCAGCACAGGTACAGCTGCAGCAGTCAGG
Omni_VH_rev_woEsp3I	VH	TATATATGCTCTTCTGGCTGARGAGACAGTGACCR
Omni_K-GGA_1	VL kappa	ATATATGCTCTTCAGCTGACATCCAGATGACCCAGTCTCC
Omni_K-GGA_2	VL kappa	ATATATGCTCTTCAGCTGMCATCCRGWTGACCCAGTCTCC
Omni_K-GGA_3	VL kappa	ATATATGCTCTTCAGCTGATRTTGTGATGACYCAGWCTCC
Omni_K-GGA_4	VL kappa	ATATATGCTCTTCAGCTGAAATWGTGWTGACRCAGTCTCC
Omni_K-GGA_5	VL kappa	ATATATGCTCTTCAGCTGACATCGTGATGACCCAGTCTCC
Omni_K-GGA_6	VL kappa	ATATATGCTCTTCAGCTGAAACGACACTCACGCAGTCTCC
Omni_K-GGA_7	VL kappa	ATATATGCTCTTCAGCTGAAATTGTGCTGACTCAGTCTCC
Omni_K-GGA_rev1	VL kappa	GCGCGCGCTCTTCATCGTTTGATHCCASYTTGGTCCC
Omni_K-GGA_rev2	VL kappa	GCGCGCGCTCTTCATCGTTTAATCTCCAGTCGTGTC

Overhang sequence

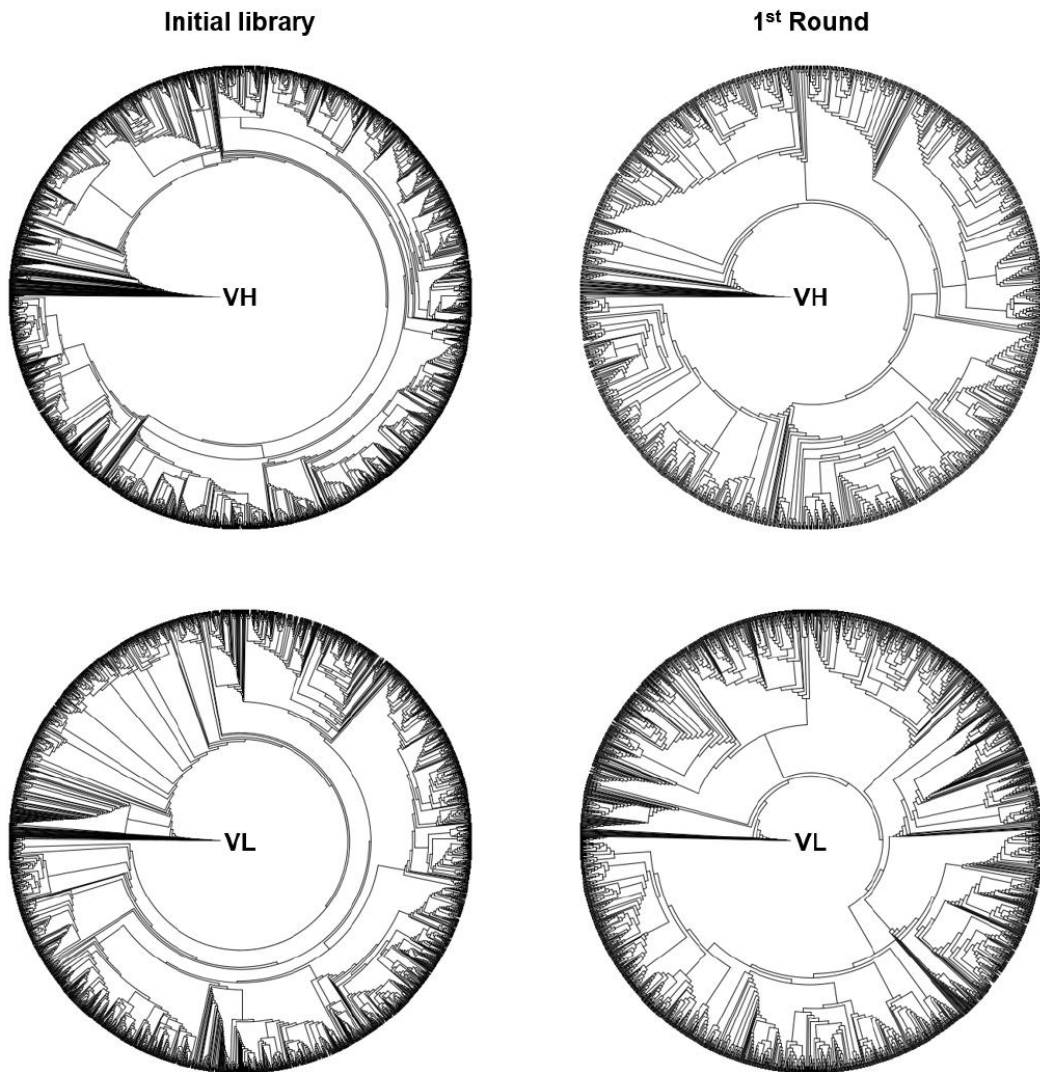
Primer sequence

Supplementary Table 2: Number of cleavage sites in the OmniRat repertoire. A total of 44 VH and 20 Vk germline genes are present. *BsaI* serves as a reference, compared to the three type IIS enzymes used to establish the workflow presented in this work.

Type IIS Enzyme	Number of cleavage sites in OmniRat germlines	
	VH	Vk
<i>SapI</i>	0	0
<i>BbsI</i>	2	0
<i>Esp3I</i>	1	0
<i>BsaI</i>	15	0

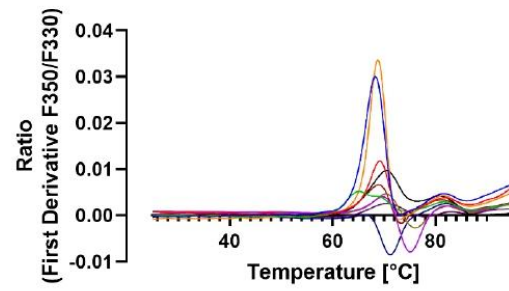


Supplementary Figure 1: Tree map of VH-VL pairs after reformatting into the MD vector. 14 unique candidates based on sequence differences were revealed.

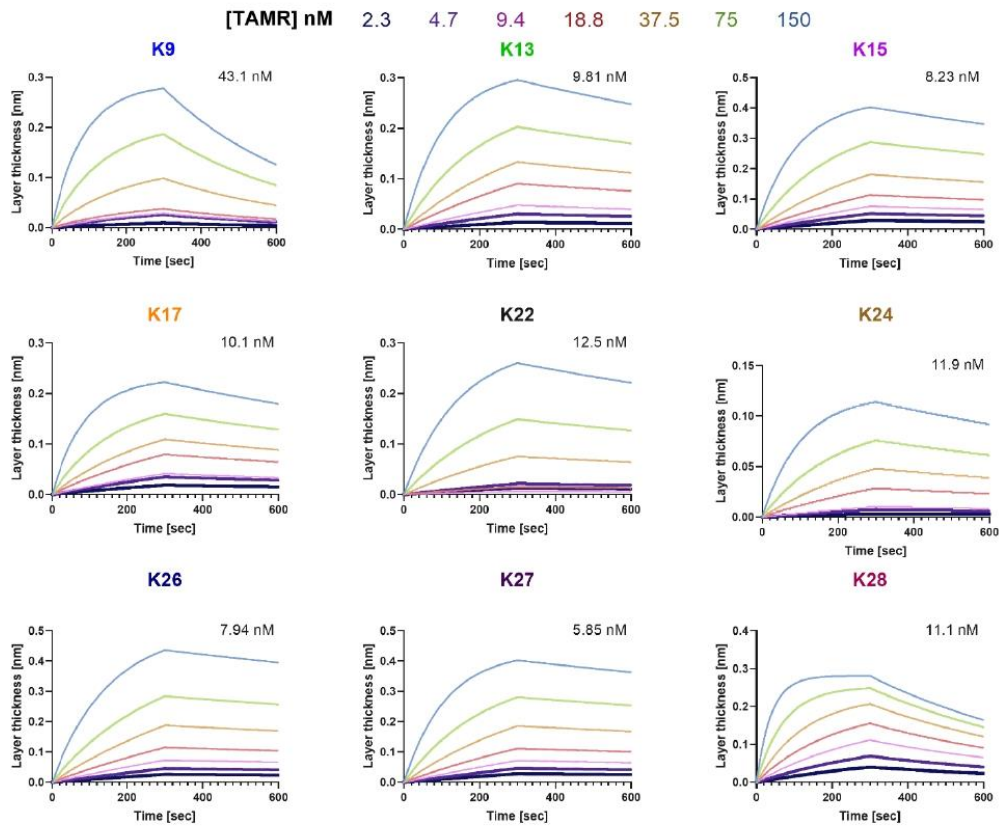


Supplementary Figure 2: VH and VL diversity of the initial library and after the 1st screening round on the left and right, respectively, after NGS analysis.

Clone	T _M [°C]
K9	68.1
K13	65.7
K15	69.0
K17	68.6
K22	70.3
K26	70.5
K27	68.5
K28	70.8



Supplementary Figure 3: Melting temperatures of TAMR-binding variants. NanoDSF-assisted thermal stability studies were performed. The ratio of the integrated fluorescence at 350 nm / 330 nm was calculated. Colour-coding of the clone names correlates with the curves.



Supplementary Figure 4: Kinetics determination of variants targeting TAMR. Antibodies were immobilized at a concentration of 10 $\mu\text{g/ml}$ on AHC biosensor tips and associated to different concentrations of soluble antigen in a range from 0 – 150 nM.

4.4 Targeted phagocytosis induction for cancer immunotherapy *via* bispecific MerTK-engaging antibodies

Title:

Targeted phagocytosis induction for cancer immunotherapy *via* bispecific MerTK-engaging antibodies

Authors:

Stefania Candela Carrara, Jan Patrick Bogen, David Fiebig, Julius Grzeschik, Björn Hock, Harald Kolmar

Bibliographic Data:

Journal – *International Journal of Molecular Sciences (MDPI)*

Special Issue – *Advances in Single Domain-Based Antibodies*

DOI: 10.3390/ijms232415673

Contributions by S.C. Carrara:

- Initial idea & project planning
- Cloning and production of bispecifics
- Testing of monospecific and bispecific variants in biophysical and biological assays
- Writing of manuscript
- Generation of all figures



Article

Targeted Phagocytosis Induction for Cancer Immunotherapy via Bispecific MerTK-Engaging Antibodies

Stefania C. Carrara ^{1,2}, Jan P. Bogen ^{1,2}, David Fiebig ^{1,2}, Julius Grzeschik ³, Björn Hock ⁴ and Harald Kolmar ^{1,5,*}

¹ Institute for Organic Chemistry and Biochemistry, Technical University of Darmstadt, Alarich-Weiss-Strasse 4, D-64287 Darmstadt, Germany

² Ferring Darmstadt Laboratories, Alarich-Weiss-Strasse 4, D-64287 Darmstadt, Germany

³ Ferring Biologics Innovation Centre, Biopôle, CH-1066 Epalinges, Switzerland

⁴ Aerium Therapeutics, Biopôle, CH-1066 Epalinges, Switzerland

⁵ Centre for Synthetic Biology, Technical University of Darmstadt, Alarich-Weiss-Strasse 4, D-64287 Darmstadt, Germany

* Correspondence: harald.kolmar@tu-darmstadt.de



Citation: Carrara, S.C.; Bogen, J.P.; Fiebig, D.; Grzeschik, J.; Hock, B.; Kolmar, H. Targeted Phagocytosis Induction for Cancer Immunotherapy via Bispecific MerTK-Engaging Antibodies. *Int. J. Mol. Sci.* **2022**, *23*, 15673. <https://doi.org/10.3390/ijms232415673>

Academic Editor: Sergei V. Tilib

Received: 31 October 2022

Accepted: 7 December 2022

Published: 10 December 2022

Publisher's Note: MDPI stays neutral with regard to jurisdictional claims in published maps and institutional affiliations.



Copyright: © 2022 by the authors. Licensee MDPI, Basel, Switzerland. This article is an open access article distributed under the terms and conditions of the Creative Commons Attribution (CC BY) license (<https://creativecommons.org/licenses/by/4.0/>).

Abstract: The Tyro, Axl, and MerTK receptors (TAMRs) play a significant role in the clearance of apoptotic cells. In this work, the spotlight was set on MerTK, as it is one of the prominent TAMRs expressed on the surface of macrophages and dendritic cells. MerTK-specific antibodies were previously isolated from a transgenic rat-derived immune library with suitable biophysical properties. Further characterisation resulted in an agonistic MerTK antibody that led to phospho AKT activation in a dose-dependent manner. In this proof-of-concept study, a MerTK-specific antibody, MerK28, was combined with tandem, biparatopic EGFR-binding VHH camelid antibody domains (7D9G) in different architectures to generate bispecific antibodies with the capacity to bind EGFR and MerTK simultaneously. The bispecific molecules exhibited appropriate binding properties with regard to both targets in their soluble forms as well as to cells, which resulted in the engagement of macrophage-like THP-1 cells with epidermoid carcinoma A431 cells. Furthermore, targeted phagocytosis in co-culture experiments was observed only with the bispecific variants and not the parental MerTK-binding antibody. This work paves the way for the generation of bispecific macrophage-engaging antibodies for targeted phagocytosis harnessing the immune-modulating roles of MerTK in immunotherapy.

Keywords: macrophages; targeted phagocytosis; MerTK; EGFR; bispecific antibody; BiME

1. Introduction

A specialised family of receptor tyrosine kinases is the Tyro3, Axl, and MerTK receptor (TAMR) family, which plays a number of crucial roles maintaining tissue homeostasis [1]. Structurally, the extracellular domains of all TAMRs are similar, being composed of two immunoglobulin-like domains that mediate ligand binding and two fibronectin type III repeats, with a conserved intracellular kinase domain, as with all other RTKs [2–5]. Two endogenous ligands, growth arrest-specific gene 6 (Gas6) [6] and anticoagulation factor protein S (Pros1) [7], bind the TAMRs, with Gas6 having a strong affinity for Axl but not for Tyro3 and MerTK, and Pros1 preferring Tyro3 and MerTK but not activating Axl [3,8]. Activation of the receptors is mediated by homo- and hetero-dimerisation of both the receptors and the ligands, resulting in TAMR-mediated signalling [5]. On macrophages, the most well-characterised signalling cascade is the phosphoinositide 3 kinase (PI3K)/AKT pathway, ultimately resulting in the phosphorylation of AKT (pAKT) through mediators in the signal transduction and altered gene expression [2,9,10].

Macrophages are commonly known as the professional phagocytes of apoptotic cells (AC), as they spend most of their time phagocytosing apoptotic cells and fragments, with >10⁹ ACs generated in humans per day [3,11]. The maintenance of tissue homeostasis

by efficient clearance of AC by macrophages is crucial to inhibit inflammatory and auto-immune responses against “self” antigens. MerTK is mainly expressed on myeloid cells pertaining to the immune system, including macrophages and dendritic cells (DC), and is involved in the clearance of ACs by recognising phosphatidylserine (PtdSer) exposed on ACs through bridging with its endogenous ligands, Gas6 and Pros1 [3,12–15]. Being largely absent on monocytes, MerTK becomes strongly upregulated upon monocyte-to-macrophage differentiation [2,16]. Furthermore, MerTK has been largely associated with “alternatively activated” M2 macrophages that aid in tissue homeostasis, wound healing, and fighting infections by secreting anti-inflammatory cytokines [2,17]. In line with their wound-healing immunosuppressive phenotype, M2-like macrophages have a greater capacity to clear ACs compared to the “classically activated” M1-like macrophages [2,18]. In vivo studies with mice containing a truncated version of MerTK showed reduced clearance of ACs, highlighting the importance of MerTK in this mechanism [13]. Additionally, a triple Tyro3/Axl/MerTK mice knock-out model showed normal development of the mice but exhibited elevated levels of pro-inflammatory cytokines (e.g., TNF α , IL-6). Furthermore, a diminished ability to clear ACs and increased auto-antibody production could be observed, which over time resulted in symptoms evocative of systemic lupus erythematosus, rheumatoid arthritis (RA), and psoriasis. A deeper analysis of single TAMR knock-outs exposed the role of MerTK in autoimmunity, contributing largely to the effects seen in the triple knock-out mice [19,20].

Nevertheless, MerTK may be seen as a double-edged sword, as it modulates the immune system by reducing immune cell activation through the clearance of ACs, but it has also been implied to have tumour-intrinsic functions due to its aberrant expression on several types of cancerous cells [21]. Targeting and inhibiting MerTK and other members of the TAMR family have been considered interesting anti-cancer strategies for reducing tumour development and promoting survival via the alleged MerTK-mediated signalling pathways, including the development of several pan-TAMR small molecule inhibitors and monoclonal antibodies [22–27].

However, evidence has emerged to cast doubt on TAMR blockage as a suitable anti-cancer therapy. As reported by Bosurgi et al., MerTK-deficient mice resulted in increased pro-inflammatory cytokine secretion and decreased AC clearance in colon cancer models, ultimately sponsoring a tumour-promoting tumour microenvironment (TME) [28,29]. Furthermore, on-target retinal toxicities were observed with treatment with an antagonistic MerTK antibody in cynomolgus monkeys, warranting the need for further investigation of MerTK-targeting therapy [22,29]. MerTK activity has also been shown to play a role in endothelial cell recruitment to the TME and to inhibit angiogenesis, thus hindering tumour development and growth [29,30].

To harness the increased expression of MerTK on tumour-associated macrophages (TAMs) in the TME, bispecific antibodies (bsAbs) were generated targeting a tumour-associated antigen (TAA) to generate bispecific macrophage engagers (BiMEs). While BiMEs have been previously described, they mediate macrophage engagement and activation by inhibiting the classical SIRP α and simultaneously targeting a TAA [31]. Along similar lines, CD47-directed bsAbs target the CD47/SIRP α axis by blocking CD47 signalling and restoring phagocytosis of tumour cells by macrophages [32]. In the hereby presented proof-of-concept study, targeted phagocytosis for cancer immunotherapy was substituted by targeting MerTK on macrophages and the epidermal growth factor receptor (EGFR) that is overexpressed on a plethora of tumour types [33–35]. By harnessing MerTK’s expression on phagocytes, this could ameliorate the immunosuppressive environment in the TME and result in targeted phagocytosis of malignant cells. This is, to the best of our knowledge, the first MerTK-mediated macrophage engager for immunotherapy.

2. Results

2.1. Characterisation of MerTK Monoclonal Antibody

As previously reported [36], an OmniRat-based immunisation campaign was initiated by genetic immunisation with the extracellular domain of MerTK. After fluorescence-activated cell sorting (FACS) of a Fab-library by yeast surface display (YSD), a panel of antibodies (mAbs) were isolated with favourable biophysical properties and high affinity binding to soluble human MerTK (hMerTK). Ten antibody candidates were reformatted as full-length IgG1 molecules, expressed via transient transfection in Expi293-F cells and purified by protein A chromatography. To further characterise these antibodies, all variants were initially tested for binding to the MerTK⁺ Jurkat cell line (Figure S1a) and to HEK293 cells (Figure S1b). While several antibody candidates showed decent binding to both cell lines, MerK17 and MerK28 were chosen for further characterisation as they displayed the highest binding in flow cytometric cell binding assays.

Their effect on the modulation of MerTK's signalling transduction cascade was measured, as this is an important mechanism of action for the differentiation of macrophages and clearance of apoptotic cells. To this end, MerTK⁺ A431 cells were incubated with mAbs overnight, and subsequently the activation of pAKT was measured by homogenous time-resolved fluorescence (HTRF). While no activation was observed in the presence of MerK17, moderate pAKT activation was noted for MerK28, indicating agonistic properties of this antibody (Figure S1c). The most suitable stimulation time was investigated by a time-course on A431 and HEK293 cells, resulting in the strongest pAKT activation after 30 min with relative fold changes of 2.5 and 4.5 compared to the unstimulated control for A431 and HEK293 cells, respectively (Figure S1d,e). With the optimal stimulation time of 30 min, the HTRF pAKT assay was repeated on A431 cells to ensure MerK17 did not result in different activation profiles. Unsurprisingly, no stimulation was observed with MerK17, and dose-dependent stimulation was detected with MerK28 (Figure S1f).

To further characterise the agonistic MerK28, its binding affinities to both hMerTK and murine MerTK (mMerTK) were determined by biolayer interferometry (BLI). A one-armed variant of MerK28, oaMerK28, was generated, and its MerTK-binding capability was also tested. Using in-house produced antigens, MerK28 and oaMerK28 were loaded onto AHC biosensors and associated to varying concentrations of either hMerTK-TS or mMerTK-Fc. Kinetics revealed low single-digit nanomolar affinity of MerK28 to hMerTK-TS (Figure 1a, Table 1) and a slight decrease in affinity with oaMerK28 (Figure 1b, Table 1). Cross-reactivity to mMerTK-Fc was revealed for both the bivalent and the one-armed MerK28 in the low-nanomolar range (Figure 1c,d). MerK17 did not exhibit cross-reactivity with murine MerTK. Dose-dependent activation of pAKT after mAb incubation was observed on both A431 (Figure 1e) and HEK293 (Figure 1f) cells for the bivalent MerK28, but not for the oaMerK28.

Due to the different effects on cell signalling of MerK17 and MerK28, an epitope binning via BLI was performed to confirm that different epitopes were being addressed. As seen in Figure 1g, MerK28 and MerK17 did not possess overlapping epitopes, as they were both able to bind to hMerTK-His₆ simultaneously. These results were confirmed by reversing the order of association of the mAbs (Figure S2a). Additionally, it was investigated whether MerK28 competed for the ligand binding site of one of the MerTK ligands, Pros1. By pre-incubating MerTK with an equimolar amount of Pros1 and associating it to MerK28, a decreased layer thickness was observed over time compared to MerTK binding only, indicating that MerK28 competed for the Pros1 ligand binding site (Figure 1h). This effect was not noted with MerK17 (Figure S2b). These results further epitomise the agonistic characteristic of MerK28, as Pros1 naturally leads to receptor activation. Thus, MerK28 was chosen for further studies, as it allows the choice between an agonistic mAb in the bivalent form or binding in its monovalent form and is also cross-reactive to murine MerTK.

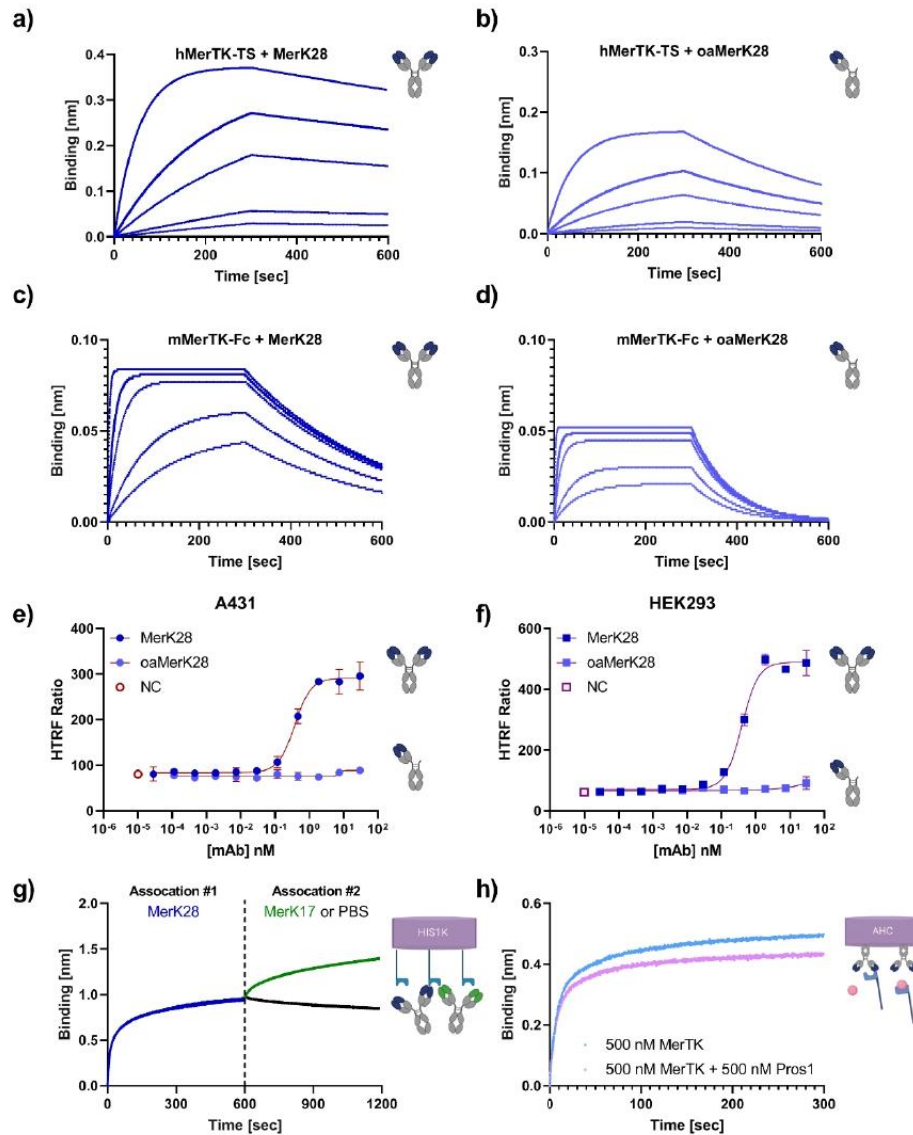


Figure 1. Characterisation of parental MerTK antibodies. Kinetics determination against soluble hMerTK-TS for either (a) MerK28 or (b) oaMerK28, and against mMerTK-Fc for (c) MerK28 or (d) oaMerK28. (e,f) Activation of signalling transduction with MerK28. pAKT HTRF assays with either A431 (e) or HEK293 (f) cells. Unstimulated cells are shown as “NC”, and the bivalent MerK28 and one-armed MerK28 (oaMerK28) are plotted. Error bars represent biological duplicate measurements. (g) Epitope binning of MerK28 (blue) and MerK17 (green) via BLI. Human MerTK-His₆ was immobilised on HIS1K biosensors and associated to the indicated antibodies for 600 s each. PBS is shown in black. (h) Ligand competition assay for MerK28. Association to hMerTK (light blue) alone or to MerTK pre-incubated with Pros1 ligand (pink).

Table 1. Biophysical properties of MerK28 and its derived bispecifics. Abbreviations: TS—TwinStrepII-Tag, n.d.—not determined.

Variant	Affinity Determination			Yield for 1 L (mg)	Thermal Stability (°C)
	hMerTK-TS (nM)	mMerTK-Fc (nM)	EGFR (pM)		
MerK28	26.9 ± 0.238	2.31 ± 0.0845	-	67.8	75.0
oaMerK28	30.5 ± 0.499	4.83 ± 0.205	-	56.2	74.0
MerK28-7D9G	34.0 ± 0.271	n.d.	155 ± 68.3	90.1	75.0
KiH MerK28-7D9G	34.7 ± 0.307	n.d.	389 ± 22.0	154.0	76.0

2.2. Generation and Characterisation of Bispecific MerTK/EGFR Variants

After characterisation of the monovalent anti-MerTK antibody MerK28 and its one-armed counterpart oaMerK28, bispecific antibodies were generated by fusing tandem, biparatopic VHHs targeting EGFR (termed 7D9G), which were previously described elsewhere [37]. Two different architectures were chosen; one with the bivalent MerK28 antibody and a C-terminal fusion of 7D9G (hereafter termed MerK28-7D9G), and a bispecific with a single MerTK-binding moiety and only one 7D9G using the Knob-into-Hole technology (hereafter dubbed KiH MerK28-7D9G). All molecules and their respective architectures are depicted in Figure 2a. As the KiH MerK28-7D9G variant was equivalent to the oaMerK28 in terms of MerTK binding valency, the agonistic properties of the molecule were bypassed, allowing for a simple macrophage-engager instead of -activator (Figure 2b).

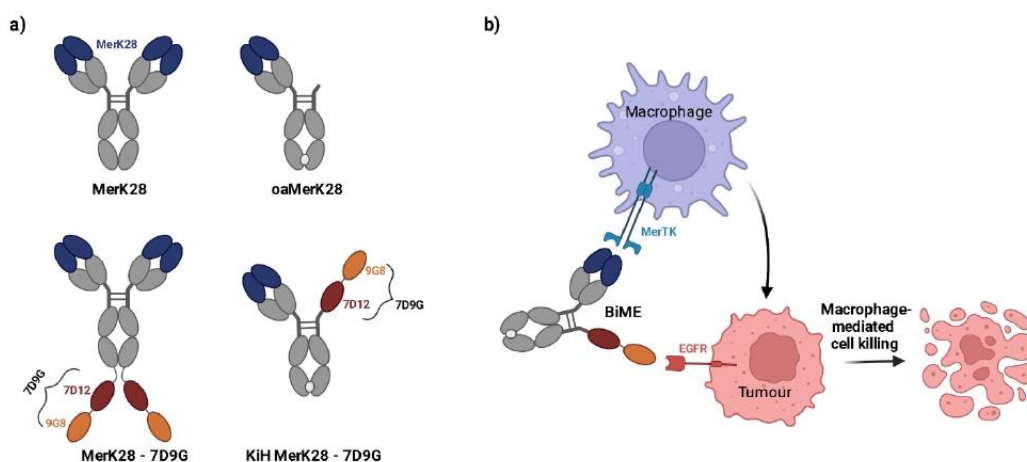


Figure 2. Bispecific MerTK/EGFR antibodies. (a) Architectures of the mono- and bispecific antibodies. VH and VL domains depicted in blue represent those for MerK28. The tandem VHHs together are termed 7D9G, with the red representing 7D12 and the orange 9G8 nanobodies. (b) Macrophage-tumour cells engagement with a bispecific macrophage engager (BiME). The blue cell represents macrophages expressing MerTK on their surface, whereas the pink cells represent tumour cells overexpressing EGFR.

After transient production in Expi293-F cells and purification either via Protein A chromatography or a His/Strep purification for MerK28-7D9G or KiH MerK28-7D9G, respectively, SDS-PAGE gel analysis revealed the expected bands under both reducing and non-reducing conditions (Figure S3). For the MerK28-7D9G variant, additional bands were noticeable under non-reducing conditions, indicating decreased stability, likely due to the addition of two tandem VHHs with significant flexibility. Yields and thermal stability were within acceptable ranges for bispecific antibodies, with surprisingly higher yields

for both bispecifics compared to the parental MerK28 clone (Table 1). Thermal stability investigation by SYPRO-Orange incorporation indicated exceptional stability with melting temperatures (T_M) between 74.0–75.0 °C (Table 1). The high global T_M s for the molecules suggest decent stability.

To ensure that the bispecific molecules could bind both targets simultaneously in the soluble form, a BLI-based assay was performed by first associating the antibodies to hMerTK and then to EGFR. As can be observed in Figure 3a, the bsAbs were able to bind both antigens. The same result was observed in the opposing order, verifying its simultaneous binding capacity (Figure S2c).

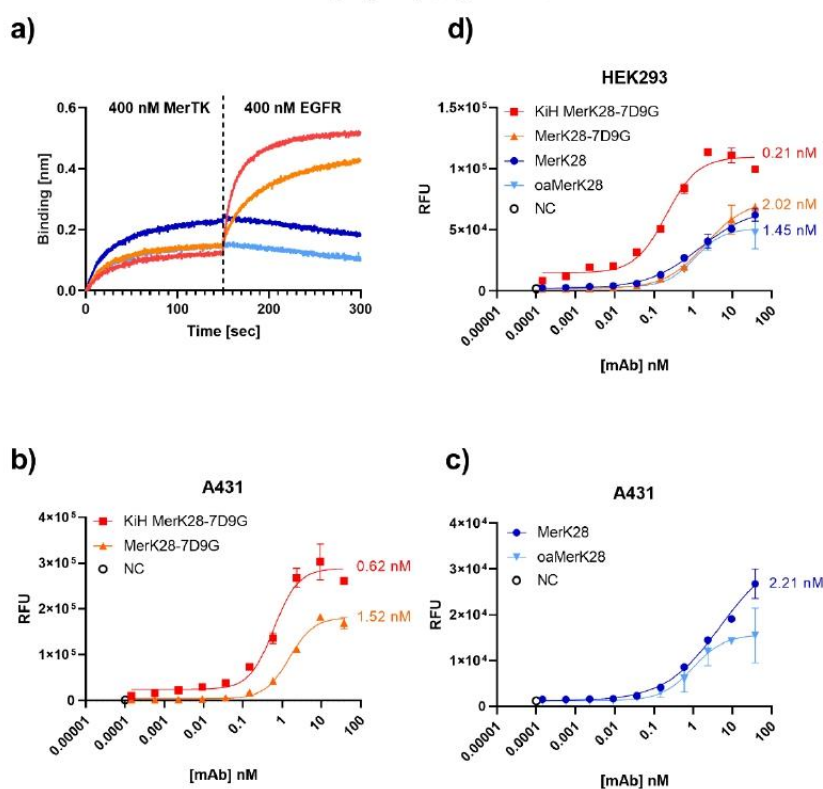


Figure 3. Bispecific MerTK/EGFR antibodies and their binding capabilities. (a) Simultaneous binding of hMerTK and EGFR via BLI. Antibodies were loaded onto AHC biosensors and then associated first to MerTK and then to EGFR for 300 s. The colour-coding is the same as represented in the legend for (d). Cell titration on (b,c) A431 and (d) HEK293 cell lines by staining the antibodies with anti-human Fc PE and plotting the relative fluorescence units (RFU) versus the antibody concentration. The negative controls incubated only with secondary antibodies are shown as “NC”. Error bars represent biological duplicates.

To determine an on-cell affinity, A431 and HEK293 cells were titrated. On A431 cells, which are EGFR⁺⁺⁺/MerTK⁺, 620 pM and 1.52 nM on-cell binding affinities were determined for KiH MerK28-7D9G and MerK28-7D9G, respectively (Figure 3b). MerK28 had an on-cell affinity of 2.21 nM, even though the fold induction was significantly lower, as no EGFR binding was possible (Figure 3c). While HEK293 cells are also EGFR⁺, the lower expression compared to A431 cells was a more realistic model. The on-cell affinities on HEK293 cells remained in a similar range, with 0.21 nM and 2.02 nM for KiH MerK28-7D9G and MerK28-7D9G, respectively, and 1.45 nM for MerK28 (Figure 3d). The on-cell affinity was unexpectedly higher for the KiH bispecific compared to MerK28-7D9G, as the latter

should have been able to bind both MerTK and EGFR more effectively due to having two and four binding moieties, respectively. An explanation for this could be the intermittent molecule flexibility not providing any advantage in this precise architecture compared to the KiH variant. Nevertheless, on-cell affinity in the single-digit to low nanomolar range was determined for the EGFRxMerTK bispecifics. Unspecific binding to other cell-surface proteins by the parental MerK28 antibody was ruled out by staining MerTK⁺ ExpiCHO cells (Figure S2d). For verification, affinity was determined by BLI for soluble EGFR and hMerTK (Figure S4, Table 1). Both bsAbs exhibited picomolar affinities towards EGFR and very similar K_D s for hMerTK, comparable to the parental MerK28.

2.3. Influence of Bispecifics on EGFR Signalling Cascade

With the promising biophysical properties of the bispecific molecules, their ability to inhibit the EGF/EGFR signalling cascade was examined. An EGF competition assay was first performed via BLI by incubating EGFR with an excess of EGF and observing the ability of the antibodies to bind to the complex. For both KiH MerK28-7D9G and MerK28-7D9G, binding to EGF-competing epitopes could be observed (Figure 4a,b), suggesting that it could inhibit the EGF-mediated signalling transduction cascade of EGFR. The binding of the biparatopic VHH 7D9G to EGFR was mapped by using EGFR mutants displayed on yeast cells, as previously described [38]. By measuring the binding of KiH MerK28-7DG to the different YSD-displayed fragments by flow cytometry, binding to EGFR could be allocated to domain III, one of the EGF-binding domains on the receptor [39], confirming previous results [37] (Figure S5).

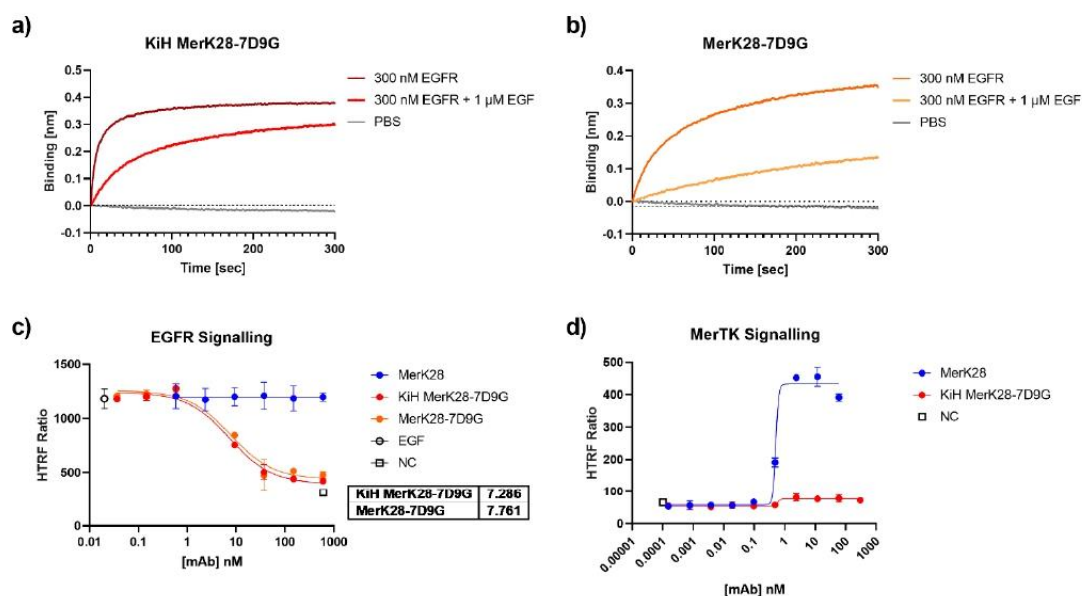


Figure 4. EGF competition and inhibition through 7D9G. EGF competition assay via BLI for (a) KiH MerK28-7D9G and (b) MerK28-7D9G. Antibodies were loaded onto AHC biosensors and either associated to 300 nM EGFR (dark red or orange), 300 nM EGF pre-incubated with 1 μM EGF (lighter red and orange), or only PBS (grey). (c) HTRF pAKT of A549 cells stimulated with 20 ng/mL EGF after pre-incubation with the indicated antibodies and respective concentrations. Negative control (NC) represents unstimulated cells, while EGF control shows maximum activation of pAKT. (d) Investigation of MerTK signalling pathway on HEK293 cells after 30 min incubation with either parental MerK28 (blue) or KiH MerK28-7D9G (red). Error bars represent the standard deviation of biological duplicates.

To verify these results in a cellular setting, A549 cells were pre-incubated with varying concentrations of antibodies for 1 h and subsequently stimulated with EGF for 10 min. Analysis of pAKT by HTRF resulted in IC₅₀ values of 7.29 and 7.76 nM for KiH MerK28-7D9G and MerK28-7D9G, respectively (Figure 4c). Further, as the KiH bispecific variant should be equivalent to the one-armed MerK28 (oaMerK28) variant concerning its ability to activate the MerTK signalling pathway, or rather lack thereof, HEK293 cells were incubated with the bsAbs and downstream signalling by pAKT activation was measured. While the parental mAb MerK28 resulted in strong activation, the bispecific KiH MerK28-7D9G did not (Figure 4d). Thus, this construct could be used as a macrophage-engager without activating MerTK signalling.

2.4. Differentiation of THP-1 Cells from Monocytic (M0) to Macrophage-like (M0) State

To assess the phagocytic capabilities of macrophages, the THP-1 cell line first had to be differentiated into a macrophage-like state, hereafter termed M0, through the addition of phorbol 12-myristate-13-acetate (PMA). Cells were incubated with 20 ng/mL PMA for 24 h and specific markers were subsequently measured to ensure the successful differentiation of THP-1 cells into an M0 macrophage-like state. Initial gene expression data revealed over 15-fold and nearly 300-fold relative mRNA increase in *Itgam* (*Cd11b*) and *Il-1b* after 24 h PMA incubation (Figure S6a) and the expected change in morphology was observed (Figure S6b). To confirm the gene expression data, THP-1 cells were stained with anti-CD11b or anti-CD14 antibodies. Both markers showed a significant increase after PMA differentiation, with a 40-fold increase in cell-surface CD11b, and a nearly 4-fold increase in CD14 levels compared to M0 THP-1s (Figure S6c,d). More importantly, members of the TAMR family were also analysed by gene expression, resulting in a significant increase in *MerTK*, as well as *Axl* (Figure S6e). Nevertheless, only a very modest increase in mRNA levels was observed for *Axl* compared to *MerTK*, which is in line with MerTK playing a more significant role on macrophages compared to its other TAMR members. Further, increased levels of *Cd274* (*Pd-1*) were also observed (Figure S6e). The increase in *MerTK* mRNA levels was also corroborated by measuring the cell-surface levels by flow cytometry (Figure S6f). The significant increase at both gene and protein levels of such M0 markers and the very evident change in morphology confirmed the macrophage-like state of M0 PMA-primed THP-1 cells.

2.5. M1- and M2-Polarised Macrophage-like Characteristics of THP-1 Cells

While THP-1 cells do not represent the complexity of human monocyte-derived macrophages, they are widely used as a model system for in vitro studies. To this end, macrophage-like M0 THP-1 cells were further differentiated by external stimuli to an M1-like or M2-like differentiation state by the addition of lipopolysaccharide (LPS) or IL-4 and IL-13, respectively. Characterisation of M1-differentiated cells was performed by measuring *Il-6*, *Il-1β*, and *Tnfα* mRNA levels (Figure 5a). Compared to the M0 control, significant upregulation was observed for all three genes upon incubating THP-1 cells with LPS, but not with IL-4 and IL-13 as expected. Secretion of cytokines (IL-6 and TNFα) was determined by ELISA and were in line with the gene expression data (Figure 5b). For IL-6, an M1-specific increase was noted, whereas TNFα secretion was already increased after PMA incubation (M0), which was then increased further upon LPS treatment (Figure 5b).

As MerTK is involved in M2-differentiated macrophages, M0 THP-1 cells were differentiated to investigate its phagocytic capabilities. To this end, M0 THP-1 cells were incubated with either PMA (M0) or PMA with IL-4 and IL-13 simultaneously (designated M2). M2 markers were investigated by comparing M0 and M2 macrophage-like THP-1 cells after 24 and 48 h incubation. By gene expression, two important M2 markers, *Il-10*, and *Ccl22*, were shown to increase upon the addition of IL-4 and IL-13 compared to only PMA incubation (Figure 5c). While only a modest increase was shown after 24 h, the relative normalised mRNA expression was drastically increased after 48 h incubation, with

a 12-fold and a 450-fold increase for *Il-10* and *Ccl22*, respectively, relative to the 24 h M0 control (Figure 5c).

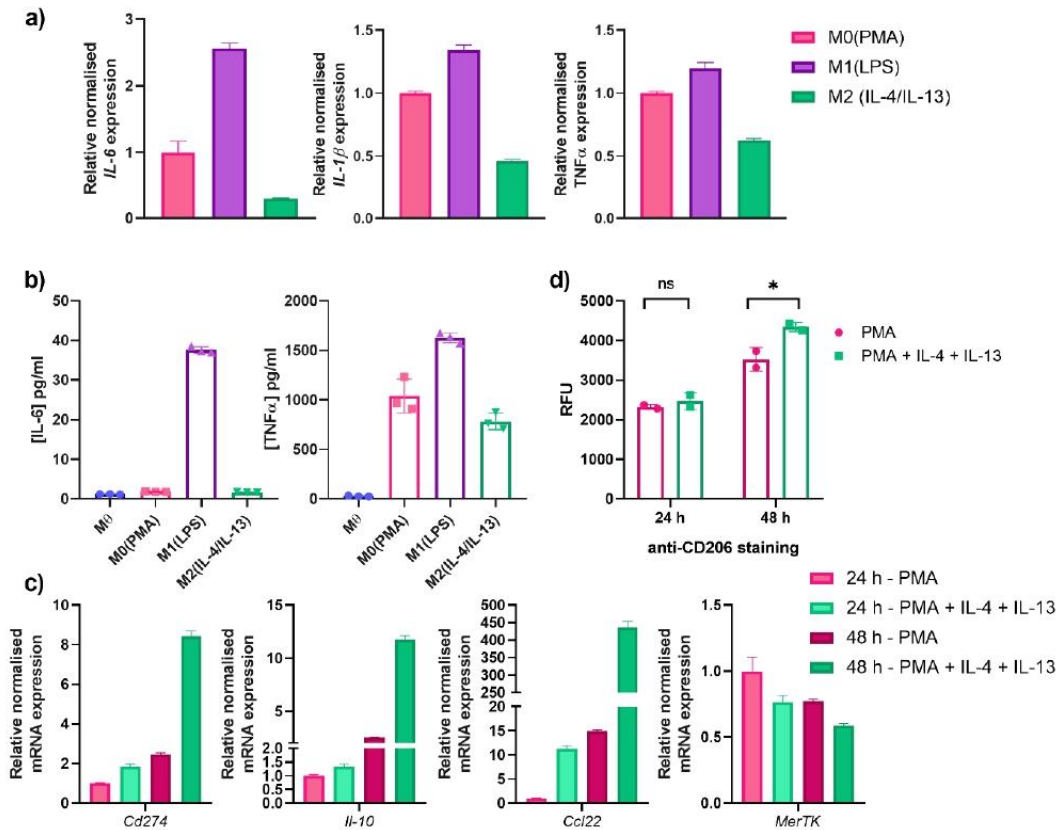


Figure 5. Differentiation of macrophage-like THP-1 cells to M1- and M2-state. (a) Gene expression analysis of THP-1 cells differentiation with PMA (M0—pink), LPS (M1—violet) or IL-4/IL-13 (M2—teal) for 24 h. The data are normalised to housekeeping genes and set relative to the M0(PMA) control. (b) Secretion of IL-6 and TNF α in cell culture supernatants as determined by ELISA. (c) Gene expression analysis of PMA- (M0—pink shades) and PMA/IL-4/IL-13-incubated cells (M2—greens shades) after either 24 h (lighter colours) or 48 h (darker shades) incubation. Analysis was performed by normalising the data to housekeeping genes and setting the values relative to the M0 24 h control. (d) CD206-cell surface staining of differentiated cells by flow cytometry. After differentiation, THP-1 cells were stained with anti-CD206 PE-conjugate and measured by flow cytometry. The mean relative fluorescence units (RFU) were determined and plotted for each individual duplicate. One-way ANOVA analysis performed using GraphPad Prism: ns: non-significant, * p value < 0.05.

In the peculiar case of *MerTK* levels, an unexpected, modest decrease was observed compared to the 24 h M0 control (Figure 5c). While this was not particularly expected, as literature reports upregulation of *MerTK* in an M2-state, an explanation for this could be the increase in metalloproteinases, such as a disintegrin and metalloproteinase 17 (ADAM17), which is known to cause *MerTK* shedding and could thus have an influence on its expression levels [40]. Furthermore, the time-dependent decrease in the PMA M0 control from 24 to 48 h also substantiates this supposition. RT-qPCR revealed an 8-fold increase in relative *Cd274* mRNA levels—another marker of *MerTK*-dependent M2 differentiation—after 48 h incubation with IL-4 and IL-13 compared to the 24 h M0 control (Figure 5c). A further important M2-specific marker is CD206, which is known to not be expressed on

M1 macrophages [41]. Staining of differentiated THP-1 cells with an anti-CD206 antibody revealed no significant difference between PMA- (M0) and PMA/IL-4/IL-13 (M2)-differentiated THP-1 cells after 24 h incubation (Figure 5d). Nonetheless, a longer incubation time of 48 h revealed a statistically significant increase in CD206 surface levels in M2-differentiated macrophage-like cells (Figure 5d). The increase in M1- and M2-specific markers confirmed the successful THP-1 differentiation to the respective macrophage-like states.

2.6. Phagocytosis of Anti-MerTK Parental Antibodies and Anti-MerTK/EGFR Bispecifics

The simultaneous binding of macrophages and tumour cells is crucial for a macrophage-engaging bispecific antibody. To test this in a cellular context, THP-1 cells were pre-incubated with the respective antibodies and then stained with a PE-conjugated secondary antibody. Calcein-AM-stained A431 cells were added to the stained THP-1 cells and simultaneous MerTK-binding on THP-1 and EGFR-binding on A431 cells was measured using a flow cytometer. The MerK28 and oaMerK28 antibodies only displayed THP-1 binding in both monoculture and co-culture with A431 cells (Figure 6a,b). The quantification of their binding compared to the negative control resulted in 80% and 35% binding for MerK28 and oaMerK28, respectively, which corroborates with their MerTK-binding valency (Figure 6a,b). After co-incubation of pre-stained THP-1 cells and Calcein-AM-stained A431 cells, double positive events were only observed for the bispecific molecules (Figure 6a,b), as they are capable of binding both cell types. The quantitation of THP-1-only binding resulted in similar frequencies compared to the respective monospecific control (MerK28 for MerK28-7D9G, or oaMerK28 for KiH MerK28-7D9G). As MerK28-7D9G has two sets of tandem VHHs fused C-terminally, its EGFR-binding resulted in a higher engagement compared to the KiH variant (Figure 6b).

Furthermore, the ability of targeted phagocytosis with pre-characterised THP-1 macrophage-like states (M0, M1, or M2) was tested via flow cytometric analysis after co-incubation of the differentiated THP-1 cells with the respective antibody variants and Calcein-AM red—orange stained A431 cells. The entire complex after co-incubation was stained with an anti-CD14-FITC conjugated antibody to be able to gate the THP-1 cells. For both M0 and M1-like THP-1 cells, treatment with the bispecific antibodies led to a significant increase in double-positive events (Figures 6c, S7 and S8). In the case of M2 macrophages, the cell-surface CD14 levels were very low, and thus no significant differences were observed. These double-positive events were gated further to determine the phagocytosis rate, as exemplified in Figure S9 for M1-like macrophages.

Quantitation of phagocytosis resulted in a significant increase for all differentiation states with both bispecific variants compared to the negative control, and non-significant changes upon incubation of the cells with MerTK-binding antibodies only (Figure 6d). In the case of M2-differentiated THP-1 cells, higher basal phagocytosis was observed, and moderate differences were noted with the bsAbs (Figure 6d). Thus, targeted phagocytosis with EGFR⁺ tumour cells was seen for all macrophage-like states in vitro.

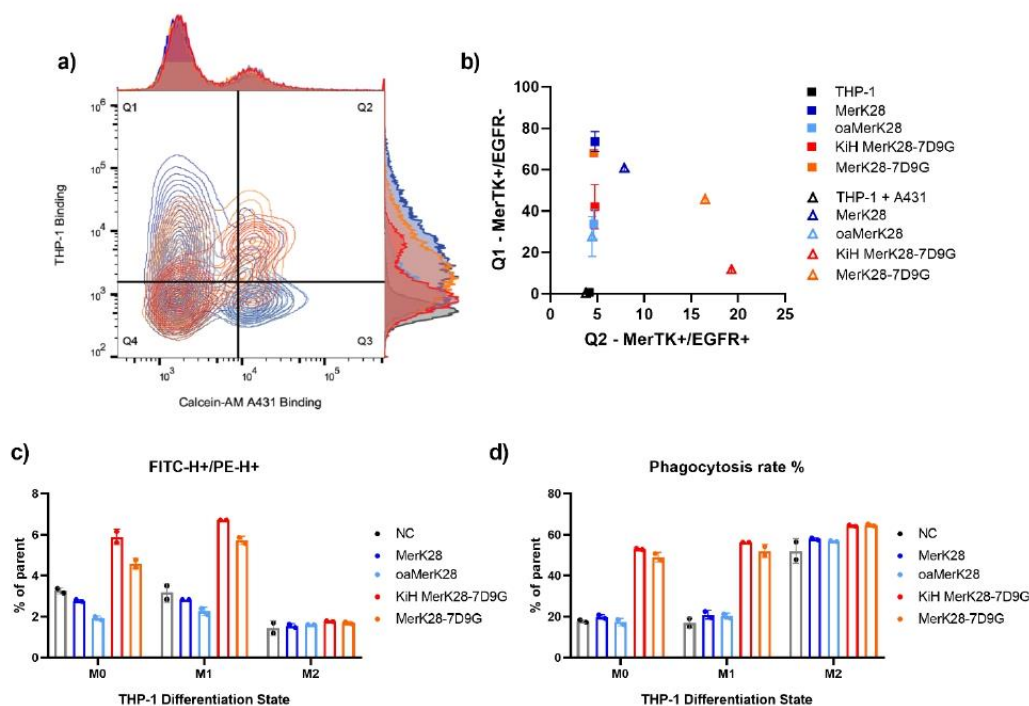


Figure 6. Macrophage-engagement and phagocytosis of tumour cells. (a) Contour plots of A431 binding on the x-axis (FITC fluorescence) and THP-1 binding on the y-axis (PE fluorescence) following the colour-coding of (b). Double-positive events in the upper-right Q2 quadrant show simultaneous engagement of THP-1 and A431 cells, whereas the upper-left Q1 quadrant represents MerTK-binding only. (b) Frequency of parent of Q1 and Q2 from (a). Coloured squares represent incubation of antibodies only on THP-1 cells, whereas the triangles represent co-incubation of pre-stained THP-1 cells and Calcein-AM-stained A431 cells. (c) Quantitation of CD14⁺ THP-1 cells and Calcein-AM red—orange stained A431 cells for phagocytosis assays. The negative control (NC) represents co-incubation of both cell types without antibody treatment. (d) Determination of phagocytosis rate (%) after co-incubation of THP-1 cells in different differentiation states together with A431 cells. Error bars represent the standard deviation of at least biological duplicates.

3. Discussion

In this proof-of-concept study, bispecific macrophage-engaging antibodies were generated by combining MerTK-binding Fabs with tandem, biparatopic EGFR-targeting VHHs in different architectures. Contrary to MerK17, MerK28 exhibited cross-specific binding to human and murine MerTK, and was thus considered further. The parental MerTK clone, MerK28, exhibited agonistic properties in the bivalent form, losing its ability to activate MerTK-dependent signalling transduction when a one-armed variant was generated. Thus, the two bispecific antibodies had either mono- or bivalent MerTK binding to mediate the activation of MerTK. As activation of MerTK is said to lead to an immunosuppressive environment, the KiH MerK28-7D9G variant would be a more suitable fit for immunotherapy, as its capacity to activate pAKT through MerTK signalling was abolished. Further, no robust advantages for bivalent MerTK-binding were observed throughout this study when comparing both bispecific molecules. Due to the flexible nature of VHHs, and especially tandem VHHs, it may not be suitable to combine a total of four VHHs to the C-terminus of the Fc fragment, as the resulting molecule could have very flexible termini and could therefore be relatively unstable.

Characterisation of the 7D9G tandem VHHs resulted in picomolar affinity to EGFR as reported previously [37], inhibition of EGF binding to its receptor, and inhibition of EGF-mediated signal transduction through pAKT. The binding of 7D9G was mapped to domain III of the extracellular EGFR, which is involved in EGF binding [39], confirming its mechanism of action. By combining a potent EGFR binder with a medium-affine MerTK binder, the bispecific molecules will be more likely to reach the tumour microenvironment, where MerTK binding can take place to bridge tumour-associated and tumour-infiltrating macrophages with tumour cells and lead to phagocytosis in a targeted manner. In this context, no MerTK activation is required, and might even lead to counterproductive repercussions, as previously reported by Waterborg and colleagues [42]. For M0-like and M1-like THP-1 cells, targeted engagement and phagocytosis were observed with the bispecific antibodies after co-incubation with epidermoid carcinoma cells overexpressing EGFR. On the other hand, M2-differentiated THP-1 cells resulted in higher basal phagocytosis, as expected. Differences in phagocytosis with the bsAbs compared to the parental mAb were observed, however they were not as large as in the other differentiation states. An explanation for this could be the protease-mediated cleavage of MerTK, compromising the ability of the antibodies to bind to the THP-1 cells.

Proteolytic cleavage via ADAM17 results in soluble forms of MerTK that compete with surface-bound MerTK and inhibits efferocytosis [43]. A possible advantage of a bispecific antibody with bivalent agonism to MerTK might be in the recruitment of soluble MerTK after ADAM17 cleavage and shedding to restore TAMR-dependent efferocytosis; however, this requires further investigation. Further experiments with macrophages in conjunction with an appropriate mouse model will reveal the potential of bispecific MerTK×EGFR antibodies for cancer immunotherapy. Additionally, a thorough analysis of the role of these bispecific molecules and their activation of the MerTK pathway in the clearance of apoptotic cells should be performed, as the clearance of apoptotic cells within the TME is largely hindered by chronic inflammation. Effective clearance of ACs may have the potential to ameliorate the immunosuppressive environment and thus reduce anti-inflammatory effects from non-efficiently cleared ACs. Furthermore, combination therapy or the addition of PD-L1-binding moieties to the bispecific antibodies generated herein could enhance tumour cell-killing and avoid the upregulation of PD-L1 by MerTK in a potentially immunosuppressed TME. Taken together, harnessing MerTK expression on tumour-infiltrating macrophages via bispecific antibodies binding to tumour-specific markers might pave the way for interesting therapeutic strategies resulting in the targeted phagocytosis of tumour cells.

4. Materials and Methods

4.1. Cell Culture

The following cell lines were purchased from DSMZ (Brunswick, Germany): human epidermoid carcinoma A431 (ACC 91), human embryonic kidney HEK293 (ACC 305), human lung carcinoma A549 (ACC 107), and human acute monocytic leukaemia THP-1 (ACC 16). Cell maintenance and production of soluble proteins were performed as previously described [44,45]. The cancer cell lines were chosen based on their EGFR overexpression in the case of A431 and A549, and the endogenous expression of MerTK on HEK293 cells.

Monocytic THP-1 cells (M0) were differentiated into macrophage-like cells (M0) by incubating with 20 ng/mL phorbol 13-myristate 13-acetate (PMA, Sigma Aldrich, Taufkirchen, Germany) for 24 or 48 h. Afterwards, the medium was exchanged and the M0 THP-1 cells were incubated in growth medium or differentiated further. Differentiation into an M1-like state was achieved by incubating with 250 ng/mL lipopolysaccharides (LPS) for 24 h. For an M2-like state, THP-1 cells were differentiated with 20 ng/mL PMA, 20 ng/mL IL-4 and 20 ng/mL IL-13 for 48 h.

4.2. Gene Expression Analysis for THP-1 Differentiation

RNA isolation was performed after lysis of cells using the RNeasy Mini Kit (QIAGEN, Hilden, Germany). Pure RNA was ensured by determining the concentration and ensuring an absorbance ratio ($A_{260/280}$) of 2.0. For RT-qPCR, iTaq Universal SYBR Green One-Step kit (Bio-Rad, Feldkirchen, Germany) was used, primers for *Gapdh*, *Hprt1*, *MerTK*, and *Axl* were ordered from IDT (Coralville, IA, USA), while the rest were ordered from Sigma Aldrich (Sequences in Table S1). RT-qPCR and subsequent gene expression analysis were performed using a CFX Connect instrument (Bio-Rad) with the integrated CFX Manager software. Normalised relative mRNA expression was determined by normalising the data to the housekeeping genes (*Gapdh* and *Hprt1*) and setting gene expression relative to the M0 THP-1 sample.

4.3. Cloning and Production of Antibodies

The generation of anti-MerTK antibody clone MerK28 was described previously [36]. For the generation of bispecific antibodies, two tandem, biparatopic VHHs (termed 7D9G) binding EGFR were chosen [37]. Cloning of the bispecific variants was performed using Golden Gate Cloning. Primers with *SapI* overhangs were designed and ordered at Sigma Aldrich. For MerK28-7D9G, 7D9G was added to the C-terminus of the Fc region. For the KiH MerK28-7D9G, the MerK28 VH region was re-cloned into a plasmid containing a CH1 domain and a Knob-mutated Fc fragment, and the 7D9G was added to a Hole-mutated Fc fragment (lacking a CH1 region and containing a partial hinge). The knob-into-hole (KiH) technology was used to ensure heterodimerisation of the Fc fragments. Cloning was performed using Q5 DNA Polymerase (New England Biolabs, Frankfurt am Main, Germany), and Golden Gate cloning was performed with *SapI* restriction enzyme (New England Biolabs).

For production and purification of the antibodies, Expi293-F cells were transfected as described above. Five days post-transfection, the cells were harvested by centrifugation and the supernatant was sterile-filtered. MerK28 and MerK28-7D9G were subsequently purified using Protein A chromatography followed by a desalting step into PBS. The one-armed MerK28 (oaMerK28) and the KiH bispecific variant were purified by a two-step purification through His₆- and StrepII-tags to ensure heterodimers, as previously described [45].

4.4. Affinity Determination, EGF Competition and Epitope Binning with Biolayer Interferometry (BLI)

For affinity determination, 10 µg/mL of the respective antibody was loaded onto anti-human Fc capture biosensors (AHC, Sartorius, Göttingen, Germany) until a threshold of 0.8 nm was reached. Different antigen concentrations were associated to the antibodies for 300 s, followed by a dissociation step for 300 s in Kinetics Buffer (KB). For soluble human MerTK and EGFR, a range of 200 nM–0 nM was measured using in-house produced antigens (hMerTK-TS, His-EGFR-TS). Murine MerTK as an Fc-fusion was used in a concentration range of 300–0 nM for MerK28.

EGF competition, epitope binning, and simultaneous binding assays were performed as previously described [45]. In brief, EGF competition was performed by pre-incubating 300 nM His-EGFR-TS (in-house produced) with 1 µM EGF and associating the loaded antibodies for 300 s. Similarly, Pros1 competition was performed with 500 nM hMerTK-TS (produced in-house) and equimolar amounts of Pros1 (R&D Systems, Wiesbaden, Germany). Epitope binning was performed by loading hMerTK-His₆ onto anti-HIS1K biosensors (Sartorius, Göttingen, Germany). MerK28 was first associated to hMerTK for 600 s, followed by associating to MerK17 or PBS afterwards. Lastly, simultaneous binding was performed by loading antibodies onto AHC biosensors, and similarly to the epitope binning, sequentially associating to different antigens.

4.5. Phospho AKT Signalling Assays

To investigate either MerTK- or EGFR-signal transduction pathways, 50,000 or 200,000 cells/well were seeded onto either 96-well or 24-well plates for HTRF and Western blot analysis, respectively, in complete growth medium, and incubated at 37 °C in 5% CO₂ until cells became adherent. Thereafter, cells were serum-starved for 12–18 h in growth medium deprived of FBS. For MerTK activation, serum-starved cells were incubated with the indicated antibodies for 30 min. For EGFR-signalling, the cells were pre-treated with antibodies for 1 h and subsequently stimulated with 20 ng/mL EGF for 10 min. After stimulation, the cells were lysed in either 30 or 80 µL/well lysis buffer for 96- and 24-well plates, respectively. The lysis buffer for subsequent western blot analysis was composed of 1x Tris MSD lysis buffer supplemented with 1x PhosSTOP (Roche, Basel, Switzerland) and 1x Halt Protease and Phosphatase Inhibitor cocktail (ThermoFisher Scientific, Erlangen, Germany). For the phospho AKT HTRF kit (64AKSPEG, Cisbio/Perkin Elmer, Codolet, France), the lysis buffer was prepared according to the manufacturer's instructions.

Western blot analysis was performed by loading 15 µL sample onto a 4%–15% Mini-PROTEAN TGX precast gel (Bio-Rad) in reducing Laemmli buffer. After separation by SDS PAGE, the Trans-Blot Turbo Transfer System (Bio-Rad) was used to transfer the proteins onto a nitrocellulose membrane. The membranes were initially blocked in TBS-T (TBS containing 0.1% Tween-20) with 5% bovine serum albumin (BSA) for 1 h at RT. After 3 wash steps with TBS-T, the membranes were incubated with primary antibody diluted in TBS-T for 1 h. Washing was repeated three times and incubated with AP-conjugated secondary antibody in TBS-T for a further hour. After the final washing steps, 5 mL 1-step NBT/BCIP substrate solution (ThermoFisher Scientific) was added per membrane and incubated until colour was developed. In order to stop the reaction, the membranes were washed thoroughly with water. Antibodies used: phospho AKT (Ser473) (#4060, Cell Signaling Technology, Frankfurt am Main, Germany), total AKT (#9272, Cell Signaling Technology).

4.6. Cell Titration, Macrophage Markers and Simultaneous Binding by Flow Cytometry

To determine an on-cell EC₅₀, target cells were washed with ice-cold PBS-F (PBS containing 2% FBS) and incubated with the desired antibody concentration diluted in PBS-F for 30 min on ice in a 96-well U-bottom plate. After a washing step, the pelleted cells were incubated with anti-human Fc-PE conjugated antibody (1:80 dilution, ThermoFisher Scientific) for 15 min on ice. Washing with ice-cold PBS-F was performed three times before measuring on a CytoFlex S (Beckman Coulter, Krefeld, Germany) flow cytometer. Cells stained only with secondary antibody were used as a negative control and in order to adjust the parameters. As a negative cell line, ExpiCHO-S (ThermoFisher Scientific) were stained in the same way.

Simultaneous binding of M0 THP-1 cells and the A431 tumour cells was performed by pre-incubating THP-1 cells with the desired antibody concentration and stained with anti-human Fc-PE as described above. A431 cells were stained with 1 µM Calcein-AM according to the manufacturer's protocol and subsequently co-incubated with pre-stained THP-1 cells. After 30 min, duplets were analysed by flow cytometry.

Cell surface expression of macrophage markers were measured by flow cytometry using the same procedure as above. Antibodies used: mouse anti-human CD11b-PE (#12-0118-42, ThermoFisher Scientific), mouse anti-human CD14-FITC (#11-0149-42, ThermoFisher Scientific), and mouse anti-CD206 PE-conjugate (Clone 19.2, ThermoFisher Scientific). Data visualisation was performed using FlowJo v10 software (BD Biosciences, Franklin Lakes, NJ, USA) and GraphPad Prism 8.0. (San Diego, CA, USA).

4.7. Phagocytosis

To determine the rate of phagocytosis, differentiated THP-1 cells were trypsinised and washed thoroughly before incubating with the desired antibody concentration for 1 h at 37 °C. Simultaneously, target cells were trypsinised, washed, and stained with 5 µM Calcein-AM red–orange for 1 h at 37 °C. Subsequently, both cell types were mixed

in a 1:5 effector-to-target ratio and incubated further. Then, the mixture was washed three times with ice-cold PBS and stained with anti-CD14-FITC for 20 min on ice. A final wash series was performed, and then the cells were analysed via flow cytometry on a CytoFlex S cytometer. Macrophages were gated through their CD14⁺ expression, and then the number of CD14⁺/Calcein-AM red–orange events were considered as phagocytosed A431 cells by the macrophages. The rate of phagocytosis was determined by the frequency of CD14⁺/Calcein-AM red–orange⁺ as a percentage of the parent population.

Supplementary Materials: The supporting information can be downloaded at: <https://www.mdpi.com/article/10.3390/ijms232415673/s1>.

Author Contributions: Conceptualization, S.C.C.; methodology, S.C.C.; investigation, S.C.C., J.P.B. and D.F.; curation, S.C.C. and J.G.; writing—original draft preparation, S.C.C.; writing—review and editing, S.C.C., J.P.B., D.F., J.G., B.H. and H.K.; supervision, B.H. and H.K. All authors have read and agreed to the published version of the manuscript.

Funding: This research was funded by the Department of GPRD at Ferring Pharmaceuticals. We acknowledge support by the Deutsche Forschungsgemeinschaft (DFG, German Research Foundation) and the Open Access Publishing fund of Technical University of Darmstadt.

Institutional Review Board Statement: Not applicable.

Informed Consent Statement: Not applicable.

Data Availability Statement: Data are contained within the article or supplementary material.

Acknowledgments: The authors would like to acknowledge the Department of GPRD at Ferring Pharmaceuticals for funding. The funders played no part in the study design, data collection, or curation.

Conflicts of Interest: The authors declare no conflict of interest.

References

1. Lai, C.; Lemke, G. An extended family of protein-tyrosine kinase genes differentially expressed in the vertebrate nervous system. *Neuron* **1991**, *6*, 691–704. [[CrossRef](#)]
2. Myers, K.V.; Amend, S.R.; Pienta, K.J. Targeting Tyro3, Axl and MerTK (TAM receptors): Implications for macrophages in the tumor microenvironment. *Mol. Cancer* **2019**, *18*, 94. [[CrossRef](#)] [[PubMed](#)]
3. Lemke, G. Biology of the TAM Receptors. *Cold Spring Harb. Perspect Biol.* **2013**, *5*, a009076. [[CrossRef](#)] [[PubMed](#)]
4. Huang, X.; Finerty, P.; Walker, J.R.; Butler-Cole, C.; Vedadi, M.; Schapira, M.; Parker, S.A.; Turk, B.E.; Thompson, D.A.; Dhe-Paganon, S. Structural insights into the inhibited states of the Mer receptor tyrosine kinase. *J. Struct Biol.* **2009**, *165*, 88–96. [[CrossRef](#)] [[PubMed](#)]
5. Linger, R.M.A.; Keating, A.K.; Earp, H.S.; Graham, D.K. TAM Receptor Tyrosine Kinases: Biologic Functions, Signaling, and Potential Therapeutic Targeting in Human Cancer. *Adv. Cancer Res.* **2008**, *100*, 35–83. [[CrossRef](#)]
6. Manfioletti, G.; Brancolini, C.; Avanzi, G.; Schneider, C. The protein encoded by a growth arrest-specific gene (gas6) is a new member of the vitamin K-dependent proteins related to protein S, a negative coregulator in the blood coagulation cascade. *Mol. Cell Biol.* **1993**, *13*, 4976–4985. [[CrossRef](#)]
7. Stitt, T.N.; Conn, G.; Goret, M.; Lai, C.; Bruno, J.; Radzilewski, C.; Mattsson, K.; Fisher, J.; Gies, D.R.; Jones, P.F.; et al. The anticoagulation factor protein S and its relative, Gas6, are ligands for the Tyro 3/Axl family of receptor tyrosine kinases. *Cell* **1995**, *80*, 661–670. [[CrossRef](#)]
8. Davra, V.; Kimani, S.; Calianese, D.; Birge, R. Ligand Activation of TAM Family Receptors-Implications for Tumor Biology and Therapeutic Response. *Cancers* **2016**, *8*, 107. [[CrossRef](#)]
9. Vergadi, E.; Ieronymaki, E.; Lyroni, K.; Vaporidi, K.; Tsatsanis, C. Akt Signaling Pathway in Macrophage Activation and M1/M2 Polarization. *J. Immunol.* **2017**, *198*, 1006–1014. [[CrossRef](#)]
10. Cummings, C.T.; DeRyckere, D.; Earp, H.S.; Graham, D.K. Molecular Pathways: MERTK Signaling in Cancer. *Clin. Cancer Res.* **2013**, *19*, 5275–5280. [[CrossRef](#)]
11. Gregory, C.D.; Devitt, A. The macrophage and the apoptotic cell: An innate immune interaction viewed simplistically? *Immunology* **2004**, *113*, 1–14. [[CrossRef](#)]
12. Zizzo, G.; Hilliard, B.A.; Monestier, M.; Cohen, P.L. Efficient Clearance of Early Apoptotic Cells by Human Macrophages Requires M2c Polarization and MerTK Induction. *J. Immunol.* **2012**, *189*, 3508–3520. [[CrossRef](#)] [[PubMed](#)]
13. Scott, R.S.; McMahon, E.J.; Pop, S.M.; Reap, E.A.; Caricchio, R.; Cohen, P.L.; Earp, H.S.; Matsushima, G.K. Phagocytosis and clearance of apoptotic cells is mediated by MER. *Nature* **2001**, *411*, 207–211. [[CrossRef](#)] [[PubMed](#)]

14. Rothlin, C.v.; Carrera-Silva, E.A.; Bosurgi, L.; Ghosh, S. TAM Receptor Signaling in Immune Homeostasis. *Annu. Rev. Immunol.* **2015**, *33*, 355–391. [CrossRef] [PubMed]
15. Lemke, G.; Burstyn-Cohen, T. TAM receptors and the clearance of apoptotic cells. *Ann. N. Y. Acad. Sci.* **2010**, *1209*, 23–29. [CrossRef]
16. Huelse, J.M.; Fridlyand, D.M.; Earp, S.; DeRyckere, D.; Graham, D.K. MERTK in cancer therapy: Targeting the receptor tyrosine kinase in tumor cells and the immune system. *Pharm. Ther.* **2020**, *213*, 107577. [CrossRef]
17. Troidl, C.; Möllmann, H.; Nef, H.; Masseli, F.; Voss, S.; Szardien, S.; Willmer, M.; Rolf, A.; Rixe, J.; Troidl, K.; et al. Classically and alternatively activated macrophages contribute to tissue remodelling after myocardial infarction. *J. Cell Mol. Med.* **2009**, *13*, 3485–3496. [CrossRef] [PubMed]
18. Grabiec, A.M.; Goenka, A.; Fife, M.E.; Fujimori, T.; Hussell, T. Axl and MerTK receptor tyrosine kinases maintain human macrophage efferocytic capacity in the presence of viral triggers. *Eur. J. Immunol.* **2018**, *48*, 855–860. [CrossRef]
19. Tsou, W.-I.; Nguyen, K.-Q.N.; Calarese, D.A.; Garforth, S.J.; Antes, A.L.; Smirnov, S.V.; Almo, S.C.; Birge, R.B.; Kotenko, S.V. Receptor Tyrosine Kinases, TYRO3, AXL, and MER, Demonstrate Distinct Patterns and Complex Regulation of Ligand-induced Activation. *J. Biol. Chem.* **2014**, *289*, 25750–25763. [CrossRef]
20. Lu, Q.; Lemke, G. Homeostatic Regulation of the Immune System by Receptor Tyrosine Kinases of the Tyro 3 Family. *Science* **2001**, *293*, 306–311. [CrossRef]
21. Graham, D.K.; DeRyckere, D.; Davies, K.D.; Earp, H.S. The TAM family: Phosphatidylserine-sensing receptor tyrosine kinases gone awry in cancer. *Nat. Rev. Cancer* **2014**, *14*, 769–785. [CrossRef] [PubMed]
22. White, K.F.; Rausch, M.; Hua, J.; Walsh, K.H.; Miller, C.E.; Wells, C.C.; Moodley, D.; Lee, B.H.; Chappel, S.C.; Holland, P.M.; et al. Abstract 558: MERTK-specific antibodies that have therapeutic antitumor activity in mice disrupt the integrity of the retinal pigmented epithelium in cynomolgus monkeys. *Cancer Res.* **2019**, *79*, 558. [CrossRef]
23. Caetano, M.S.; Younes, A.I.; Barsoumian, H.B.; Quigley, M.; Menon, H.; Gao, C.; Spires, T.; Reilly, T.P.; Cadena, A.P.; Cushman, T.R.; et al. Triple Therapy with MerTK and PD1 Inhibition Plus Radiotherapy Promotes Abscopal Antitumor Immune Responses. *Clin. Cancer Res.* **2019**, *25*, 7576–7584. [CrossRef] [PubMed]
24. Kasikara, C.; Davra, V.; Calianese, D.; Geng, K.; Spires, T.E.; Quigley, M.; Wichroski, M.; Sriram, G.; Suarez-Lopez, L.; Yaffe, M.B.; et al. Pan-TAM Tyrosine Kinase Inhibitor BMS-777607 Enhances Anti-PD-1 mAb Efficacy in a Murine Model of Triple-Negative Breast Cancer. *Cancer Res.* **2019**, *79*, 2669–2683. [CrossRef]
25. Kimani, S.G.; Kumar, S.; Bansal, N.; Singh, K.; Kholodovych, V.; Comollo, T.; Peng, Y.; Kotenko, S.V.; Sarafianos, S.G.; Bertino, J.R.; et al. Small molecule inhibitors block Gas6-inducible TAM activation and tumorigenicity. *Sci. Rep.* **2017**, *7*, 43908. [CrossRef]
26. Branchford, B.R.; Stalker, T.J.; Law, L.; Acevedo, G.; Sather, S.; Brzezinski, C.; Wilson, K.M.; Minson, K.; Lee-Sherick, A.B.; Davison-Castillo, P.; et al. The small-molecule MERTK inhibitor UNC2025 decreases platelet activation and prevents thrombosis. *J. Thromb. Haemost.* **2018**, *16*, 352–363. [CrossRef] [PubMed]
27. Cummings, C.T.; Zhang, W.; Davies, K.D.; Kirkpatrick, G.D.; Zhang, D.; DeRyckere, D.; Wang, X.; Frye, S.V.; Earp, H.S.; Graham, D.K. Small Molecule Inhibition of MERTK Is Efficacious in Non-Small Cell Lung Cancer Models Independent of Driver Oncogene Status. *Mol. Cancer* **2015**, *14*, 2014–2022. [CrossRef] [PubMed]
28. Bosurgi, L.; Bermink, J.H.; Cuevas, V.D.; Gagliani, N.; Joannas, L.; Schmid, E.T.; Booth, C.J.; Ghosh, S.; Rothlin, C.V. Paradoxical role of the proto-oncogene Axl and Mer receptor tyrosine kinases in colon cancer. *Proc. Natl. Acad. Sci. USA* **2013**, *110*, 13091–13096. [CrossRef] [PubMed]
29. Zhou, Y.; Wang, Y.; Chen, H.; Xu, Y.; Luo, Y.; Deng, Y.; Zhang, J.; Shao, A. Immuno-oncology: Are TAM receptors in glioblastoma friends or foes? *Cell Commun. Signal.* **2021**, *19*, 11. [CrossRef]
30. Png, K.J.; Halberg, N.; Yoshida, M.; Tavazoie, S.F. A microRNA regulon that mediates endothelial recruitment and metastasis by cancer cells. *Nature* **2012**, *481*, 190–194. [CrossRef]
31. Elpiscience Biopharma. Pipeline-ES028. Available online: <https://www.elpiscience.com/pipeline/125.html> (accessed on 8 September 2022).
32. Yang, Y.; Yang, Z.; Yang, Y. Potential Role of CD47-Directed Bispecific Antibodies in Cancer Immunotherapy. *Front. Immunol.* **2021**, *12*, 2773. [CrossRef]
33. Yarden, Y.; Pines, G. The ERBB network: At last, cancer therapy meets systems biology. *Nat. Rev. Cancer* **2012**, *12*, 553–563. [CrossRef] [PubMed]
34. Nicholson, R.I.; Gee, J.M.W.; Harper, M.E. EGFR and cancer prognosis. *Eur. J. Cancer* **2001**, *37*, 9–15. [CrossRef] [PubMed]
35. Mitsudomi, T.; Yatabe, Y. Epidermal growth factor receptor in relation to tumor development: EGFR gene and cancer. *FEBS J.* **2010**, *277*, 301–308. [CrossRef]
36. Fiebig, D.; Bogen, J.P.; Carrara, S.C.; Deweid, L.; Zielonka, S.; Grzeschik, J.; Hock, B.; Kolmar, H. Streamlining the Transition From Yeast Surface Display of Antibody Fragment Immune Libraries to the Production as IgG Format in Mammalian Cells. *Front. Bioeng Biotechnol.* **2022**, *10*, 794389. [CrossRef] [PubMed]
37. Pirzer, T.; Becher, K.-S.; Rieker, M.; Meckel, T.; Mootz, H.D.; Kolmar, H. Generation of Potent Anti-HER1/2 Immunotoxins by Protein Ligation Using Split Inteins. *ACS Chem. Biol.* **2018**, *13*, 2058–2066. [CrossRef]
38. Bogen, J.P.; Carrara, S.C.; Fiebig, D.; Grzeschik, J.; Hock, B.; Kolmar, H. Expedient Generation of Biparatopic Common Light Chain Antibodies via Chicken Immunization and Yeast Display Screening. *Front. Immunol.* **2020**, *11*. [CrossRef]

39. Huang, Y.; Ognjenovic, J.; Karandur, D.; Miller, K.; Merk, A.; Subramaniam, S.; Kuriyan, J. A molecular mechanism for the generation of ligand-dependent differential outputs by the epidermal growth factor receptor. *Elife* **2021**, *10*, e73218. [[CrossRef](#)]
40. Worley, J.R.; Baugh, M.D.; Hughes, D.A.; Edwards, D.R.; Hogan, A.; Sampson, M.J.; Gavrilovic, J. Metalloproteinase Expression in PMA-stimulated THP-1 Cells. *J. Biol. Chem.* **2003**, *278*, 51340–51346. [[CrossRef](#)]
41. Xu, Z.-J.; Gu, Y.; Wang, C.-Z.; Jin, Y.; Wen, X.-M.; Ma, J.-C.; Tang, L.-J.; Mao, Z.-W.; Qian, J.; Lin, J. The M2 macrophage marker CD206: A novel prognostic indicator for acute myeloid leukemia. *Oncoimmunology* **2020**, *9*, 1683347. [[CrossRef](#)]
42. Waterborg, C.E.J.; Beermann, S.; Broeren, M.G.A.; Bennink, M.B.; Koenders, M.I.; Van Lent, P.L.E.M.; van den Berg, W.B.; Van Der Kraan, P.M.; Van De Loo, F.A.J. Protective Role of the MER Tyrosine Kinase via Efferocytosis in Rheumatoid Arthritis Models. *Front. Immunol.* **2018**, *9*, 742. [[CrossRef](#)] [[PubMed](#)]
43. Thorp, E.; Vaisar, T.; Subramanian, M.; Mautner, L.; Blobel, C.; Tabas, I. Shedding of the Mer Tyrosine Kinase Receptor Is Mediated by ADAM17 Protein through a Pathway Involving Reactive Oxygen Species, Protein Kinase C δ , and p38 Mitogen-activated Protein Kinase (MAPK). *J. Biol. Chem.* **2011**, *286*, 33335–33344. [[CrossRef](#)] [[PubMed](#)]
44. Harwardt, J.; Bogen, J.P.; Carrara, S.C.; Ulitzka, M.; Grzeschik, J.; Hock, B.; Kolmar, H. A Generic Strategy to Generate Bifunctional Two-in-One Antibodies by Chicken Immunization. *Front. Immunol.* **2022**, *13*, 888838. [[CrossRef](#)] [[PubMed](#)]
45. Bogen, J.P.; Carrara, S.C.; Fiebig, D.; Grzeschik, J.; Hock, B.; Kolmar, H. Design of a Trispecific Checkpoint Inhibitor and Natural Killer Cell Engager Based on a 2 + 1 Common Light Chain Antibody Architecture. *Front. Immunol.* **2021**, *12*, 669496. [[CrossRef](#)]

Supplementary Information

Targeted phagocytosis induction for cancer immunotherapy *via* bispecific MerTK-engaging antibodies

Stefania C. Carrara ^{1,2}, Jan P. Bogen ^{1,2}, David Fiebig ^{1,2}, Julius Grzeschik ³, Björn Hock ⁴ and Harald Kolmar ^{1,5,*}

Table S1: RT-qPCR SYBR Green primers

Gene Name	Forward	Reverse
<i>Gapdh</i>	ACATCGCTCAGACACCATG	TGTAGTTGAGGTCAATGAAGGG
<i>Hprt1</i>	TTGTTGTAGGATATGCCCTTGA	GCGATGTCAATAGGACTCCAG
<i>MerTK</i>	CTGTGTTTCTGAATGAATCTAGTGA	GCCAACTTCCTCCAAGAGC
<i>Axl</i>	TGGCTGTGAAGACGATGAAG	GTCAAATTCCTTCATGCAGACC
<i>Itgam</i>	GCCTGGATTATAAGGATGTC	TTGAAAAGCTAATCCAACCC
<i>Il-1β</i>	CTAAACAGATGAAGTGCTCC	GGTCATTCTCCTGGAAGG
<i>Ccl22</i>	GTGGTGTGCTAACCTTC	GGCTCAGCTTATTGAGAATC
<i>Il-10</i>	GCCTTTAATAAGCTCCAAGAG	ATCTTCATTGTCATGTAGGC

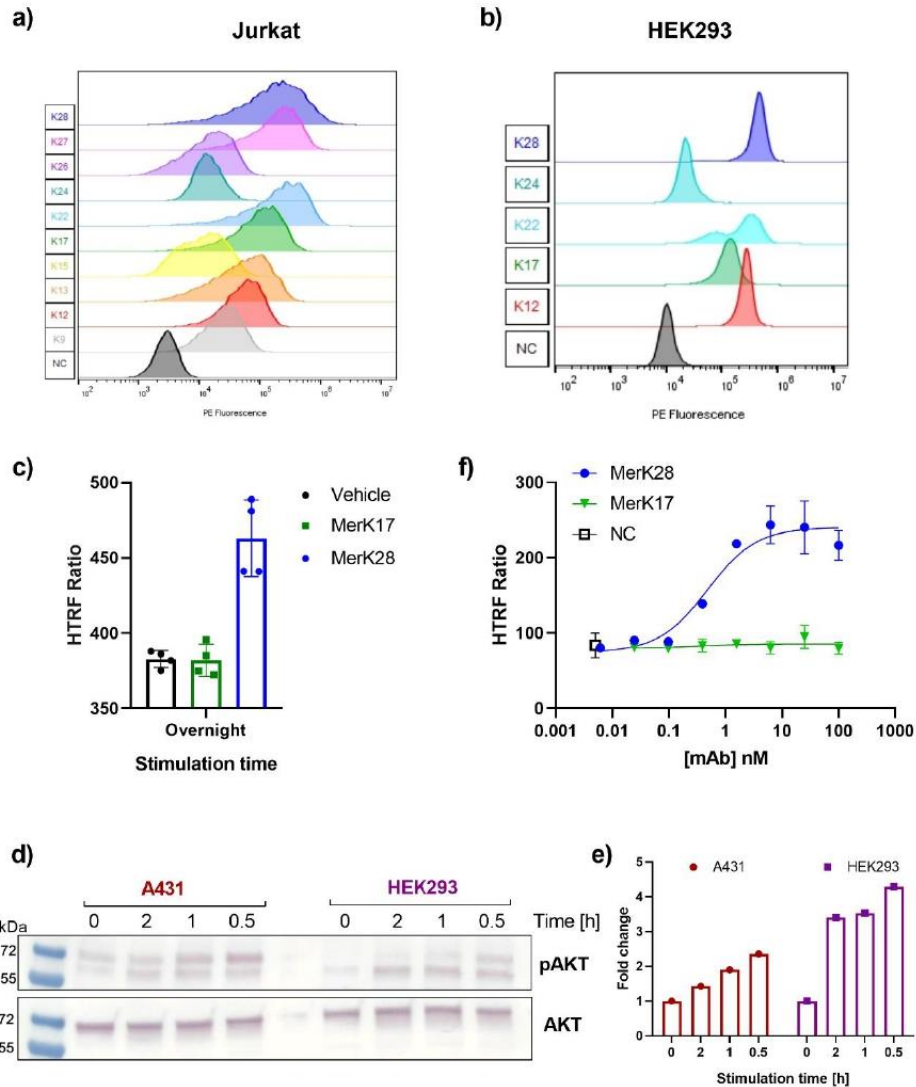


Figure S1: Characterisation of all MerTK antibodies and signalling activation of MerK17 and MerK28. Cell staining with 250 nM anti-MerTK antibodies of a) Jurkat or b) HEK293. Bound antibodies were detected with an anti-human Fc PE-conjugate. Colour-coding represents the different clone numbers. C) Overnight stimulation of A549 cells with either 50 $\mu\text{g/ml}$ MerK17 or MerK28 or a vehicle (PBS). d) Stimulation with 50 $\mu\text{g/ml}$ MerK28 on either A431 or HEK293 cells for the indicated time points. The pAKT levels were normalized to total AKT and set relative to the negative control to determine the fold change induction of pAKT after stimulation (e). f) 30 min incubation of A549 cells with the indicated antibody concentration. HTRF Ratio represents the ratio of donor and acceptor values as suggested by the manufacturer.

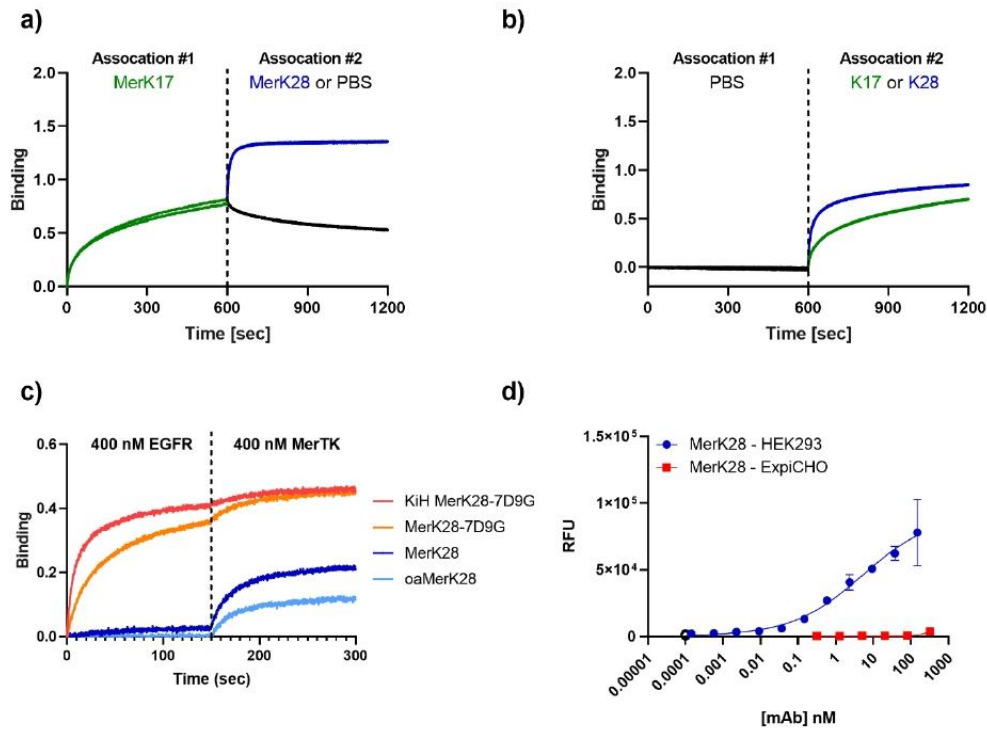


Figure S2: Epitope binning and characterisation of bispecific antibodies. a) Epitope binning by BLI. Association of MerK17 (green) followed by either MerK28 (blue) or PBS (black). b) Competition assay of MerK17 for the ligand binding site of Pros1 *via* BLI. MerK17 was loaded onto AHC biosensors and sequentially associated to either 500 nM MerTK (light blue) or 500 nM MerTK pre-incubated with equimolar Pros1 (pink). c) Simultaneous binding of human MerTK and EGFR via BLI. Antibodies were loaded onto AHC biosensors and then associated first to EGFR and then to MerTK over 300 seconds. d) Cellular binding of MerK28 on either HEK293 (blue) or ExpiCHO cells as a negative control shown in red.

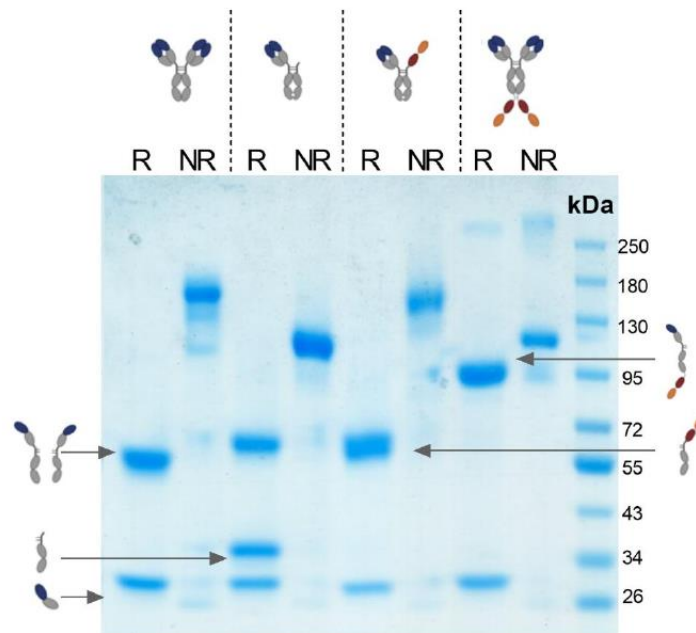


Figure S3: SDS-PAGE gel analysis of all variants in reducing and non-reducing conditions, respectively. The reduced fragments of the variants are indicated with arrows at their expected sizes. Abbreviations: R – reduced, NR – non-reducing, kDa- kilodaltons.

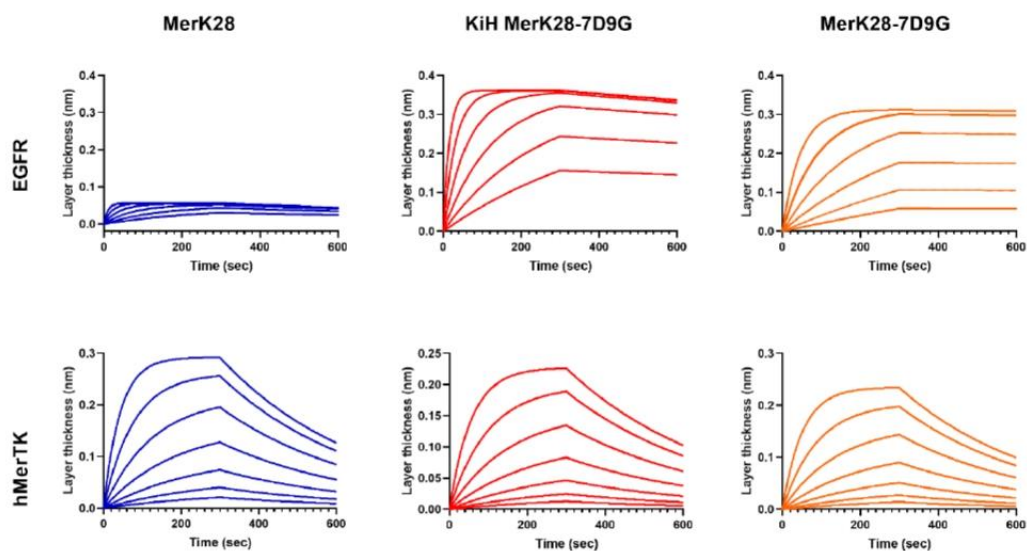


Figure S4: Kinetics Determination. The indicated antibodies were immobilised onto anti-human Fc capture (AHC) biosensors and associated to different target antigen concentrations. For both hMerTK and EGFR, a range of 200 – 0 nM were measured using a 2-fold serial dilution.

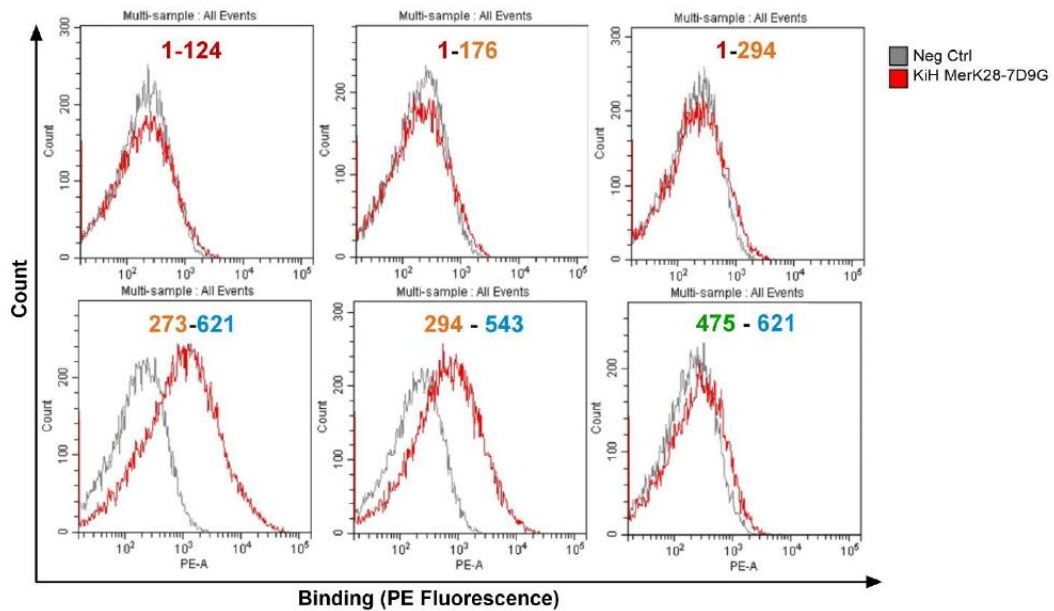


Figure S5: EGFR domain mapping on YSD. Numbers represent the amino acids of the extracellular domain of EGFR, as displayed on yeast cells. The grey histograms present the negative control staining with only secondary Ab, while the red represents KiH MerK28-7D9G. EGFR domain mapping colour-coding: red – domain I, orange – domain II, green – domain III, and blue – domain IV. Yeast cells were stained with 100 nM of the indicated mAbs followed by anti-human Fc-PE-conjugate staining (1:75 dilution). 10'000 events were measured for each.

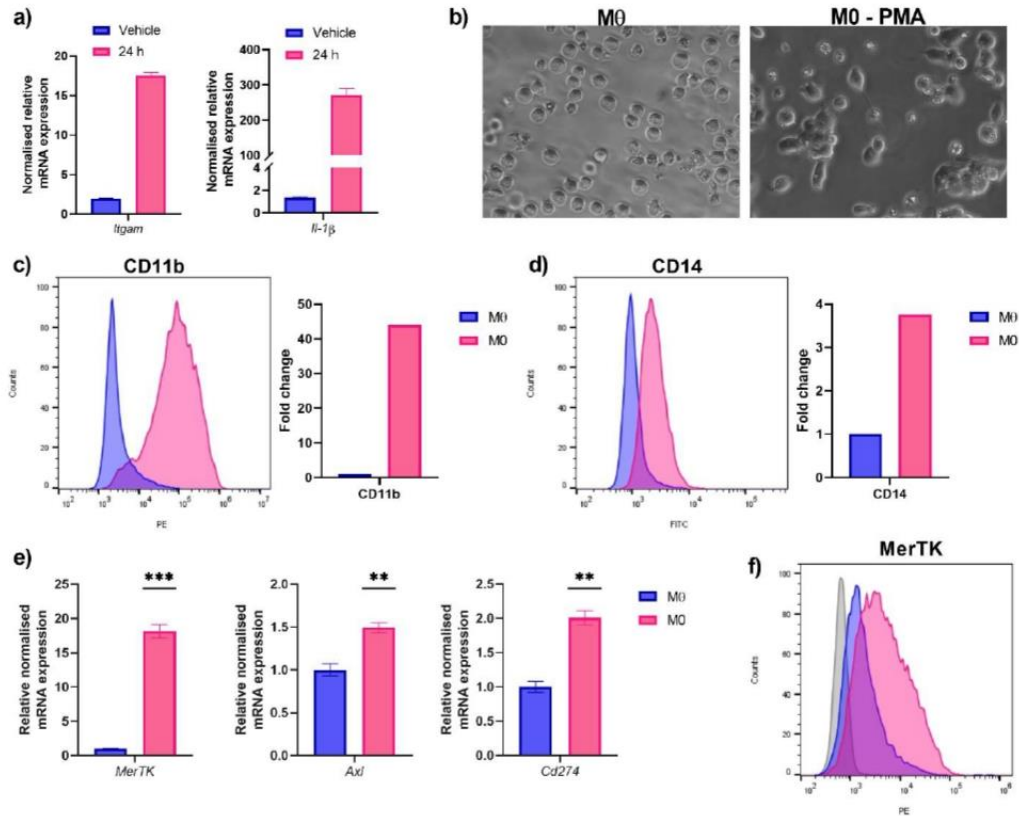


Figure S6: Differentiation of THP-1 cells after PMA incubation. a) Gene expression analysis of unstimulated (blue) or PMA-stimulated THP-1 cells (pink). *Itgam* and *Il-1b* mRNA levels were determined and set relative to the unstimulated control, normalised to internal housekeeping genes. b) Brightfield microscopy images of THP-1 cells before and after PMA incubation. c) Flow cytometric analysis of cell-surface CD11b measured with an anti-CD11b PE-conjugate. d) Cell surface expression of CD14 measuring using an anti-CD14 FITC-conjugate. Fold change was determined for c) and d) by calculating the mean fluorescence and setting the data relative to the M0 control. e) Relative normalised mRNA expression of *MerTK*, *Axl* and *Cd274*. f) MerTK cell surface levels as determined by staining with 50 $\mu\text{g/ml}$ MerK28 and an anti-human Fc PE-conjugate. The grey histogram represents the secondary antibody only, while the blue and pink represent M0 and M0 THP-1s, respectively. Error bars for RT-qPCR represent SEM of triplicate measurements, while flow cytometric analysis is representative of a single experiment while it was repeated at least three times.

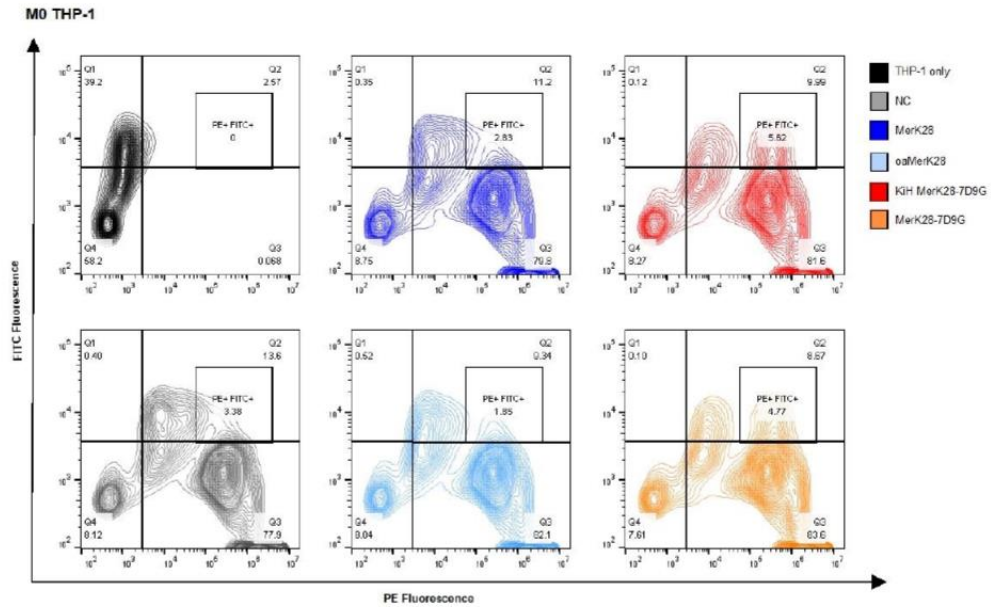


Figure S7: Contour plots of M0-like THP-1 cells after co-incubation with A431 cells. A431 cells were stained with Calcein-AM red-orange and measured using the PE channel (x-axis), whereas THP-1 cells were gated after staining with an anti-CD14-FITC antibody (y-axis). To determine phagocytosis, the double-positive PE+/FITC+ events in the upper right quadrant Q2 were analysed and gated further. Signal in Q3 only represents possible unspecific A431 cells sticking to the THP-1 cells. Colour-coding is indicated in the legend. The negative control (NC, gray) represents THP-1 and A431 cells without any antibody treatment. Visualisation was performed using FlowJo v10 software.

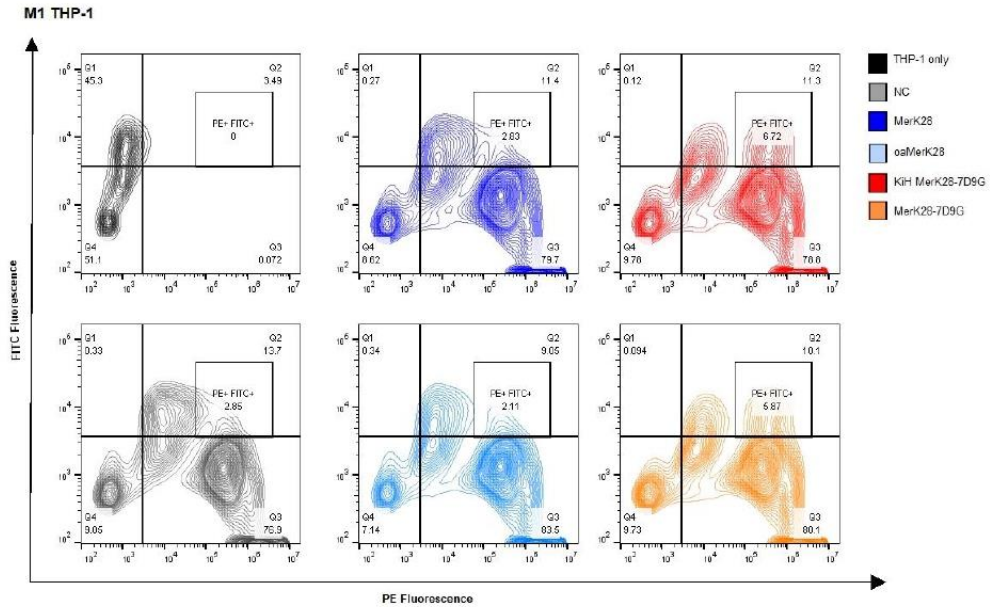


Figure S8: Contour plots of M1-like THP-1 cells after co-incubation with A431 cells. A431 cells were stained with Calcein-AM red-orange and measured using the PE channel (x-axis), whereas THP-1 cells were gated after staining with an anti-CD14-FITC antibody (y-axis). To determine phagocytosis, the double-positive PE+/FITC+ events in the upper right quadrant Q2 were analysed and gated further. Signal in Q3 only represents possible unspecific A431 cells sticking to the THP-1 cells. Colour-coding is indicated in the legend. The negative control (NC, gray) represents THP-1 and A431 cells without any antibody treatment. Visualisation was performed using FlowJo v10 software.

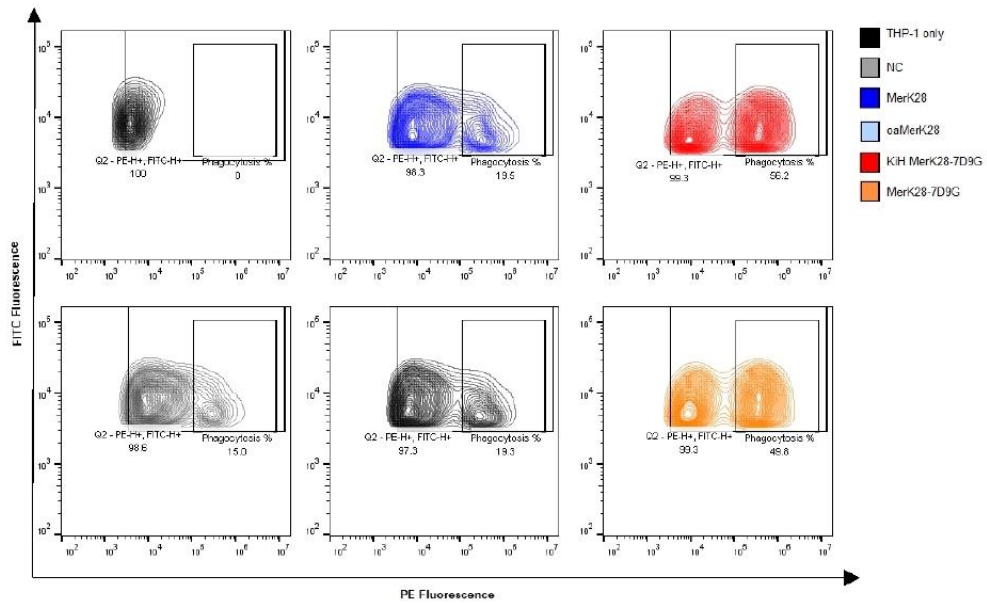


Figure S9: Phagocytosis rate % determination by gating the PE++ events as exemplified by M1-like THP-1 cells. From the gated PE+/FITC+ cells in Figure S8, the co-incubation of cells were gated further to ensure the THP-1 cells had taken up the A431 cells and were not bound lightly to their surface (“phagocytosis %”). A431 cells were stained with Calcein-AM red-orange and measured using the PE channel (x-axis), whereas THP-1 cells were gated after staining with an anti-CD14-FITC antibody (y-axis). Colour-coding is indicated in the legend. The negative control (NC, gray) represents THP-1 and A431 cells without any antibody treatment. Visualisation was performed using FlowJo v10 software.

4.5 TriTECM: A Tetrafunctional T-Cell Engaging Antibody with Built-In Risk Mitigation of Cytokine Release Syndrome

Title:

TriTECM: A Tetrafunctional T-Cell Engaging Antibody with Built-In Risk Mitigation of Cytokine Release Syndrome

Authors:

Stefania Candela Carrara, Julia Harwardt, Julius Grzeschik, Björn Hock, Harald Kolmar

Bibliographic Data:

Journal – *Frontiers in Immunology*

Accepted for publication on 21st October 2022

DOI: 10.3389/fimmu.2022.1051875

Contributions by S.C. Carrara:

- Initial idea & project planning
- Cloning and production of multispecific variants
- Testing of all variants on cell lines and isolated PBMCs
- Writing of manuscript
- Generation of all figures



OPEN ACCESS

EDITED BY
Markus Philipp Radsak,
Johannes Gutenberg University Mainz,
Germany

REVIEWED BY
Hakim Echchannaoui,
Johannes Gutenberg University Mainz,
Germany
Chan Hyuk Kim,
Korea Advanced Institute of Science
and Technology (KAIST), South Korea

*CORRESPONDENCE
Harald Kolmar
Harald.Kolmar@TU-Darmstadt.de

SPECIALTY SECTION
This article was submitted to
Vaccines and Molecular Therapeutics,
a section of the journal
Frontiers in Immunology

RECEIVED 23 September 2022
ACCEPTED 21 October 2022
PUBLISHED 10 November 2022

CITATION
Carrara SC, Harwardt J, Grzeschik J,
Hock B and Kolmar H (2022) TriTECM:
A tetrafunctional T-cell engaging
antibody with built-in risk mitigation of
cytokine release syndrome.
Front. Immunol. 13:1051875.
doi: 10.3389/fimmu.2022.1051875

COPYRIGHT
© 2022 Carrara, Harwardt, Grzeschik,
Hock and Kolmar. This is an open-
access article distributed under the
terms of the [Creative Commons
Attribution License \(CC BY\)](https://creativecommons.org/licenses/by/4.0/). The use,
distribution or reproduction in other
forums is permitted, provided the
original author(s) and the copyright
owner(s) are credited and that the
original publication in this journal is
cited, in accordance with accepted
academic practice. No use,
distribution or reproduction is
permitted which does not comply with
these terms.

TriTECM: A tetrafunctional T-cell engaging antibody with built-in risk mitigation of cytokine release syndrome

Stefania C. Carrara^{1,2}, Julia Harwardt¹, Julius Grzeschik³,
Björn Hock⁴ and Harald Kolmar^{1,5*}

¹Institute for Organic Chemistry and Biochemistry, Technische Universität Darmstadt, Darmstadt, Germany, ²Ferring Darmstadt Laboratory, Biologics Technology and Development, Darmstadt, Germany, ³Ferring Biologics Innovation Centre, Epalinges, Switzerland, ⁴Aerium Therapeutics, Epalinges, Switzerland, ⁵Centre for Synthetic Biology, Technische Universität Darmstadt, Darmstadt, Germany

Harnessing the innate power of T cells for therapeutic benefit has seen many shortcomings due to cytotoxicity in the past, but still remains a very attractive mechanism of action for immune-modulating biotherapeutics. With the intent of expanding the therapeutic window for T-cell targeting biotherapeutics, we present an attenuated trispesific T-cell engager (TCE) combined with an anti-interleukin 6 receptor (IL-6R) binding moiety in order to modulate cytokine activity (TriTECM). Overshooting cytokine release, culminating in cytokine release syndrome (CRS), is one of the severest adverse effects observed with T-cell immunotherapies, where the IL-6/IL-6R axis is known to play a pivotal role. By targeting two tumour-associated antigens, epidermal growth factor receptor (EGFR) and programmed death ligand 1 (PD-L1), simultaneously with a bispecific two-in-one antibody, high tumour selectivity together with checkpoint inhibition was achieved. We generated tetrafunctional molecules that contained additional CD3- and IL-6R-binding modules. Ligand competition for both PD-L1 and IL-6R as well as inhibition of both EGF- and IL-6-mediated signalling pathways was observed. Furthermore, TriTECM molecules were able to activate T cells and trigger T-cell-mediated cytotoxicity through CD3-binding in an attenuated fashion. A decrease in pro-inflammatory cytokine interferon γ (IFN γ) after T-cell activation was observed for the TriTECM molecules compared to their respective controls lacking IL-6R binding, hinting at a successful attenuation and potential modulation *via* IL-6R. As IL-6 is a key player in cytokine release syndrome as well as being implicated in enhancing tumour progression, such molecule designs could reduce side effects and cytotoxicity observed with previous TCEs and widen their therapeutic windows.

KEYWORDS

T-cell engager, multispecific antibody, cytokine release syndrome, IL-6R, CRS, tetraspecifics

Introduction

Therapeutic strategies for solid cancers have led to the rise of monoclonal antibodies (mAbs), targeting a single target that is overexpressed on tumour cells. Moreover, bispecific antibodies (BsAbs) and multispecific antibodies are now gaining importance due to their power of binding multiple tumour-associated antigens (TAA) simultaneously and/or redirecting immune cells to the tumour microenvironment to enhance anti-tumour activities and combining different mechanisms of action (1–4). Besides other immune cells, T lymphocytes (T cells) have been a central focus point in the battle against cancer in recent years. A plethora of T cell-based immunotherapies showing moderate to good success, particularly in hematologic cancers, have been developed and approved, including the renowned immune-checkpoint inhibitors and engineered chimeric antigen receptor T cells (CAR-Ts) (5, 6).

A special class of BsAbs termed bispecific T-cell engagers (BiTEs) was introduced by Micromet (now owned by Amgen Inc.) in 2008, where T cells are redirected to tumour cells through the binding of both a TAA and a T cell surface antigen, allowing for enhanced tumour lysis and redirecting of T cells to the tumour microenvironment (7–9). BiTEs consist of two linked single-chain variable fragments (scFvs) and are thus relatively small molecules with a short half-life. The first-in-class BiTE molecule to be approved for therapy was Blinatumomab (Blinicyto) in 2014 for the treatment of B-cell malignancies by simultaneously targeting CD19 on B cells and CD3 on T-cells (7, 10–13). Another T cell-engaging bispecific molecule approved for clinical use in the European Union is catumaxomab (Removab) of the TrioMab format, which targets epithelial cell adhesion molecule (EPCAM) and CD3 with a functional Fc region mediating effector functions resulting in a trifunctional antibody (14, 15). While the breakthrough of bispecific T-cell engagers was validated with the regulatory approval of both molecules, they both have shortcomings. Catumaxomab, a rat-mouse hybrid IgG2 antibody with a very high affinity for CD3, led to T cell over-activation and cytokine release syndrome (CRS) and was later voluntarily withdrawn due to commercial reasons (16). Similarly, treatment with blinatumomab was reported to be associated with a high risk of CRS, narrowing its therapeutic window and additionally requiring frequent infusion due to its short half-life (17–21). The first monoclonal antibody ever approved for clinical use, muromonab-CD3 (Orthoclone-OKT3), a mouse antibody binding CD3, was deployed for the treatment of acute kidney allograft rejection and additionally investigated for its use against T cell acute lymphoblastic leukemia (22). In 2010, the manufacturing of Muromonab-CD3 was voluntarily withdrawn due to severe side effects after administration and the growing number of better-tolerated alternatives that were available (23). It was also the coiner for the term “cytokine release syndrome” back in the 1990s (19, 24, 25).

Cytokine release syndrome is one of the most frequent grave adverse effects of T cell-engaging immunotherapies, resulting in a systemic inflammatory response after immunotherapy (19). Though grade 1 and 2 CRS result in mild reactions such as fever and hypotension, intravenous fluids or low-dose vasopressors are generally required. Grade 3 CRS results in hospitalisation, high-dose vasopressors are administered, and signs of organ dysfunction appear to begin. Lastly, severe CRS, namely grade 4, embodies life-threatening situations where mechanical ventilation support is required, grade 4 organ toxicities are observed, and occurring hypotension requires the application of multiple high-dose vasopressors (19, 26–28). While the pathophysiology of CRS is not wholly understood, interleukin-6 (IL-6), interleukin-10 (IL-10), and interferon- γ (IFN γ) are known to be the main drivers of CRS. Initially, activated T cells release IFN γ which is secreted and in turn activates macrophages, leading to the excessive production of IL-6, IL-10, and TNF α (19, 29). While all cytokines presumably play an important role, IL-6 seems to be a key player in the pathophysiology of CRS and contributes to many key symptoms (19, 30, 31). Currently, grade 3 or 4 CRS are managed by treating patients with tocilizumab, a therapeutic anti-IL-6R antibody that blocks receptor activation by IL-6. Tocilizumab (Actemra) was approved by the U.S. Food and Drug Administration (FDA) in 2010 for rheumatoid arthritis treatment and more recently received emergency use authorisation for the management of CRS (32–34). Furthermore, in light of the unprecedented COVID-19 pandemic where life-threatening infections were observed resulting in CRS, not only tocilizumab but also sarilumab, another antibody directed against IL-6R, have gained importance in the management of CRS in critically ill patients (35–42). Although risk- and grade-management of CRS with the administration of tocilizumab appears to work well, improvements are required to widen the therapeutic index of immunotherapies and boost their efficacies, particularly in solid tumours.

Due to IL-6's pleiotropic nature, it has also been shown to play critical roles in tumour growth, angiogenesis, and metastasis of different cancer types by activating signalling pathways after assembly and dimerization with its receptor IL-6R and glycoprotein 130 (gp130) (43). The IL-6/IL-6R/gp130 complex is able to activate signal transduction by the Janus kinase/signal transducer and activator of transcription (JAK/STAT) pathway by either membrane-bound IL-6R and gp130 (classical signalling) or by soluble forms of IL-6R (sIL-6R) that then joins membrane-bound gp130 (*trans* signalling) to mitigate downstream signalling (44). The JAK/STAT pathway plays a critical role in solid tumour progression and thus inhibition of downstream events by IL-6 or IL-6R blockage is a promising strategy for the development of new anti-cancer combination therapies (43, 45). Furthermore, co-targeting of the EGFR and IL-6R pathways through blockage of oncogenic signalling may aid in overcoming acquired EGFR resistance that is observed after treatment with anti-EGFR drugs such as small molecule inhibitors gefitinib or erlotinib (46–49).

Tumour-associated macrophages (TAMs) are a key element of the heterogeneous tumour microenvironment (TME) and can take on both tumour-impairing or tumour-promoting roles by differentiation of infiltrating or resident macrophages to either M1- or M2-type TAMs, respectively (50). Previous studies have shown the implication of TAMs and their ability to produce IL-6 to promote tumorigenesis in hepatocellular carcinoma stem cells (51), K-ras mutant lung cancer mouse models (52), and breast cancer (44). Under hypoxic conditions in an immunosuppressive TME, upregulation of IL-6R expression on tumour cells and increased IL-6 production have been reported, inducing M2-TAMs and further promoting tumour progression and expansion, and survival resistance (51, 53, 54). The complexity of the TME culminates in the difficulty of efficaciously targeting tumours by monospecific therapies due to the involvement of many key players. Thus, combinatorial approaches through multispecific antibodies targeting multiple pathways might encourage redefining and reprogramming the TME to efficaciously eradicate tumours, and inhibiting TAM-derived IL-6-mediated signalling transduction pathways. Eventually, this strategy may contribute to the activation of immunologically cold tumours (55).

While many antibody formats exist for T cell-redirecting antibodies, the preclinical and clinical efficacy of such antibodies is often hampered by high toxicities in early stages. In recent years, researchers have investigated the role of CD3 affinity to improve the therapeutic index of T-cell engagers (TCEs) (56–60). This requires the development and characterisation of novel CD3 binders with less critical cytokine release profiles. Trispecific T-cell engager (TriTE) antibodies have been described in literature as next-generation T-cell engager therapies, though studies in humans are yet to be concluded (7, 61, 62). For example, in the antibody described by Tapia-Galisteo and colleagues, a CD3-specific single-chain variable fragment (scFv) was flanked by two different tumour-targeting V_{HH} antibody fragments directed against epidermal growth factor receptor (EGFR) and EpCAM for the treatment of colorectal cancer (61). Another novel trispecific T-cell engager concept was described by Wu and co-workers by binding not only to CD3 but also its co-stimulatory receptor CD28 by using the cross-over dual variable (CODV) bispecific antibody format and additionally targeting CD38 on myeloma cells (62). Moreover, eight TCE mAbs are in late-stage clinical studies targeting several different TAA for different indications, including CD7, BCMA, CD20, and CD123 (63). A further three candidates are currently undergoing regulatory review, namely teclistamab (BCMAxCD3), glofitamab (CD20xCD3), and teplizumab (humanised OKT3) (64). Two additional bispecific molecules were approved for therapeutic use in the USA and the EU in 2022, targeting gp100xCD3 as a bispecific fusion protein (tebentafusp), and CD20xCD3 as a bispecific antibody (mosunetuzumab). The vast number of preclinical and clinical programs investigating CD3-binding either as mono- or bispecific antibodies further highlights the unmet need and interest in pursuing T cell-activating immunotherapies.

To overcome the limitations of current clinical approaches, we present a first-in-class trispecific T-cell engager and TME and cytokine modulator (TriTECM), by engineering a two-in-one dual-TAA targeting antibody with anti-CD3 and anti-IL-6R binding moieties. This tetrafunctional antibody results in high tumour selectivity by targeting EGFR and the checkpoint inhibitor programmed death-ligand 1 (PD-L1) simultaneously, and has attenuated CD3 ϵ binding, diminishing the cytokine release and toxicity effects. On top, an anti-IL-6R binding moiety that modulates the signalling of IL-6 released after T cell and macrophage activation is present to not only potentially support tumour eradication but also to mitigate CRS events. This concept may allow the usage of previously developed high potency anti-CD3 antibodies in the long term, obviating the need to discover novel functionally attenuated CD3-binders. For the first time, to the best of our knowledge, an anti-IL-6R moiety is fused directly to a trispecific T cell-engager to inhibit both *cis*- and *trans*-IL-6-mediated signalling, aimed at directly modulating but not completely abolishing cytokine release after T-cell activation.

Materials & methods

Cell culture

A431 (ACC 91), A549 (ACC 107), and THP-1 (ACC 16) cells were obtained from DSMZ (German Collection of Microorganisms and Cell Cultures GmbH). Adherent cell lines (A431, A549) were maintained in Dulbecco's Minimal Eagle Medium (DMEM) supplemented with 10% FBS and 1x penicillin/streptomycin. THP-1 cells were maintained in RPMI 1640 supplemented with 10% FBS and 1x penicillin/streptomycin. Cells were subcultured every 2–3 days and incubated at 37°C, 5% CO₂.

Cloning, production and purification of antibody constructs

The HCP-LCE IgG backbone was used as a starting block (65). For the different scFvs, gene fragments were ordered from Twist Biosciences based on their published protein sequences (66) with respective *SapI* overhangs. The various architectures were cloned using Q5 DNA Polymerase and subsequent *SapI*-mediated Golden Gate Cloning (GGC). The sequences were verified by Sanger Sequencing at Microsynth (Göttingen). An effector-silenced Fc-backbone carrying LALA mutations was used (67), as well as the Knob-into-Hole (KiH) technology to ensure heterodimerisation (68).

For the production of the antibodies, Expi293-F (Thermo Fisher Scientific) cells were transfected with Expifectamine293 (Thermo Fisher Scientific), following the manufacturer's instructions. The cells were cultured in Expi293 Expression Medium (Thermo Fisher Scientific), sub-cultured every 3–4 days

and incubated at 37°C, 8% CO₂. Transfections were harvested 5 days post-transfection. The supernatants were sterile filtered and supplemented with 18.1 mL/L BioLock (IBA Lifesciences). Purification of all KiH variants was performed by a two-step purification using an ÄKTA Pure25 (Cytiva Lifesciences); a His-tag purification using a HisTrap™ excel column (Cytiva Lifesciences) was performed followed by TwinStrep®-tag purification using a Streptactin®XT 4Flow® column. In this manner, heterodimeric heavy chains were ensured.

Biophysical characterisation (SDS-PAGE, Thermal stability)

To characterise the produced antibodies, SDS-PAGE analysis was performed. To this end, 4 µg purified mAb were loaded onto a Mini-PROTEAN TGX 4-15% Gel (BioRad) with either reducing- or non-reducing-Lämmli buffer, and subsequently stained with Coomassie.

For thermal stability determination, antibodies were incubated with SYPRO Orange (Thermo Fisher Scientific) and a thermal shift assay was performed using a CFX Connect Real-Time PCR System (BioRad). The temperature gradient was set from 10°C to 95°C with an increment of 0.5°C/10 s. The derivatives of the melt curves were determined with the CFX Maestro software to determine the melt temperature (T_M).

Affinity determination, simultaneous binding and competition assays *via* BLI

Affinities were determined using biolayer interferometry (BLI) on an Octet RED96. For kinetics determination, 60 nM antibody was loaded onto anti-human Fc capture (AHC) biosensors and incubated with varying concentrations of antigen, in a range from 0 – 500 nM for EGFR and PD-L1, and 0 – 200 nM for IL-6R. Fitting of the curves for affinity determination was performed based on Savitzky-Golay filtering and a 1:1 Langmuir binding model.

For simultaneous binding studies with BLI, 10 µg/ml antibody was loaded onto an AHC biosensor and sequentially associated to 200 nM IL-6R, followed by 500 nM EGFR and PD-L1. A negative control with PBS was included to eliminate unspecific binding of the self-produced antigens.

Competition assays for PD-L1/PD-1 and IL-6/IL-6R were performed as previously described (65, 69, 70).

T-cell activation assays

To determine the potency of T-cell engagement, the T-cell activation Bioassay (NFAT) (Promega) was performed following the manufacturer's instructions. In brief, 4×10^4

A431 cells/well were seeded in sterile 96-well plates and allowed to adhere overnight. The following morning, 1×10^5 effector cells/well were added with the indicated antibody dilutions (3x concentrations). The co-culture was incubated for 6 h at 37°C, 5% CO₂, followed by the addition of Bio-Glo reagent. After 5-10 min, the plate was measured on a luminescence plate reader.

PBMC isolation

Peripheral blood mononuclear cells (PBMCs) were obtained from buffy coats from healthy human donors obtained from the Deutsche Rotes Kreuz (Frankfurt). To this end, 25 ml blood was mixed 1:1 with PBS- 2% FBS (PBS-F) and PBMCs were purified using SepMate-50 tubes following the manufacturer's instructions (StemCell Technologies). The isolated PBMCs were frozen in 70% RPMI 1640, 20% FBS and 10% DMSO and thawed directly when required. All work was performed according to local ethics and welfare regulations.

Cytokine release assay

For cytokine release assays, PBMCs were thawed and seeded onto 48-well plates at 3×10^5 cells/well. The desired antibody concentration was added to the cells, and the mixture was incubated at 37°C, 5% CO₂ for 72 h. After 72 h, the supernatant was collected and centrifuged to remove any cell debris. The cells were separated for further flow cytometric analysis. A minimum of four healthy donors were used and at least biological duplicates were measured in independent experiments.

Signalling assays

To detect phosphoproteins and signalling inhibition, HTRF (Perkin Elmer) kits were used. Therefore, 5×10^4 A549 cells/well were seeded onto 96-well tissue-culture plates and allowed to adhere for 4 h, cells were subsequently serum-starved overnight. The serum-starved cells were pre-treated with the desired antibody concentrations for 1 h before the addition of 20 ng/ml ligand for 10 or 40 min for EGF and IL-6, respectively. Immediately afterwards, the cells were washed with ice-cold PBS and lysed in the appropriate lysis buffer according to the manufacturer's instructions. The investigation of the EGF/EGFR pathway was performed using the Phospho-Akt (Ser4739 cellular HTRF Kit (Perkin Elmer), and the IL-6/IL-6R pathway was investigated using the Phospho-STAT3 (Tyr705) cellular HTRF kit (Perkin Elmer). Data was graphed using GraphPad Prism 8.0.1. Assays were repeated at least three times with biological duplicates.

Cytokine ELISAs

Quantification of secreted cytokines from cell culture supernatants was measured using commercially available ELISAs following the manufacturer's instructions. ELISA kit was purchased from R&D Systems: Human IFN- γ DuoSet ELISA (DY285B).

T-cell-mediated cytotoxicity

Evaluation of cytotoxicity was performed by incubating A431 cells with PBMCs (effector-to-target ratio 10:1) in 96-well tissue culture plates with the desired antibody concentration for 24 – 48 h. After different time points, the supernatant was used to measure released LDH by the LDH-Glo Cytotoxicity Assay (Promega) following the manufacturer's instructions. Plates were observed under a bright-field microscope to evaluate potential cell killing. Further, dead cell staining was performed by trypsinising and collecting all cells, staining with propidium iodide (PI) (Sigma Aldrich) and measuring PE fluorescence using a flow cytometer.

Flow cytometry

Flow cytometric analysis was performed by first washing the cells of interest with ice-cold PBS- 2% FBS (PBS-F). Cells were then stained with primary antibodies and incubated on ice for 30 min. Subsequently, the cell pellets were washed with ice-cold PBS-F and resuspended in an appropriate volume of PBS-F for measurement using a CytoFlex S (Beckman Coulter) flow cytometer. If the primary antibody was not directly conjugated, a secondary antibody incubation was performed on ice for 15 min before measurement. The antibodies used in this study were: anti-human Fc-PE (Thermo Fisher Scientific), anti-human CD69-FITC (Thermo Fisher Scientific), anti-human CD25-APC (Thermo Fisher Scientific). Dot plots were generated using FlowJo V10 software.

Results

Design & generation of TriTECM variants

In this proof-of-concept study, we combined existing and well-characterised binding modules in different antibody formats to generate a trispecific T-cell engager with TME and cytokine release modulation (TriTECM). Due to its ability to bind and block both EGFR and PD-L1 pathways and having two binding sites for each target, a recently isolated two-in-one antibody (65) was chosen as the backbone, carrying an effector-silenced Fc to minimise cytotoxicity and extend the

half-life. This molecule carries dual targeting abilities in a generic IgG1 antibody format, where the light chain mainly contributes to EGFR-binding and the heavy chain to PD-L1-binding. Moreover, while individual binding to each target occurs with moderate affinity, tumour cells expressing both antigens were bound with high affinity, indicating that the antibody, besides being able to inhibit the PD-1/PD-L1 axis, displays enhanced tumour selectivity.

For CD3 ϵ -engagement, the fully human monoclonal antibody foralumab (NI0401, abbreviated as α CD3 ϵ) was considered (71, 72), from which a single-chain variable fragment (scFv) was derived. Clinical investigations have been performed using different formulations of foralumab for several indications, including non-alcoholic steatohepatitis (NASH), type 2 diabetes mellitus, primary and secondary multiple sclerosis, and more recently for COVID-19 infections (71, 73). According to a reported study by Moreira et al., nasal administration of foralumab in a pilot study using patients with mild to moderate COVID-19 disease severity led to no CRS and lowered IL-6 blood levels 10 days after administration (72). For this proof-of-concept study, the anti-CD3 scFv was used as a CD3-based T-cell engager.

For inhibition of the IL6-IL-6R-gp130 pathway, a sarilumab-derived scFv (abbreviated with α IL-6R) was generated as sarilumab exhibits exceptional affinity to the IL-6R α with 61.9 pM, approximately 20-fold higher than tocilizumab, and is able to block both the classical- and trans-mediated signalling pathways (74). Furthermore, recent studies showed its ability to modulate CRS events in SARS-CoV2-infected patients (35–42).

With these building blocks, different TCEs were designed. To have better control over the positioning of the scFvs added, all molecules were designed with the Knob into Hole (KiH) technology (68). To avoid hyper-cytokine release, a single CD3-binding scFv was fused onto the HCP-LCE KiH backbone. As well recognised, the distance and relative positioning of TAA and CD3 binding modules of T-cell recruiting antibodies matter, influencing their ability to bridge the immune synapse between a tumour-associated antigen and the TCR on the surface of T cells (56, 75). For this purpose, a classical approach was taken, fusing the anti-CD3 ϵ scFv to the N-terminus of the VH domain with a (G₄S)₃ linker, providing a relatively small distance between CD3-engagement and the surface of the tumour cell upon binding. Conversely, a C-terminal fusion to the Knob-Fc with a (G₄S)₃ linker was also generated, providing the largest distance between the tumour-binding Fab and the engaging T cell (Figure 1A). The anti-IL-6R scFv was placed either at the C-termini of both heavy chain (HC) Fc-fragments or only at the Hole-Fc heavy chain, respectively. The control variants are all depicted and named in Figure 1B. For simplicity, the nomenclature is based on the positioning of the scFvs (either N- or C-terminal) to the heavy chain and either for the Knob (K) or Hole (H) HCs. As an example, a fusion of anti-CD3 ϵ scFv N-

terminal to the VH of the Knob HC together with a C-terminal fusion of the anti-IL-6R scFv to both the Knob and Hole HC is denoted as $(\alpha\text{CD}3\epsilon)\text{K}(\alpha\text{IL-6R}) + \text{H}(\alpha\text{IL-6R})$. The parental two-in-one antibody is termed K + H.

Biophysical characterisation of variants

Production of the antibodies was performed in Expi293-F cells by transient transfection with expression plasmids using Expiectamine293. To ensure exclusive isolation of heterodimers, a Twin-StrepII-tag sequence was placed at the C-terminus of the CH3 domain of the Knob-Fc, while a His₆-tag was placed C-terminally to the Hole-Fc, as previously described (76). Subsequently, the cell culture supernatant was purified *via* a two-step purification, namely an IMAC followed by StrepTactin purification to purify only heterodimeric antibodies carrying both a Knob- and a Hole-HC. SDS-PAGE analysis revealed all the expected heavy- and light-chain bands under reducing conditions, as well as the expected molecular size under non-reducing conditions with no degradation products (Figure 1C). The antibodies unveiled appropriate yields for all

variants, with the yield decreasing with increasing number of fused scFvs as expected (Table 1). Thermal stability investigated by SYPRO Orange revealed melting temperatures between 63.50°C and 78.00°C, with the parental K + H exhibiting 66.50°C, revealing no large reduction in thermal stability (Table 1; Supplementary Figure 1).

Affinity towards the different antigens was determined *via* biolayer interferometry (BLI). Antibodies were loaded onto AHC biosensors and varying concentrations of antigen were associated to the mAb. The determined affinities were in similar ranges to those cited in literature from previous studies (65, 74), with only minor changes where the fused scFvs could presumably interfere with binding (Table 2; Supplementary Figure 2). Nevertheless, the affinity to neither EGFR nor PD-L1 was greatly influenced by N- or C-terminal scFv fusions. The affinity towards soluble IL-6R (sIL-6R-TS) was not determined for all IL-6R-binding variants due to the very slow dissociation (Supplementary Figure 2), however both K ($\alpha\text{CD}3\epsilon$) + H($\alpha\text{IL-6R}$) and $(\alpha\text{CD}3\epsilon)\text{K}(\alpha\text{IL-6R}) + \text{H}(\alpha\text{IL-6R})$ showed single-digit nanomolar affinity towards IL-6R, substantiating the very high affinity of the full-length variant from literature (74).

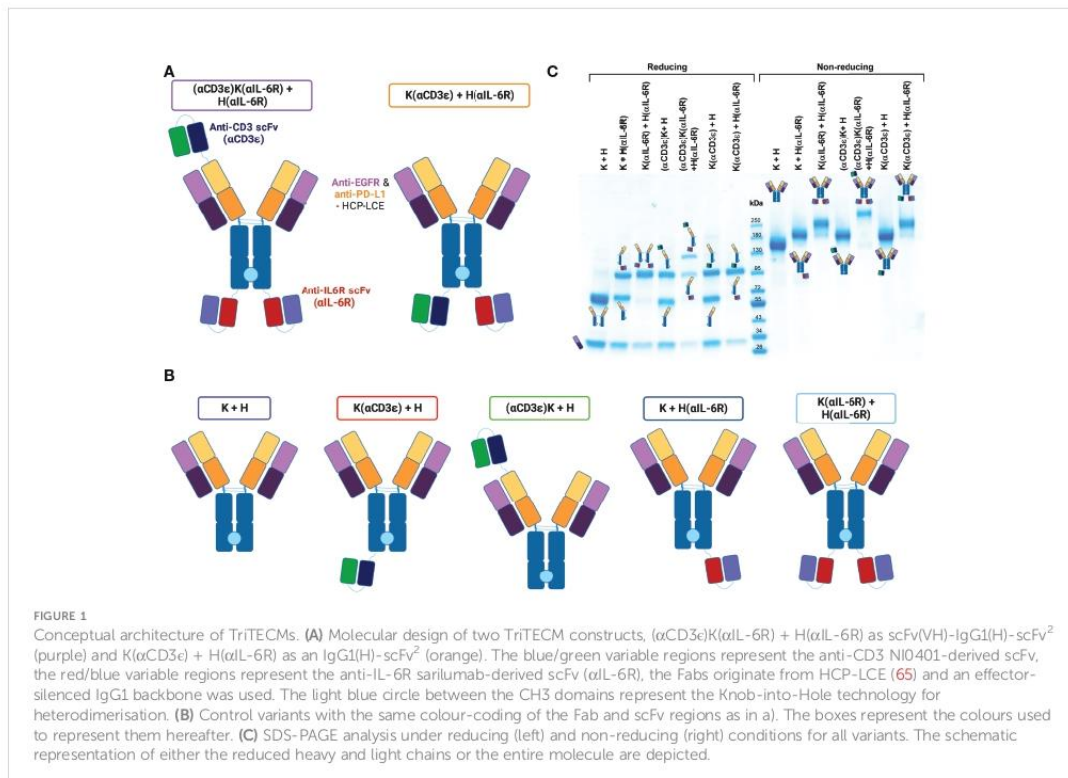


TABLE 1 Yields and thermal stability of all variants.

Variants	Yield per 1 L (mg)	T _M (°C)
K + H	122.344	66.50
K + H(α IL-6R)	54.512	70.00
K(α CD3e) + H	63.170	78.00
K(α CD3e) + H(α IL-6R)	22.478	69.50
K(α IL-6R) + H(α IL-6R)	31.635	63.50
(α CD3e)K + H	101.765	74.50
(α CD3e)K(α IL-6R) + H(α IL-6R)	23.643	64.00
oa(α CD3e)K(α IL-6R)	26.074	71.00

On-cell affinities and simultaneous binding

To ensure the tumour-targeting ability of the two-in-one backbone remained intact, A431 cells were examined that are both positive for EGFR and PD-L1, revealing very similar on-cell affinities for all variants (Supplementary Table 1; Supplementary Figure 3). The parental K + H antibody showed an affinity of 2.5 nM, similar to previous studies (65), and the two TriTECM molecules revealed 12.3 and 21.2 nM for (α CD3e)K(α IL-6R) + H(α IL-6R) and K(α CD3e) + H(α IL-6R), respectively. Nonetheless, very good on-cell affinities were measured for all variants. CD3 binding was observed on Jurkat cells, with the (α CD3e)K + H and K(α CD3e) + H variants binding with two-digit nanomolar affinities. A reduction in CD3-binding was observed for both TriTECM variants, presumably due to different conformations of the molecules (Supplementary Table 1; Supplementary Figure 3). Lastly, IL-6R-binding was confirmed on macrophage-like THP-1 cells (Supplementary Table 1; Supplementary Figure 3).

For T-cell engagers, simultaneous binding and engagement of both tumour- and T-cells is crucial. Accordingly, simultaneous binding of Calcein AM-stained A431 tumour cells and pre-incubated CD3-stained Jurkat cells was investigated by flow cytometry (Figure 2A). Quantification of FITC⁺/PE⁺ and FITC⁺/PE⁻ binding events were considered as

successful co-binding, as both CD3-binding on Jurkat cells was observed through the antibodies, as well as to A431 cells via EGFR and PD-L1 (Figure 2B). The two best candidates were (α CD3e)K + H and (α CD3e)K(α IL-6R) + H(α IL-6R), followed by K(α CD3e) + H and K(α CD3e) + H(α IL-6R). Weaker simultaneous binding was observed for (α CD3e)K(α IL-6R) + H(α IL-6R) and K(α CD3e) + H(α IL-6R) compared to their counterparts without the anti-IL-6R scFv, as expected from their reduced on-cell affinity, however still significant compared to K + H or K + H(α IL-6R) which are not able to bind Jurkat cells due to the absence of the CD3 binding module.

Furthermore, simultaneous binding to IL-6R, EGFR and PD-L1 was confirmed via BLI by loading the different constructs onto AHC biosensors and associating to the three antigens sequentially for 300 seconds each (Figure 2C). A one-armed variant of (α CD3e)K(α IL-6R) + H(α IL-6R) (dubbed oa (α CD3e)K(α IL-6R)) was generated to test whether a single arm could still bind all three targets. Interestingly, the one-armed variant was also able to bind IL-6R, EGFR and PD-L1, though with decreased layer thickness increase due to only monovalent binding to each antigen. This indicated that the two-in-one Fab retained its ability to simultaneously bind EGFR and PD-L1 with scFvs fused to its N-terminus. Overall, the tetraspecificity of both TriTECM molecules was confirmed.

Ligand competition and signalling pathway inhibition

For a full therapeutic effect, it is important that the antibodies binding to EGFR, PD-L1 and IL-6R have antagonistic effects. Sarilumab is well-known to compete with the IL-6 binding site on the IL-6R (77), and the previously identified parental K + H antibody competes with PD-1 for binding to PD-L1 (65). Via BLI, a competition assay was performed for both TriTECM molecules and full-length sarilumab or K + H as controls. For IL-6/IL-6R competition, the (α CD3e)K(α IL-6R) + H(α IL-6R) construct inhibited equally

TABLE 2 Affinities towards soluble, monomeric EGFR, PD-L1 or IL-6R as determined by BLI.

Variant	K _D (nM)		
	His ₆ -EGFR-TS	His ₆ -PD-L1-TS	sIL-6R-TS
K + H	173 ± 10.8	92.9 ± 2.35	–
K + H(α IL-6R)	355 ± 19.4	68.8 ± 2.02	< 0.001*
K(α IL-6R) + H(α IL-6R)	503 ± 20.0	70.7 ± 2.51	< 0.001*
K(α CD3e) + H	228 ± 12.4	105.0 ± 2.80	–
K(α CD3e) + H(α IL-6R)	172 ± 10.5	112 ± 3.14	1.80 ± 0.188
(α CD3e)K + H	236 ± 11.5	108.0 ± 2.85	–
(α CD3e)K(α IL-6R) + H(α IL-6R)	271 ± 14.4	130 ± 3.73	2.71 ± 0.0848

*curves were not fittable due to very slow dissociation that precludes exact off-rate determination. TS – TwinStrepII tag.

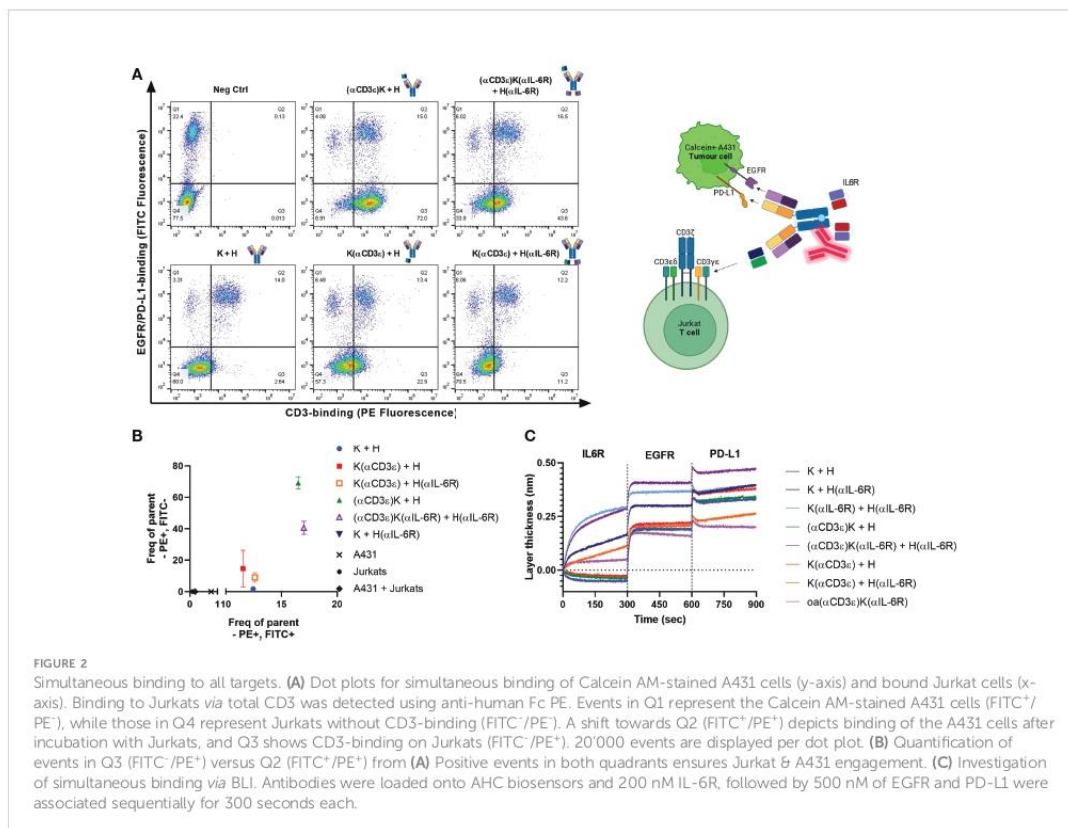
well compared with sarilumab IL-6R binding and ligand competition, however, the K(α CD3 ϵ) + H(α IL-6R) showed weaker competition (Figure 3A). This is presumably due to monovalent IL-6R binding, whereas both sarilumab and (α CD3 ϵ)K(α IL-6R) + H(α IL-6R) are bivalent. For PD-L1, all antibodies displayed good binding to PD-L1, which became weaker upon pre-incubation with PD-1, confirming competition of binding (Figure 3B).

As the parental K + H antibody binds to domain II of EGFR, it does not compete with its ligand EGF. However, it still inhibits the EGF-mediated signalling pathway (65). Similarly, sarilumab is able to inhibit IL-6-mediated signalling (77). Hence, pAKT and pSTAT3 were measured for EGF- and IL-6-mediated signalling inhibition, respectively. For IL-6/IL-6R, pSTAT3 analysis by HTRF assays revealed dose-dependent inhibition for both TriTECMs and the K(α IL-6R) + H(α IL-6R) control mAb (Figure 3C). While a slight reduction was noticed with 300 nM of either (α CD3 ϵ)K + H or K(α CD3 ϵ) + H, the inhibition was not as high as for the molecules with the anti-IL-6R scFv and similar to that of K + H. For EGF/EGFR signalling, pAKT was measured and all antibodies exhibited dose-dependent

inhibition compared to the EGF control, all very similar to the parental K + H antibody (Figure 3D). Furthermore, to investigate whether the antibodies could inhibit both pathways simultaneously, cells were pre-incubated with mAbs and then stimulated with a combination of EGF and IL-6. HTRF analysis revealed dose-dependent inhibition of both pathways as seen by pSTAT3 and pAKT inhibition (Figures 3E, F). Thus, despite minor differences in EGFR/PD-L1 binding of the TriTECMs as measured by affinity determination or on-cell affinities, their functionalities were retained compared to the parental two-in-one antibody in the K + H format.

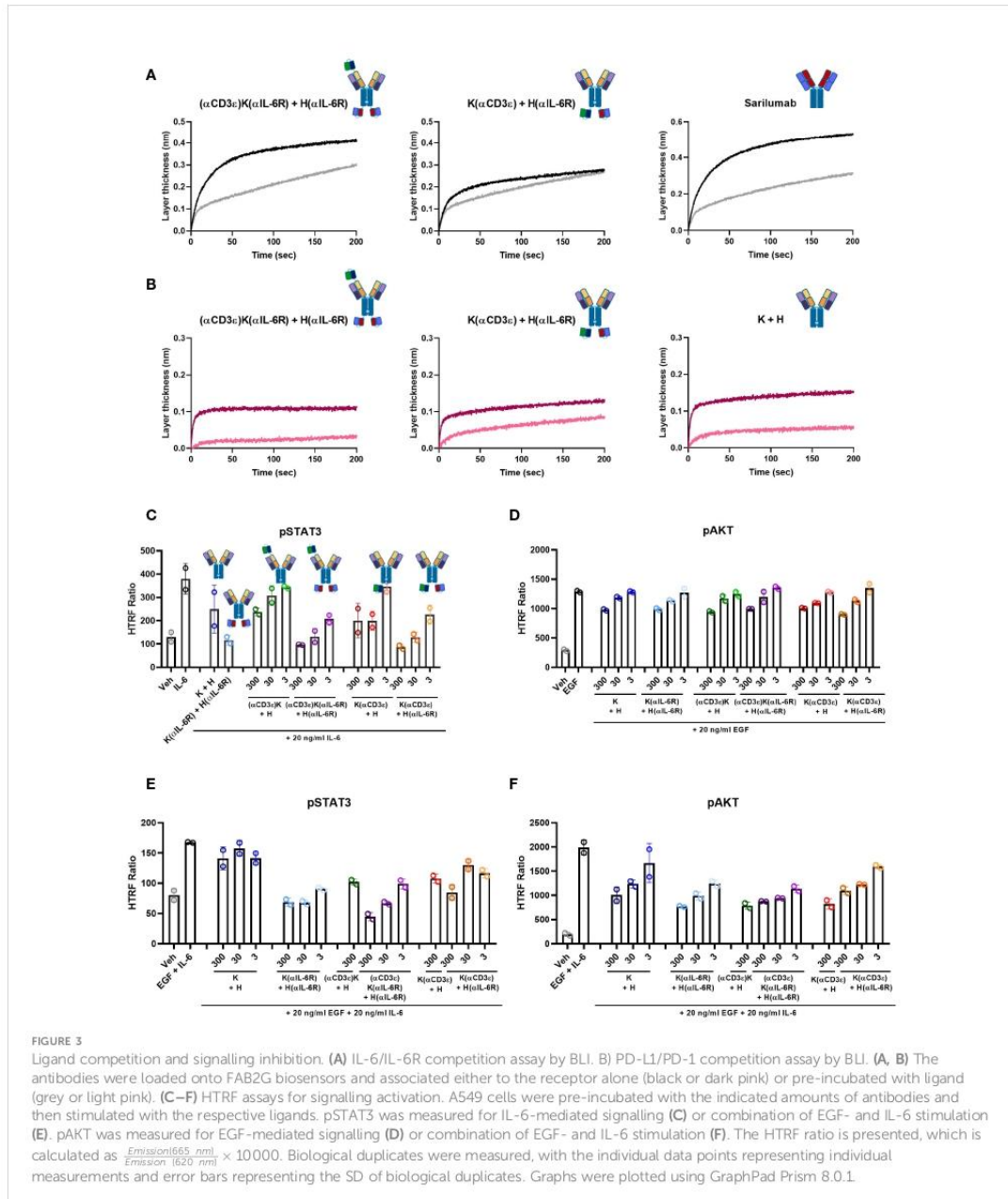
T-cell activation

A fundamental aspect of a T-cell engager is the ability of the CD3-binding moiety to activate T cells upon binding and engagement with tumour cells. To this end, a commercially available kit was used to measure activation of the NFAT pathway after engagement of effector (TCR/CD3 cells) and tumour cells (A431). Potent T-cell activation was observed for



the two variants carrying only NI0401 with EC₅₀ of 0.59 and 0.63 nM for (αCD3ε)K + H and K(αCD3ε)+H, respectively (Figures 4A, B). For the TriTECMs, a 5- and 10-fold reduction in EC₅₀ was observed compared to their counterparts lacking anti-IL-6R scFvs, with 2.51 and 5.60 nM for (αCD3ε)K(αIL-6R) +

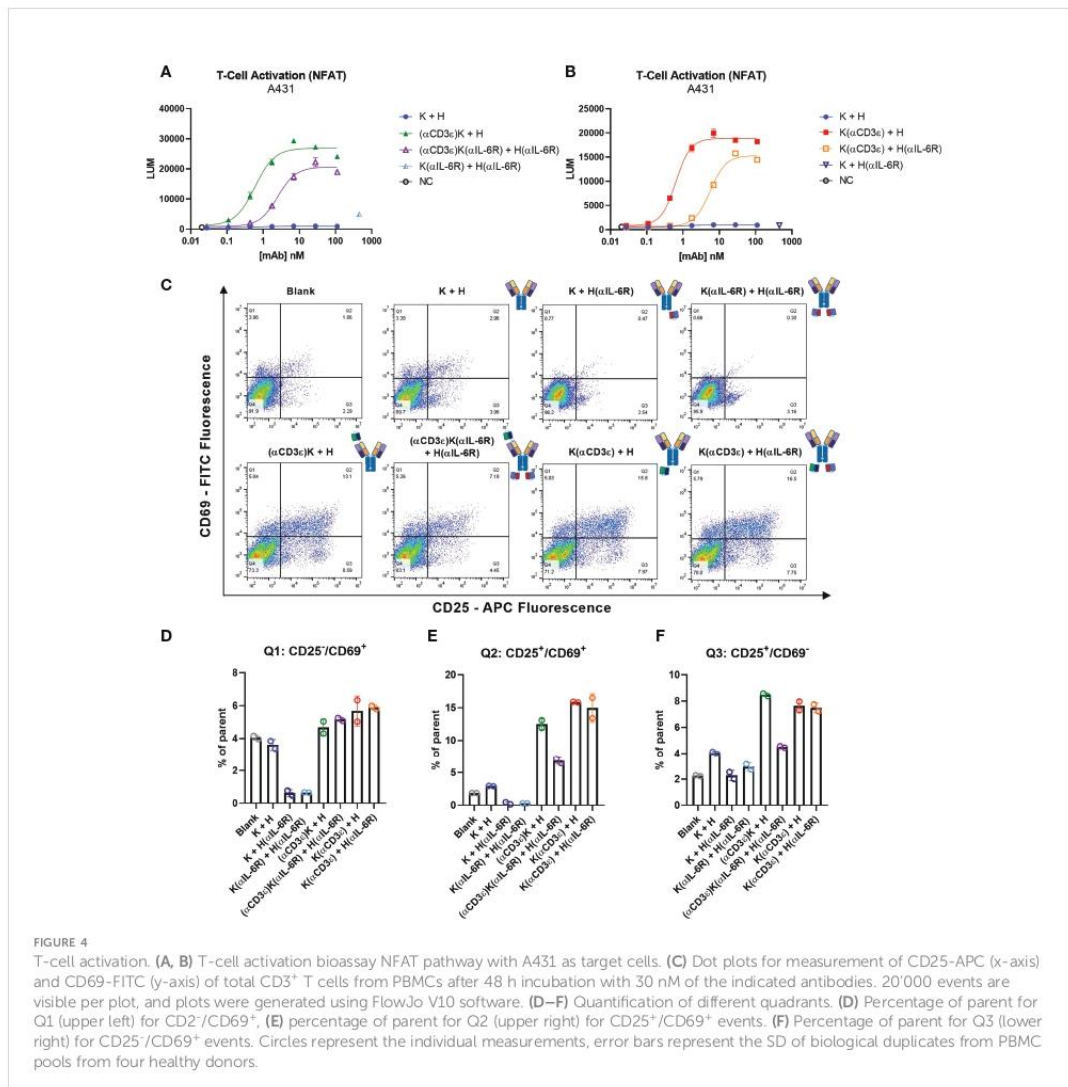
H(αIL-6R) and K(αCD3ε) + H(αIL-6R), respectively (Figures 4A, B). Nonetheless, significant T-cell activation was observed, meaning no complete loss-of-function occurred through the diminished CD3 binding on effector cells (Supplementary Table 1).



While immortalised cell lines can provide an estimate of *in vitro* potency, human peripheral blood mononuclear cells (PBMCs) isolated from healthy donors are a more reliable source. Subsequently, PBMCs were incubated with 30 nM of the indicated antibodies for 48 h and the early and late stage T-cell activation markers CD69 and CD25, respectively, were measured by flow cytometry (Figure 4C). While the control antibodies and blank measurements all showed similar levels, a significant increase in both activation markers (upper right quadrant) was observed where the CD3-binding NI0401 scFv was present, as expected. Quantification of the different quadrants showed increased expression in CD25/CD69 and

CD25 for all four NI0401-containing molecules, with a significant reduction for $(\alpha\text{CD3}\epsilon)\text{K}(\alpha\text{IL-6R}) + \text{H}(\alpha\text{IL-6R})$ compared to $(\alpha\text{CD3}\epsilon)\text{K} + \text{H}$, as previously observed (Figures 4E, F). Not many CD69⁺/CD25⁻ events were observed compared to the controls, however this could be due to the gradual decrease of CD69 with longer incubation times, as known from literature (78, 79) (Figure 4D).

In summary, T-cell activation was observed for all molecules with the CD3-binding NI0401 scFv, with the $(\alpha\text{CD3}\epsilon)\text{K}(\alpha\text{IL-6R}) + \text{H}(\alpha\text{IL-6R})$ showing the most attenuated T-cell activation, which might aid in the search for T-cell engagers with increased safety profiles.

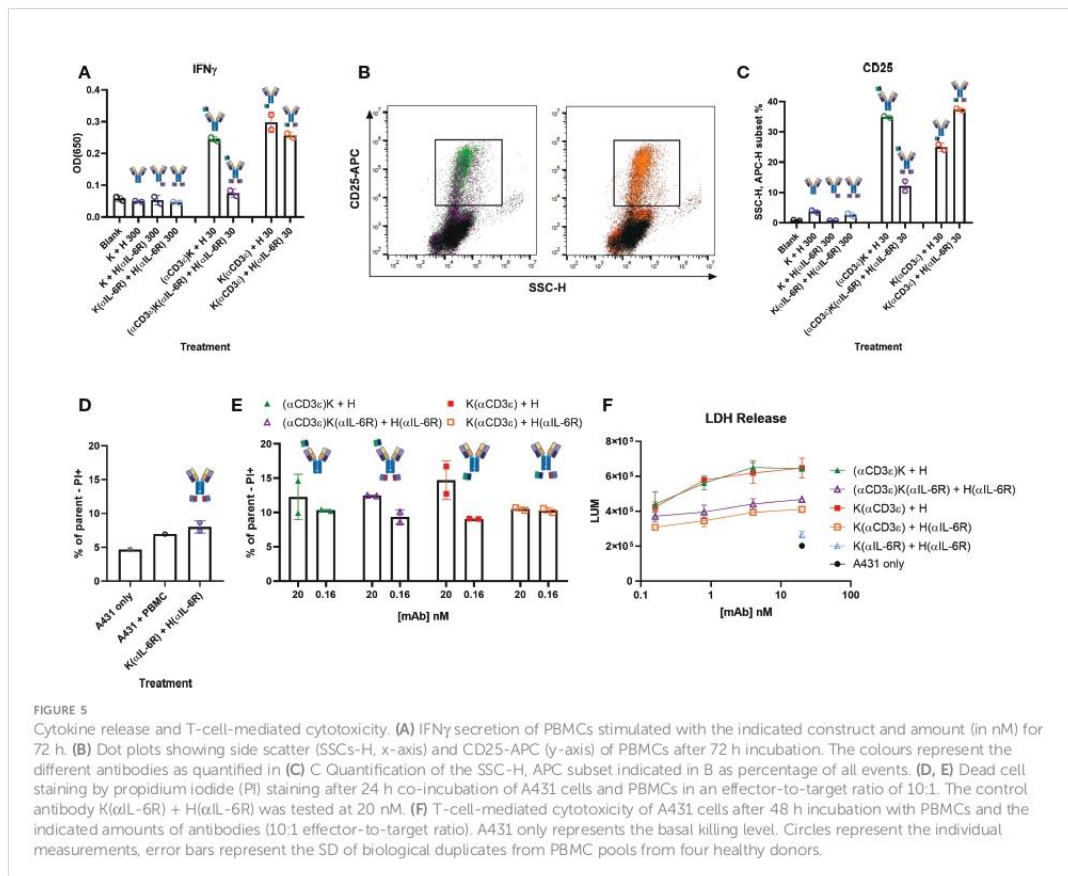


Attenuated cytokine release and cytotoxicity with TriTECMs

One of the large drawbacks of T-cell engagers is the increase in pro-inflammatory cytokines such as TNF α and IFN γ upon T-cell activation, leading to the hyperactivation of macrophages. A hyperactivation of macrophages leads to the secretion of high levels of IL-6 and other cytokines, ultimately resulting in a cytokine storm. To investigate whether the addition of the anti-IL-6R scFv module resulted in decreased pro-inflammatory cytokine release, PBMCs were stimulated with 30 nM of the respective antibodies and stimulated over 72 h. Thereafter, the release of pro-inflammatory IFN γ was measured in the supernatant (Figure 5A), and the cells themselves were stained with an APC-conjugated anti-CD25 antibody to measure T-cell activation (Figures 5B, C). In both cases, significant increases in either IFN γ or CD25 were observed compared to the controls (K +

H, K + H(α IL-6R), and K(α IL-6R) + H(α IL-6R)). In the case of IFN γ , a decrease was noted with the TriTECM (α CD3 ϵ)K(α IL-6R) + H(α IL-6R) compared to (α CD3 ϵ)K + H, hinting at both an attenuated activation and a decrease in cytokine release due to the anti-IL-6R scFv (Figure 5A). This effect was also noted for K(α CD3 ϵ) + H(α IL-6R) compared to K(α CD3 ϵ) + H but to a smaller extent, presumably due to monovalent IL-6R binding (Figure 5A). CD25 staining revealed significant T-cell activation with the TriTECM molecules compared to their controls (Figure 5C).

To ensure the attenuation of CD3-binding still led to decent T-cell-mediated cytotoxicity, cell killing of tumour cells by co-incubation with PBMCs was investigated. Dose-dependent cytotoxicity was observed through PI staining after 24 h co-incubation (Figures 5D, E; Supplementary Figure 4), with a slight reduction of activation for both TriTECM variants compared to their controls without Sar. Longer incubation



times of 48 h revealed T-cell-mediated cytotoxicity as measured by lactate dehydrogenase (LDH) release (Figure 5F; Supplementary Figure 5). While the tetraspecific molecules resulted in lowered cytotoxicity, these results, combined with previous T-cell activation studies (Figure 4) prove the attenuated nature of TriTECMs and their potential use as TCEs with a cytokine release and activity modulating function.

Discussion

With the increasing demand and interest for the development of new therapeutics in the fight against cancer, T-cell engagers and multispecific antibodies have been set in the spotlight as they are able to trigger and combine multiple mechanisms of action. For TCEs in particular, their safety profiles are often hindered by hyperstimulation of immune cells resulting in cytokine storms or cytokine release syndrome.

Within the scope of this work, proof-of-concept TriTECM molecules were designed consisting of a CD3-binding moiety derived from foralumab (71), an IL-6R binding module derived from sarilumab, and a bispecific two-in-one antibody binding both EGFR and PD-L1 (65). Production and purification of the antibodies as well as their respective controls using the KiH technology resulted in reasonable yields of pure product, considering the complexity of the molecules (80). High-affinity binding to both tumour targets, EGFR and PD-L1, as well as to IL-6R was observed *via* biolayer interferometry. On-cell affinities revealed high affinities to tumour cells but were decreased on both T cells and macrophages/monocytes, which could lead to improved tumour-penetration and accessibility into the tumour microenvironment without being captured before reaching the tumour site. Furthermore, the tetravalent TriTECMs were able to bind all antigens simultaneously. They retained the mechanism of action of the single antibody fragments when combined, including EGF- and IL-6 mediated signalling inhibition, and PD-L1/PD-1 axis blockade as determined by competition assays.

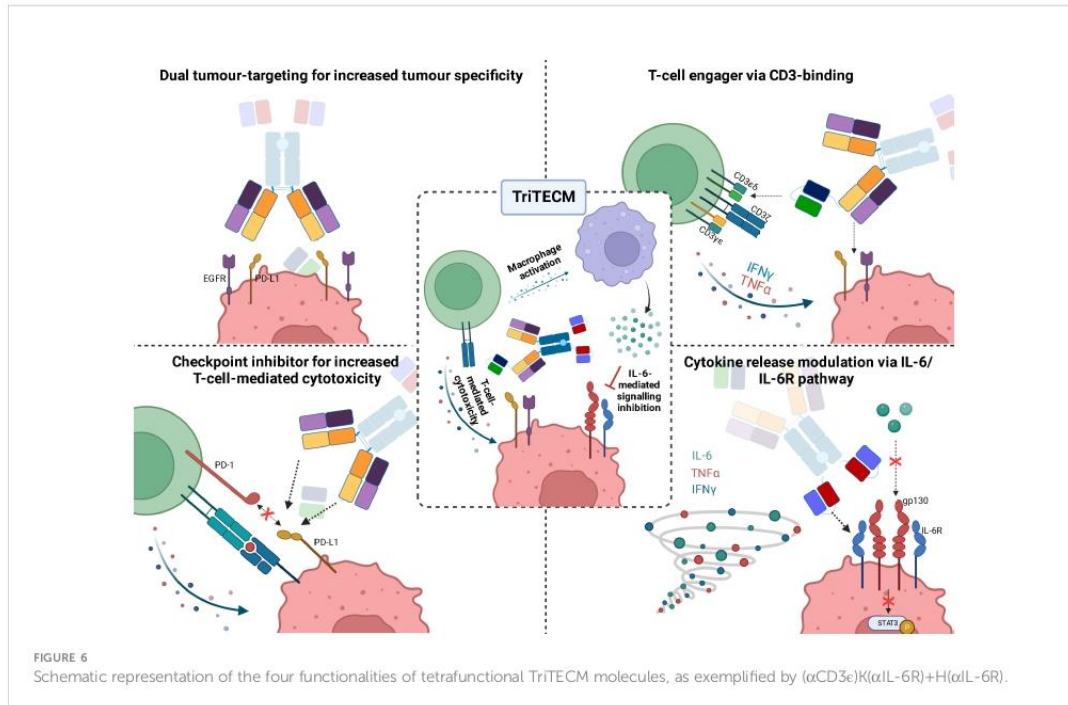
The design of the two reported TriTECMs vary mainly in their valency towards IL-6R, with $(\alpha\text{CD3}\epsilon)\text{K}(\alpha\text{IL-6R}) + \text{H}(\alpha\text{IL-6R})$ binding bivalently and $\text{K}(\alpha\text{CD3}\epsilon) + \text{H}(\alpha\text{IL-6R})$ only monovalently. The effect of monovalent IL-6R binding was primarily seen in the competition assay *via* BLI and inhibition of IL-6-mediated signalling when compared to either sarilumab itself or $(\alpha\text{CD3}\epsilon)\text{K}(\alpha\text{IL-6R}) + \text{H}(\alpha\text{IL-6R})$, which resulted in much stronger competition as well as inhibition. Additionally, the positioning of the anti-CD3 scFv was considered, either being placed in close proximity to the TAA-engaging Fab arm by an N-terminal VH fusion [for $(\alpha\text{CD3}\epsilon)\text{K}(\alpha\text{IL-6R}) + \text{H}(\alpha\text{IL-6R})$], or a C-terminal fusion to the CH3 domain of the Fc region [for $\text{K}(\alpha\text{CD3}\epsilon) + \text{H}(\alpha\text{IL-6R})$]. While previous results have identified higher potencies when the CD3-binder and the TAA-binder are in close proximity (75, 81), no significant

differences were noted in the T-cell activation bioassay performed in this study. An explanation for this could be the different conformations of the molecule due to the fused scFvs, possibly bridging the molecule in closer proximity and thus having similar effects for both architectures.

An attenuated T-cell engager was developed which nonetheless resulted in T-cell activation and T-cell-mediated cytotoxicity as seen both on immortalized cell lines and human-derived PBMCs. The decreased affinity to CD3 on cells might also prevent the over-stimulation of immune cells, as is the case for next-generation TCEs which are being developed with lower affinities to avoid cytotoxicity (81). Secretion of T cell-released IFN γ was found to be significantly reduced after incubation with $(\alpha\text{CD3}\epsilon)\text{K}(\alpha\text{IL-6R}) + \text{H}(\alpha\text{IL-6R})$ compared to $(\alpha\text{CD3}\epsilon)\text{K} + \text{H}$, noting the potential of such a molecule to mitigate cytokine storm events when combined directly with IL-6R inhibition. Further understanding of the modulation *via* IL-6R remains to be investigated. The functionality of this type of molecule with such a large number of modules having different modes of action requires extensive animal studies which were out-of-scope for this proof-of-concept study.

While combination therapies with anti-IL-6R agents (tocilizumab, sarilumab) have been investigated and approved for therapeutics-induced cytokine release syndrome (31, 33, 40), simultaneous administration by being fused to the mAb itself might prove beneficial. Hypothetical clinical findings after CAR T-cell therapy report dramatic increases in cytokine levels 3 days after infusion, with tocilizumab having to be administered at day 6 or 7 (31, 82, 83). By using a full-length IgG1 backbone, the serum half-life of such a molecule would be approximately 21 days (84, 86), thus being in frame with the current management approaches or interventions required when grade 2 CRS is reached. Furthermore, the direct fusion of an anti-IL-6R JAK/STAT pathway further downstream signalling by inhibiting the JAK/STAT pathway responsible for the promotion of tumour growth and metastasis could provide beneficial anti-tumour properties. Such a synergistic effect may be promoted by direct fusion to tumour-targeting antibodies rather than co-administration, thereby enhancing the accumulation of an IL-6R blocking entity in the tumour microenvironment.

In summary, the tetrafunctional TriTECMs could consist of: i) dual tumour-targeting for increased tumour specificity by targeting EGFR and PD-L1, ii) engagement of T cells *via* CD3 ϵ binding and bridging T cells in close proximity to tumour cells for tumour cell lysis, iii) increased T-cell-mediated cytotoxicity by blocking the PD-L1/PD-1 axis (checkpoint inhibitors), and iv) modulating cytokine storms or CRS by inhibiting the IL-6/IL-6R pathway by an anti-IL-6R scFv (Figure 6). Altogether, the advantages of TriTECMs may pave the way to finding novel biologicals for cancer therapies by harnessing the power of T cells. To further test this concept, other CD3-binding antibody



fragments could be tested, and more importantly, already-existing antibodies which were shown to be toxic due to CRS or other side-effects might be able to be recycled in such a format due to the attenuation and modulation of both T-cell activation and IL-6-mediated signalling. Due to the attenuation of the CD3-binding moiety, bivalent binding to CD3 could also be investigated. In order to avoid unwanted on-target off-tumour effects *via* IL-6R binding to other cell types, further antibody engineering may be required to fine-tune the affinity of the IL-6R binding moiety. Alternative strategies might also include pH-responsive binders to only allow binding of the mAb to IL-6R within the acidified tumour microenvironment, or alternatively masking this binding unit with an anti-idiotypic binder connected *via* a cleavable linker. Ultimately, highly complex models are required to elucidate the efficacy of TriTECMs in modulating CRS *in vivo*. Additionally, pentafunctional molecules could be envisioned by using an Fc that induces effector functions and compare the effects of both variants on cytokine release and T-cell-mediated cytotoxicity.

Data availability statement

The original contributions presented in the study are included in the article/Supplementary Material. Further inquiries can be directed to the corresponding author.

Author contributions

SC and HK conceived and designed experiments. SC, JG and JH performed experiments. SC, BH and HK analysed the data. JG, BH and HK have scientific advice and guidance. SC wrote the manuscript. All authors contributed to the article and approved the submitted version.

Acknowledgments

The authors would like to thank Janine Becker and Michael Ullitzka for their assistance in cell maintenance and antibody purification. Furthermore, we would like to thank the department of GPRD at Ferring Pharmaceuticals for funding. The funders played no role in study design, data collection/analysis, nor decision to publish. We acknowledge support by the Deutsche Forschungsgemeinschaft (DFG – German Research Foundation) and the Open Access Publishing Fund of the Technical University of Darmstadt.

Conflict of interest

Authors SCC and JG were employed by company Ferring Pharmaceuticals. Author BH was employed by company Aermium

Therapeutics. Authors SCC, JH, and HK are inventors of a patent related to the parental two-in-one antibody (EP22159491.4).

Publisher's note

All claims expressed in this article are solely those of the authors and do not necessarily represent those of their affiliated organizations, or those of the publisher, the editors and the reviewers. Any product that may be

evaluated in this article, or claim that may be made by its manufacturer, is not guaranteed or endorsed by the publisher.

Supplementary material

The Supplementary Material for this article can be found online at: <https://www.frontiersin.org/articles/10.3389/fimmu.2022.1051875/full#supplementary-material>

References

- Tian Z, Liu M, Zhang Y, Wang X. Bispecific T cell engagers: an emerging therapy for management of hematologic malignancies. *J Hematol Oncol* (2021) 14:75. doi: 10.1186/s13045-021-01084-4
- Runcie K, Budman DR, John V, Seetharamu N. Bi-specific and tri-specific antibodies- the next big thing in solid tumor therapeutics. *Mol Med* (2018) 24:50. doi: 10.1186/s10020-018-0051-4
- Elshiaty M, Schindler H, Christopoulos P. Principles and current clinical landscape of multispecific antibodies against cancer. *Int J Mol Sci* (2021) 22:5632. doi: 10.3390/ijms22115632
- Klein C, Schaefer W, Regula JT. The use of CrossMab technology for the generation of bi- and multispecific antibodies. *Mabs* (2016) 8:1010–20. doi: 10.1080/19420862.2016.1197457
- Waldman AD, Fritz JM, Lenardo MJ. A guide to cancer immunotherapy: from T cell basic science to clinical practice. *Nat Rev Immunol* (2020) 20:651–68. doi: 10.1038/s41577-020-0306-5
- Goebeler M-E, Bargou RC. T Cell-engaging therapies — BiTEs and beyond. *Nat Rev Clin Oncol* (2020) 17:418–34. doi: 10.1038/s41571-020-0347-5
- Zhou S, Liu M, Ren F, Meng X, Yu J. The landscape of bispecific T cell engager in cancer treatment. *Biomark Res* (2021) 9:38. doi: 10.1186/s40364-021-00294-9
- Cheadle EJ. MT-103 Micromet/ModImmune. *Curr Opin Mol Ther* (2006) 8:62–8.
- Helwick C. Novel BiTE antibody mediates contact between T cells and cancer cells, in: *Oncology NEWS international* (2008). Available at: <https://www.cancernetwork.com/view/novel-bite-antibody-mediates-contact-between-t-cells-and-cancer-cells> (Accessed August 22, 2022).
- European Medicines Agency. *Blinicyto* (2015). Available at: <https://www.ema.europa.eu/en/medicines/human/EPAR/blincyto> (Accessed June 27, 2022).
- Goebeler M-E, Bargou R. Blinatumomab: a CD19/CD3 bispecific T cell engager (BiTE) with unique anti-tumor efficacy. *Leuk Lymphoma* (2016) 57:1021–32. doi: 10.3109/10428194.2016.1161185
- Wu J, Fu J, Zhang M, Liu D. Blinatumomab: a bispecific T cell engager (BiTE) antibody against CD19/CD3 for refractory acute lymphoid leukemia. *J Hematol Oncol* (2015) 8:104. doi: 10.1186/s13045-015-0195-4
- Burt R, Warcel D, Fielding AK. Blinatumomab, a bispecific b-cell and T-cell engaging antibody, in the treatment of b-cell malignancies. *Hum Vaccin Immunother* (2019) 15:594–602. doi: 10.1080/21645515.2018.1540828
- Wu Y, Yi M, Zhu S, Wang H, Wu K. Recent advances and challenges of bispecific antibodies in solid tumors. *Exp Hematol Oncol* (2021) 10:56. doi: 10.1186/s40164-021-00250-1
- Linke R, Klein A, Seimetz D. Catumaxomab. *Mabs* (2010) 2:129–36. doi: 10.4161/mabs.2.2.11221
- Ma J, Mo Y, Tang M, Shen J, Qi Y, Zhao W, et al. Bispecific antibodies: From research to clinical application. *Front Immunol* (2021) 12:626616. doi: 10.3389/fimmu.2021.626616
- Jain T, Litzow MR. Management of toxicities associated with novel immunotherapy agents in acute lymphoblastic leukemia. *Ther Adv Hematol* (2020) 11:204062071989989. doi: 10.1177/2040620719899899
- Frey NV, Porter DL. Cytokine release syndrome with novel therapeutics for acute lymphoblastic leukemia. *Hematology* (2016) 2016:567–72. doi: 10.1182/asheducation-2016.1.567
- Shimabukuro-Vornhagen A, Gödel P, Subklewe M, Stemmler HJ, Schlöfer HA, Schlaak M, et al. Cytokine release syndrome. *J Immunother Cancer* (2018) 6:56. doi: 10.1186/s40425-018-0343-9
- Li X, Shao M, Zeng X, Qian P, Huang H. Signaling pathways in the regulation of cytokine release syndrome in human diseases and intervention therapy. *Signal Transduct Target Ther* (2021) 6:367. doi: 10.1038/s41392-021-00764-4
- Teachey DT, Rheingold SR, Maude SL, Zugmaier G, Barrett DM, Seif AE, et al. Cytokine release syndrome after blinatumomab treatment related to abnormal macrophage activation and ameliorated with cytokine-directed therapy. *Blood* (2013) 121:5154–7. doi: 10.1182/blood-2013-02-485623
- Gramatzki M, Burger R, Strobel G, Trautmann U, Bartram CR, Helm G, et al. Therapy with OKT3 monoclonal antibody in refractory T cell acute lymphoblastic leukemia induces interleukin-2 responsiveness. *Leukemia* (1995) 9:382–90.
- Mahmud N, Klipa D, Ahsan N. Antibody immunosuppressive therapy in solid-organ transplant. *Mabs* (2010) 2:148–56. doi: 10.4161/mabs.2.2.11159
- Chatenoud L, Ferran C, Reuter A, Legendre C, Gevaert Y, Kreis H, et al. Systemic reaction to the anti-T-Cell monoclonal antibody OKT3 in relation to serum levels of tumor necrosis factor and interferon- α . *New Engl J Med* (1989) 320:1420–1. doi: 10.1056/NEJM198905253202117
- Chatenoud L, Ferran C, Legendre C, Thouard I, Merite S, Reuter A, et al. *In vivo* cell activation following OKT3 administration. *Transplantation* (1990) 49:697–702. doi: 10.1097/00007890-199004000-00009
- Neelapu SS, Tummala S, Kebriaei P, Wierda W, Gutierrez C, Locke FL, et al. Chimeric antigen receptor T-cell therapy — assessment and management of toxicities. *Nat Rev Clin Oncol* (2018) 15:47–62. doi: 10.1038/nrclinonc.2017.148
- Schuster SJ, Maziarz RT, Rusch ES, Li J, Signorovitch JE, Romanov VV, et al. Grading and management of cytokine release syndrome in patients treated with tisagenlecleucel in the JULIET trial. *Blood Adv* (2020) 4:1432–9. doi: 10.1182/bloodadvances.2019001304
- Lee DW, Santomaso BD, Locke FL, Ghobadi A, Turtle CJ, Brudno JN, et al. ASTCT consensus grading for cytokine release syndrome and neurologic toxicity associated with immune effector cells. *Biol Blood Marrow Transplant* (2019) 25:625–38. doi: 10.1016/j.bbmt.2018.12.758
- Matthys P, Dillen C, Proost P, Heremans H, And JVD, Billiau A. Modification of the anti-CD3-induced cytokine release syndrome by anti-interferon- γ or anti-interleukin-6 antibody treatment: Protective effects and biphasic changes in blood cytokine levels. *Eur J Immunol* (1993) 23:2209–16. doi: 10.1002/eji.1830230924
- Tanaka T, Narazaki M, Kishimoto T. Immunotherapeutic implications of IL-6 blockade for cytokine storm. *Immunotherapy* (2016) 8:959–70. doi: 10.2217/imt-2016-0020
- Lee DW, Gardner R, Porter DL, Louis CU, Ahmed N, Jensen M, et al. Current concepts in the diagnosis and management of cytokine release syndrome. *Blood* (2014) 124:188–95. doi: 10.1182/blood-2014-05-552729
- Le RQ, Li L, Yuan W, Shord SS, Nie L, Habtemariam BA, et al. FDA Approval summary: Tocilizumab for treatment of chimeric antigen receptor T cell-induced severe or life-threatening cytokine release syndrome. *Oncologist* (2018) 23:943–7. doi: 10.1634/theoncologist.2018-0028
- Si S, Teachey DT. Spotlight on tocilizumab in the treatment of CAR-T-Cell-Induced cytokine release syndrome: Clinical evidence to date. *Ther Clin Risk Manag* (2020) 16:705–14. doi: 10.2147/TCRM.S223468

34. Kadauke S, Myers RM, Li Y, Aplenc R, Baniewicz D, Barrett DM, et al. Risk-adapted preemptive tocilizumab to prevent severe cytokine release syndrome after CTL019 for pediatric b-cell acute lymphoblastic leukemia: A prospective clinical trial. *J Clin Oncol* (2021) 39:920–30. doi: 10.1200/JCO.20.02477
35. Chen J-J, Zhang L-N, Hou H, Xu L, Ji K. Interleukin-6 signaling blockade treatment for cytokine release syndrome in COVID-19 (Review). *Exp Ther Med* (2020) 21:1–1. doi: 10.3892/etm.2020.9456
36. REMAP-CAP. Interleukin-6 receptor antagonists in critically ill patients with covid-19. *N Engl J Med* (2021) 384:1491–502. doi: 10.1056/NEJMoa2100433
37. Chamlagain R, Shah S, Sharma Paudel B, Dhital R, Kandel B. Efficacy and safety of sarilumab in COVID-19: A systematic review. *Interdiscip Perspect Infect Dis* (2021) 2021:1–8. doi: 10.1155/2021/8903435
38. Mariette X, Hermine O, Tharaux P-L, Resche-Rigon M, Porcher R, Ravaud P, et al. Sarilumab in adults hospitalised with moderate-to-severe COVID-19 pneumonia (CORIMUNO-SARI-1): An open-label randomised controlled trial. *Lancet Rheumatol* (2022) 4:e24–32. doi: 10.1016/S2665-9913(21)00315-5
39. Rubin EJ, Longo DL, Baden LR. Interleukin-6 receptor inhibition in covid-19 — cooling the inflammatory soup. *N Engl J Med* (2021) 384:1564–5. doi: 10.1056/NEJMe2103108
40. León López R, Fernández SC, Limia Pérez L, Romero Palacios A, Fernández-Roldán MC, Aguilar Alonso E, et al. Efficacy and safety of early treatment with sarilumab in hospitalised adults with COVID-19 presenting cytokine release syndrome (SARICOR STUDY): protocol of a phase II, open-label, randomised, multicentre, controlled clinical trial. *BMJ Open* (2020) 10:e039951. doi: 10.1136/bmjopen-2020-039951
41. Meanwathana J, Majam T. Interleukin-6 antagonists: Lessons from cytokine release syndrome to the therapeutic application in severe COVID-19 infection. *J Pharm Pract* (2021) 35, 089719002110006. doi: 10.1177/08971900211000691
42. Corominas H, Castellví I, Diaz-Torné C, Matas L, de la Rosa D, Mangués MA, et al. Sarilumab (IL-6R antagonist) in critically ill patients with cytokine release syndrome by SARS-CoV2. *Medicine* (2021) 100:e25923. doi: 10.1097/MD.00000000000025923
43. Johnson DE, O'Keefe RA, Grandis JR. Targeting the IL-6/JAK/STAT3 signalling axis in cancer. *Nat Rev Clin Oncol* (2018) 15:234–48. doi: 10.1038/nrclinonc.2018.8
44. Heo T-H, Wahler J, Suh N. Potential therapeutic implications of IL-6/IL-6R/gp130-targeting agents in breast cancer. *Oncotarget* (2016) 7:15460–73. doi: 10.18632/oncotarget.7102
45. Thomas SJ, Snowden JA, Zeidler MP, Danson SJ. The role of JAK/STAT signalling in the pathogenesis, prognosis and treatment of solid tumours. *Br J Cancer* (2015) 113:365–71. doi: 10.1038/bjc.2015.233
46. Tumberink HL, Heimsoth A, Sos ML. The next tier of EGFR resistance mutations in lung cancer. *Oncogene* (2021) 40:1–11. doi: 10.1038/s41388-020-01510-w
47. Yun C-H, Mengwasser KE, Toms A v., Woo MS, Greulich H, Wong K-K, et al. The T790M mutation in EGFR kinase causes drug resistance by increasing the affinity for ATP. *Proc Natl Acad Sci* (2008) 105:2070–5. doi: 10.1073/pnas.0709662105
48. Ray K, Ujvari B, Ramana V, Donald J. Cross-talk between EGFR and IL-6 drives oncogenic signaling and offers therapeutic opportunities in cancer. *Cytokine Growth Factor Rev* (2018) 41:18–27. doi: 10.1016/j.cytogfr.2018.04.002
49. Colomiere M, Ward AC, Riley C, Trenerry MK, Cameron-Smith D, Findlay J, et al. Cross talk of signals between EGFR and IL-6R through JAK2/STAT3 mediate epithelial-mesenchymal transition in ovarian carcinomas. *Br J Cancer* (2009) 100:134–44. doi: 10.1038/sj.bjc.6604794
50. Lin Y, Xu J, Lan H. Tumor-associated macrophages in tumor metastasis: biological roles and clinical therapeutic applications. *J Hematol Oncol* (2019) 12:76. doi: 10.1186/s13045-019-0760-3
51. Wan S, Zhao E, Kryczek I, Vatan L, Sadvokaya A, Ludema G, et al. Tumor-associated macrophages produce interleukin 6 and signal via STAT3 to promote expansion of human hepatocellular carcinoma stem cells. *Gastroenterology* (2014) 147:1393–404. doi: 10.1053/j.gastro.2014.08.039
52. Caetano MS, Zhang H, Cumpian AM, Gong L, Unver N, Ostrin EJ, et al. IL6 blockade reprograms the lung tumor microenvironment to limit the development and progression of k-ras-mutant lung cancer. *Cancer Res* (2016) 76:3189–99. doi: 10.1158/0008-5472.CAN-15-2840
53. Jeong SK, Kim JS, Lee CG, Park Y-S, Kim SD, Yoon SO, et al. Tumor associated macrophages provide the survival resistance of tumor cells to hypoxic microenvironmental condition through IL-6 receptor-mediated signals. *Immunobiology* (2017) 222:55–65. doi: 10.1016/j.imbio.2015.11.010
54. Sarode P, Schaefer MB, Grimminger F, Seeger W, Savai R. Macrophage and tumor cell cross-talk is fundamental for lung tumor progression: We need to talk. *Front Oncol* (2020) 10:324. doi: 10.3389/fonc.2020.00324
55. Hu R, Han Q, Zhang J. STAT3: A key signaling molecule for converting cold to hot tumors. *Cancer Lett* (2020) 489:29–40. doi: 10.1016/j.canlet.2020.05.035
56. Chen W, Yang F, Wang C, Narula J, Pascua E, Ni I, et al. One size does not fit all: navigating the multi-dimensional space to optimize T-cell engaging protein therapeutics. *MAbs* (2021) 13:1–18. doi: 10.1080/19420862.2020.1871171
57. Wang S, Chen K, Lei Q, Ma P, Yuan AQ, Zhao Y, et al. The state of the art of bispecific antibodies for treating human malignancies. *EMBO Mol Med* (2021) 13:1–13. doi: 10.15252/emmm.202114291
58. Haber L, Olson K, Kelly MP, Crawford A, DiLillo DJ, Tavaré R, et al. Generation of T-cell-redirecting bispecific antibodies with differentiated profiles of cytokine release and biodistribution by CD3 affinity tuning. *Sci Rep* (2021) 11:14397. doi: 10.1038/s41598-021-93842-0
59. Dang K, Castello G, Clarke SC, Li Y, Balasubramani A, Boudreau A, et al. Attenuating CD3 affinity in a PSMAXCD3 bispecific antibody enables killing of prostate tumor cells with reduced cytokine release. *J Immunother Cancer* (2021) 9:e002488. doi: 10.1136/jitc-2021-002488
60. Staffin K, Zuch de Zafra CL, Schutt LK, Clark V, Zhong F, Hristopoulos M, et al. Target arm affinities determine preclinical efficacy and safety of anti-HER2/CD3 bispecific antibody. *JCI Insight* (2020) 5:1–15. doi: 10.1172/jci.insight.133757
61. Tapia-Galisteo A, Sánchez Rodríguez I, Aguilar-Sopena O, Harwood SL, Narbona J, Ferreras Gutierrez M, et al. Trispecific T-cell engagers for dual tumor-targeting of colorectal cancer. *Oncimmunology* (2022) 11:1–14. doi: 10.1080/2162402X.2022.2034355
62. Wu L, Seung E, Xu L, Rao E, Lord DM, Wei RR, et al. Trispecific antibodies enhance the therapeutic efficacy of tumor-directed T cells through T cell receptor co-stimulation. *Nat Cancer* (2020) 1:86–98. doi: 10.1038/s43018-019-0004-z
63. Society TA. *Antibody therapeutics in late-stage clinical studies* (2022). Available at: <https://www.antibodysociety.org/antibodies-in-late-stage-clinical-studies/> (Accessed June 28, 2022).
64. Society TA. *Antibody therapeutics product data* (2022). Available at: <https://www.antibodysociety.org/antibody-therapeutics-product-data/> (Accessed June 28, 2022).
65. Harwardt J, Bogen JP, Carrara SC, Ulitzka M, Grzeschik J, Hock B, et al. A generic strategy to generate bifunctional two-in-One antibodies by chicken immunization. *Front Immunol* (2022) 13:888838. doi: 10.3389/fimmu.2022.888838
66. Omx Personal Health Analytics Inc. *DrugBank*. Available at: <https://www.drugbank.com/> (Accessed August 16, 2022).
67. Lund J, Pound JD, Jones PT, Duncan AR, Bentley T, Goodall M, et al. Multiple binding sites on the CH2 domain of IgG for mouse FcγR11. *Mol Immunol* (1992) 29:53–9. doi: 10.1016/0161-5890(92)90156-R
68. Ridgway JBB, Presta LG, Carter P. 'Knobs-into-holes' engineering of antibody CH3 domains for heavy chain heterodimerization. *Protein Engineering Design Selection* (1996) 9:617–21. doi: 10.1093/protein/9.7.617
69. Bogen JP, Carrara SC, Fiebig D, Grzeschik J, Hock B, Kolmar H. Expedient generation of biparatopic common light chain antibodies via chicken immunization and yeast display screening. *Front Immunol* (2020) 11:606878. doi: 10.3389/fimmu.2020.606878
70. Bogen JP, Carrara SC, Fiebig D, Grzeschik J, Hock B, Kolmar H. Design of a trispecific checkpoint inhibitor and natural killer cell engager based on a 2 + 1 common light chain antibody architecture. *Front Immunol* (2021) 12:669496. doi: 10.3389/fimmu.2021.669496
71. Ogura M, Deng S, Preston-Hurlburt P, Ogura H, Shaibubhai K, Kuhn C, et al. Oral treatment with foralumab, a fully human anti-CD3 monoclonal antibody, prevents skin xenograft rejection in humanized mice. *Clin Immunol* (2017) 183:240–6. doi: 10.1016/j.clim.2017.07.005
72. Moreira TG, Matos KTF, De Paula GS, Santana TMM, Da Mata RG, Pansera FC, et al. Nasal administration of anti-CD3 monoclonal antibody (Foralumab) reduces lung inflammation and blood inflammatory biomarkers in mild to moderate COVID-19 patients: A pilot study. *Front Immunol* (2021) 12:709861. doi: 10.3389/fimmu.2021.709861
73. Clinical Trials. (2022). Available at: <https://clinicaltrials.gov/> (Accessed August 17, 2022).
74. Xu C, Rafique A, Potocky T, Pacaly A, Nolain P, Lu Q, et al. Differential binding of sarilumab and tocilizumab to IL-6Rα and effects of receptor occupancy on clinical parameters. *J Clin Pharmacol* (2021) 61:714–24. doi: 10.1002/jcph.1795
75. Dickopf S, Georges GJ, Brinkmann U. Format and geometries matter: Structure-based design defines the functionality of bispecific antibodies. *Comput Struct Biotechnol J* (2020) 18:1221–7. doi: 10.1016/j.csbj.2020.05.006
76. Raimondo MG, Biggioggero M, Crotti C, Becciolini A, Favalli EG. Profile of sarilumab and its potential in the treatment of rheumatoid arthritis. *Drug Des Devel Ther* (2017) 11:1593–603. doi: 10.2147/DDDT.S100302
77. Testi R, D'Ambrosio D, de Maria R, Santoni A. The CD69 receptor: a multipurpose cell-surface trigger for hematopoietic cells. *Immunol Today* (1994) 15:479–83. doi: 10.1016/0167-5699(94)90193-7

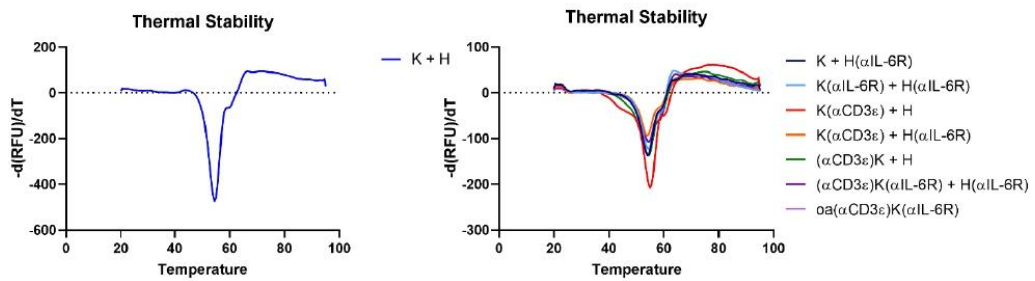
78. Ziegler SF, Ramsdell F, Alderson MR. The activation antigen CD69. *Stem Cells* (1994) 12:456–65. doi: 10.1002/stem.5530120502
79. Fang XT, Sehlin D, Lannfelt L, Syvänen S, Hultqvist G. Efficient and inexpensive transient expression of multispecific multivalent antibodies in Expi293 cells. *Biol Proced Online* (2017) 19:11. doi: 10.1186/s12575-017-0060-7
80. Vafa O, Trinklein ND. Perspective: Designing T-cell engagers with better therapeutic windows. *Front Oncol* (2020) 10:446. doi: 10.3389/fonc.2020.00446
81. Zhang Y, Zhou F, Wu Z, Li Y, Li C, Du M, et al. Timing of tocilizumab administration under the guidance of IL-6 in CAR-T therapy for R/R acute lymphoblastic leukemia. *Front Immunol* (2022) 13:914959. doi: 10.3389/fimmu.2022.914959
82. Morris EC, Neelapu SS, Giavridis T, Sadelain M. Cytokine release syndrome and associated neurotoxicity in cancer immunotherapy. *Nat Rev Immunol* (2022) 22:85–96. doi: 10.1038/s41577-021-00547-6
83. Saxena A, Wu D. Advances in therapeutic fc engineering – modulation of IgG-associated effector functions and serum half-life. *Front Immunol* (2016) 7:580. doi: 10.3389/fimmu.2016.00580
84. Mankarious S, Lee M, Fischer S, Pyun KH, Ochs HD, Oxelius VA, et al. The half-lives of IgG subclasses and specific antibodies in patients with primary immunodeficiency who are receiving intravenously administered immunoglobulin. *J Lab Clin Med* (1988) 112:634–40.

Supplementary Material

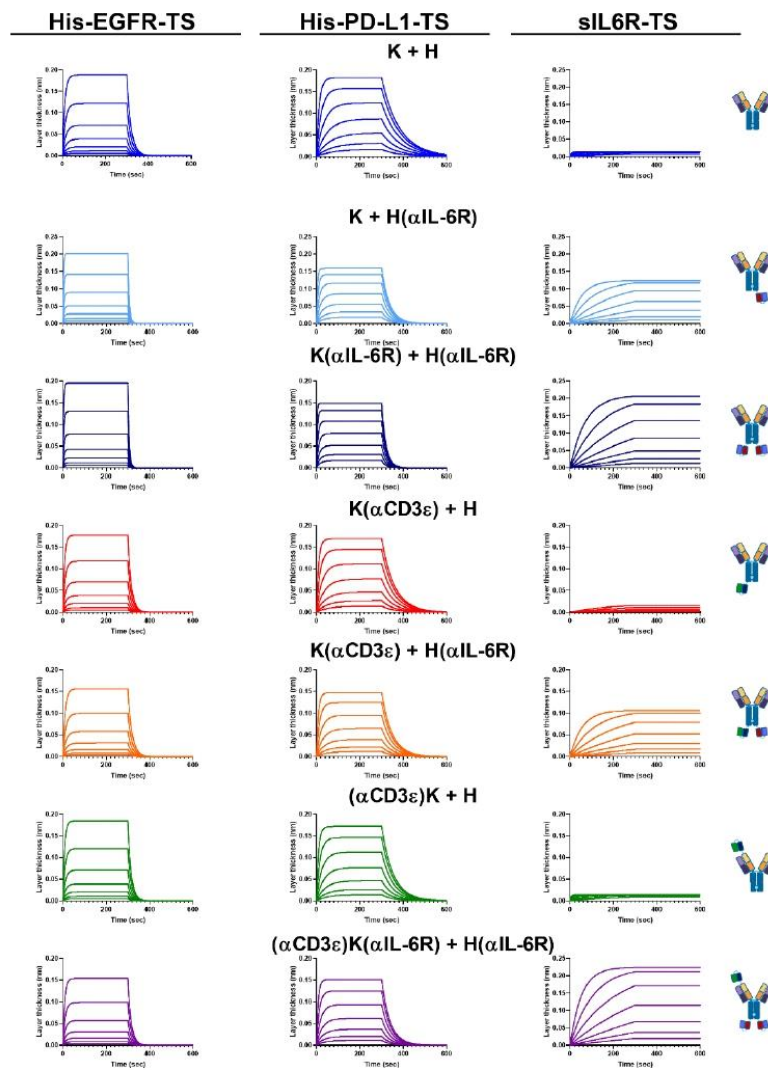
TriTECM: A Tetrafunctional T-Cell Engaging Antibody with Built-In Risk Mitigation of Cytokine Release Syndrome

Stefania C. Carrara^{1,2}, Julia Harwardt¹, Julius Grzeschik³, Björn Hock⁴, Harald Kolmar^{1,5*}

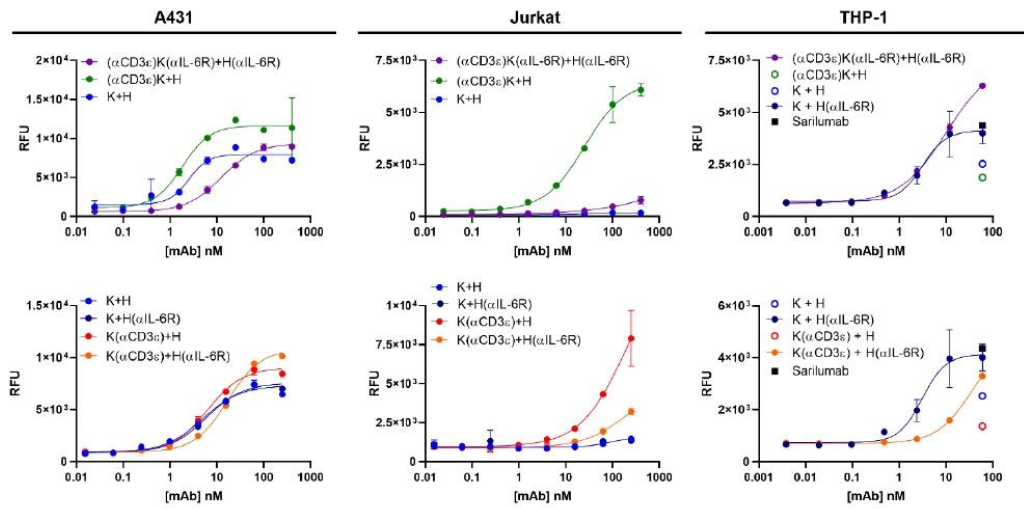
1 Supplementary Figures and Tables



Supplementary Figure 1: Melt peaks after thermal shift assay by SYPRO Orange. RFU – relative fluorescence units. The derivative of RFU is plotted against temperature in a range from 20 – 95 °C. The dotted line represents the threshold set to determine the melt temperature.



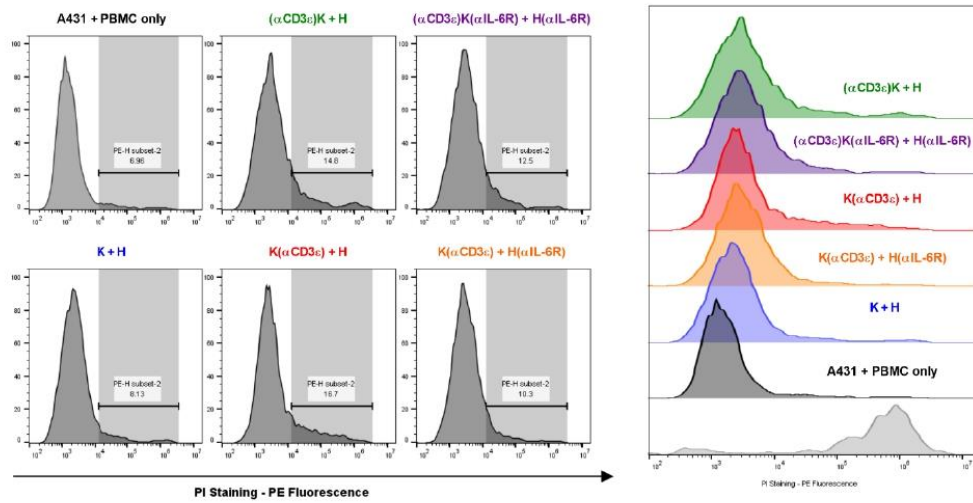
Supplementary Figure 2: Affinity determination by biolayer interferometry. The binding curves for His-EGFR-TS (left), His-PD-L1-TS (middle) or soluble IL6R-TS (right) are displayed for all antibodies. The colour-coding represents the different variants. For His-EGFR-TS and His-PD-L1-TS, a concentration range of 7.8 – 500 nM was measured, while for sIL6R-TS a range from 3.125 – 200 nM was measured.



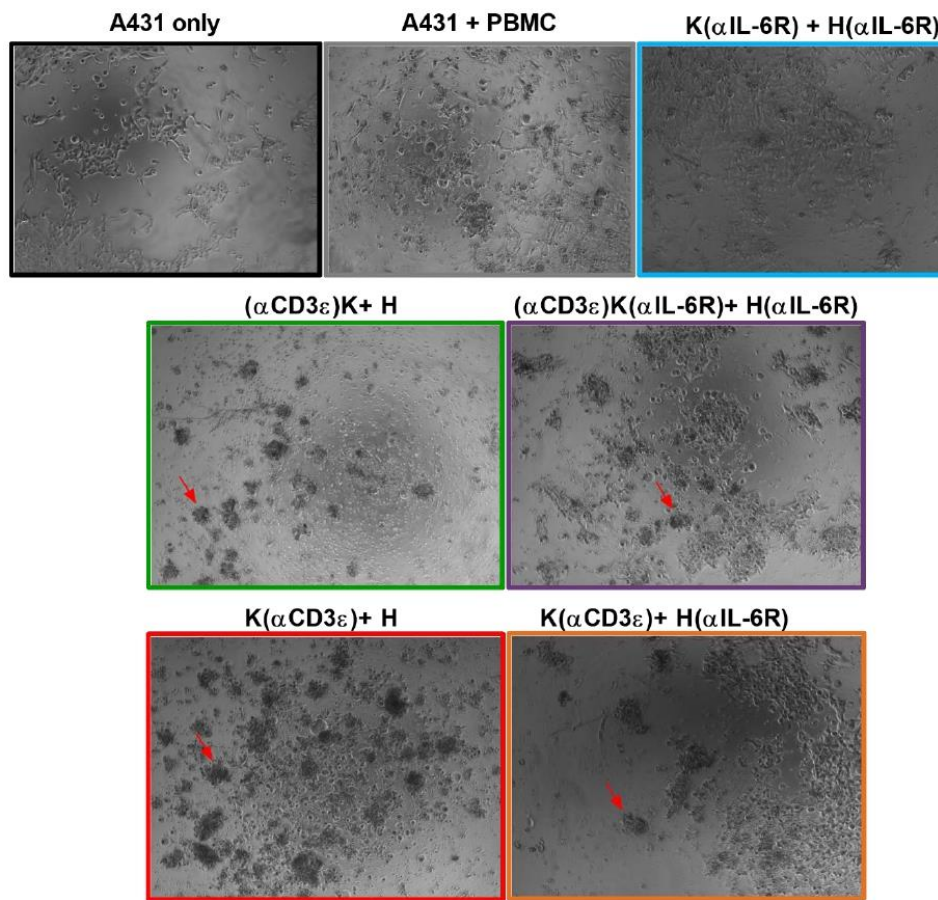
Supplementary Figure 3: On-cell titrations. The antibodies were tested for either CD3-binding (Jurkat), IL6R-binding (THP-1) or EGFR/PD-L1-binding (A431). The top panel show the variants with an N-terminal NI0401 scFv fusion, whereas the bottom panel shows the C-terminal NI0401 scFv variants with the respective controls. The mean fluorescence was determined and plotted using GraphPad prism. A non-linear regression was determined to calculate the on-cell affinities. RFU – relative fluorescence units.

Supplementary Table 1: On-cell affinities on A431 (EGFR⁺⁺⁺/PD-L1⁺), Jurkat (CD3⁺) and THP-1 (IL6R⁺/PD-L1⁺).

Variant	On-cell affinity (nM)		
	A431	Jurkat	THP-1
K + H	2.50	-	-
K + H(αIL-6R)	4.30	-	3.10
K(αCD3ϵ) + H	4.50	195.90	-
K(αCD3ϵ) + H(αIL-6R)	21.24	213.80	36.66
(αCD3ϵ)K + H	1.82	25.38	-
(αCD3ϵ)K(αIL-6R) + H(αIL-6R)	12.34	n.d.	10.08



Supplementary Figure 4: Histograms and half-offset overlays for dead cell staining with propidium iodide (PI) after co-culture of A431 and PBMCs for 24 h to measure T-cell-mediated cytotoxicity. Histograms and overlays were generated using FlowJo V10 software.



Supplementary Figure 5: Bright field images of A431 and PBMC co-culture in combination with 20 nM of the indicated antibodies after 48 h incubation. Black dead target cell clusters are exemplified by red arrows in each of the relevant images.

4.6 Antibody Library Screening Using Yeast Biopanning and Fluorescence-Activated Cell Sorting

Title:

Antibody Library Screening Using Yeast Biopanning and Fluorescence-Activated Cell Sorting

Authors:

Stefania Candela Carrara*, Jan Patrick Bogen*, Julius Grzeschik, Björn Hock, Harald Kolmar.
(* shared first authorship)

Bibliographic Data:

Book – *Methods in Molecular Biology* Book Series

Volume 2491, Yeast Surface Display pp. 177-193

First online: 29th April 2022

DOI: 10.1007/978-1-0716-2285-8_10

© 2022 under exclusive license to Springer Science+ Business Media, LLC part of Springer Nature

Contributions by S.C. Carrara:

- Writing of manuscript together with J.P. Bogen.
- Design and generation of figures with J.P. Bogen.



Chapter 10

Antibody Library Screening Using Yeast Biopanning and Fluorescence-Activated Cell Sorting

Stefania C. Carrara, Jan P. Bogen, Julius Grzeschik, Björn Hock, and Harald Kolmar

Abstract

Yeast surface display (YSD) emerged as a prominent screening methodology for the isolation of monoclonal antibodies (mAbs) against various antigens. However, phage display remains the gold standard in cell panning-based screenings to isolate mAbs against difficult-to-screen targets, such as G-protein coupled receptors (GPCR) and ion channels. Herein we describe a step-by-step protocol to establish and perform the isolation of mAbs using YSD in a fluorescence-activated cell sorting (FACS)-assisted biopanning manner, yielding a variety of antibodies binding their antigen with high affinity in the natural environment of the cell. Upon mixing antibody-displaying yeast cells with antigen-displaying mammalian cells, complexes are specifically formed and isolated for enrichment of yeast cells encoding binders against the antigen. The utilization of mammalian cells expressing the respective target accounts for accessibility of the epitope and the correct conformation of the antigen. Furthermore, critical characterization methods mandatory for this kind of antibodies are illuminated.

Key words Yeast biopanning, FACS, Yeast surface display, Antibody library screening, Hit discovery

1 Introduction

Ion channels, receptor tyrosine kinases, and G-protein coupled receptors (GPCR) are protein classes of major interest for therapeutic drug targets. However, the isolation of antibodies specific for those molecules remains a challenge. Due to the difficulties presented in expressing and producing such antigens in a soluble form, phage display, first described in 1985, is the state-of-the-art technology to perform cell panning-based antibody screening campaigns to isolate GPCR binders [1, 2]. Cell panning approaches allow for the isolation of antibodies binding to their respective antigen in its natural environment and conformation and evades

Stefania C. Carrara and Jan P. Bogen contributed equally to this work.

Michael W. Traxlmayr (ed.), *Yeast Surface Display*, Methods in Molecular Biology, vol. 2491, https://doi.org/10.1007/978-1-0716-2285-8_10, © The Author(s), under exclusive license to Springer Science+Business Media, LLC, part of Springer Nature 2022

the need to produce and purify soluble target proteins [3]. Nonetheless, phage display comes with intrinsic disadvantages due to the prokaryotic expression host. Furthermore, antibodies screened via phage display can be troublesome to convert into full-length antibodies, as the screening is mostly performed utilizing single-chain fragment variables (scFv), resulting in the loss of potential binders.

Yeast surface display (YSD) is a prominent method to circumvent these intrinsic disadvantages by allowing the display of a fragment antigen-binding (Fab) on the surface of a eukaryotic cell [4]. Even though yeast cells can be applied in a panning approach [5–11], one main advantage is lost, namely the online tracking of enrichment over multiple sorting rounds by fluorescence-activated cell sorting (FACS). Herein, we describe a protocol for FACS-assisted YSD that can be applied for cell panning to enrich antibodies against receptors naturally expressed on standard cancer cell lines. As a proof-of-concept study, we demonstrate the enrichment of highly affine antibodies utilizing an anti-EGFR chicken-derived common light chain library panned against EGFR⁺⁺⁺ A431 mammalian cancer cells [12] (Fig. 1).

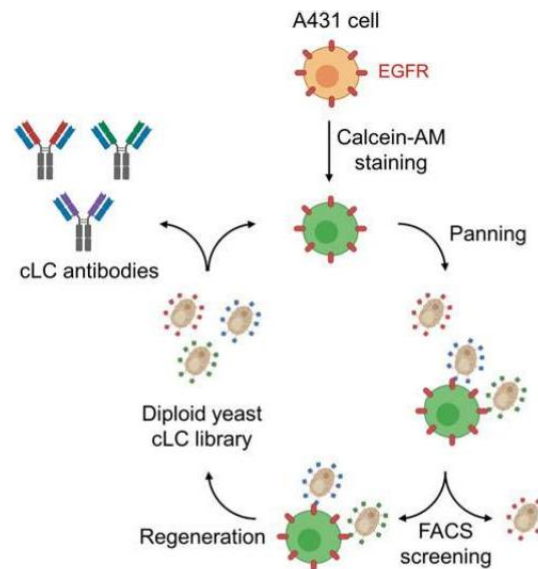


Fig. 1 Schematic representation of FACS-assisted yeast biopanning, utilizing Calcein-AM stained A431 cells and an anti-EGFR cLC chicken library. (Created with BioRender.com)

2 Materials

2.1 Mammalian Cells and Media

1. A431 human epidermoid carcinoma cells (ATCC).
2. Dulbecco's Modified Eagle Medium (DMEM) high glucose.
3. Complete growth medium (DMEM, 10% FBS, 1× P/S).
4. Fetal Bovine Serum (FBS) superior.
5. Penicillin-Streptomycin (P/S).
6. Trypsin-EDTA 0.25%.
7. Phosphate buffered saline (PBS).
8. T75 cm² cell culture flasks.
9. Calcein-AM cell stain (Fisher Scientific).

2.2 FACS-Assisted Sorting and Panning

1. User provided yeast library (*see* Subheading 3.1) in *Saccharomyces cerevisiae* strain EBY100.
2. SD-CAA: 8.6 g/L NaH₂PO₄ · H₂O, 5.4 g/L Na₂HPO₄, 1.7 g/L yeast nitrogen base without amino acids, 5 g/L ammonium sulfate, 5 g/L Bacto Casamino Acids, 20 g/L glucose, and 100 µg/mL ampicillin (+12 g/L agar agar for agar plates).
3. SG-CAA: 8.6 g/L NaH₂PO₄ · H₂O, 5.4 g/L Na₂HPO₄, 1.7 g/L yeast nitrogen base without amino acids, 5 g/L ammonium sulfate, 5 g/L Bacto Casamino Acids, 20 g/L galactose, and 100 µg/mL ampicillin.
4. PBS-B: PBS with 0.1% (w/v) bovine serum albumin.
5. Fc-tagged EGFR extracellular domain (ECD) (R&D Systems).
6. Goat anti-human Kappa-Alexa Fluor 647 antibody (1 mg/mL) (SouthernBiotech).
7. Goat anti-human IgG-Fc-PE-conjugate antibody (Fisher Scientific).
8. BD Influx (nozzle size 100 µm) or similar cell sorter.

2.3 Reformating, Production and Characterization

2.3.1 Reformating via Golden Gate Assembly

1. Zymoprep Yeast Plasmid Miniprep I (Zymo Research).
2. Q5[®] High-Fidelity DNA polymerase (New England Biolabs).
3. 5× Q5[®] buffer (New England Biolabs).
4. dNTPs (New England Biolabs).
5. Nuclease-free water.
6. Primers (*see* Table 1).
7. Thermocycler.
8. pTT5-derived destination vector [12].
9. CH1-CH2-CH3 entry vector [12].

Table 1
Primers utilized for reformatting of chicken VH and VL genes. Overhangs encoding SapI restriction sites are highlighted in red

Primer Name	Sequence 5'-3'
Chicken VH to pTT5 SapI GGA for	AAAAAGCTCTTCAAGTGGCCGTGACGTTGGACGAG
Chicken VH to pTT5 CH1 SapI GGA rev	TTTTTGCTCTTCTGGCGGAGGAGACGATGACTTCGGT
Chicken VL to pTT5 SapI GGA for	AAAAAGCTCTTCAAGTGCGCTGACTCAGCCGTCCTCG
Chicken Lam VL to pTT5 SapI GGA rev	TTTTTGCTCTTCACCCTAGGACGGTCAGGGTTGTCCG

10. Lambda entry vector [12].
11. T4 DNA ligase Buffer (New England Biolabs).
12. T4 DNA Ligase (New England Biolabs).
13. SapI (New England Biolabs).
14. Competent XL1 blue *E. coli* cells.
15. Ampicillin LB agar plates and media (100 µg/mL).
16. PureYield Plasmid Midiprep System (Promega).

2.3.2 Production and Purification of mAbs

1. Expi293F™ (Thermo Fisher).
2. Expifectamine™ 293 Transfection Kit (Thermo Fisher).
3. New Brunswick™ S41i (Eppendorf) or comparable cell culture shaker.
4. Chromatography system and Protein A purification columns.

2.3.3 Characterization of Isolated Antibodies

1. TSKgel SuperSW3000 column (Tosoh Bioscience).
2. 1260 Infinity chromatography system (Agilent Technologies).
3. Prometheus NT.48 nanoDSF Instrument (NanoTemper Technologies).
4. Nunc MaxiSorp™ flat-bottom 96-well plate (Thermo Fisher).
5. Sterile 96-well flat-bottom microtiter plates.
6. PBS-T: PBS with 0.05% Tween-20.
7. Blocking solution: PBS with 5% bovine serum.

8. Goat anti-human Fc-HRP conjugate.
9. TMB One solution (Promega).
10. Stop solution: 160 μ M sulfuric acid.
11. BMG ClarioStar microplate reader (or similar, compatible with absorbance measurements).

3 Methods

This chapter describes a FACS-assisted screening process by panning yeast cells displaying a common light chain Fab immune library against standard A431 cancer cells to enrich EGFR-specific antibodies. This straightforward method can be rapidly implemented and yields binders targeting different epitopes and exhibiting favorable biophysical properties. For immune libraries, any commonly used immunization host can be used, such as mice or rats. In this chapter, antibodies derived from immunized chickens are exemplarily used. Other library types, like semisynthetic libraries, might be suitable as well (*see Note 1*).

3.1 Yeast Libraries

Multiple protocols exist for the generation of yeast libraries, among them homologous recombination of scFv fragments [13] or Golden Gate cloning for Fab libraries [14]. We will illuminate the FACS-assisted YSD panning exemplarily on homologous recombination- and yeast mating-based library. However, library generation is not the focus of this chapter. A detailed description of how the utilized library was generated can be found here [12]. Nonetheless, other library generation methodologies are also potentially suitable for the panning approach.

3.2 Pre-screening: Cell Staining and Library Sorting by FACS

In this and the following section, the screening of immune libraries via FACS will be discussed. For this model study, we decided to perform the first sorting round utilizing soluble EGFR extracellular domain (ECD)-Fc in a standard FACS sorting procedure to reduce the library size before panning with mammalian cells (*see Note 2*). If screening is performed against ion channels or GPCRs, where such a pre-screening is not possible, continue with Subheading 3.3 (*see Note 3*).

1. Cultivate the yeast library in 50 mL up to 1 L SG-CAA at an OD_{600} of 1.0 overnight at 30 °C and 180 rpm. The total number of cultivated cells should exceed the diversity of the initial library by the factor 10 while an OD_{600} of 1 represents 1×10^7 cells per mL.
2. Harvest 1×10^7 cells (OD_{600} of 1.0 in 1 mL) by centrifugation at $8000 \times g$ for 3 min and wash with 1 mL PBS-B.

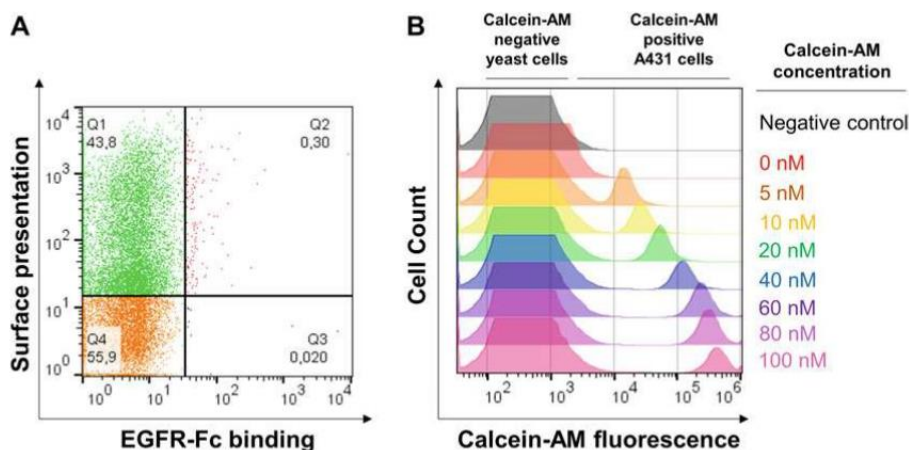


Fig. 2 Pre-screening and Calcein-AM titration. (a) Pre-screening of yeast cells with 250 nM soluble EGFR-Fc. Surface presentation (*y*-axis) and EGFR-Fc binding (*x*-axis) are depicted. Yeast cells not exhibiting Fab presentation are shown in Q4 (orange), while Fab-presenting yeast cells are depicted in Q1 (green). The right-shifting population displaying EGFR-Fc binding can be observed in Q2 (red). A total of 50,000 events are plotted. (b) Calcein-AM titration on A431 cells mixed with yeast cells. A range of 0–100 nM Calcein-AM was used. The population to the left with lower fluorescence depicts the uninduced yeast population, with a right-shifting mammalian cell population with increasing Calcein-AM concentration. The optimal concentration in this case was 80 nM, as the difference in fluorescence between the yeast population and the stained, live A431 cells was the highest within the detection threshold of the FACS instrument

3. Incubate cells with a 1:75 dilution (13.3 $\mu\text{g}/\text{mL}$) of an anti-human Kappa-AF647 antibody (*see Note 4*) in the presence of 250 nM Fc-tagged EGFR-ECD for 30 min. Subsequently, centrifuge cells, wash with 1 mL PBS-B, and incubate with a 1:50 dilution of an anti-human Fc-PE antibody for 15 min. For a negative control, perform a separate reaction in absence of the antigen.
4. Wash yeast cells twice with 1 mL ice-cold PBS-B and resuspend in 1 mL PBS-B for subsequent FACS analysis.
5. Apply a suitable sorting gate, which should comprise a suitable number of double-positive cells while no more than 0.3% of cells of the negative control should be included. As this sorting is done as a pre-screening, the “sort enrich mode” is utilized. The number of sorted cells should at least exceed the initial library by a factor 10. An exemplary FACS plot is shown in Fig. 2a.
6. All sorted cells are plated on SD-CAA agar plates and incubated for 48 h at 30 °C. Cells are transferred to SD-CAA media and incubated overnight at 30 °C. Subsequently, 50 mL SG-CAA media is inoculated at an initial OD_{600} of 1.0 and further incubated overnight at 30 °C. Induced cells can be applied to the biopanning process.

3.3 Yeast Biopanning

This section describes the cultivation and preparation of mammalian target cells to perform the subsequent FACS-assisted YSD biopanning. As a first step, the staining of mammalian cells utilizing the viability dye Calcein-AM needs to be optimized to enable the subsequent panning and FACS-assisted sorting.

3.3.1 Cultivation of Mammalian Cells

Human epidermoid carcinoma A431 cells naturally overexpressing EGFR (EGFR⁺⁺⁺) are cultured at 37 °C in a humidified atmosphere with 5% CO₂. When the cells reach a confluency of 80–90%, sub-passage the cells by first washing with PBS and trypsinizing using 0.25% Trypsin-EDTA. Incubate the cells at 37 °C until signs of detachment are visible. Resuspend the detached cells using complete growth medium and centrifuge at 500 × *g*, 5 min to remove trypsin. Resuspend the cell pellet in fresh complete growth medium and dilute the cells as required in T75 cm² cell culture flasks and incubate further at 37 °C, 5% CO₂.

3.3.2 Staining of A431 Cells

Contrary to other biopanning methods described in literature [8], this method relies on the endogenous overexpression of EGFR without requiring transfection or engineering of cell lines. By using a live cell marker, namely Calcein-AM, the enrichment of antibodies against the correct and native conformation of the receptor of interest on the cell surface is ensured, a current bottleneck in the separation of binders against membrane-bound targets of interest, such as receptor tyrosine kinases (RTK), GPCRs or ion channels. In an initial experiment, the optimal Calcein-AM concentration is determined to ensure a clear separation of yeast cells and viable mammalian cells. For this initial experiment, uninduced yeast cells should be utilized to circumvent any display-mediated binding effects.

1. Trypsinize cells from cell culture flask and centrifuge cells as described above.
2. Resuspend the cell pellet in PBS to a final concentration of 1×10^7 cells/mL.
3. To stain the cells, test different Calcein-AM concentrations in a range of 5–100 nM and incubate at room temperature for 20 min. Following staining, centrifuge and resuspend cells in pre-warmed complete growth medium. Incubate at 37 °C, 5% CO₂ for 10 min.
4. Wash Calcein-AM treated cells with PBS and mix 20:1 with untreated yeast cells (yeast:A431 cells). Yeast cells were previously grown overnight in SD-CAA and were washed once with PBS before incubation with Calcein-AM stained mammalian cells.
5. Analyze the cell mixture in FACS, which is intended to be used for subsequent sorting. Determination of the optimal Calcein-AM concentration is dependent on both the cell line and FACS

instrument used and must be determined for each set of experiments (*see Note 5*). As seen in Fig. 2b, the Calcein-AM concentration leading to the best separation for A431 was at 80 nM in this model experiment, as there was a clear separation of yeast cells and mammalian cells without exceeding the fluorescence threshold of the FACS device.

3.3.3 FACS-Assisted Biopanning of Mammalian and Yeast Cells

After having established antibody surface-presentation on yeast cells (Subheading 3.2) and the appropriate Calcein-AM concentration for live cell staining (Subheading 3.3.2), the library can now be sorted by yeast biopanning.

1. A431 cells are stained utilizing Calcein-AM at the concentration determined in Subheading 3.3.2. The number of stained cells is dependent on the number of yeast cells intended to be screened and the yeast:mammalian cell ratio (*see below*). Following staining, centrifuge and resuspend cells in pre-warmed complete growth medium. Incubate at 37 °C, 5% CO₂ for 10 min, followed by a PBS washing step.
2. During Calcein-AM staining of A431 cells, incubate a suitable number of yeast cells (*see below*) from the induced library (either initial or derived from the pre-screening) with a 1:75 dilution (13.3 µg/mL) of the anti-human Kappa-AF647 antibody for 15 min at 4 °C in a final volume of up to 500 µL, and subsequently wash yeast cells with PBS-B.
3. In this exemplary study, A431 cells were mixed at a ratio of 20:1 (yeast:mammalian cells, *see Note 6*) and subsequently incubated at 4 °C for 30 min while gently shaking at 30 rpm. Choose a volume appropriate for the number of mixed cells, as no additional washing step is performed before FACS analysis. A final volume of 1 mL is adequate for most applications.
4. After incubation, resuspend sedimented cells carefully and perform FACS analysis utilizing a BD Influx FACS Cell Sorter (Software 1.00.0.650) or a comparable sorting device.
5. When applying gates to the double-positive cell mixture, do not gate for singlets, as the mammalian-yeast cell complexes are cell–cell interaction-based events. Double-positive events were sorted utilizing the “sort enrich mode.” An exemplary FACS plot can be seen in Fig. 3.
6. Plate all sorted cells on SD-CAA agar plates and incubate for 48 h at 30 °C. While yeast cells will grow on SD-CAA media, sorted mammalian cells will die.
7. Subsequently, transfer yeast cells to SD-CAA media and incubate overnight at 30 °C. Inoculate 50 mL SG-CAA media at an initial OD₆₀₀ of 1.0 and incubate further overnight at 30 °C. Induced cells can be applied to subsequent biopanning rounds.

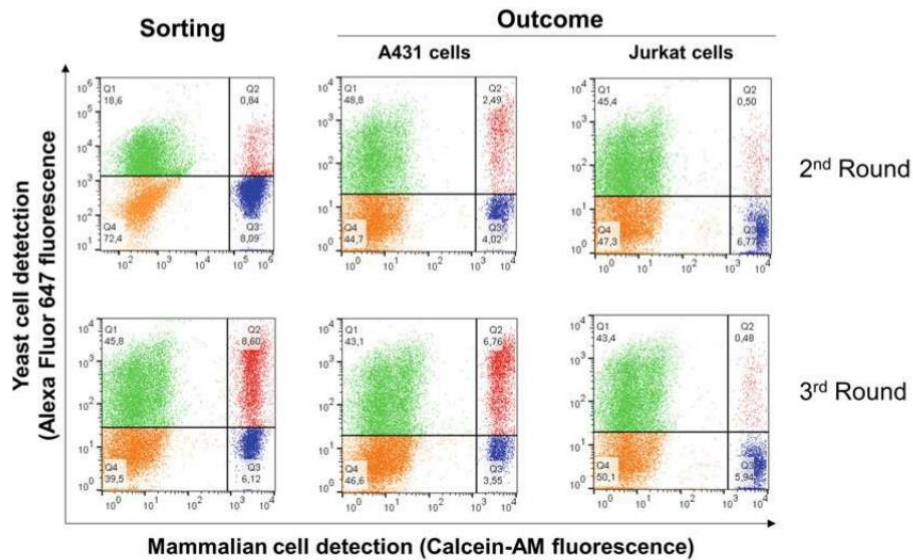


Fig. 3 Sorting and outcome FACS plots of the second and third round of yeast biopanning using target cells (A431) and control (Jurkat) cells. Fab surface presentation (y -axis) and Calcein-AM fluorescence (x -axis) are depicted. Four populations are visible in the FACS dot plots. The left side of the FACS plots shows yeast cells—Q4 (orange) depicts yeast cells with no Fab surface expression, while Q1 (green) are those yeast cells displaying Fabs on their surface. In Q3 (blue), Calcein-AM stained A431 cells are visible. The population of interest for yeast biopanning is shown in the upper right quadrant (Q2, red), showing double-positive cells, namely Fab-displaying yeast cells binding to stained mammalian target cells. With sequential rounds, an enrichment in Q2 can be observed. Jurkat cells were used as negative control. Per FACS plot, 50,000 events are visible

If library screening is complete, the SD-CAA culture can be used for plasmid isolation (Subheading 3.4.1). Alternatively, single clones derived from the final screening round can be picked from the SD-CAA agar plate and induced separately in SG-CAA media, allowing subsequent single clone analysis using cell-bound antigen or soluble antigen (Subheading 3.3.4).

Enrichment of antigen-binding population can be observed with repeating library staining and cell sorting rounds. The number of repeating sorting rounds is to be determined on a case-by-case basis (*see Note 7*).

3.3.4 Target Binding Analysis of Isolated Single Clones

As screening is performed with a 20:1 ratio of yeast cells to A431 cells, it is not expected to observe a complete shift of all Fab-displaying yeast cells. Therefore, FACS-assisted YSD biopanning-based single clone analysis can be utilized to

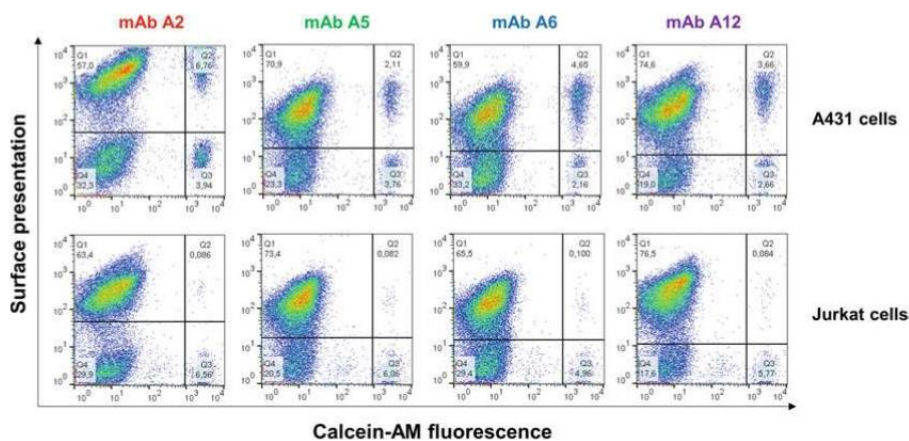


Fig. 4 Single clone analysis via FACS-assisted biopanning. Single clones were tested against binding on A431 (EGFR⁺⁺⁺) cells and Jurkat (EGFR⁻) cells. Fab surface presentation on yeast cells (y -axis) and mammalian cells via Calcein-AM fluorescence (x -axis) are depicted. The left side of the FACS plots shows yeast cells—Q4 depicts yeast cells with no Fab surface expression, while Q1 are Fab-displaying yeast cells. In Q3, stained mammalian cells are visible. The population of interest is shown in the upper right quadrant (Q2), showing double-positive cells, namely Fab-displaying yeast cells binding to stained target mammalian cells. For all four clones, binding to target A431 cells can be observed, with minimal binding of the single clones to Jurkat cells in Q2. Per FACS plot, 50,000 events are visible

distinguish binders from non-binders. Furthermore, if multiple cell lines are at hand expressing the same antigen of interest, cross-validation can be performed to ensure the specificity of isolated antibodies. Single clone biopanning is performed analogously to the staining of a library as described in Subheading 3.3.3. Exemplary plots of yeast cells derived from the screening effort expressing EGFR-specific binders are shown in Fig. 4. As a control, an EGFR-negative Jurkat cell line was utilized.

As the surface of mammalian cells comprises many proteins, it is crucial to ensure that the specificity of the enriched binders is against the target of interest and not against other surface proteins expressed (*see Note 8*). If possible, flow cytometric analysis can be performed as described in Subheading 3.2 utilizing soluble EGFR-ECD-Fc and the isolated single clones from Fig. 4. With strong binding shown toward the EGFR-ECD-chimera, this approach confirmed the successful isolation of EGFR-specific antibodies by combining yeast biopanning and FACS (Fig. 5).

3.4 Reformating, Antibody Production, and Characterization

FACS-assisted biopanning utilizing YSD is a novel screening tool without broad application in literature, therefore general conclusions on the biophysical properties of antibodies isolated that way are hardly drawn. In comparison, mAbs isolated utilizing a standard FACS-assisted campaign utilizing soluble antigens often have

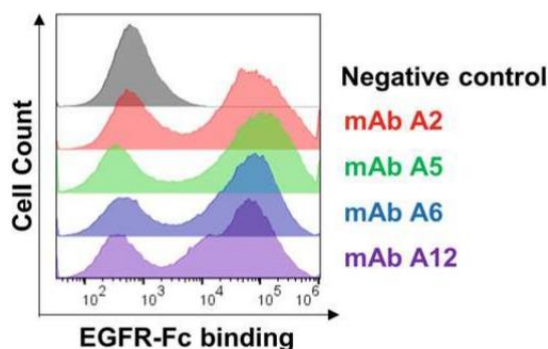


Fig. 5 Binding of soluble EGFR-ECD-Fc to isolated single yeast clones to confirm target binding. mAbs A2, A5, A6, and A12 were successfully isolated using biopanning, as depicted here in red, green, blue, and violet, respectively. The yeast cells were stained with 100 nM EGFR-Fc as described in Subheading 3.2

favorable biophysical properties due to the eukaryotic expression host [15]. However, biopanning of yeast cells could lead to the enrichment of antibodies binding to A431 cells in an unspecific manner. Furthermore, the panning approach is based on cell clustering of yeast cells and mammalian cells, potentially resulting in mAbs with unfavorable aggregation profiles. In addition, panning is based on strong avidity effects, which might result in the isolation of low-affinity binders. To assess those risks, a robust and rigorous characterization of full-length antibodies is mandatory. This section describes some of the most straightforward methods to assess the biophysical properties of panning-derived antibodies after reformatting, production, and purification of the lead candidates (*see Note 9*).

3.4.1 Reformatting via Golden Gate Assembly

This section describes the reformatting of Fabs displayed on yeast cells to full-length antibodies expressed in mammalian cell culture. Since we utilized common light chain Fabs, the VH genes can be amplified from a cell population and can be reformatted using batch-cloning. If a haploid yeast Fab library was used, consisting of a diverse set of heavy and light chains, plasmids encoding the respective domains need to be isolated from individual clones to ensure correct light chain-heavy chain pairing. The selection of those single clones is described in Subheading 3.3.4.

The primers used for VH and VL amplification are specific to chicken-derived antibodies and introduce overhangs containing SapI restriction sites, enabling subsequent Golden Gate cloning into a pTT5-derived vector suitable for mammalian transfection.

1. Cultivate yeast cells derived from the final panning round in SD-CAA media overnight at 30 °C.

Table 2
PCR protocol for amplification of chicken-derived VH and VL genes utilizing Q5 DNA-polymerase

98 °C	30 s	
98 °C	15 s	30 cycles
63 °C	15 s	
72 °C	30 s	
72 °C	2 min	

2. Harvest cells by centrifugation and isolate plasmid DNA utilizing the Zymoprep Yeast Plasmid Miniprep I kit according to the manufacturer's instruction (*see Note 10*).
3. Amplify VH and VL genes via PCR utilizing Q5 DNA polymerase. Respective primers for VH and VL amplification can be found in Table 1. The PCR protocol is depicted in Table 2. In brief, one reaction comprises:
 - (a) 10 μ L 5 \times Q5 Reaction Buffer.
 - (b) 1 μ L dNTPs (10 mM each).
 - (c) 2.5 μ L of a 10 μ M solution of forward primers for either VH or VL.
 - (d) 2.5 μ L of a 10 μ M solution of reverse primers for either VH or VL.
 - (e) 1 μ L of plasmid DNA isolated from yeast cells.
 - (f) 0.5 μ L Q5[®] High-Fidelity DNA polymerase.
 - (g) Nuclease-free water to a volume of 50 μ L.
4. Verify successful amplification of chicken-derived VH and VL sequences by performing gel electrophoresis using 1% (w/v) agarose.
5. Purify the VH and VL amplicons using the Promega Wizard[®] SV Gel and PCR Clean-up System or a comparable kit and determine the DNA concentration.
6. VH amplicons are inserted into a pTT5-derived destination vector utilizing the entry vector encoding the CH1-CH2-CH3 sequence of a human IgG1. VL amplicons are inserted into a pTT5-derived destination vector utilizing the Lambda CL entry vector. The detailed Golden Gate procedure is described here [12]. In brief:
 - (a) 2.5 μ L T4 Ligase Buffer.
 - (b) 75 ng pTT5-derived entry vector [12].
 - (c) 75 ng CH1-CH2-CH3 OR Lambda entry vector [12].
 - (d) 75 ng VH or VL amplicon.

Table 3
Temperature protocol for Golden Gate Assembly of VH and VL genes

37 °C	1 min	30 cycles
16 °C	1 min	
55 °C	5 min	
4 °C	∞	

- (e) 20 U SapI.
 - (f) 1000 U T4 Ligase.
 - (g) Nuclease-free water to 25 μ L.
7. Golden Gate reaction is performed in a thermocycler following the temperature protocol from Table 3.
 8. Transform 5 μ L of the reaction mixture into chemical competent *E. coli* XL1-Blue, plate transformed cells onto ampicillin LB agar plates, and incubate cells overnight at 37 °C.
 9. Perform Sanger sequencing of an appropriate number of clones to identify unique sequences. *E. coli* carrying the plasmid of desired antibodies are inoculated to 50 mL LB ampicillin media and incubated overnight at 37 °C, 180 rpm.
 10. Isolate plasmid DNA utilizing the PureYield Plasmid Midiprep System (Promega) kit and determine the DNA concentration.
1. Transfect Expi293F™ cells utilizing Expifectamine™ 293 and 30 μ g vector DNA according to the manufacturer's instructions (*see Note 11*).
 2. After 18–24 h, feed transfected cells using the Expi293 feed and enhancer solutions. Subsequently, incubate the cells further for 5 days at 37 °C, 8.0% CO₂, and 110 rpm.
 3. Harvest cells by centrifugation at 3000 $\times g$ at 4 °C for 3 min and sterile filter (0.22 or 0.4 μ m) the supernatant.
 4. Utilizing standard Protein A chromatography, purify the chimeric full-length antibodies and subsequently dialyze against PBS buffer.

3.4.2 Production and Purification of mAbs

From the reformatted and purified antibodies, their crucial characteristics were analyzed by means of size exclusion chromatography, thermal stability, unspecific binding, and EC₅₀ determination on cells. From the established FACS-assisted, yeast surface display-based panning approach, antibodies were isolated, exhibiting remarkable biophysical properties and prominent affinities.

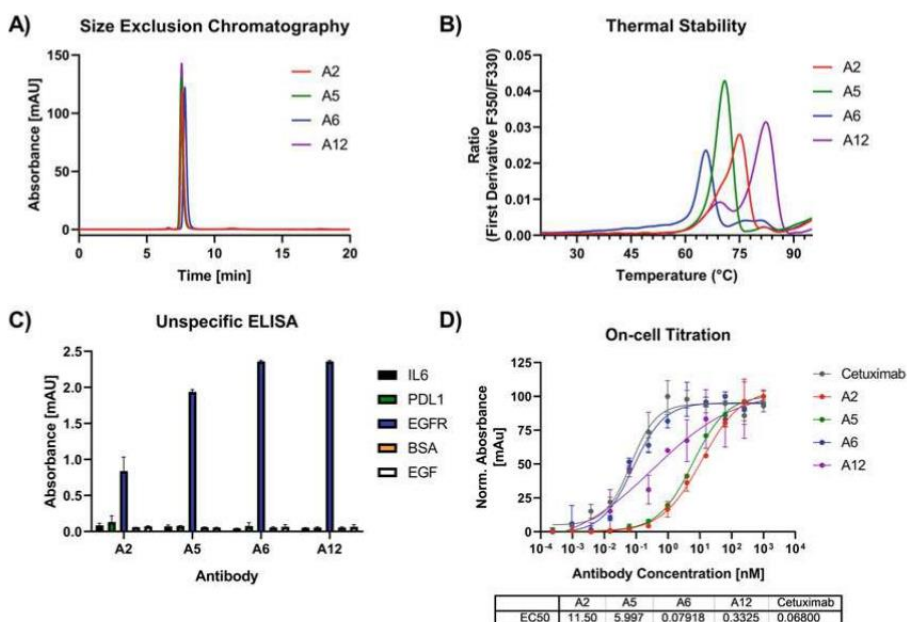


Fig. 6 Characterization of isolated binders. (a) Size Exclusion Chromatography analysis using native conditions. All four antibodies showed minimal aggregation propensity. (b) Thermal stability experiments carried out using nanoDSF instrument. (c) Unspecific binding behavior of isolated antibodies. Binding was only observed against EGFR and not against other antigens tested (IL-6, PD-L1, BSA, EGF). (d) On-cell antibody titration for EC₅₀ determination, using Cetuximab as a positive control on A431 cells

3.4.3 Size Exclusion Chromatography (SEC)

Using a TSKgel SuperSW3000 column combined with the 1260 Infinity Chromatography system, SEC was performed to characterize the aggregation propensity of the isolated antibodies. All isolated antibodies exhibited only minimal aggregation tendencies (Fig. 6a).

3.4.4 Thermal Stability

To assess protein stability, the melting temperature (T_M) was determined using Prometheus NT.48 Protein Stability Instrument. From a 1 mg/mL sample, the tryptophan fluorescence was measured at 350 and 330 nm at temperatures from 20 to 90 °C with a heating rate of 1 °C/min. The T_M was extrapolated from the ratios of the first derivative at 330 and 350 nm at the first maxima using the integrated software, and notable stabilities were observed (Fig. 6b).

3.4.5 Unspecific Binding ELISA

To ensure the isolated EGFR binders did not exhibit unspecific behavior toward other targets, an unspecific binding ELISA was performed against different antigens (Fig. 6c). Standard ELISA protocols can be applied. A detailed protocol can be found here [12].

3.4.6 On-Cell EC50 Determination

Multiple technologies exist to determine binding properties, such as biolayer interferometry (BLI) or surface plasmon resonance spectroscopy (SPR). However, for targets like GPCRs or ion channels, such assays can be challenging to perform. As the panning-based screening is done to assure binding specificity to the antigen in the natural environment of the cell, on-cell titration is a suitable method to determine binding behavior of isolated mAbs (*see Note 12*). An on-cell antibody titration was carried out in 96-well plates, allowing for triplicate measurements in a straightforward manner (Fig. 6d). The exact protocol can be found elsewhere [12] (*see Note 13*).

4 Notes

1. (Semi-)synthetic and naïve libraries comprise binders against a variety of antigens, so binders against membrane proteins that are not the intended target antigen might be enriched. In such cases, a good strategy is to switch cell lines between sorting rounds derived from different host organisms but express the same antigen of interest. This can, for example, be applied by performing two enrichment rounds on the intended human cell line and a third sorting round on transfected CHO cells.
2. For FACS sorting utilizing soluble antigens, all staining steps should be performed at 4 °C.
3. A pre-screening is not necessary; however, it can drastically reduce the diversity of the initial library in favor of specific binders, easing the panning campaign.
4. This antibody recognizes the CL domain of the displayed Fab fragment and allows for the detection of surface display of the protein of interest. The best-suited antibody for display detection is based on the utilized library.
5. The concentration of Calcein-AM must be determined for each cell type and FACS device in order to find the optimal separation of fluorescence signal between mammalian and yeast cells, without reaching the threshold of the FACS machine. The fluorescence intensity of the Calcein-AM-stained A431 cells should be as high as possible within the instrument's detection limit. At lower Calcein-AM concentrations, an overlap of both the yeast and mammalian cell populations was observed, leading to poor sorting conditions.
6. The authors recommend determining the most suitable yeast-to-mammalian cell ratio on a case-to-case basis, depending on the mammalian cells being used.
7. The number of sorting rounds is to be determined based on the number of positive hits. The authors recommend at least three sorting rounds.

8. In cases where no soluble antigen is available, other cell lines derived from other host organisms can be utilized upon transfection of the respective target antigen as described in Subheading 3.3.4.
9. Up to now, all panning-derived mAbs isolated from immunized animals from our group exhibited exclusively favorable biophysical properties. However, the utilization of naïve or (semi-)synthetic libraries might result in binders with unspecific binding behaviours or higher aggregation tendencies, making the assessment of biophysical properties mandatory.
10. Other yeast plasmid DNA isolation kits and protocols are suitable as well. A straightforward way that does not require commercial kits is described elsewhere [16].
11. Determine the volume of culture and vessel size required for characterization of single clones. Depending on the number of unique clones after biopanning, transient transfection of Expi293F™ cells can be carried out in smaller vessels, such as 24-deep well plates, to increase throughput and lower material consumption, while producing and purifying enough material for subsequent analysis.
12. On-cell titration is an excellent method to determine binding characteristics of mAbs against antigens that are hard to produce in a soluble form. However, one must keep in mind that the binding of a bivalent mAb to a cell exhibiting multiple copies of the target antigen comes with an avidity effect.
13. As this is an on-cell titration, the authors recommend using gentle pipetting when washing the cells. While A431 cells retain their adherence very well, other cell types may be more prone to detaching during the washing steps, ultimately leading to loss of cells.

References

1. Smith GP (1985) Filamentous fusion phage: novel expression vectors that display cloned antigens on the virion surface. *Science* 228(4705):1315. <https://doi.org/10.1126/science.4001944>
2. Jo M, Jung ST (2016) Engineering therapeutic antibodies targeting G-protein-coupled receptors. *Exp Mol Med* 48(2):e207–e207. <https://doi.org/10.1038/emm.2015.105>
3. Alfaleh MA, Jones ML, Howard CB, Mahler SM (2017) Strategies for selecting membrane protein-specific antibodies using phage display with cell-based panning. *Antibodies* 6(3):10. <https://doi.org/10.3390/antib6030010>
4. Pepper LR, Cho YK, Boder ET, Shusta EV (2008) A decade of yeast surface display technology: where are we now? *Comb Chem High Throughput Screen* 11(2):127–134. <https://doi.org/10.2174/138620708783744516>
5. Wang XX, Shusta EV (2005) The use of scFv-displaying yeast in mammalian cell surface selections. *J Immunol Methods* 304(1–2):30–42. <https://doi.org/10.1016/j.jim.2005.05.006>
6. Wang XX, Cho YK, Shusta EV (2007) Mining a yeast library for brain endothelial cell-binding antibodies. *Nat Methods* 4(2):143–145. <https://doi.org/10.1038/nmeth993>
7. Williams RM, Hajiran CJ, Nayeem S, Sooter LJ (2014) Identification of an antibody fragment specific for androgen-dependent prostate

- cancer cells. *BMC Biotechnol* 14:81. <https://doi.org/10.1186/1472-6750-14-81>
8. Yang Z, Wan Y, Tao P, Qiang M, Dong X, Lin CW, Yang G, Zheng T, Lerner RA (2019) A cell-cell interaction format for selection of high-affinity antibodies to membrane proteins. *Proc Natl Acad Sci U S A* 116(30):14971–14978. <https://doi.org/10.1073/pnas.1908571116>
 9. Stern LA, Schrack IA, Johnson SM, Deshpande A, Bennett NR, Harasymiw LA, Gardner MK, Hackel BJ (2016) Geometry and expression enhance enrichment of functional yeast-displayed ligands via cell panning. *Biotechnol Bioeng* 113(11):2328–2341. <https://doi.org/10.1002/bit.26001>
 10. Hu D, Zhu Z, Li S, Deng Y, Wu Y, Zhang N, Puri V, Wang C, Zou P, Lei C, Tian X, Wang Y, Zhao Q, Li W, Prabakaran P, Feng Y, Cardosa J, Qin C, Zhou X, Dimitrov DS, Ying T (2019) A broadly neutralizing germline-like human monoclonal antibody against dengue virus envelope domain III. *PLoS Pathog* 15(6):e1007836. <https://doi.org/10.1371/journal.ppat.1007836>
 11. Stern LA, Lown PS, Kobe AC, Abou-Elkacem L, Willmann JK, Hackel BJ (2019) Cellular-based selections aid yeast-display discovery of genuine cell-binding ligands: targeting oncology vascular biomarker CD276. *ACS Comb Sci* 21(3):207–222. <https://doi.org/10.1021/acscombsci.8b00156>
 12. Bogen JP, Storka J, Yanakieva D, Fiebig D, Grzeschik J, Hock B, Kolmar H (2020) Isolation of common light chain antibodies from immunized chickens using yeast biopanning and fluorescence-activated cell sorting. *Biotechnol J* 16(3):2000240. <https://doi.org/10.1002/biot.202000240>
 13. Bogen JP, Grzeschik J, Krah S, Zielonka S, Kolmar H (2020) Rapid generation of chicken immune libraries for yeast surface display. *Methods Mol Biol* 2070:289–302. https://doi.org/10.1007/978-1-4939-9853-1_16
 14. Krah S, Grzeschik J, Rosowski S, Gaa R, Willenbuecher I, Demir D, Toleikis L, Kolmar H, Becker S, Zielonka S (2018) A streamlined approach for the construction of large yeast surface display fab antibody libraries. *Methods Mol Biol* 1827:145–161. https://doi.org/10.1007/978-1-4939-8648-4_8
 15. Cherf GM, Cochran JR (2015) Applications of yeast surface display for protein engineering. *Methods Mol Biol* 1319:155–175. https://doi.org/10.1007/978-1-4939-2748-7_8
 16. Holm C, Meeks-Wagner DW, Fangman WL, Botstein D (1986) A rapid, efficient method for isolating DNA from yeast. *Gene* 42(2):169–173. [https://doi.org/10.1016/0378-1119\(86\)90293-3](https://doi.org/10.1016/0378-1119(86)90293-3)

5 Acknowledgements

To kick off the list of people I have to thank, I would like to thank **Prof. Dr. Harald Kolmar** for his mentorship over the last three years and making my move to Darmstadt worthwhile. Your unconditional trust and the flexibility you gave me to investigate and follow my own ideas and molecules has only further inspired me to continue trusting in the process and never giving up. Your work ethic has been of utmost motivation and a path to follow, from always finding the time to answer questions to writing e-mails at ungodly hours. From the annual retreat to scientific discussions in the biergarten, being part of AK Kolmar was a great honour and something I will tribute forever!

Further, I would like to thank **PD. Dr. Björn Hock** for agreeing to take me on as a PhD student and being my second examiner. Your industry- and business-driven view of scientific discoveries has helped shape my way of thinking to focus on the big things and get things done productively. I am thankful that you still took the time for scientific discussions and meetings and continued to guide me until the very end.

I would like to thank **PD. Dr. Tobias Meckel** and **Prof. Dr. Beatrix Süß** for agreeing to take on the role as subject examiners.

I would like to thank **Dr. Alex Bähre** for her guidance during our time as members at FDL. Your warm welcome and our weekly 1-to-1 sessions were instrumental for my smooth transition upon moving to Darmstadt. You were always willing to invest time to make sure we were all doing okay. Our time at Christmas markets, around Copenhagen or at dinners will not be forgotten! I hope our paths manage to cross again.

Dr. Julius Grzeschik has been instrumental not only at FDL but in always helping with many Ferring-related questions. Thank you for making times more bearable and for always being ready to drink a beer together. You have a particular way of questioning people to make them reflect about what they are thinking or why they think that, and I hope to learn from that. Thank you for all your scientific contributions, guidance, and assistance! The speed at which I have seen you grow as a leader within the past three years is nothing short of amazing and I am sure this is just the beginning for you!

I would like to address **Dr. Jan P. Bogen** for his relentless and contagious attitude in the lab. Your help at introducing me to new technologies was influential for the remainder of my PhD! It was a pleasure working with you and bouncing around scientific ideas. Your trispecific antibody was the inspiration for the Frankenstein variants! I wish you nothing but the best for your future and I am sure you will leave a great mark within the scientific community.

Thereafter I would like to thank **Dr. Dafi Fiebig** whose work ethic is nothing short of astounding. Thank you for always pushing us to find the root cause of problems and not just shove them in a cupboard, even though we might have found it annoying at the time. The spontaneous beers and endless conversations at late hours waiting for runs/experiments to finish were definitely a highlight. Any company would be lucky to have such a hard-working and dedicated scientist like you!

Furthermore, I would like to thank the entire Ferring team **Dr. Lukas Deweid, Dr. Benjamin Mattes and Michael Ulitzka** for the great collaboration and your willingness to help within your area of expertise. The conferences and trips we were able to take together were great fun!

Thank you to **Dr. Adrian Elter** for always listening to my rants about weird results I was getting during my last year and always providing insightful input. Stay cool!

Thank you to **Julia Harwardt** for the fruitful dynamic we had to make the best out of bad situations! It was great working together and trying to troubleshoot why things weren't working as planned! I wish you all the best for the remainder of your PhD.

Thank you to **Barbara Diestelmann, Dana Schmidt, Cecilia Gorus, Dr. Olga Avrutina, and Dr. Andreas Christmann** for always being ready to help with administrative or laboratory issues and making AK Kolmar run the way it does. A special thank you to **Janine Becker** for your contributions with the cell culture and your willingness to help facilitate my day-to-day by taking over some of my workload!

Dominic Happel and Jan Habermann thank you for always being willing to help with general things in the lab that no one finds themselves responsible for, and for knowing where everything was located when I couldn't find something. The lab would not work as smoothly without the things you do in the "background"!

I would like to thank **Dr. Steffen Hinz, Dr. Hendrick Schneider, Simon Englert, Dr. Ataurehman Ali, Dr. Arturo Maccarón Palacios, and Dr. Desislava Yanakieva** for the many fruitful conversations outside on the balcony. A big thank you to **Jorge Lerma Romero, Sebastian Bitsch, Peter Bitsch, Carolin Dombrowsky, Katrin Schoenfeld, Sarah Hofmann, Ingo Bork, Lieke van Gijzel** and the entire **AK Kolmar** for their help when needed and for the great times both within the lab and at KWT!

Mi agradecimiento más grande va dirigido hacia mi familia, por sobre todo mis papás **Flavia Bozzetto** y **Dr. Dario Carrara**, a quienes me gustaría dedicarle esta tesis. Gracias por siempre apoyarme y permitirme llegar a este punto. Sin el apoyo incondicional que me vienen dando desde siempre, nada de esto hubiera sido posible. Los dos son un ejemplo a seguir, tanto en cuestiones laborales como personales. Estoy eternamente agradecida, y espero algún día poder devolverles todo lo que me dieron! To my sestra **Coni Carrara** and nephew **Maxi**, thank you for never giving up on “pushing” me to find the time to spend together. I may not be the best at keeping in touch, but know you are always on my mind. No one can give us back those moments, and you helped me remember that! I cannot wait to meet the newest member of the **Van der Graaf** family that is on the way. To my brother **Augusto Carrara**, who has always been there in good times and bad! Thank you for always having my back and always knowing how to have a good time. I wish you the best for your further studies and hope I will be able to help you like you have helped me! A toda mi familia en Argentina que siempre están presentes y sé que de lejos me ayudaron a cumplir esta meta, ¡mil gracias!

Por último, me gustaría expresar mi profundo agradecimiento a **Amanda Dávila Lezama**, quien nunca dudó de mí y me puso primera los últimos años. Te agradezco por todo lo que tuviste que aguantar, yo sé que no siempre soy fácil. Volver a casa después de días muy largos llena de frustración o con ganas de celebrar y saber que siempre estabas dispuesta a ayudarme, escucharme o abrirme una cerveza son sentimientos impagables. Gracias por dejarme disfrutar de momentos y lugares juntas para que pueda volver a motivarme y seguir adelante. Espero algún día poder ayudarte a cumplir un sueño tuyo, así como lo hiciste por mí. No podría pedir una mejor compañera de vida and I can't wait for what the future has in store for us, sea donde sea!

6 Curriculum Vitae

Name: Stefania Candela Carrara
Birth date: 08.04.1995
Birth place: Buenos Aires, Argentina
Nationality: Swiss

Education

Doctoral student - Technische Universität Darmstadt 11/2019 – 12/2022

PhD candidate at the Clemens-Schöpf-Institute for Organic Chemistry and Biochemistry under the direction of Prof. Dr. Harald Kolmar.

M.Sc. in Biochemistry – Universität Zürich 08/2016 – 08/2018

Master thesis completed at the Department of Biochemistry under supervision of Prof. Dr. Andreas Plückthun: Selection and characterization of DARPins binding different hROR2 epitopes. Final grade: 5.2/6.

B.Sc. in Biochemistry and Molecular Biology – Universität Bern 08/2013 – 07/2016

Bachelor thesis completed at the Institute of Biochemistry and Molecular Medicine under PD Dr. Roch-Philippe Charles: Discovery of new key players in anaplastic thyroid cancer.

International Baccalaureate – International School of Basel 08/2011 – 05/2013

International Baccalaureate (IB) with 35 points.

7 Erklärung laut Promotionsordnung

§8 Abs. 1 lit. c der Promotionsordnung der TU Darmstadt

Ich versichere hiermit, dass die elektronische Version meiner Dissertation mit der schriftlichen Version übereinstimmt und für die Durchführung des Promotionsverfahrens vorliegt.

§8 Abs. 1 lit. d der Promotionsordnung der TU Darmstadt

Ich versichere hiermit, dass zu einem vorherigen Zeitpunkt noch keine Promotion versucht wurde und zu keinem früheren Zeitpunkt an einer in- oder ausländischen Hochschule eingereicht wurde. In diesem Fall sind nähere Angaben über Zeitpunkt, Hochschule, Dissertationsthema und Ergebnis dieses Versuchs mitzuteilen.

§9 Abs. 1 der Promotionsordnung der TU Darmstadt

Ich versichere hiermit, dass die vorliegende Dissertation selbstständig und nur unter Verwendung der angegebenen Quellen verfasst wurde.

§9 Abs. 2 der Promotionsordnung der TU Darmstadt

Die Arbeit hat bisher noch nicht zu Prüfungszwecken gedient.

Darmstadt, den 31. Oktober 2022

Stefania C. Carrara

DECLARATION ON OWN CONTRIBUTION TO PUBLICATIONS

In the following you will find a list of the percentage of publications I have been involved in.

My share in the following publication is 90%.

[1] Carrara SC et al. (2021). From cell line development to the formulated drug product: The art of manufacturing therapeutic monoclonal antibodies. *International Journal of Pharmaceutics* 10.1016/j.ijpharm.2020.120164.

My share in the following publication is 30%.

[2] Carrara SC*, Fiebig D*, Bogen JP*, Grzeschik J, Hock B, Kolmar H (2021). Recombinant antibody production using a dual-promoter single plasmid system. *Antibodies (Basel)* 10.3390/antib10020018. (* shared first authorship)

My share in the following publication is 30%.

[3] Fiebig D*, Bogen JP*, Carrara SC* et al. (2022). Streamlining the transition from yeast surface display of antibody fragment immune libraries to the production as IgG format in mammalian cells. *Frontiers in Bioengineering & Biotechnology* 10.3389/fbioe.2022.794389 (* shared first authorship)

My share in the following publication is 85% (accepted for publication).

[4] Carrara SC et al. (2022). Bulk reformatting of antibody fragments displayed on the surface of yeast cells to final IgG format for mammalian production. *Methods in Molecular Biology*, accepted.

My share in the following publication is 90% (under review).

[5] Carrara SC et al. (2022). TriTECM: a tetrafunctional T-cell engaging antibody with built-in risk mitigation of cytokine release syndrome. *Frontiers in Immunology*, revision.

My share in the following publication is 90% (manuscript in final preparation).

[6] Carrara SC et al. (2022). Targeted phagocytosis induction for cancer immunotherapy via bispecific MerTK-engaging antibodies. *International Journal of Molecular Sciences*.

My share in the following publication is 45%.

[7] Carrara SC*, Bogen JP*, Grzeschik J, Hock B, Kolmar H (2022). Antibody library screening using yeast biopanning and fluorescence-activated cell sorting. *Methods in Molecular Biology* 10.1007/978-1-0716-2285-8_10. (* shared first authorship)

.....

Date 17.10.22



Signature of applicant



DECLARATION ON THE REVIEW OF PUBLICATIONS

___Prof. Dr. Harald Kolmar___
Referee

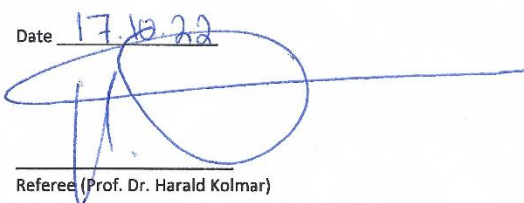
___PD. Dr. Björn Hock___
Co-Referee

17.10.22
Date

Neither referee (Prof. Dr. Harald Kolmar) nor co-referee (PD. Dr. Björn Hock) of this cumulative doctoral thesis were involved in the review of the following publications:

- [1] Carrara SC et al. (2021). From cell line development to the formulated drug product: The art of manufacturing therapeutic monoclonal antibodies.
- [2] Carrara SC*, Fiebig D*, Bogen JP*, Grzeschik J, Hock B, Kolmar H (2021). Recombinant antibody production using a dual-promoter single plasmid system.
- [3] Fiebig D*, Bogen JP*, Carrara SC* et al. (2022). Streamlining the transition from yeast surface display of antibody fragment immune libraries to the production as IgG format in mammalian cells.
- [4] Carrara SC et al. (2022). Bulk reformatting of antibody fragments displayed on the surface of yeast cells to final IgG format for mammalian production.
- [5] Carrara SC et al. (2022). TriTECM: a tetrafunctional T-cell engaging antibody with built-in risk mitigation of cytokine release syndrome.
- [6] Carrara SC et al. (2022). Targeted phagocytosis induction for cancer immunotherapy via bispecific MerTK-engaging antibodies. *International Journal of Molecular Sciences*.
- [7] Carrara SC*, Bogen JP*, Grzeschik J, Hock B, Kolmar H (2022). Antibody library screening using yeast biopanning and fluorescence-activated cell sorting.
-

Date 17.10.22


Referee (Prof. Dr. Harald Kolmar)

Björn Hock
Co-Referee (PD Dr. Björn Hock)